NSF/CEE-82102

STRUCTURES & MECHANICS

PB83-204875

# UNIVERSITY OF WASHINGTON

## COLLEGE OF ENGINEERING

## DEPARTMENT OF CIVIL ENGINEERING

SM 82-1

# ANCHORAGE OF REINFORCING BARS FOR REVERSED CYCLIC LOADING

by

Ing-Jaung Lin and Neil M. Hawkins

SEATTLE, WASHINGTON

98195

50272-101

| REPORT DOCUMENTATION PAGE | 1. REPORT NO. NSF/CEE-82102 | 2. | 3. Recipient's Accession No. PB83-204875 |
|---|---|---|---|
| 4. Title and Subtitle<br>Anchorage of Reinforcing Bars for Reversed Cyclic Loading | | | 5. Report Date<br>June 1982 |
| | | | 6. |
| 7. Author(s)<br>I.J. Lin, N.M. Hawkins | | | 8. Performing Organization Rept. No.<br>SM 82-1 |
| 9. Performing Organization Name and Address<br>University of Washington<br>Department of Civil Engineering<br>Seattle, WA 98195 | | | 10. Project/Task/Work Unit No. |
| | | | 11. Contract(C) or Grant(G) No.<br>(C) ENV7615366<br>(G) |
| 12. Sponsoring Organization Name and Address<br>Directorate for Engineering (ENG)<br>National Science Foundation<br>1800 G Street, N.W.<br>Washington, DC 20550 | | | 13. Type of Report & Period Covered |
| | | | 14. |

15. Supplementary Notes

Submitted by: Communications Program (OPRM)
National Science Foundation
Washington, DC 20550

16. Abstract (Limit: 200 words)

An analytical model is developed that predicts the load-slip characteristics of reinforcing bars anchored within exterior beam-column joints in reinforced concrete structures subject to earthquake loading. The model is developed from knowledge of fundamental mechanical characteristics for the reinforcing bar, for the interface between that bar and the surrounding concrete, and from the requirements for continuity of forces and displacements along the anchorage length for the bar. The analytical results predicted by the model are compared to experimental results for 22 specimens. Variables included in the specimens were the loading history for the bar, the yield strength for the bar, the size of the bar, the embedment length for the bar, the strength of the concrete and the use of a straight bar or a bar terminating with a standard 90 degree hook. Good agreement is obtained between the measured results and those predicted by the model for both monotonic and reversed cyclic loading.

17. Document Analysis a. Descriptors

Reinforced concrete
Structural members
Reinforcing steels
Dynamic structural analysis
Structural design

b. Identifiers/Open-Ended Terms

EQ resistant construction
Concrete steel
N.M. Hawkins, /PI

c. COSATI Field/Group

| 18. Availability Statement | 19. Security Class (This Report) | 21. No. of Pages |
|---|---|---|
| NTIS | 20. Security Class (This Page) | 22. Price |

Abstract

ANCHORAGE CHARACTERISTICS FOR REINFORCING BARS SUBJECTED TO REVERSED CYCLIC LOADING

by Ing-Jaung Lin and Neil M. Hawkins

An analytical model is developed that predicts the load-slip characteristics of reinforcing bars anchored within exterior beam-column joints in reinforced concrete structures subject to earthquake loading. The model is developed from knowledge of fundamental mechanical characteristics for the reinforcing bar, for the interface between that bar and the surrounding concrete, and from the requirements for continuity of forces and displacements along the anchorage length for the bar. The analytical results predicted by the model are compared to experimental results for 22 specimens. Variables included in the specimens were the loading history for the bar, the yield strength for the bar, the size of the bar, the embedment length for the bar, the strength of the concrete and the use of a straight bar or a bar terminating with a standard 90 degree hook. Good agreement is obtained between the measured results and those predicted by the model for both monotonic and reversed cyclic loading.

TABLE OF CONTENTS

LIST OF TABLES

## LIST OF FIGURES

Figure | Page

| Figure | | Page |
|---|---|---|

Figure | Page

| Figure | | Page |
|---|---|---|

Figure | Page

Figure | Page

| Figure | | Page |
|---|---|---|

NOTATION

$\sigma_s$ = steel stress (Ksi)

$\sigma_y$ = yield stress of steel (Ksi)

$\varepsilon_s$ = steel strain

$\varepsilon_y$ = yield strain of steel

$\varepsilon_{sh}$ = strain at the beginning of strain-hardening

$E_s$ = modulus of elasticity (Ksi)

$E_{sh}$ = slope in strain-hardening range (Ksi)

$\sigma_{sA}$ = stress coordinate of point A' in Fig. 11

$\varepsilon_{sA}$ = strain coordinate of point A' in Fig. 11

$f'_c$ = concrete strength (psi)

$\tau$ = local bond stress (Ksi)

$S$ = local slip (in.)

$\tau_{max}$ = maximum local bond stress for monotonic loading (Ksi)

$S_o$ = local slip corresponding to $\tau_{max}$ (in.)

$\tau_c$ = local bond stress which induces cone-like cracking around the bar for monotonic loading

$S_c$ = local slip corresponding to $\tau_c$ (in.)

$\Delta S$ = slip increment for the previous half cycle in the same loading direction

$A_b$ = bar cross-sectional area (in$^2$)

$\varepsilon_o$ = bar perimeter (in.)

$h$ = height of lug (in.)

$d_b$ = bar diameter (in.)

$a$ = lug spacing (in.)

$L_t$ = total embedment length for straight bar

$L_{em}$ = effective embedment length for straight bar before the formation of a wedge at the tail end

$L_{ec}$ = effective embedment length for straight bar after the formation of a wedge at the tail end

$L_a$ = length of bond stress distribution affected by unloading

$L_p$ = length for bond stress distribution before unloading

$L_b$ = length for bond stress distribution under severe reversed loading

$L_e$ = equivalent anchorage length for hooked bars under reversed cyclic loading

$L_s$ = lead-in length to the hook

$R_h$ = radius of the hook

$L_{t(ACI)}$ = development length required by ACI 318-77

$L_{s(ACI)}$ = lead-in length required by ACI 318-77

$\tau_1(x_1)$, $\tau_2(x_2)$, $\tau_3(x_3)$, $\tau_4(x_4)$ = bond stress functions

$\sigma_1(x_1)$, $\sigma_2(x_2)$, $\sigma_3(x_3)$, $\sigma_4(x_4)$ = steel stress functions

$\varepsilon_1(x_1)$, $\varepsilon_2(x_2)$, $\varepsilon_3(x_3)$, $\varepsilon_4(x_4)$ = steel strain functions

$S_1(x_1)$, $S_2(x_2)$, $S_3(x_3)$, $S_4(x_4)$ = local slip functions

## ACKNOWLEDGEMENTS

This report was prepared as a Ph.D. thesis by Dr. Ing-Jaung Lin working under the supervision of Professor Neil M. Hawkins. The experimental portions of the study were carried out in the Structural Research Laboratory of the University of Washington. The study was made possible by the support of the National Science Foundation through grant ENV 76-15366. The National Science Foundation program manager for that grant was Dr. M. P. Gauss.

Contributions made to the execution of this investigation by Professor A. S. Koyayashi, and Messrs. A. Chen, T. L. Su, Y. H. Liu and S. L. Lok are gratefully acknowledged.

## PREFACE

This report forms part of an on-going study at the University of Washington into the bond and anchorage characteristics of reinforcing bars for seismic type loadings. That investigation has been sponsored by the National Science Foundation since 1974, first under Grant GI-43443 and later under Grant ENV 76-15366.

The long-range goals of the study are two-fold. First the development of practical techniques and instrumentation permitting assessment of the degree of deterioration of the bond between reinforcement and concrete in a structure surviving an earthquake. Second, the development of design recommendations for predicting the effects of bond deterioration on the strength and stiffness of reinforced concrete structures subjected to earthquake motions.

Initially, basic data were developed on bar force slip relationships for beam bars embedded within simulated columns. A Ph.D. thesis on that work was published as a Structures and Mechanics Report of the University (P1), and two papers, one reporting the results of those tests (P2), and the other a model for prediction of the results were published in the archival press. Following some improvement in the form of the test specimen, additional tests were made in which the prime emphasis was examination of the feasibility of using holographic and acoustic emissions techniques to determine bond deterioration. The initial phase of those investigations was reported in detail in Reference P4 and published in the archival press in References P11 and P12. The significance of the bar force-slip relationships measured in those tests was evaluated in Reference P7. In a subsequent phase of that investigation, additional simulated beam-column specimens were tested (P5, P6), and additional acoustic emission data developed (P6, P7).

As a result of the foregoing investigations, it was decided that a fundamental study should be made, experimentally and analytically, of the feasibility of modeling the bond behavior of beam bars anchored within columns as the sum of the responses for three components: the reinforcing steel; the concrete locally around the bar; and the compatibility relationship for forces and displacements along the bar. Accordingly, one series of tests were made to determine the stress-strain relationships for full section reinforcing bars subject to inelastic reversed loads (P8); three series of tests were made to determine bar force-local bond strength relationships for bars bonded deep within a concrete block (P9, P10, P15, P16), and studies made of possible compatibility models. This report describes those studies and develops an analytical model that utilizes those three components to predict load-slip characteristics measured in the simulated beam-column tests.

This report is an adaptation of the Ph.D. thesis of Ing-Juang Lin. That thesis was supervised by Professor Neil M. Hawkins.

## REFERENCES


P1. Hassan, F.M., "Bond Deterioration Under Simulated Seismic Loading," Ph.D. Thesis, Seattle, WA, 1973. Also Report SM-73-2 Department of Civil Engineering, University of Washington, Seattle, WA, Mar 1973.

P2. Hassan, F.M. and Hawkins, N.M., "Anchorage of Reinforcing Bars for Seismic Forces," Reinforced Concrete in Earthquake Zones, SP-53, American Concrete Institute, Detroit, MI 1977.

P3. Hassan, F.M. and Hawkins, N.M., "Prediction of Seismic Loading Characteristics of Reinforced Bars," Reinforced Concrete in Earthquake Zones, SP-53, American Concrete Institute, Detroit, MI, 1977.

P4. Hawkins, N.M., Kobayashi, A.S. and Fourney, M.E., "Reversed Cyclic Loading Bond Deterioration Tests," Report SM-75-5, Department of Civil Engineering, University of Washington, Seattle, WA, Nov. 1975.

P5. Hawkins, N.M., Kobayashi, A.S., Chan, Y-L.A. and Lin, I.J., "Bond Deterioration Under Seismic Loading," SM-79-1, Department of Civil Engineering, University of Washington, Seattle, WA, May 1979.

P6. Aminian, K., "Effect of Cyclic Loading on Bond Deterioration of Na. 6 Reinforcing Bars," MSCE Thesis, University of Washington, Seattle, WA, 1977.

P7. Hawkins, N.M. and Lin, I.J., "Bond Deterioration of Reinforcing Bars for Seismic Loadings," Third Canadian Conference on Earthquake Engineering, Proceedings, Vol. 2, Montreal, 1979.

P8. Su, T.L., "Behavior of Reinforcing Bars Under Inelastic Reversed Loadings," MSCE Thesis, University of Washington, Seattle, WA, 1979.

P9. Liu, Y.H., "Local Bond Strength of Concrete Under Cyclic Loading," MSCE Report, University of Washington, Seattle, WA, 1978.

P10. Jeang, F.L. "Local Bond Strength of Concrete Under Reversed Cyclic Loadings," MSCE Thesis, University of Washington, Seattle, WA, 1980.

P11. Hawkins, N.M., Kobayashi, A.S. and Fourney, M.E., "Use of Acoustic Emission and Holographic Techniques to Detect Debonding in Cyclically-loaded Concrete Structures," Proceedings of ASCE-EMD Specialty Conference, Los Angeles, March, 1976.

P12. Hawkins, N.M., Kobayashi, A.S. and Fourney, M.E., "Use of Holographic and Acoustic Emission Techniques to Detect Structural Damage in Concrete Members," Experimental Methods in Concrete Structures for Practitioners, American Concrete Institute, Detroit, MI, 1979.

P13. Hawkins, N.M., Kobayashi, A.S., "A Feasibility Study of Detecting Reinforcing Bar Debonding by Acoustic Emission Technique," Experimental Mechanics, Sept. 1980, pp. 301-308.

P14. Lin, I.J. "Anchorage Characteristics of Reinforcing Bars Subjected to Reversed Cyclic Loadings," Ph.D. Thesis, University of Washington, Seattle, WA, March, 1981. Also Report SM 82-1 Department of Civil Engineering, University of Washington, Seattle, WA, June 1982.

P15. Liu, J.P. "Influence of Bar Deformation and Concrete Cover on Local Bond Strength," MSCE Thesis, University of Washington, June 1982.

P16. Hawkins, N.M., Lin, I.J. and Jeang, F.L., "Local Bond Strength of Concrete for Cyclic Reversed Loadings," International Conference on Bond, Paisley Institute of Technology, Paisley, Scotland, June, 1982.

# CHAPTER 1

# INTRODUCTION

## 1.1 General

When earthquake occurs, structures are subjected to reversed and cyclic lateral loadings. The overall response of a structure in an earthquake depends primarily on the dynamic characteristics of the structure. The dynamic characteristics of the structure vary with its strength, stiffness and damping. Experience (1, 2, 3) has shown that the response of structures during earthquake is often governed by the connections between beams and columns since a large portion of the ductility and energy absorption of the structure must be supplied by those connections or at sections immediately adjacent to those connections.

For reinforced concrete to perform adequately as a structural material, stresses must be transferred between the reinforcement and the concrete. It is desirable that this "bonding" be achieved with only a limited amount of slip between the reinforcement and the concrete. Otherwise progressive degeneration in stiffness, cumulative damage and eventually pull-out of the bar are possible under seismic loading.

At many sections there is a simultaneous occurrence of maximum shear, bending and bond effects. It is, therefore, frequently difficult to obtain aduquate anchorage for the reinforcing bars within the joint. In order to develop the full strengeth of the bar at the face of the joint, the bar must be bent or mechanical devices used to ensure the required anchorage length.

Traditional reinforced concrete design (4) separates shear, moment and bond resistance for calculation purposes, since for monotonic load-



ing to failure an unfavorable interaction of these effects is virtually unknown. However, the inadequate performance of many different types of connections during earthquakes and in simulated laboratory tests suggests that such simplifications are not appropriate for reversed cyclic loading. Experiments (5, 6) have shown that as the effectiveness of the bond decreases, the chance of a shear failure increases. It is also known that the bond between a reinforcing bar and concrete deteriorates more rapidly (7) under reversed cyclic loading than under monotonic loading. Shear failures in joints and stiffness degeneration of joints are prime causes of poor earthquake performance. In concrete structures, in earthquake regions, not only must bond transfer provide anchorage for the embedded reinforcement under static loads, it must also maintain that anchorage when the structure is subjected to the earthquake loads creating stress reversals and high shear stress levels that both deteriorate bond transfer capability.

## 1.2 Previous Experimental Research

Research has been conducted previously into both the effects on bond transfer of cyclic loading, and of repeated reversed cyclic loading of the magnitude likely during a severe earthquake.

In 1958, Nordby (8) reviewed the available information for repeated loading and reported that results were extremely erratic. Since then, Bresler and Bertero (9) have reported tests on push-out specimens subjected to low frequency cyclic loading producing bar stresses in the service load range and in the tensile range only. They observed that bond effectiveness was dependent on loading history. Previous peaks in applied stress reduced effectiveness for lower stress levels in subsequent cycles. Further, the degree of reduction increased as the previous peak stress increased. Brown and Jirsa (10) have conducted tests on concrete cantilever beams subjected to a reversed cyclic overload in which they determined the effects of load history on the strength, ductility and mode of failure of the beams. They found the response to be markedly non-linear, and they attributed this behavior to shear deformations and to slip of the longitudinal reinforcement where it was.

Perry and Jundi (11) subjected eccentric pullout specimens to repeated unidirectional static and dynamic loading to determine their effect on bond transfer. The No. 6 bars of their specimens were internally instrumented with electrical resistance strain gages to provide information on the degree of degradation resulting from the loading procedure. They concluded that for loading in excess of 80% of the ultimate capacity of the specimen, the peak bond transfer stress shifts from the loaded end to the unloaded end as the number of cycles increases; and this bond transfer distribution stabilized after a few hundred cycles. They also found that failure of their specimens would not occur for repeated loadings, unless the applied load level was at least 80% of the ultimate load or greater.

Japanese observations on internal cracking adjacent to the lugs of a bar suggest that a tension-compression loading cycle could cause a greater reduction in bond effectiveness than a tension-tension loading cycle. Goto (12) has observed that, as a bar is stressed in tension, internal cracks develop as indicated by the solid lines in Fig. 1. If loading reversals cause high compressive stresses in the bar, a second



pattern of crossing cracks can be expected as indicated by the broken lines. These cracks may join up some distance from the bar surface and result in a zone surrounding the bar in which the concrete crumbles permitting considerable bond deterioration. This concept implies that the rate of bond deterioration will vary with the geometry of the lugs on the bar, the stress state in the concrete surrounding the bar, the reinforcement surrounding the bar and the loading history. Okamura and Takahashi (13) have observed that the bond strength of lightweight concretes are only 80% of those of normal weight concretes with comparable tensile splitting and compressive strengths. They attribute this difference to the enhanced ability of stiff normal weight aggregate particles to spread the lugs over a wider area of concrete.

Research conducted by Ismail (14) examined the effects of repeated tensile loading on the bond transfer mechanism of pullout specimens for both the elastic and post yield regions. He reported that, under peak stress levels less than the yield stress, the magnitude of the peak stress was the major factor affecting the bond transfer mechanism. He also confirmed Bresler and Bertero's conclusion that a high stress level considerably influenced subsequent behavior at lower stress levels. His study indicated that the peak stress level was of more importance to the specimen's behavior than the number of cycles of loading below the yield stress of the bar. Conversely, for loading above the yield stress, the number of cycles became more important for determining the specimen's behavior. He also found that repeated, reversed loading produced greater bond transfer deterioration than repeated loading alone.

Ismail (15) continued his research into the effects of cyclic loading on bond transfer by investigating the behavior of simulated beam-column connections. Those specimens were subjected to loads, causing both elastic and post-yield stresses in the bars. The elastic load histories were repeated tensile loadings in which the peak load was applied for a various number of cycles. The post-yield load histories consisted of repeated tensile loads of constant magnitude and repeated, reversible loads of constant magnitude. He found that, for both loading cases, bond deterioration occurred over a significant distance between the beam-column interface and the anchored end of the reinforcing bar. He also determined that the amount of bond deterioration and yield penetration depended on the relative stiffness of the member and the joint and that the magnitude of the load was of more importance than the number of cycles in determining the amount of bond deterioration.

In a series of investigations, conducted by Ismail and Jirsa (16, 17), on both pullout and simulated beam-column connections similar in concept to the specimens tested by Ismail, the influence of various load histories on bond transfer was studied in greater detail. The results of these investigations confirmed the findings of the earlier studies. However, it was concluded that extensive research would still be necessary before a quantitative understanding of the effects of large cyclic overloads on bond transfer could be achieved.

A significant deterioration of bond resistance with cyclic loading has also been observed in conjunction with laboratory tests on building components. During reversed cyclic loading tests on shear walls at the University of California at Berkeley and at the Portland Cement Association (18), considerable bond slip has occurred for the vertical wall



reinforcement anchored within the foundation mat. For both monotonic and reversed cyclic loading tests on flat plate to column connections at the University of Washington (19, 20), bond slip of the reinforcing bars anchored within the column has been found to be one of the main factors controlling the stiffness of the connection.

There have been other investigations conducted recently at the University of Washington and concerned with bond deterioration under high intensity cyclic loading. Hassan and Hawkins (21) have reported tests on 13 specimens simulating exterior beam-column connections. Variables were the type of bar (plain and two types of deformed bar), the presence or absence of an 180 degree hook on the end of the bar and the load history. Grade 40 No. 10 bars were used in all specimens and the concrete strength was about 4,000 psi. Sufficient additional bonded hoop and column reinforcement were added to the specimens to prevent a shear failure and not affect the bond deterioration mechanism. From their tests they concluded that high intensity reversed cyclic loading induces a progressive bond deterioration causing subsequent loss in stiffness for a reinforced concrete beam-column connection in which such bars are anchored. They quantitized the importance of the character of the loading history for their tests, surface goemetry for the bar and the lead-in length to the hook. They showed how their results could provide a useful practical tool to assess the likely extent of damage that had occurred to a beam-column joint in a building surviving an earthquake.

In subsequent investigations conducted by Hawkins et al. (22, 23), the previous work by Hassan and Hawkins was extended to No. 10 and

No. 8 Grade 60 bars and the effect of 90 degree hooks examined. A study was also made of the feasibility of using acoustic emission, holographic interferometry and paint injection techniques to detect the progress of bond degradation. It was concluded that the load-displacement relationships, the strain data, the acoustic emission data, the holographic interferometry data and the paint injection data all clearly indicated a fundamental difference in the behavior and bonding mechanism for bent and straight bars. Large movements of the hook occurred once the yielding penetrated to the end of the lead-in zone for the hook. The 90 degree hook always provided additional strengths for tensile loadings characterized by increasing displacements. However, for compressive loadings the hook became less effective as the magnitude of the applied compressive displacement increased.

Seven cyclic pull-out tests on No. 6 Grade 60 bars were carried out by Aminian (24). The specimens, chosen to simulate an exterior beam-column connection, were 6 in. thick, 16 in. deep and 66 in. high. The test bars were placed in the center of the 6 in. dimension at a distance 25.5 in. from the top. The effect of the loading history on the strength, stiffness and energy absorption of the simulated beam-column connections was studied. The loading histories included monotonic tension loading and repeated tension and compression loading of constant and varying magnitudes. Aminian reported that cyclic loading induced bond deterioration and subsequent loss in stiffness and energy absorption for beam bars anchored within beam-column connections. The character of the loading history affected the rate of bond deterioration, Stiffness and energy absorption. By comparing his results with those



for similar specimens containing No. 10 bars (22), Aminian concluded that the diameter of the bar directly affected the energy absorption of the bonding mechanism and that the current ACI Code 318-77 anchorage length provisions were non-conservative for bars reversed cyclically loaded into their yield range.

More recently additional experimental work on bond deterioration has been carried out at the University of California at Berkeley (25, 26). Tests have been made on concrete blocks simulating conditions existing at a typical interior beam-column joint. During a severe overload due to lateral forces a crack forms in the beam adjacent to the column face. With loading reversals, another crack forms through the adjoining beam on the opposite side of the column. If the applied lateral forces are sufficiently intense, cracks form through the whole depth of the beams on both sides of a column. Moreover, at large overloads due to inelastic straining of steel such cracks never close and the continuous longitudinal bars of the beams are simultaneously pulled from one side and pushed from the other. The experimental set-up was designed to simulate this condition for a single bar. A series of bond tests with No. 6, No. 8 and No. 10 bars embedded in various width concrete blocks were made. In the experiments, both normal weight and lightweight concretes of different strengths were used and the bars were subjected either to monotonic or cyclic loadings to failure. Some tests were also made on epoxy-repaired specimens to study the possibility of using epoxy for restoring bond. Several loading histories for different specimens were investigated. These loading histories included a monotonic pull from one side, a monotonic simultaneous pull, T, from one side and push, C, from the other with T = C, and several types of cyclic experiments with T = C. In this study most of the bars were instrumented with strain gages placed in grooves machined into the bars. Those gages allowed determination of the development of strains during the progress of the tests. They found that the strains caused by a pushing force were very different to those caused by a pulling force. pushing forces were very rapidly transferred to the concrete and the development length for the bar for a given stress was much less than for a pulling force. In cyclic loading tests it was observed that all of the cyclic curves were below the monotonic one and that considerable displacements of the bars occurred even at stress levels below the working stress level. For both normal weight and lightweight concretes, it was found that the concrete strength was a very important parameter affecting the bond strength. The higher the concrete strength, the higher was the bond strength. On the basis of the test data, it was concluded that lightweight concretes consistently developed lower maximum steel strengths and bond strengths than normal weight concretes of comparable strengths. For epoxy-repaired specimens, although two different epoxies and methods of injection were employed, both were found too difficult to make. These two methods of epoxy injection could restore sufficient bond strength for sustained working stresses, but neither method was able to restore the bar's full capacity in bond for inelastic loadings. They concluded that epoxy had difficulty in penetrating through the powered concrete surrounding a bar that had slipped.

The following major conclusions can be drawn from previous experimental studies of bond deterioration in reinforced concrete structures.



(1) The response of reinforced concrete frames during earthquakes is often governed by the characteristics of the beam-column connections. The failures that have occurred have been due mainly to failures of beam-column connections. Deterioration of the bond between concrete and reinforcing bars has been one of the major causes for failure of beam-column connections.

(2) Reversed cyclic loading induces a progressive deterioration of the bond between reinforcing bars and concrete so that there is a subsequent loss in stiffness for reinforced concrete connections.

(3) The characteristics of the loading history have a marked effect on the rate of bond deterioration and the mode of failure. For monotonic loading the rate of degradation is less than that for reversed cyclic loading.

(4) For reversed cyclic loading at least two modes of failure are possible:

(a) failure by attainment of the same ultimate load and deformation capacities as those developed by the same joint for monotonic loading, and

(b) failure due to bond deterioration at an ultimate load and deformation considerably less than those for monotonic loading. Failure occurs in the first mode when the maximum displacement in the compression cycle is less than half that for the tension cycle or the maximum displacements for both half cycles are equal with values decreasing with cycling except for the final half cycle to failure. The type of loading affects the stiffness of the bond joint but not the ultimate capacity. Failure in the second mode dominates for cases where the maximum displacement in the tension and compression cycles are approximately equal, and values remain constant or increase with cycling.

(5) The bar surface geometry plays a significant role in the rate of bond deterioration. The greater the lug spacing to nominal diameter ratio the greater is the rate of bond deterioration. Bars with different surface geometries can have similar load-slip characteristics for monotonic loading and significantly different load-slip characteristics for reversed cyclic loading.

(6) For reversed cyclic loading the bond characteristics of a reinforcing bar with V-type deformations are better than those for a bar of the same size with bamboo-type deformations.

(7) When hooked bars are subjected to severe reversed cyclic loading, bond resistance and energy absorption are provided primarily by the "lead-in" length to the hook. Because a hook shortens the "lead-in" length, it can have an adverse effect on energy absorption. The response for severe reversed cyclic loading between equal tension and compression displacements for a bond joint with an 180 degree hooked bar or a 90 degree hooked bar is poorer than that for a bond joint with a straight bar. A 90 degree hook has, however, two advantages over an 180 degree hook: (a) the connection with a 90 degree hook maintains good characteristics considerably longer with tensile loadings than with compressive loadings. If the reversed cyclic loading results in a maximum compressive displacement considerably less than the maximum tensile displacement, the bar



with a 90 degree hook can show characteristics as good or better than those of a straight bar, and (b) for tensile loadings to displacements beyond the displacement for the peak capacity, there is some regain of strength with increasing tensile displacements for a 90 degree hook. The same is not true for a 180 degree hook.

(8) The appearance of the test specimens with hooks after failure suggests that, in buildings surviving an earthquake, loss of cover from behind the hook should be interpreted as a warning that the anchorage for such bars has been largely destroyed.

(9) The grade of the loaded reinforcing bar has less effect on bond deterioration than the general form of its stress-strain characteristics. The slope of the load-slip curve after yielding depends on the length of the yield plateau in the bar's stress-strain curve and the bar's strain hardening modulus. For bars with similar strain hardening moduli the slope of the post-yield load-slip curve decreases as the length of the yield plateau increases and for bars with similar yield plateau lengths the slope of the post-yield load-slip curve increases as the strain hardening modulus increases. When a bar is first stressed inelastically the yielding length is small and the initial slope of the post-yield load-slip curve depends primarily on the strain hardening modulus. The bond stress that can be developed with a yielding bar is considerably less than that with an elastic bar. Therefore, for increasing loads beyond yielding, the length of bar that is yielding increases rapidly and the length of the yield plateau becomes increasingly important in determining the slope of the load-slip curve.

(10) The amount of hoop reinforcement in a connection has a significant influence on the load-slip characteristics for bars anchored within that connection.

(11) For bond joints of the same geometry subjected to the same load history the slip for maximum load is approximately inversely proportional to the yield strength of the bar and directly proportional to the concrete compresseve strength.

(12) The diameter of the bar directly affects the energy absorption of the bonding mechanism.

(13) The formulas recommended in ACI 318-77 for calculating the development length of reinforcing bars are slightly nonconservative for bars severely reversed cyclically loaded into the inelastic range.

## 1.3 Previous Analytical Research

Serval attempts have been made to develop analytical models to predict the force-slip relationships measured in tests on simulated beam-column connections.

Hassan (7) developed two models for the prediction of his results. One model was for a bar subjected to reversed cyclic loading and the other for a bar subjected to monotonically increasing or unidirectional cyclic loadings. Hassan's model predicts well his test results which were all for Grade 40 No. 10 bars. However, as shown in this section, there are several shortcomings to his models that limit their reality, applicability and usefulness. Shown in Table 1 are the properties of the test specimens used for the comparisons made in this section.



### (a) Hassan's Reversed Cyclic Loading Model

For a bar subjected to reversed cyclic loading the bond stress distribution assumed by Hassan for his model and the constitutive relationships assumed for the reinforcement are shown in Fig. 1. The transfer length is divided into three rigions. In region 1, adjacent to the tail end of the bar, the steel strain is less than the yield strain and cracking has not developed around the bar. The bond stress is assumed to build up from zero at the end of the bar to a maximum at the junction between region 1 and region 2. In region 2 internal cracking has developed around the bar as a result of the lugs digging into the concrete. As shown in Fig. 1, the $i^{th}$ half cycle of loading is assumed to have extended the cracking from a distance $C_{i-1}$ from the loaded end of the bar to a distance $C_i$ from the loaded end. The steel in this region responds according to its stress-strain relationship for virgin loading and the bond stress has a constant value $u^*$. In region 3, compression loading in the $(i - 1)^{th}$ half cycle has generated reversed cracking to a distance $C_{i-1}$ from the loaded end of the bar. The bar responds according to its stress-strain relationshop for reversed cyclic loading and the reversed cracking causes a bond deterioration according to a power law from the value of $u^*$ at the junction with region 2 to zero at the loaded end of the bar. In region 4 the steel follows the same law as that in region 3. The steel stress variation in region 1 was derived based on the results of finite element plane stress analysis and the steel stress variations in other regions were derived from equilibrium in the axial direction. Therefore, the displacement at the loaded end of the bar could be derived from the steel stresses distributed along the overall length of the bar.

The shortcomings of the model are:

(1) It is necessary to know the length of the bond joint to apply the model. Thus the model cannot be readily used for design, nor can it be readily applied to a bar continuous through a joint or a bar with an extremely long anchorage length.

(2) As apparent from Fig. 2, the length of the bond joint directly affects predictions of the load-displacement relationship. Fig. 2 shows predicted relationships for a 3,500 psi concrete, a No. 10 Grade 40 bar, and a joint length of 24 in. (curve), 36 and 48 in. respectively. The longer the length of the bond joint the greater is the amount of displacement predicted for a given load. That result does not seem realistic.

(3) The model assumes that there is a bond stress acting at every point along the length of the bar no matter how small the external loading or how long the bar. That assumption is not realistic and not in agreement with steel strains measured along the length of the bar.

(4) In the model, the maximum bond stress, $u^*$, between the reinforcing bar and the concrete is derived as a function of the external loading. It is commonly recognized that the maximum bond stress is sensitive to many factors such as confinement, concrete strength, surface geometry for the reinforcing bar, ect. It is also reasonable to expect the some cut-off exists on the maximum bond stress that can be developed.

(5) The model implies that the length of the crack along the reinforcing bar governs the response of the bond joint. Other factors such as the bar size, the type of deformation, the stress-strain characteristics for the bar, the reinforcement in the joint and the concrete strength may also significantly affect the propagation of the crack along the bar. As currently formulated Hassan's model does not include the effects of those factors. Comparisons of the predictions of Hassan's model and the results for specimens having properties significantly different from those of the specimens for which Hassan's model was developed are shown in Figs. 3 through 5. The predicted responses are not in good agreement with the test results for bond joints containing a No. 10 Grade 60 bar, S104, or a No. 6 Grade 60 bar, S61, or for a concrete strength, $f_c'$ of 2640 psi, S107, significantly different from the 3,500 psi strength used in Hassan's specimens.



(6) Hassan's results indicated that cracking propagated progressively along the bar once the loading was increased beyond a certain range. The maximum increase in crack length for a particular half cycle must be achieved when the loading is at its peak value for that particular half cycle. However, Hassan's model assumed that the crack increment for the whole half cycle, which was predetermined, existed once the external loading was applied to the bar. Further, the length of each region in his model (Fig. 1) remained constant throughout a given half cycle.

(b) <u>Hassan's Monotonic Loading Model</u>

The bond stress distribution assumed for that model is shown in Fig. 6. One fundamental difference in this model, as compared to the reversed cyclic loading model, is that the crack increments are generated as the loading increases so that the crack length, C, from the loaded end of the bar is changing continuously with the axial force, $F_o$.

Besides the first five shortcomings mentioned already for the reversed cyclic loading model, there is an additional shortcoming for the monotonic model. The model assumes that the bond stress in the cracked region is constant and equal to $u^*$. However, it is probably more realistic to assume a transfer length divided into three regions once the cracked length, C, exceeds a certain distance and to assume that the bond stress distribution for the third region near the loaded end of the bar follows a power law.

It is obviously desirable to have available a more realistic and more widely applicable model than Hassan's model. Such a model would probably need to utilize a limiting maximum value for the peak bond stress, permit variable values for the bond stress along the bar as a function of displacements and variable lengths for the uncracked portion of the bond joint that are a function of the loading history.

Recently Hawkins et al. (27, 28) developed a simplified mathematical model, as shown in Fig. 7, to determine the values for bond-slip effects for slab-to-column connections transferring reversing moments. The curve OABC defines the response for monotonic tensile loading and OB'C' the response for monotonic compressive loading. The stiffness for OB, $K_s$, and that for BC, $K_{sh}$, are calculated from the following equations:

$$K_s = (1{,}250\ d_b^2 + 1{,}900)\left(\sqrt{\frac{f'_c}{3200}}\right)\ \text{(Kips/in.)} \qquad \text{.........(1-1)}$$



$$K_{sh} = \frac{E_{sh}}{E_s} K_s \qquad \text{.........(1-2)}$$

Where:

$d_b$ = bar diameter (in.)

$f'_c$ = concrete strength (psi)

$E_s$ = modulus of elasticity

$E_{sh}$ = slope in strain-hardening range

Equation (1-1) is applicable for $d_b$ values ranging from 0.5 through 2.25 inches. Rules for construction of the model are as follows:

Condition 1 - The yield load $P_y$ has not been exceeded. The bar force is $P_1$. Unloading follows a straight line from A towards E. The unloading stiffness, $K_u$, is twice that given by Equation (1-1). Once the direction of loading reverses, the stiffness reverts to $K_s$. When unloading commences at A', the stiffness again changes to $K_u$.

Condition 2 - The yield load, $P_y$, has been exceeded for tensil loading. The bar force is $P_2$ and the slip $S_2$. The capacity decreases with no change in slip until the initial yield load is reached. The unloading stiffness then becomes $K_u$ until the load drops to zero. For compressive loadings, the response follows a straight line directed towards the load and slip for yielding in compression B'. When unloading commences at the slip, $S_2'$, the stiffness is $K_u$ until the load drops to zero. For tensile loadings, the response then follows a straight line directed towards the load and slip for yielding in tension.

As reported in Reference 28, the responses predicted by the simplified mathematical model are in good agreement with test results. In Reference 27 it is shown the simplified mathematical model can be easily utilized to determine reasonable values for bond-slip effects for slab-to-column connections transferring reversing moments.

## 1.4 Object and Scope

The objective of this study is to demonstrate that the load-slip characteristics of reinforcing bars subject to inelastic reversed cyclic loadings can be determined directly from knowledge of the fundamental mechanical characteristics for the reinforcing bar and its interface with the surrounding concrete. This study is concerned with the development of an analytical model for predicting the load-slip characteristics of bars anchored within beam-column joints in reinforced concrete structures subject to earthquake loadings.

A model is developed using three basic building blocks:

(1) the mechanical characteristics for the reinforcing steel,

(2) the local bond stress properties for bars anchored in concrete,

and (3) constitutive relationships that effectively require continuity of forces and displacements along the length of the anchored bar.

In the general model, necessary to predict cyclic loading behavior, the anchored length is divided into a number of discrete elements and the stress-strain relationship for each element tracked. The approach is necessary because under inelastic cyclic loading the stress in a loaded bar can change from compression to tension or vice versa within the stressed length of the bar. For monotonic loading a simpler model is possible because the basic mechanical properties for the steel and concrete, and the displacements along the length of the bar can be represented by continuous functions.

As part of this investigation tests were made on 22 specimens



simulating exterior beam-column connections and for which load-slip relationships were determined for a beam bar anchored within the connection. The beam-column connection test results were described in References 22, 23 and 24. The parameters studied in those tests included load history, concrete strength, bar size, bar grade, and the effect of a go degree hook at the end of the bar. The properties of those 22 connection specimens are summarized in Table 2.

The monotonic and reversed cyclic stress-strain characteristics for one typical size of reinforcing steel used in those specimens were studied in an investigation reported in Reference 29. Two analytical models that could predict those results were developed in Reference 29 and the extension of one of those models to prediction of the stress-strain characteristics of the beam bars is discussed in Chapter 2.

Local bond stress-slip characteristics for the bar sizes and range of concrete strengths used in the beam-column specimens were studied in investigations reported in References 30 and 31. An analytical model that can predict the results reported in Reference 30 is developed in Chapter 3.

In Chapter 4 an analytical model is developed for predictions of the force-displacement relationships for an anchored bar subjected to monotonic or cyclic loading. That model integrates the analytical models developed in Chapters 2 and 3 for the stress-strain characteristics for the reinforcing steel and the local bond stress-slip relationship for the steel-concrete interface. The experimental results for the 22 beam-column specimens are compared with the results predicted by the analytical model. The FORTRAN programs that constitute the analytical force-displacement model are included as Appendices A and B.

# CHAPTER 2

# CONSTITUTIVE RELATIONSHIPS FOR REINFORCING STEEL

## 2.1 Introduction

If a structure is to absorb and ultimately dissipate large amounts of energy during an earthquake the reinforcing steel at selected maximum moment locations must yield. Generally, in a ductile frame those locations are at the ends of the beams adjacent to the columns. Since the beam steel passing into the column is loaded inelastically, accurate information is needed on the cyclic stress-strain characteristics for those bars if their force-slip relationships are to be accurately predicted.

The relatively simple stress-strain characteristics of steels for monotonic loading are abundantly documented. For example, it is widely recognized that a low strength steel, such as a Grade 40 steel, will generally have a longer plastic plateau and show a greater ultimate to yield strength ratio than a higher strength steel, such as a Grade 60 steel. By contrast, there is only a limited amount of information available on cyclic stress-strain relationships for steel and the factors affecting those relationships are not widely understood.

The increased interest in earthquake engineering has resulted in the cyclic stress-strain relationships for steels being the subject of several investigations in recent years. It has generally been found that the cyclic behavior of such steels is best represented by a Ramberg-Osgood equation. Popov (32), for example, developed such a model, applying the Ramberg-Osgood equation and a set of rules, to predict the measured stress-strain relationships for conventional No. 5 and No. 6 Grade

60 reinforcing steels subjected to repeated and reversed cyclic loadings simulating those likely under seismic conditions. The Ramberg-Osgood equation can describe both the Bauschinger effect of strain-softening under reversed loadings as well as the general cyclic strain-hardening behavior. Popov concluded that with his model the ordinary stress-strain curve for monotonic loading was sufficient to define the parameters needed to describe the properties of the same steel for cyclic loading. Su (29) conducted recently a series of tests on No. 8 Grade 60 bars at the University of Washington. He found that the accuracy of the Ramberg-Osgood expression depended strongly on the value of the parameters $\alpha$, $\beta$ and n, used to describe the non-linear term in that expression and that the values in Popov's model had to be modified to fit his test results.

For this thesis the strain-hardening range of the monotonic stress-strain relationship for the reinforcing bars was linearized and Su's model used to predict the stress-strain characteristics of bars for inelastic reversed cyclic loadings. Su's parameters rather than those of Popov's were used because the properties of the No. 8 full section bars tested by Su are likely to be more indicative of the properties of the bars used in the beam-column specimens than the properties of the No. 5 and No. 6 reduced section bars tested by Popov.

## 2.2 Monotonic Model

Linear constitutive equations that predict reasonably well the stress-strain properties of steel for monotonic loading are as follow:

$$\sigma_s = E_s \varepsilon_s \qquad \text{.........(2-1)}$$

$$\sigma_s = \sigma_y \qquad \text{.........(2-2)}$$



$$\sigma_s = \sigma_y + E_{sh}(\varepsilon_s - \varepsilon_{sh}) \qquad \text{.........(2-3)}$$

where:

$E_s$ = modulus of elasticity

$E_{sh}$ = slope in strain-hardening range

$\sigma_y$ = stress at first yield

and $\varepsilon_{sh}$ = strain at beginning of strain-hardening

For the test bars, values of the above constants were determined from the results for simple tension tests on the steels used in the beam-column specimens. Those constants are listed in Table 3.

Comparisons of the measured and idealized monotonic stress-strain relationships for the reinforcing bars used in this study are shown in Figs. 8 through 10. It is apparent that little would be gained by using more complex constitutive relationships than Eqs. (2-1) through (2-3) to represent the test results.

## 2.3 Cyclic Model

If a bar is stressed into its strain-hardening range, the stress-strain relationship for reversed loading can be constructed as illustrated in Fig. 11. The response follows that for monotonic loading OCA until unloading begins. Then the following rules apply:

(1) As the magnitude of stress is reduced from the post-yield stress level A to the initial yield stress level A', the stress-strain relationship is assumed to be linear-elastic.

(2) Once the level is reduced below the initial yield level A', but not below the stress level B, the stress-strain relationship is given by the Ramberg-Osgood equation:

$$\bar{\varepsilon}_s = \beta(\bar{\sigma}_s - \alpha|\bar{\sigma}_s|^n) \qquad \text{.........(2-4)}$$

where:

$$\bar{\varepsilon}_s = \frac{\varepsilon_s - \varepsilon_{sA}}{2\varepsilon_y}$$

$$\bar{\sigma}_s = \frac{\sigma_s - \sigma_{sA}}{2\sigma_y}$$

$$\alpha = 3.1\left(\frac{\varepsilon_{pmax}}{0.016}\right) < 3.1$$

$$\beta = (1.0 + 0.8\bar{\varepsilon}_p - 0.3\bar{\varepsilon}_p^3) < 1.5$$

$$\varepsilon_{pmax} = \left|\varepsilon_{sA} - \frac{\sigma_{sA}}{E_s}\right|$$

$$\bar{\varepsilon}_p = \frac{\varepsilon_{pmax}}{70 \times 10^{-3}}$$

$n = 6$

$\sigma_{sA}$ and $\varepsilon_{sA}$ = stress and strain values of point A', respectively.

$\sigma_y$ and $\varepsilon_y$ = stress and strain values at first yield, respectively.

$\sigma_s$ and $\varepsilon_s$ = stress and strain values of a point on the reversal curve, respectively.

The point B is the point at which the magnitude of steel stress reaches the initial yield stress level during reversed loading, or where the magnitude of strain, $\Delta\varepsilon_s$, that occurs during reversed loading reaches the value of 0.016.

(3) If loading continues beyond point B, the stress-strain relationship is assumed to be given by the rotated and translated monotonic



strain-hardening curve, CA.

(4) If Loading reverses a second time at say point E, the stress-strain relationship of the ascending reversal curve is assumed to be given by the previous descending curve, provided there is no change in the value of $\varepsilon_{pmax}$ from that for the last reversal of loading. The ascending reversal curve is established by rotating the curve AE through 180 degrees and shifting it so that point A coincides with point E. For loading beyond point A, the stress-strain relationship is assumed to be given by the monotonic strain-hardening curve. The reversal at G is based on the parameter $\varepsilon_{pmax}$ corresponding to that point.

Detailed comparisons of the cyclic stress-strain characteristics of reinforcing bars measured by Su and the characteristics predicted by the foregoing expressions are presented in Reference 29. Comparisons for three specimens R-03, R-04 and R-06 subject to loading histories similar to those applied to the beam bars of the beam-column specimens are presented in Appendix C.

## 2.4 Discussion

The behavior of reinforcing bars under reversed cyclic loading is quite different to that for reinforcing bars under monotonic loading. That difference is caused by what is known as the Bauschinger effect. That effect results in a changing character for the stress-strain curve with loading reversals and a stress-strain behavior that becomes strongly influenced by the prior strain history. In general, cyclic stress-strain test results show that for reinforcing bars Bauschinger effects become more pronounced as the magnitude of the plastic strain increases. To use the Ramberg-Osgood equation to predict the behavior of the reinforcing steels under cyclic loading, the stress-strain curve is divided into three sections as detailed previously and three different equations or rules used to predict each section of the curve. Therefore, the first and second derivatives of the curve are not continuous from one section of the curve to the next. There are three parameters, $\alpha$, $\beta$ and n, involved in the Ramberg-Osgood equation. The curvature of the stress-strain curve is dependent on the parameter n, which is taken as constant and equal to 6 in this study. It is believed that the differences in the values of $\alpha$, $\beta$ and n for the specimens reported in Reference 29 and in Reference 32 are related to differences in the monotonic stress-strain characteristics for the bars used in those two investigations. The No. 5 and No. 6 reduced section bars reported in Reference 32 had more marked and considerably longer yield plateaus than the No. 8 full section bars reported in Reference 29.

The simple constitutive relationships proposed in this Chapter for monotonic loading permit the development of a simple force-displacement model for monotonic loading as detailed in Chapter 4 because the steel stress corresponding to strain greater than $\varepsilon_{sh}$ is unique and can easily be determined. As reported in Reference 29, the constants of the Ramberg-Osgood equation can always be adjusted so that the resulting model predicts accurately the stress-strain characteristics of reinforcing bars for reversed cyclic loadings and permits ready determination of the steel strain corresponding to a given stress. The latter characteristic is very important for developing the cyclic force-displacement model described in Chapter 4. Several models other than those based on Ramberg-



Osgood equations have been proposed (29) but in all those models the determination of the steel strain corresponding to a given steel stress when a bar is inelastically and reversed cyclically loaded is more difficult than with a model based on the Ramberg-Osgood equation. The prime disadvantage of the two models proposed in this Chapter is that an increase in strain always results in an increase in stress and the desirable limiting conditions corresponding to the ultimate strength of the bar, namely, $df_s/d\varepsilon_s = 0$ and $f_s = f_{su}$ when $\varepsilon_s = \varepsilon_{su}$, cannot be satisfied. Thus, the two models proposed here are only applicable when $\varepsilon_s$ is considerably smaller than $\varepsilon_{su}$. It is suggested that in accordance with the data presented in Figs. 8, 9 and 10, use of these models should be discontinued when $\varepsilon_s$ become greater than about 0.05.

# CHAPTER 3

## LOCAL BOND STRESS-SLIP RELATIONSHIPS FOR REINFORCING BARS

### 3.1 Introduction

When subjected to severe earthquake or wind loading, the response of reinforced concrete structures is largely influenced by the behavior of the beam-column connections. It is well known that the bond deterioration between steel and concrete is a significant factor affecting the behavior of beam-column connections under load reversals. Therefore, to predict the behavior of reinforced concrete structures subjected to earthquakes, information is needed on local bond stress-slip characteristics for reinforcing bars.

Morita and Kaku (33, 34) studied the effects of load history on the local bond stress-slip relationships for pull-out and push-out specimens containing reinforcing bars bonded to the concrete over a short length. They reported that the local bond deterioration depends on the magnitude of the previous maximum local slip, and that the larger the previous slip the greater was the reduction in bond stress at lower slip levels in subsequent loading cycles. Based on their test results they proposed a highly simplified law for construction of the envelope curve, the unloading curves and the reversed loading curves for local bond stress-slip relationships for repeated and reversed cyclic loading. The envelope curve was approximated by a bi-linear relationship and defined as the local bond stress-slip curve for monotonic loading to failure. That local bond stress-slip law was then utilized to predict the load-slip relationships for pull-out specimens and reinforced concrete prisms subject to load reversals.



Recently Liu (30) conducted reversed cyclic loading local bond-slip tests on 13 reinforced concrete blocks containing centrally embedded No. 10 bars with their bamboo style deformations bonded to the block over a short length only. Liu reported that the shorter the bonded length, the higher was the ultimate local bond stress, that the reduction in the maximum local bond stress due to cyclic loading increased with decreasing bonded length and that the initial stiffness was approximately proportional to bonded length and to the square root of the concrete compressive strength.

In this Chapter six of Liu's test results for specimens subjected to various load histories are used to develop monotonic and cyclic load models for local bond stress-slip relationships for reinforcing bars. The properties of those six specimens are listed in Table 4.

### 3.2 Monotonic Model

The local bond stress-slip curve proposed for monotonic loading is shown in Fig. 12 and is given by the following linear functions:

$$\tau = k_1 S \quad , \text{ for } S \leq S_c \qquad \text{.........(3-1)}$$

$$\tau = \tau_c + k_2(S-S_c) \quad , \text{ for } S_c < S \leq S_o \qquad \text{.........(3-2)}$$

and $$\tau = \tau_{max} - k_3(S-S_o), \text{ for } S > S_o \qquad \text{.........(3-3)}$$

where:

$$k_1 = 5\sqrt{f'_c} \qquad (\text{Kip/in}^3) \qquad \text{.........(3-4)}$$

$$k_2 = \left(\frac{f'_c}{1400}\right)^3 \qquad (\text{Kip/in}^3) \qquad \text{.........(3-5)}$$

$$k_3 = 4.0 \qquad (\text{Kip/in}^3) \qquad \text{.........(3-6)}$$

$$S_c = \frac{\tau_{max} - k_2 S_o}{k_1 - k_2} \quad \text{.........(3-7)}$$

$$\tau_c = k_1 S_c \quad \text{.........(3-8)}$$

$$\tau_{max} = \left(\frac{f'_c - 2300}{300}\right)^{\frac{2}{3}} \quad \text{.........(3-9)}$$

$$S_o = \frac{160}{f'_c} \quad \text{........(3-10)}$$

Measured and predicted monotonic local bond stress-slip curves are shown in Figs. 13 through 15. While the results might be better represented by non-linear expressions, the form proposed above is simpler for computational purposes. The physical significance of the relationship is discussed in Section 3.4.

### 3.3 Cyclic Model

The rules proposed for determining the unloading and reversed loading curves are indicated schematically in Fig. 16. The stiffness $k_4$ for linear unloading and the coefficients $\alpha$ and $\beta$, which define the magnitude of bond deterioration, were based on the test results. The values for $k_4$, $\alpha$ and $\beta$ are as follows:

$k_4 = 3.0 \times 10^3$ (Kip/in$^3$) ........(3-11)

$\alpha = 0.15$ ........(3-12)

$\beta = 0.9$, for the loading dirction for which $|\tau|$ has never been greater than $\tau_c$ ........(3-13)

$0.9 \geq \beta = 0.9 - 15 \times \Delta S \geq 0.75$, for the loading direction for which $|\tau|$ has been greater than $\tau_c$ ........(3-14)



where $\Delta S$ is defined as the slip increment for the previous half cycle in the same loading direction.

For cyclic loading the envelope curve for positive loading is also assumed to apply for negative loading. Cyclic loading is assumed to cause a reduction in the local bond capacity for a loading direction for which $\tau_c$ is exceeded in a prior loading half cycle. The degenerated envelope is CM'N' for positive loading and C"m'n' for negative loading. The rules for the degenerated envelope are as follows:

$\tau_{M'} = 0.9\ \tau_M,\quad S_{M'} = S_M$

$\tau_{N'} = 0.9\ \tau_N,\quad S_{N'} = S_N$

and $\tau_{m'} = 0.9\ \tau_m,\quad S_{m'} = S_m$

$\tau_{n'} = 0.9\ \tau_n,\quad S_{n'} = S_n$

The rules for unloading and reloading depend on whether $\tau$ has exceeded $\tau_c$ and whether the cycle is the first or a second or subsequent loading to a given slip.

Cycle O'ABZC"C'DEF illustrates the rules for loading to a given slip for the first time. Between O' and A the response is that for monotonic loading. For unloading from A

$\tau_B = \tau_Z = -\alpha\tau_A,\quad S_B = S_A - (1+\alpha)\tau_A/k_4$

Between B and Z, the bond resistance remains constant while the slip changes. From Z to C', the response follows that for monotonic loading since $\tau$ had not exceeded $\tau_c$ in the negative loading direction in previous cycles. From C' to E the response follows the same rules as from B to Z

$\tau_D = \tau_E = -\alpha\tau_{C'},\quad S_D = S_{C'} - (1+\alpha)\tau_{C'}/k_4$

except that the change in slip at a constant stress with reversal of the direction of loading depends on the range in slip L and is as follows

$$S_E = S_{C'} - \tau_{C'}/k_4 + L'$$

where

$$L' = 0.65\ L \text{ and } L = S_A - S_{C'}$$

From E to F there is a reduced stiffness defined by

$$\tau_F = \beta\tau_A, \quad S_F = S_A - (1-\beta)\tau_A/k_4$$

and $\beta = 0.9$ since $\tau_A < \tau_c$

Cycle FGHIKLOP illustrates the response for a subsequent cycle to new peak slips. Since $\tau$ has not exceeded $\tau_c$ in the previous positive half cycle, the response from F to G follows the monotonic envelop. Unloading rules from G to H and from K to L are the same as those from A to B and loading reversal rules from H to I and L to O follow those from D to E. Since $\tau$ has previously exceeded $\tau_c$ in the negative direction in Cycle O'ABZC"C'DEF, for determining the stiffness from I to J, $\beta$ is defined as follows:

$$0.9 \geq \beta = 0.9 - 15 \times \Delta S \geq 0.75$$

and $\Delta S = |S_{c'}|$

If the loading is increased beyond P, the response from P to P' follows the degenerated envelope since $\tau$ has exceeded $\tau_c$ in the positive loading direction.

The rules for determining the stiffnesses from O to P, R to T and V to W are the same as those from I to J but the values for $\Delta S$ are taken as $|S_G| - |S_A|$, $|S_K| - |S_{c'}|$ and $|S_P| - |S_G|$ respectively.

The test results and the load histories for the cyclically loaded local bond specimens used in this study are presented in Reference 30. In Figs. 17 through 22 the test results are compared with the results



predicted by the foregoing cyclic load model.

## 3.4 Discussion

This section discusses the parameters affecting the local bond stress-slip characteristics, interprets the physical significance of the models presented in Sections 3.2 and 3.3, and compares the results predicted by Morita's proposals and those predicted by the two foregoing models. The limitations for those two models are also discussed in this section.

### 3.4.1 Monotonic Response

For bars bonded to concrete over a short length and stressed under monotonic loading, initial stiffnesses are very large and sensitive to concrete strength. The higher the concrete strength, the larger is the initial stiffness. Once the local bond stress exceeds about 70% of the maximum local bond stress achieved subsequently in the test, significant decreases in stiffness develop for increasing loads. It is believed that the decrease in stiffness is caused by cone-like cracks that have the form shown in Fig. 23. Those cracks originate from the extremities of the bar's lugs and are a result of the high stress concentrations on that perimeter. As the loading is increased, the cone-like cracks propagate further and further into the concrete around the bar, causing the stiffness in that area to decrease and progressively larger slips to occur for equal increments in load. Eventually the local bond stress reaches its maximum value when a complete longitudinal crack forms between extremities of the lugs of the bar. After failure the local bond stress decreases as the local slip increases. The slope of descending local bond stress-slip curve is essentially constant and the sharpness of the peak in the curve increases as the concrete strength increases.

the model presented in Section 3.2 simplifies the monotonic local bond stress-slip relation into three linear functions corresponding to the three different stages in the physical behavior for a short bond joint subject to monotonic loading.

In Stage 1, the lug bears directly against the concrete in front of it. Slips are caused by the concrete compressing locally beneath the lug and there is no cracking in the surrounding concrete. The stiffness in this stage, $k_1$, in Fig. 12, is very large and assumed to be proportional to the square root of concrete compressive strength. When the bond stress reaches to $\tau_c$, Eq. (3-8), it is assumed that cone-like cracking initiates at the extremity of the lugs. This assumption is consistent with observations of other investigations and the evidence from dissected beam-column specimens (23). The cone-like cracking drastically alters the integrity of the concrete around the bar and decreases markedly the stiffness. The behavior for monotonic loading passes into a second stage. Increases in loading causes progressively greater extensions of the cone-like cracks out into the concrete and a gradual deterioration in the stiffness of the load-slip relationship. For simplification proposes, the monotonic model proposes that the stiffness $k_2$ in stage 2, defined by Eq. (3-5), is only a function of concrete strength and the increase in loading does not significantly affect that stiffness. A complete longitudinal crack is assumed to develop between sucessive lugs when the bond stress increases to $\tau_{max}$, as given by Eq. (3-9). The behavior of the bond joint moves into a third stage. For slips less than $S_o$ there is no relative movement between the lug under consideration and the concrete immediately to the front and outside that lug. For slips greater than $S_o$ relative movements occur as the lugs shear past the surrounding concrete. The slope of the local bond stress-slip curve in the third stage is given as a constant, $k_3$, and is not sensitive to concrete strength. The stiffness depends entirely on frictional and shearing of concrete on concrete effects. It is reasonable to believe that the surface of the longitudinal crack is very rough immediately after that crack forms. The surface is ground smoother little by little as the local slip increases so that the force needed to pull or push the bar through a given displacement decreases as the local slip increases. When the local slip becomes large, it is to be expected that the cracked surface will have become relatively smooth surface and the pulling or pushing force will drop to a constant value corresponding to the pure friction between the bar and the cracked concrete surface.

The monotonic model discussed above shows that for slips less than $S_o$ the concrete strength is an important factor affecting the monotonic local bond stress-slip relation. It is believed that other factors such as the degree of confinement for a bar, the type of concrete, and the bar size may also significantly affect the local bond behavior. In this study, those factors were treated as constants since the local bond-slip specimens essentially duplicated conditions for the beam-column specimens. Jeang's work (31) has shown that there is an upper limit to the increase in $\tau_{max}$ with increasing concrete strengths and a strong effect of bar size.

The monotonic local bond stress-slip law proposed by Morita and

Kaku is applicable only up to failure. They divided the behavior before failure into two stages. The stiffness for those two stages were determined by tests and essentially treated as constants for a range of concrete strengths from 4,300 psi to 5,000 psi. The monotonic model proposed by the author also divides the response into two stages but then considers that the stiffnesses before failure depend on the concrete strength. The behavior beyond $\tau_{max}$ is an essential ingredient to prediction of the behavior of the beam-column specimens. No information on that behavior is available through Morita and Kaku's work.

Comparisons between Morita's monotonic bond-slip law and the monotonic model proposed in this chapter are summarized in Table 5.

### 3.4.2 Cyclic Response

Test results showed that the behavior of a short bond joint under reversed cyclic loading was sensitive to loading history. The loading histories used in this study were categorized as Type 1 or Type 2 depending on the extent to which the direction of the slip was reversed.

Type 1 loading involved reversed cycling between constant slip limits with the limit in one direction held approximately constant at zero displacement. The slip range was held constant for three cycles before being increased for the subsequent three cycles. In the positive loading direction, the first pulling direction, the maximum peak stress for each slip limit, before attainment of the maximum capacity for cyclic loading, was greater than 70% of the maximum bond stress achieved in monotonic loading. However, in the negative loading direction, the second pulling direction, the peak stress achieved in every cycle was never greater than that 70% value. After attainment of the maximum



capacity the slip range was incremented by increasing the peak slip for the first pulling direction.

Type 2 loading involved reversed cyclic loading between constant stress limits until the maximum capacity was reached. After attainment of the maximum capacity the load was cycles between constant slip limits with the limit in one direction approximately equal but opposite in sign to the limit in the opposite direction. Generally for cycles 1 through 9, the bond joint was cycled between constant stress limits. The stress limits were increased after three cycles between the given stress limits. After cycle 9, the bond joint was cycled between constant slip limits, and the slip limits were increased after three cycles between previous slip limits.

For Type 1 loading history, it was observed that in the positive loading direction there were marked decreases in stiffness and capacity between the first and second cycles but not between the second and subsequent cycles. With an increase in the slip limits, a significant change in stiffness and capacity again occurred between the first and second cycles. For cycling between constant slip limits, the capacity and stiffness decreased with increasing number of cycles. However, the reduction in capacity and stiffness caused by the increase in slip limits was much greater than that caused by a number of repetition within a limited slip range. In the negative loading direction, there was no significant degeneration in capacity with cyclic loading.

For Type 2 loading history, when stress limits were less than 70% of the maximum bond stress for monotonic loading, the test results showed no significant degeneration in capacity or stiffness with cyclic loading but the stiffness for unloading was considerably greater the stiffness for loading. The bond stress-slip envelopes for monotonic and cyclic loadings were essentially the same. After the stress limit was increased beyond 70% of the maximum bond stress, $\tau_{max}$, for monotonic loading, there was a significant decrease in stiffness with cycling. The new peak displacement for attainment of the same stress limit was always greater than the previous displacement. For further cyclic loading between constant slip limits, in the positive loading direction, the capacity and stiffness decreased with cycling and there were always marked decreases in stiffness and capacity for the first and second cycles to increased slip limits. However, in the negative loading direction, there was no such marked decrease in stiffness and capacity. The envelope curve for cyclic loading always lay inside the monotonic curve once the bond joint had been cyclically loaded between stress limits greater than 70% of the maximum bond stress under monotonic loading. The maximum capacity for cyclic loading was about 90% of that for monotonic loading.

The author's cyclic model presented in Section 3.3 is similar to Morita's cyclic bond stress-slip law (33, 34). For the author's model 1, a set of rules, shown in Fig. 16, are used to relate the bond stress-slip curves for monotonic and cyclic loading. To predict the cyclic bond stress-slip relationship, using the model of Fig. 16, it is only necessary to know the monotonic bond stress-slip curve and the loading history. It is assumed that the relationship between the monotonic and cyclic bond stress-slip curves is essentially independent of the concrete strength. Values for the unloading stiffness $k_4$ and the coefficients $\alpha$



and $\beta$ in the cyclic model were developed based on Liu's test results. The values for $K_4$ and $\alpha$ are taken as $3.0 \times 10^3$ (Kips/in$^3$) and 0.15 respectively. However, the value for $\beta$ is assumed to depend on the previous loading history and the slip increment, $\Delta S$. For a loading direction for which the magnitude of bond stress has never exceeded $\tau_c$, the value of $\beta$ is taken as 0.9. The value of $\beta$ is expressed as a function of the slip increment, $\Delta S$, for a loading direction for which the magnitude of bond stress exceeded $\tau_c$. From the physical behavior described previously it is logical that the bond joint mechanism will not change drastically with loading reversals before cone-like cracking occurs. Thus, any deterioration in bond capacity with cycling is likely to be very small. However once the bond stress exceeds $\tau_c$ in any given direction, cone-like cracking forms for that loading direction and drastically changes the bond joint mechanism. Increasing slips for a given loading direction can be expected to cause the cone-like cracking to propagate further, damage the concrete around the bar, and cause significant deterioration in the bond capacity. In this cyclic model, the slip on reversal of loading L' in Fig. 16 is set equal to 0.65 L, Where L is the slip range. That action implies that the larger the slip range, the greater is the degree of damage. The coefficient of 0.65 was based on Liu's test results.

In Morita's cyclic bond stress-slip law, the slip limits for cyclic loading can only be increased up to $\pm$ 20 x $10^{-3}$ in. (0.5 mm) and the reloading curve is assumed to be directed towards the monotonic curve even after the bond joint has been cyclically loaded to a high stress. Morita took the value for $\beta$ to be a function of the slip value of the point from which unloading was started. The model outlined in Section

3.3, however, imposes no restriction on slip limits for cyclic loading and is still applicable even after the maximum slip for cyclic loading, $S_o$, has been exceeded. In the author's model the reloading curve is assumed to be directed towards the envelope curve for cyclic loading and the value for $\beta$ is assumed to depend on the prior loading history and the slip increment.

Values of $k_4$, $\alpha$ and $\beta$ for Morita's cyclic bond-slip law and the cyclic model proposed in this chapter are compared in Table 6.

Figures 17 through 22 show comparisons between test results and the results predicted by the cyclic bond stress-slip model. The variables for the test specimens covered in those comparisons were load history and concrete strength.

Figures 17 and 18 compare measured and predicted bond stress-slip curve for a joint subject to Type 1 loading history. The effects of increasing slip limits are studied in Fig. 17 and of repeated reversed cyclic loading between constant slip limits in Fig. 18.

Figures 19 through 22 show that the cyclic model can predict reasonable values for a bond joint with different concrete strengths and subject to Type 2 loading. Specimens LC2 and LC3 were subjected to the same type of loading history, but the concrete strength for Specimen LC3 was significantly higher than that for Specimen LC2. Effects of reversed cyclic loading between constant stress limits are shown in Figs 19 and 21. While the effects of increasing slip limits, foı a joint cycled between constant stress limits, are shown in Figs 20 and 22.

### 3.4.3 Conclusions

The foregoing comparisons show that the measured load-slip rela-



tionships and those predicted by the model developed here are in reasonable agreement. Equation (3-9), which was derived from limited test results, is applicable only to a bond joint with a concrete strength greater than 3,000 psi and less than 4,500 psi, with a degree of confinement similar to that of local bond specimens used in this study and bar sizes similar to that used in this study. Although, considerable effort was involved in developing the monotonic and cyclic models reported here, additional statistical and experimental studies are needed if accurate and comprehensive local bond stress-slip relationships for a wide variety of practical conditions and loading histories are to be developed.

# CHAPTER 4

# PREDICTION OF FORCE-DISPLACEMENT RELATIONSHIPS FOR AN ANCHORED BAR

## 4.1 Introduction

The earthquake response of a structure is sensitive to variations in its natural frequencies. Such variations are caused primarily by changes in the stiffness of the structure. Clough and Johnston (35) found that the loss in stiffness caused by inelastic deformations increased the period of vibration of a structure and that such increases lead in turn to further modifications in the response. For structures with long periods of vibration, increasing the period reduced the likelihood of resonance with the earthquake input and therefore decreased the structure's response activity significantly. In contrast, for structures with short periods of vibration, a loss in stiffness increased the response activity and, in particular, the displacement for a given earthquake input increased.

Where a maximum moment condition occurs at the face of a support the stiffness of a concrete member is sensitive to the anchorage condition for bars within the support. The force-displacement relationships characterizing those anchorage conditions depend on many factors. The more important factors are: (1) the inelastic behavior of the reinforcing steel and in particular Bauschinger effects for that steel; (2) the local bond stress-slip characteristics for reinforcing steel under various load histories; (3) the penetration of slip along the concrete-reinforcing steel interface and in particular the manner in which that penetration modifies the behavior; (4) the presence of shear deformations and diagonal cracking in the anchorage zone; and (5) the effectiveness



of confinement either by lateral members or transverse reinforcement on shear deformations, the penetration of slip along the concrere-reinforcing steel interface, and the local bond stress-slip characteristics for the concrete-steel interface.

In this study the specimens were proportioned and reinforced so that the influences of shear deformations and diagonal cracking were deliberately minimized. The confining reinforcement provided in the joint was designed so that it always remained in the elastic range throughout the loading history of the specimen.

In the following discussion a model is developed for the force-loaded end slip relationship for an inelastically loaded, anchored reinforcing bar. That model utilizes the stress-strain model for the reinforcing steel, presented in Chapter 2, and the local bond stress-slip model for a reinforcing bar, developed in Chapter 3. A general model is developed that is applicable to a bar subjected to reversed cyclic loading that extends into the inelastic range and a more simple model that is applicable for a bar subjected to monotonically increasing load that also extends into the inelastic range.

These models characterize the relationship between the axial force on a reinforcing bar and the displacement of the loaded end of that bar relative to the surrounding concrete. For reversed cyclic loading the model takes into account yielding of the reinforcing steel, Bauschinger effects, non-linearity of the bond stress distribution and the modification of that distribution caused by cyclic loading.

### 4.2 Assumptions

As mentioned previously, the local bond stress-slip model for a reinforcing bar and the stress-strain model for reinforcing steel are utilized as building blocks to develop the model for predicting the load-displacement characteristics at the attack end of an anchored bar subjected to monotonic and reversed cyclic loading. However, since the test results used for developing those two models have certain distinct limitations, it is appropriate to stress that the following limitations are inherent in those models.

(1) The local bond stress-slip relationship under monotonic loading depends primarily on the concrete strength. The size of the bar does not significantly affect the relationship.

(2) The rules defining the local bond stress-slip relationship under unloading and reversed loading are not affected by the size of the bar.

(3) The procedure for determining the cyclic stress-strain relationships for reinforcing steels is not influenced by the size of the bar and the yield strength of the bar.

### 4.3 Monotonic Force-Displacement Model

The procedure for developing the monotonic load-displacement model is described in Section 4.3.1. It was found that the concrete strength, the characteristics of the reinforcing steel and the embedment length of the bar were major factors affecting the load-displacement relationship at the attack end of the bar, the variation in bond stress along the anchored length of the bar, and the penetration of steel stress along



the anchored length of the bar. An example is presented in Section 4.3.2 in order to clarify the formulation. Failure criteria for monotonic loading are described in Section 4.3.3.

#### 4.3.1 Approach

When, as shown in Fig. 24(a), a force P is applied to the attack end of a bar, bond stresses are created along the embedded length of the bar. Unknowns can be described as the magnitude of the bond stress at the attack end, the shape of the stress distribution and the length over which bond stresses are created within the specimen. Shown in Fig. 24(b) is a free body diagram of a typical bar element of length dx. Bond stresses are assumed to be uniformly distributed over the surface of this element. Axial equilibrium gives:

$$\tau = \frac{A_b}{\Sigma_o}\frac{d\sigma}{dx} \qquad \text{.........(4-1)}$$

where:

$\tau$ = bond stress

$\sigma$ = steel stress

$A_b$ = bar cross-sectional area

$\Sigma_o$ = bar perimeter

The bond stress $\tau$ is dependent on the local slip, S, and that relationship, discussed in Section 3.2, is formulated as:

$$\tau = f(S) = \begin{cases} k_1 S & \text{, for } S \leq S_c \\ \tau_c + k_2(S - S_c) & \text{, for } S_c < S \leq S_o \\ \tau_{max} - k_3(S - S_o) & \text{, for } S > S_o \end{cases} \qquad \text{.........(4-2)}$$

where:

$$S = \int_0^x \varepsilon(\xi)d\xi \text{ .... if bond stress has not penetrated to the tail end} \qquad \text{.........(4-3)}$$

$$S = \int_0^x \varepsilon(\xi)d\xi + \text{local slip at the tail end .... if bond stress has penetrated to the tail end} \qquad \text{.........(4-4)}$$

By substituting S into Eq. (4-2) and then equating Eqs (4-1) and (4-2), a set of linear second-order differential equations can be obtained. The bond stress distribution, the steel stress distribution, and the load-displacement relationship at the attack end of the bar can be determined by solving those differential equations. The details of that procedure are illustrated through an example in the following section.

4.3.2 Example

Specimen S101 was loaded monotonically to failure. In this section, prediction of the bond stress distribution in that specimen, the penetration of steel stress into that specimen and the load-displacement relationship at the attack end of the bar are formulated step by step for the eight possible stages of behavior of that specimen.

Stage 1: As shown in Fig. 25(a), when a force P is applied to the attack end of a bar, the bond stress penetrates to a distance $L_1$ from the concrete surface. In this stage, the bar is still in the elastic range and the magnitude of the bond stress at point A is smaller than the stress $\tau_c$ at which elastic behavior ceases in the unit bond stress specimen.



Equilibrium in the axial direction gives

$$\tau_1(x_1) = \frac{A_b}{\Sigma_o}\frac{d\sigma_1(x_1)}{dx_1} \qquad \text{.........(4-5)}$$

The local bond stress-slip relation for this case is

$$\tau_1(x_1) = k_1 S_1(x_1) \qquad \text{.........(4-6)}$$

where:

$$S_1(x_1) = \int_0^{x_1} \varepsilon_1(\xi_1)d\xi_1 = \int_0^{x_1} \frac{\sigma_1(\xi_1)}{E_s}d\xi_1 \qquad \text{.........(4-7)}$$

If Eq. (4-7) is substituted into Eq. (4-6) and Eqs. (4-5) and (4-6) equated then

$$\frac{d^2\sigma_1(x_1)}{dx_1^2} = K_1^2\sigma_1(x_1) \qquad \text{.........(4-8)}$$

where:

$$K_1^2 = \frac{\Sigma_o k_1}{A_b E_s}$$

The general solution of Eq. (4-8) is

$$\sigma_1(x_1) = a_1 e^{K_1 x_1} + b_1 e^{-K_1 x_1} \qquad \text{.........(4-9)}$$

so that

$$\tau_1(x_1) = \frac{A_b K_1}{\Sigma_o}(a_1 e^{K_1 x_1} - b_1 e^{-K_1 x_1}) \qquad \text{........(4-10)}$$

The boundary conditions used to solve the three unknowns $a_1$, $b_1$ and $L_1$ are:

$$\sigma_1(0) = \sigma_o \qquad \text{........(4-11)}$$

$$\tau_1(0) = \tau_o \qquad \text{........(4-12)}$$

$$\sigma_1(L_1) = \frac{P}{A_b} \qquad \text{........(4-13)}$$

where:

$$\sigma_o = \frac{h\,\pi\, d_b\, 0.5f'_c}{A_b} \qquad \text{........(4-14)}$$

$$\tau_o = \frac{\sigma_o\, A_b}{a\, \Sigma_o} \qquad \text{........(4-15)}$$

$h$ = height of lug

$d_b$ = bar diameter

$A_b$ = bar cross-sectional area

$\Sigma_o$ = bar perimeter

and $a$ = lug spacing

It is reasonable to believe that the penetration of steel stress in the axial direction will vary incrementally according to the discrete amount of force transferred at each lug. The stress in the bar must decrease markedly after each lug. If the stress in the concrete beneath the lug is in the elastic range, it is reasonable to assume that the local slip of the bar is negligible and that the steel stress vanishes at that lug. The stress-strain curve for concrete is essentially linear up to $0.5f'_c$. Suppose, as shown in Fig. 25(b), that when the concrete beneath the lug is stressed to $0.5f'_c$, the stress in the bar immediately in front of that lug is $\sigma_o$. Then the magnitude of $\sigma_o$ can be determined from Eq. (4-14). The force acting on the lug can be represented by a uniform bond stress acting over the distance to the next lug. The magnitude of that uniform bond stress, $\tau_o$, is given by Eq. (4-15). Then,



$\tau_1(0) = \tau_o$ and $\sigma_1(0) = \sigma_o$ become the boundary conditions for solving constants $a_1$ and $b_1$ in Eqs. (4-9) and (4-10).

From Eqs. (4-11), (4-12) and (4-13),

$$a_1 = \frac{1}{2}\left(\sigma_o + \frac{\tau_o \Sigma_o}{A_b K_1}\right) \qquad \text{........(4-16)}$$

$$b_1 = \frac{1}{2}\left(\sigma_o - \frac{\tau_o \Sigma_o}{A_b K_1}\right) \qquad \text{........(4-17)}$$

and $$L_1 = \frac{1}{K_1} \ln\left(\frac{\frac{P}{A_b} + \sqrt{\frac{P^2}{A_b^2} - 4a_1 b_1}}{2a_1}\right) \qquad \text{........(4-18)}$$

The bond stress and steel stress distribution along the anchorage length of the bar can then be determined from Eqs. (4-9) and (4-10). The displacement of point B in Fig. 25(a) is equal to the local slip at point A plus the elongation of segment AB.

Stage 2: A wedge of relatively unstressed concrete forms outside the column steel. Thus, segment AA' in Fig. 25(c) provides no contribution to the bond strength and the location of the maximum value in the bond stress distribution curve shifts suddenly from point A to A'.

Pull-out tests on headed-studs and embedded bolts have clearly shown (36) that the pull-out capacity corresponds to the development of a shear stress of about $4\sqrt{f'_c}$ over the truncated cone shown in Fig. 25(d). If the average bond stress over the segment AA' is defined as $\tau_{cr}$ then

$$\tau_{cr} = \frac{4\sqrt{f'_c}\,\pi\,(d_b + L_u)}{\Sigma_o} \qquad \text{........(4-19)}$$

where:

$L_u$ = length of segment AA'

A wedge is assumed to form outside the column steel when the average bond stress reaches $\tau_{cr}$.

The displacement of point B outside the specimen equals the sum of the local slip at point A' and the elongation of segment A'B.

Stage 3: The cone-like cracking forms around the bar and penetrates to a distance $L_2$ from point A'. The bond stress distribution along the anchorage length of the bar can be divided into two regions, as shown in Fig. 26(a).

For region I:

$$\frac{d^2\sigma_1(x_1)}{dx_1^2} = K_1^2\sigma_1(x_1); \quad K_1^2 = \frac{k_1\Sigma_o}{A_bE_s} \qquad \text{........(4-20)}$$

so that

$$\sigma_1(x_1) = a_1e^{K_1x_1} + b_1e^{-K_1x_1} \qquad \text{........(4-21)}$$

$$\tau_1(x_1) = \frac{A_bK_1}{\Sigma_o}(a_1e^{K_1x_1} - b_1e^{-K_1x_1}) \qquad \text{........(4-22)}$$

For region II:

$$\frac{d^2\sigma_2(x_2)}{dx_2^2} = K_2^2\sigma_2(x_2); \quad K_2^2 = \frac{k_2\Sigma_o}{A_bE_s} \qquad \text{........(4-23)}$$

so that

$$\sigma_2(x_2) = a_2e^{K_2x_2} + b_2e^{-K_2x_2} \qquad \text{........(4-24)}$$

$$\tau_2(x_2) = \frac{A_bK_2}{\Sigma_o}(a_2e^{K_2x_2} - b_2e^{-K_2x_2}) \qquad \text{........(4-25)}$$



At ends of those two regions boundary conditions are:

$$\sigma_1(0) = \sigma_o \qquad \text{........(4-26)}$$

$$\tau_1(0) = \tau_o \qquad \text{........(4-27)}$$

$$\tau_1(L_1) = \tau_c \qquad \text{........(4-28)}$$

$$\sigma_2(0) = \sigma_1(L_1) \qquad \text{........(4-29)}$$

$$\tau_2(0) = \tau_c \qquad \text{........(4-30)}$$

$$\sigma_2(L_2) = \frac{P}{A_b} \qquad \text{........(4-31)}$$

Solution of Eqs. (4-26) through (4-31) yields:

$$a_1 = \frac{1}{2}\left(\sigma_o + \frac{\tau_o\Sigma_o}{A_bK_1}\right) \qquad \text{........(4-32)}$$

$$b_1 = \frac{1}{2}\left(\sigma_o - \frac{\tau_o\Sigma_o}{A_bK_1}\right) \qquad \text{........(4-33)}$$

$$L_1 = \frac{1}{K_1}\ln\left(\frac{\frac{\tau_c\Sigma_o}{A_bK_1} + \sqrt{\left(\frac{\tau_c\Sigma_o}{A_bK_1}\right)^2 + 4a_1b_1}}{2a_1}\right) \qquad \text{........(4-34)}$$

$$a_2 = \frac{1}{2}\left(a_1e^{K_1L_1} + b_1e^{-K_1L_1} + \frac{\tau_c\Sigma_o}{A_bK_2}\right) \qquad \text{........(4-35)}$$

$$b_2 = \frac{1}{2}\left(a_1e^{K_1L_1} + b_1e^{-K_1L_1} - \frac{\tau_c\Sigma_o}{A_bK_2}\right) \qquad \text{........(4-36)}$$

$$L_2 = \frac{1}{K_2}\ln\left(\frac{\frac{P}{A_b} + \sqrt{\left(\frac{P}{A_b}\right)^2 - 4a_2b_2}}{2a_2}\right) \qquad \text{........(4-37)}$$

The bond stress and steel stress distribution along the embedment length of the bar can then be determined from Eqs. (4-21), (4-22), (4-24) and (4-25). The displacement of point B is determined as described previously for stage 2.

Stage 4: As shown in Fig. 26(b), it is assumed that for this stage the bond stress wave has penetrated to the tail end of the bar. Then at the tail end, the bar develops a local slip relative to the surrounding concrete. In this stage, the expressions for $\tau_1(x_1)$, $\sigma_1(x_1)$, $\tau_2(x_2)$ and $\sigma_2(x_2)$ are the same as those in stage 3. However, some of the boundary conditions change. The values for $a_1$, $b_1$, $a_2$, $b_2$, $L_1$ and $L_2$ are determined by satisfying the following conditions:

$$\sigma_1(0) = 0 \qquad \text{........(4-38)}$$

$$\sigma_1(L_1) = \sigma_2(0) \qquad \text{........(4-39)}$$

$$\tau_1(L_1) = \tau_c \qquad \text{........(4-40)}$$

$$\tau_2(0) = \tau_c \qquad \text{........(4-41)}$$

$$\sigma_2(L_2) = \frac{P}{A_b} \qquad \text{........(4-42)}$$

$$L_1 + L_2 = L_{em} \qquad \text{........(4-43)}$$

Then

$$a_1 = \frac{\tau_c \Sigma_o}{A_b K_1 (e^{K_1 L_1} + e^{-K_1 L_1})} \qquad \text{........(4-44)}$$

$$b_1 = -a_1 \qquad \text{........(4-45)}$$

$$a_2 = \frac{1}{2}\left(a_1 e^{K_1 L_1} + b_1 e^{-K_1 L_1} + \frac{\tau_c \Sigma_o}{A_b K_2}\right) \qquad \text{........(4-46)}$$

$$b_2 = \frac{1}{2}\left(a_1 e^{K_1 L_1} + b_1 e^{-K_1 L_1} - \frac{\tau_c \Sigma_o}{A_b K_2}\right) \qquad \text{........(4-47)}$$

and $$\frac{P}{A_b} = a_2 e^{K_2 L_2} + b_2 e^{-K_2 L_2} \qquad \text{........(4-48)}$$

$L_1$ and $L_2$ can be obtained from Eqs. (4-43) and (4-48). While it is difficult to solve directly for $L_1$ and $L_2$, values can still be readily determined by trial-and-error methods.



Stage 5: In this stage the bar has yielded to a distance $L_3$ from point A' and the bond stress distribution along the length of the bar can be divided into three regions shown in Fig. 27(a). The unit bond stress at A' is still less than the maximum value $\tau_{max}$ cited in Chapter 3.

The differential equations derived for regions I and II are the same as those for stage 3. For region III, the differential equation is as follows:

$$\frac{d^2\sigma_3(x_3)}{dx_3^2} = K_3^2\sigma_3(x_3) + K_3^2(E_{sh}\varepsilon_{sh} - \sigma_y), \quad K_3^2 = \frac{\Sigma_o k_2}{A_b E_{sh}} \qquad \text{........(4-49)}$$

so that

$$\sigma_3(x_3) = a_3 e^{K_3 x_3} + b_3 e^{-K_3 x_3} + (\sigma_y - E_{sh}\varepsilon_{sh}) \qquad \text{........(4-50)}$$

$$\tau_3(x_3) = \frac{A_b K_3}{\Sigma_o}(a_3 e^{K_3 x_3} - b_3 e^{-K_3 x_3}) \qquad \text{........(4-51)}$$

The unknown coefficients and the lengths for each region are determined from the following conditions:

$$\sigma_1(0) = 0 \qquad \text{........(4-52)}$$

$$\tau_1(L_1) = \tau_c \qquad \text{........(4-53)}$$

$$\sigma_2(0) = \sigma_1(L_1) \qquad \text{........(4-54)}$$

$$\tau_2(0) = \tau_c \qquad \text{........(4-55)}$$

$$\sigma_2(L_2) = \sigma_y \qquad \text{........(4-56)}$$

$$\tau_2(L_2) = \tau_3(0) \qquad \text{........(4-57)}$$

$$\sigma_3(0) = \sigma_y \qquad \text{........(4-58)}$$

$$\sigma_3(L_3) = \frac{P}{A_b} \qquad \text{........(4-59)}$$

$$L_1 + L_2 + L_3 = L_{em} \qquad \text{........(4-60)}$$

Then

$$a_1 = \frac{\tau_c \Sigma_o}{A_b K_1 (e^{K_1 L_1} + e^{-K_1 L_1})} \qquad \text{........(4-61)}$$

$$b_1 = -a_1 \qquad \text{........(4-62)}$$

$$a_2 = \frac{1}{2}\,(a_1 e^{K_1 L_1} + b_1 e^{-K_1 L_1} + \frac{\tau_c \Sigma_o}{A_b K_2}) \qquad \text{........(4-63)}$$

$$b_2 = \frac{1}{2}\,(a_1 e^{K_1 L_1} + b_1 e^{-K_1 L_1} - \frac{\tau_c \Sigma_o}{A_b K_2}) \qquad \text{........(4-64)}$$

$$a_3 = \frac{1}{2}\,\{\varepsilon_{sh} E_{sh} + \frac{K_2}{K_3}(a_2 e^{K_2 L_2} - b_2 e^{-K_2 L_2})\} \qquad \text{........(4-65)}$$

$$b_3 = \frac{1}{2}\,\{\varepsilon_{sh} E_{sh} - \frac{K_2}{K_3}(a_2 e^{K_2 L_2} - b_2 e^{-K_2 L_2})\} \qquad \text{........(4-66)}$$

$$\sigma_y = a_2 e^{K_2 L_2} + b_2 e^{-K_2 L_2} \qquad \text{........(4-67)}$$

$$\frac{P}{A_b} = a_3 e^{K_3 L_3} + b_3 e^{-K_3 L_3} + (\sigma_y - \varepsilon_{sh} E_{sh}) \qquad \text{........(4-68)}$$

Once $L_1$, $L_2$ and $L_3$ are obtained from Eqs. (4-60), (4-67) and (4-68), the other coefficients can be readily determined.

Stage 6: As shown in Fig. 27(b), the bond stress wave is now divided into four regions since local bond slips in region IV have exceeded those for the development of $\tau_{max}$. Longitudinal cracking will have developed along the lugs for the complete length of region IV and



the bar will be yielding over a considerable distance from its attack end. The transfer length for bond stress is divided into four regions. The differential equations (4-8), (4-23) and (4-49) are appropriate for regions I, II and III respectively. The appropriate differential equation for region IV is

$$\frac{d^2\sigma_4(x_4)}{dx_4^2} + K_4^2\sigma_4(x_4) = K_4^2(\sigma_y - E_{sh}\varepsilon_{sh}), \quad K_4^2 = \frac{\Sigma_o k_3}{A_b E_{sh}} \qquad \text{........(4-68)}$$

so that

$$\sigma_4(x_4) = a_4 \sin K_4 x_4 + b_4 \cos K_4 x_4 + (\sigma_y - E_{sh}\varepsilon_{sh}) \qquad \text{........(4-69)}$$

$$\tau_4(x_4) = \frac{A_b K_4}{\Sigma_o}(a_4 \cos K_4 x_4 - b_4 \sin K_4 x_4) \qquad \text{........(4-70)}$$

The unknown coefficients and the lengths of the four regions can be determined from the following conditions:

$$\sigma_1(0) = 0 \qquad \text{........(4-71)}$$

$$\tau_1(L_1) = \tau_c \qquad \text{........(4-72)}$$

$$\sigma_2(0) = \sigma_1(L_1) \qquad \text{........(4-73)}$$

$$\tau_2(0) = \tau_c \qquad \text{........(4-74)}$$

$$\sigma_2(L_2) = \sigma_y \qquad \text{........(4-75)}$$

$$\sigma_3(0) = \sigma_y \qquad \text{........(4-76)}$$

$$\tau_3(0) = \tau_2(L_2) \qquad \text{........(4-77)}$$

$$\tau_3(L_3) = \tau_{max} \qquad \text{........(4-78)}$$

$$\sigma_4(0) = \sigma_3(L_3) \qquad \text{........(4-79)}$$

$$\tau_4(0) = \tau_{max} \qquad \text{........(4-80)}$$

$$\sigma_4(L_4) = \frac{P}{A_b} \qquad \text{........(4-81)}$$

$$L_1 + L_2 + L_3 + L_4 = L_{em} \qquad \text{........(4-82)}$$

Then

$$a_1 = \frac{\tau_c \Sigma_o}{A_b K_1 (e^{K_1 L_1} + e^{-K_1 L_1})} \qquad \text{........(4-83)}$$

$$b_1 = -a_1 \qquad \text{........(4-84)}$$

$$a_2 = \frac{1}{2}\,(a_1 e^{K_1 L_1} + b_1 e^{-K_1 L_1} + \frac{\tau_c \Sigma_o}{A_b K_2}) \qquad \text{........(4-85)}$$

$$b_2 = \frac{1}{2}\,(a_1 e^{K_1 L_1} + b_1 e^{-K_1 L_1} - \frac{\tau_c \Sigma_o}{A_b K_2}) \qquad \text{........(4-86)}$$

$$a_3 = \frac{1}{2}\,\{\varepsilon_{sh} E_{sh} + \frac{K_2}{K_3}(a_2 e^{K_2 L_2} - b_2 e^{-K_2 L_2})\} \qquad \text{........(4-87)}$$

$$b_3 = \frac{1}{2}\,\{\varepsilon_{sh} E_{sh} - \frac{K_2}{K_3}(a_2 e^{K_2 L_2} - b_2 e^{-K_2 L_2})\} \qquad \text{........(4-88)}$$

$$a_4 = \frac{\tau_{max} \Sigma_o}{A_b K_4} \qquad \text{........(4-89)}$$

$$b_4 = a_3 e^{k_3 L_3} + b_3 e^{-K_3 L_3} \qquad \text{........(4-90)}$$

$$\sigma_y = a_2 e^{K_2 L_2} + b_2 e^{-K_2 L_2} \qquad \text{........(4-91)}$$

$$\frac{P}{A_b} = a_4 \sin K_4 L_4 + b_4 \cos K_4 L_4 + \sigma_y - \varepsilon_{sh} E_{sh} \qquad \text{........(4-92)}$$

$$\frac{\tau_{max} \Sigma_o}{A_b K_3} = a_3 e^{K_3 L_3} - b_3 e^{-K_3 L_3} \qquad \text{........(4-93)}$$



The values for $L_1$, $L_2$, $L_3$ and $L_4$ can be determined from Eqs. (4-82), (4-91), (4-92) and (4-93).

Stage 7: In this stage, the cone-like cracking has penetrated to the tail end of the bar so that region I of Fig. 27(b) disappears. The bond stress distribution can be divided into three regions again, as shown in Fig. 28(a). The differential equations which characterize regions II, III and IV respectively are Eqs. (4-23), (4-49) and (4-68). In order to determine the unknowns in the expressions for the bond stress distribution and the steel stress distribution, the following boundary conditions are applicable.

$$\sigma_2(0) = 0 \qquad \text{........(4-94)}$$

$$\sigma_2(L_2) = \sigma_y \qquad \text{........(4-95)}$$

$$\tau_2(L_2) = \tau_3(0) \qquad \text{........(4-96)}$$

$$\sigma_3(0) = \sigma_y \qquad \text{........(4-97)}$$

$$\tau_3(L_3) = \tau_{max} \qquad \text{........(4-98)}$$

$$\sigma_3(L_3) = \sigma_4(0) \qquad \text{........(4-99)}$$

$$\tau_4(0) = \tau_{max} \qquad \text{.......(4-100)}$$

$$\sigma_4(L_4) = \frac{P}{A_b} \qquad \text{.......(4-101)}$$

$$L_2 + L_3 + L_4 = L_{em} \qquad \text{.......(4-102)}$$

Then

$$a_2 = \frac{\sigma_y}{e^{K_2 L_2} - e^{-K_2 L_2}} \qquad \text{.......(4-103)}$$

$$b_2 = -a_2 \qquad \text{.......(4-104)}$$

$$a_3 = \frac{1}{2}\{\varepsilon_{sh}E_{sh} + \frac{K_2}{K_3}(a_2 e^{K_2L_2} - b_2 e^{-K_2L_2})\} \qquad \text{.......(4-105)}$$

$$b_3 = \frac{1}{2}\{\varepsilon_{sh}E_{sh} + \frac{K_2}{K_3}(a_2 e^{K_2L_2} - b_2 e^{-K_2L_2})\} \qquad \text{.......(4-106)}$$

$$a_4 = \frac{\tau_{max}\Sigma_o}{A_bK_4} \qquad \text{.......(4-107)}$$

$$b_4 = a_3 e^{K_3L_3} + b_3 e^{-K_3L_3} \qquad \text{.......(4-108)}$$

$$\frac{\tau_{max}\Sigma_o}{A_bK_3} = a_3 e^{K_3L_3} - b_3 e^{-K_3L_3} \qquad \text{.......(4-109)}$$

$$\frac{P}{A_b} = a_4 \sin K_4L_4 + b_4 \cos K_4L_4 + (\sigma_y - \varepsilon_{sh}E_{sh}) \qquad \text{.......(4-110)}$$

Once $L_2$, $L_3$ and $L_4$ are determined from Eqs. (4-102), (4-109) and (4-110), the other coefficients can readily be determined.

Stage 8: As shown in *Fig.* 28(b), *in stage* 8 the *maximum* bond *stress*, $\tau_{max}$, has penetrated to the region where the bar is still in elastic range. During this stage, $\tau_{max}$ penetrates rapidly towards the tail end of the bar with small increments of loading. The bond joint is said to have failed when the local bond stress at the tail end reaches $\tau_{max}$. The bond stress distribution for this stage is divisible into three regions. The differential equations applicable for regions II and IV are Eqs. (4-23) and (4-68) respectively. However, the differential equation characterizing region V is

$$\frac{d^2\sigma_5(x_5)}{dx_5^2} + K_5^2\sigma_5(x_5) = 0, \quad K_5^2 = \frac{k_3\Sigma_o}{A_bE_s} \qquad \text{.......(4-111)}$$



then

$$\sigma_5(x_5) = a_5 \sin K_5x_5 + b_5 \cos K_5x_5 \qquad \text{.......(4-112)}$$

$$\tau_5(x_5) = \frac{A_bK_5}{\Sigma_o}(a_5 \cos K_5x_5 - b_5 \sin K_5x_5) \qquad \text{.......(4-113)}$$

The unknowns involved in this stage can be determined using the following boundary conditions:

$$\sigma_2(0) = 0 \qquad \text{.......(4-114)}$$

$$\tau_2(L_2) = \tau_{max} \qquad \text{.......(4-115)}$$

$$\sigma_2(L_2) = \sigma_5(0) \qquad \text{.......(4-116)}$$

$$\sigma_5(L_5) = \sigma_y \qquad \text{.......(4-117)}$$

$$\tau_5(0) = \tau_{max} \qquad \text{.......(4-118)}$$

$$\tau_5(L_5) = \tau_4(0) \qquad \text{.......(4-119)}$$

$$\sigma_4(0) = \sigma_y \qquad \text{.......(4-120)}$$

$$\sigma_4(L_4) = \frac{P}{A_b} \qquad \text{.......(4-121)}$$

$$L_2 + L_5 + L_4 = L_{em} \qquad \text{.......(4-122)}$$

Then

$$a_2 = \frac{\tau_{max}\Sigma_o}{A_bK_2(e^{K_2L_2} + e^{-K_2L_2})} \qquad \text{.......(4-123)}$$

$$b_2 = -a_2 \qquad \text{.......(4-124)}$$

$$a_5 = \frac{\tau_{max}\Sigma_o}{A_bK_5} \qquad \text{.......(4-125)}$$

$$b_5 = a_2 e^{K_2 L_2} + b_2 e^{-K_2 L_2} \qquad \text{.......(4-126)}$$

$$a_4 = \frac{K_5}{K_4}(a_5 \cos K_5 L_5 - b_5 \sin K_5 L_5) \qquad \text{.......(4-127)}$$

$$b_4 = \varepsilon_{sh} E_{sh} \qquad \text{.......(4-128)}$$

$$\sigma_y = a_5 \sin K_5 L_5 + b_5 \cos K_5 L_5 \qquad \text{.......(4-129)}$$

$$\frac{P}{A_b} = a_4 \sin K_4 L_4 + b_4 \cos K_4 L_4 + (\sigma_y - \varepsilon_{sh} E_{sh}) \qquad \text{.......(4-130)}$$

Trial-and-error methods are used to determine $L_2$, $L_5$ and $L_4$ from Eqs. (4-122), (4-129) and (4-130). The other unknowns can then easily be determined.

For all eight stages, the local bond stress at A or A' is determined first. Then the appropriate local bond stress-slip relationship is used to determine the local slip at A or A'. For stage 1, the displacement at point B is taken as the local slip at point A plus the elongation of segment AB. For stage 2 through stage 8, however, the sum of the local slip at point A' and the elongation of segment A'B is taken as the displacement of point B. The computer program listing for this example is presented in Appendix A.

4.3.3 Criteria for Failure

The criteria used for failure under monotonic loading for straight bars and bars terminating in hooks are as follows:

(a) Straight bar: For specimens with straight bars, as described previously, it is assumed that the bond joint fails when the maximum bond stress, $\tau_{max}$, established from unit bond tests, is developed at



the tail end of the bar. That assumption means that at failure longitudinal cracking can be expected to extend along the length of the bar almost to its tail end. That was the behavior observed in the University of Washington tests reported in Reference 22.

(b) Hooked bar: Marques and Jirsa (37) have proposed that standard hooks anchored within a joint be considered capable of developing a tensile stress in the bar reinforcment of

$$f_h = 700(1 - 0.3d_b)\psi\sqrt{f'_c} \qquad \text{.......(4-131)}$$

but not greater than $f_y$.

For comparison with the test data reported here it is proposed that the value of $\psi$ be taken as 1.4. In Reference 33, $\psi$ is a factor reflecting the confinement conditions for the joint. A $\psi$ value of 1.4 is recommended for the type of confinement conditions used in the specimens reported here. For specimens with bars terminating in hooks, it is assumed that the bond joint fails when the steel stress at the end of the lead in zone for the hook reaches $f_h$, as calculated from Eq. (4-131). Since the strain in the steel corresponding to $f_h$ is generally less than the slip strain corresponding to $\tau_{max}$ in the unit bond test and the lead-in length is relatively large, the foregoing assumption means that at failure longitudinal cracking should not be expected to have penetrated from the loaded end into the hooked region of the bar. However, as pointed out in Reference 22 the specimen with a hooked bar behaves differently to that with a straight bar and the hook tends to split the concrete surrounding it. That splitting masks the effects of longitudinal cracking.

## 4.4 Cyclic Load-Displacement Model

### 4.4.1 The Model

If an anchored bar is subjected to reversed cyclic loading applied at one end only, then, for the first tensile half cycle, the load-displacement curve, the bond stress distribution and the steel stress distribution along the anchorage length of the bar can be determined using the monotonic model described in Section 4.2. However, for the unloading half cycle and subsequent reversed loading cycles determinations of the load-displacement curve, the bond stress distribution and the steel stress distribution are considerably more complicated than for the monotonic loading discussed previously. In this section the bar's cyclic stress-strain characteristics and cyclic local bond stress-slip relationship, developed in Chapters 2 and 3 respectively, are used to derive a model to predict the behavior of a bond joint under reversed cyclic loading. In this model, the embedment length for the bar is divided into a number of discrete segments. Each segment is subject independently to loading reversals and that independent load history used to determine the segment's stress-strain characteristics and local bond stress-slip characteristics. The typical variations in bond stress distribution for loading reversals can be categorized into the four cases, shown in Figs. 29 through 32. In those figures the bond stress distributions for previous peak loads are represented by broken lines. The solid lines denote the bond stress distributions under unloadings or reversed loadings. For cases 1 and 2, since the bond stress wave has not penetrated to the free end of the bar, the displacement at the attack end is taken as the total elongation of the bar. For cases 3 and 4, however, where the bond stress



wave has penetrated to the free end of the bar, the displacement at the attack end is taken as the total elongation of the bar plus the local slip at the tail end. Details of the procedures used to develop the models for those four cases are described in the following:

Case 1: This case is shown in Fig. 29. As unloading occurs, the greatest amount of strain recovery for the bar occurs at the loaded end and the amount of the contraction decreases gradually along the length of the bar. Since the unloading stiffness for the local bond stress-slip curve is extremely large, during unloading the decreases in local slips, caused by strain recovery of the bar, result in the bond stresses near the attack end of the bar decreasing more rapidly than those on the remaining, previously stressed portions of the bar close to the free end. Thus, as shown in Fig. 29(a), unloading affects the bond stress distribution caused by the previous peak load only over a distance $L_a$ from the loaded end. For distances more remote from the loaded end than $L_a$, the bond stress distribution remains that dictated by the previous peak load. The length $L_a$, measured from point A', increases as unloading continues.

If the length $L_p$ in Fig. 29(a) is divided into a number of discrete segments, then the free body diagram for the $i^{th}$ segment is as shown in Fig. 29(b). The equations applicable to that segment are:

$$S_i = S_{i-1} + \varepsilon_{i-1}\,\Delta L_{i-1} = \sum_{j=1}^{i-1} \varepsilon_j \Delta L_j, \quad i \geq 2 \qquad .......(4\text{-}132)$$

$$\tau_i = f(S_i,\ \text{bond stress history of the } i^{th} \text{ segment}) \qquad .......(4\text{-}133)$$

$$\sigma_i = \sigma_{i-1} + \frac{\tau_i \Delta L_i \Sigma_o}{A_b} \qquad .......(4\text{-}134)$$

$$\varepsilon_i = g(\frac{\sigma_i + \sigma_{i-1}}{2}, \text{ steel stress history of the } i^{th} \text{ segment}) \quad .......(4\text{-}135)$$

where:

$S_i$ = slip of the $i^{th}$ segment

$\tau_i$ = bond stress of the $i^{th}$ segment

$\sigma_i$, $\sigma_{i-1}$ = steel stress in the $i^{th}$ segment

$\varepsilon_i$ = average strain for the $i^{th}$ segment

$\Delta L_i$ = length of the $i^{th}$ segment

f = cyclic local bond stress-slip relationship of reinforcing bar

g = cyclic stress-strain relationship of reinforcing bar

If the force at the attack end is decreased to P, the length of $L_a$, the bond stress distribution, and the steel stress distribution under unloading and the displacement of point B can be determined by following procedures:

(1) Assume a value for $L_a$.

(2) Reduce deliberately the magnitude of the bond stress over the $K^{th}$ segment, $\tau_K$, by a amount of $\Delta\tau$. The value of $\Delta\tau$ is an extremely small value and symbolizes that the effect of unloading on the bond stress distribution has penetrated to the $k^{th}$ segment. The smaller the value of $\Delta\tau$, the more accurate is the prediction for bond stress distribution under unloading. In this study, the value of $\Delta\tau$ was arbitrarily taken as 5% of the magnitude of $\tau_K$. It can then be assumed that for distances more remote from the attack end than the $k^{th}$ segment the bond



stress distribution resulting from the previous peak loading is not influenced by the decrease in loading at the attack end.

(3) Apply repetitively Eqs. (4-132) through (4-135) to every segment of the bar and thus obtain the steel stress at the attack end, $\sigma_B$, due to a decrease in stress $\Delta\tau$ for the $K^{th}$ segment.

(4) Check if $\sigma_B = \frac{P}{A_b}$. If not, repeat steps 1 through 4 varying the position of the $k^{th}$ segment until a suitable value for La is found. Then, the bond stress and steel stress distributions under the force P can be determined.

(5) The displacement of point B equals the local slip at point A' plus the elongation of segment A'B.

Case 2: When a bar is subjected to a severe reversed load of magnitude P, the bond stress distribution for the previous peak load may be totally superseded by that for the reversed loading. As shown in Fig. 30(a), if the increase in load is large, the bond stress distribution caused by the reversed loading penetrates to a distance $L_b$ from the attack end where $L_b$ is greater than the distance $L_p$ to which the bond stress penetrated for the previous peak load. The length $L_b$ is divided into a discrete number of segments and the free body diagrams for the first and $i^{th}$ segment drawn as shown in Fig. 30(b). In order to determine the length $L_b$, the load-displacement relationship at the attack end and the bond stress distribution along the anchorage length of the bar, procedures are used as follows:

(1) Assume a value for $L_b$.

(2) Since the segment CD in Fig. 30(a) has effectively been subjected to monotonic loading, take, as shown in Fig. 30(b), the bond

ess over the segment closest to the free end of the bar as $\tau_o$. The value of $\tau_o$ is calculated from Eq. (4-15).

(3) Apply Eqs. (4-132) through (4-135) to all segments. The steel stress at point B, $\sigma_B$, can then be determined.

(4) Check if $\sigma_B = \frac{P}{A_b}$. If not, repeat steps 1 through 4 until an appropriate value for $L_b$ is obtained.

(5) After the value for $L_b$ is determined, the bond stress distribution along the anchorage length of the bar can also be determined. The displacement of point B is taken as the sum of the local slip at point A' and the elongation of segment A'B.

Case 3: If, as shown in Fig. 31(a), as a result of severe loading the bond stress wave penetrates to the tail end of the bar, then the length for the bond stress distribution is taken as L and the bond stress, $\tau_1$, distributed over the first segment becomes an unknown. In order to determine the displacement at the attack end and the bond stress distribution along the length of the bar, the length L is divided into a discrete number of segments as shown in Fig. 31(b). The free body diagrams for the first and $i^{th}$ segments are also shown in Fig. 31(b).

For the $i^{th}$ segment, the equations involved are:

$$S_i = \begin{cases} S_{i-1} + \varepsilon_{i-1}\Delta L_{i-1} = S_1 + \sum_{j=1}^{i-1} \varepsilon_j \Delta L_j, & i \geq 2 \\ S_1, & i=1 \end{cases} \quad \text{.......(4-136)}$$

$$\tau_i = f(S_i, \text{ bond stress history of the } i^{th} \text{ segment}) \quad \text{.......(4-137)}$$

$$\sigma_i = \sigma_{i-1} + \frac{\tau_i \Delta L_i \Sigma_o}{A_b} \quad \text{.......(4-138)}$$



$$\varepsilon_i = g(\frac{\sigma_i + \sigma_{i-1}}{2}, \text{ steel stress history of the } i^{th} \text{ segment}) \quad \text{.......(4-139)}$$

The procedures outlined below are used to determine the value for $S_1$ or $\tau_1$, the bond stress distribution and the displacement at the attack end of the bar.

(1) Assume a value for $S_1$ or $\tau_1$. Then, determine the corresponding value for $\tau_1$ or $S_1$ from Eq. (4-137).

(2) Starting from the first segment, apply repeatedly Eqs. (4-136) through (4-139) to every segment and determine the value $\sigma_B$.

(3) Check if $\sigma_B = \frac{P}{A_b}$. If not, repeat steps 1 through 3 until an appropriate value for $S_1$ or $\tau_1$ is obtained.

(4) After determining the value for $S_1$ or $\tau_1$, the bond stress distribution and the displacement of point B can be found. The displacement of point B is taken the local slip at point A' plus the elongation of segment A'B. The local slip at point A', in this case, is equal to the sum of the local slip at the tail end of the bar and the elongation of the bar over segment A'D in Fig. 31(a).

Case 4: As shown in Fig. 32(a), if a bar is subjected to severe compressive loading, the concrete around the tail end of the bar can be pushed out as a wedge. It is assumed that a wedge forms at the tail end if the average value for the bond stresses distributed over the segment CD reaches $\tau_{cr}$, calculated from Eq. (4-19). For subsequent loadings, it is considered that the bonded length for the bar becomes $L_c$ and the segment CD does not contribute to the bond capacity. The length $L_c$ is divided into a discrete number of segments. Free body diagrams for the first and $i^{th}$ segments are shown in Fig. 32(b).

The procedures for determining the bond stress distribution along the length of the bar and the load-displacement relationship at the attack end of the bar are the same as those described in case 3.

The listing for the computer program developed using the cyclic load-displacement model is presented in Appendix B.

### 4.4.2 The Anchorage Length

For specimens with straight bars, the anchorage length is taken as the full embedment length for the bar. For bars terminating in 90-degree hooks, an equivalent anchorage length must be assumed in order to utilize the model. By comparing the test results for specimens with hooked bars and the predicted results for specimens with various arbitrarily assumed anchorage lengths, it was found that the predicted load-displacement curves were in good agreement with the measured load-displacement curves when the equivalent anchorage length was taken as:

$$L_e = L_s + R_h \qquad \text{.......(4-140)}$$

where:

$L_e$ = equivalent anchorage length

$L_s$ = lead-in length to the hook

$R_h$ = radius of the hook

## 4.5 Discussion

Measured load-displacement curves for the twenty-two simulated beam-column specimens are shown in Figs. 33 through 54. The broken lines



on each load-displacement diagram represent the result for a specimen identical to that shown, having a straight bar and loaded monotonically to failure. Also shown on each figure are load histories defined in terms of ductility ratios for sucessive half cycles of loading. The ductility ratio was taken as the relative displacement at the attack end between the displacement for the previous zero load and the displacement for the peak load divided by the displacement for yielding in the first inelastic half cycle. The displacements for first yielding were very similar for all specimens and equal to $40 \times 10^{-3}$ inches.

Variables examined in those tests were the loading history, the yield strength for the bar, the size of the bar, the embedment length for the bar, the strength of the concrete and the use of a straight bar or a bar terminating with a standard 90-degree hook.

### 4.5.1 Monotonic Model

Comparisons between the test results and the results predicted by the monotonic model, described in Section 4.3, are shown in Figs. 55 through 73. Predicted results are shown by solid curves and experimental results, corresponding to actual measured values of load and displacement for each loading increment, are shown by crosses. Where the test specimens were subjected to reversed cyclic loading, experimental results are shown for the first loading half cycle only. Thus, no particular significance should be attached to the correlation between the points at which the measured and predicted relationships reach their maximum values except for specimens S101 and B81 which were loaded monotonically to failure. From these comparisons it can be seen that the measured load-displacement curves are in good agreement with the predicted curves and that for S101 and B81 measured and predicted failure conditions are in close agreement. On the average the model predicts stiffnesses for the elastic range that are slightly greater than those measured for No. 10 bars, and slightly less than those measured for No. 6 bars.

The model predicts that for specimens with straight bars, the behavior of the bond joint under monotonic loading is determined by the strength of the concrete, the stress-strain characteristics of the bar and the embedment length for the bar. Fig. 74 shows the effect of concrete strength on predicted load-displacement curves. In Fig. 74 the responses predicted for 5000 psi, 4000 psi and 3200 psi concretes are compared with that for an identical joint of 2890 psi concrete, S101. From that comparison, it is clear that the higher the concrete strength, the larger are the maximum capacity and the stiffnesses for the elastic and inelastic range. The displacements corresponding to the maximum capacity for 5000 psi and 4000 psi concretes are predicted to be considerably smaller than that for the 2890 psi concrete. However, for 3200 psi concrete the displacement corresponding to the maximum capacity is almost the same as that for the 2890 psi concrete. The bar embedded into 5000 psi, 4000 psi and 3200 psi were predicted as fracturing at the maximum load whereas the bar embedded in the 2890 psi concrete was predicted as pulling out of the concrete. When a bar is stressed into the inelastic range, the slope of the load-displacement curve decreases markedly. It is believed that the yield strength of the bar, $f_y$, the length of the yield plateau in the bar's stress-strain curve, $\Delta_{sh}$, and the bar's strain hardening modulus, $E_{sh}$, all affect the behavior of the



bond joint. The theoretical effects of those three factors on predicted load-displacement curves are shown in Figs. 75, 76 and 77 respectively. In Fig. 75, the predicted load-displacement curve for a Grade 60 bar is compared with that for a Grade 40 bar with identical $\Delta_{sh}$ and $E_{sh}$. Before yielding of the Grade 40 bar, the load-displacement curves are identical. The predicted curve for Grade 40 bar deviates from elastic curve earlier than that for Grade 60 bar. After yielding of those bars, the predicted load-displacement curves are essentially parallel to each other. The effects of the strain hardening modulus on predicted load-displacement curves are shown in Fig. 76. It can be seen that the greater the strain hardening modulus, the greater are the maximum capacity and the stiffness for the inelastic range. However, the overall response for the bar with greater $E_{sh}$ is less ductile. In Fig. 77, the effect of the length of the yield plateau on the bar's stress-strain curve is studied. The length of the yield plateau has marked effect on the predicted load-displacement curve immediately after yielding of the bar. However, the displacement is increased further, the load-displacement curves remain essentially parallel to each other. The maximum capacity and the displacement corresponding to the maximum capacity for the bar with the smaller $\Delta_{sh}$ are less than those for a bar with an identical $f_y$ and $E_{sh}$, but larger $\Delta_{sh}$. Fig. 78 shows that before attainment of the maximum capacity the load-displacement curve is not sensitive to the embedment length of the bar. The embedment length of the bar, however, affects greatly the maximum capacity of the joint and the displacement corresponding to the maximum capacity once the bar reaches its ultimate strength. In the monotonic load-displacement model, it is assumed when the bond stress reaches $\tau_c$, cone-like cracking occurs around the bar and drastically changes the mechanism of stress transfer to the concrete around the bar. The slope of the load-displacement curve decreases with increase in loading. As shown in Fig. 79, the penetration of $\tau_c$ along the length of the bar indicates the distance to which cone-like cracking can be expected. It is assumed that the longitudinal crack between lugs forms as the bond stress reaches $\tau_{max}$. The length of the longitudinal crack, measured from the attack end, is determined by the penetration of of $\tau_{max}$. In the simulated beam-column specimens, it was found that bond stresses near the attack end of the bar did not reach $\tau_{max}$ until after yielding of the bar, *as shown in* Fig. 79. The distance at which $\tau_{max}$ was achieved moved gradually towards the tail end of the bar as the loading increased. When loading was increased to close to the maximum capacity of the specimen, the rate at which $\tau_{max}$ penetrated along the bar increased very rapidly. Finally, $\tau_{max}$ penetrated to the tail end of the bar as the bond joint failed.

For bond joints terminating in 90 degree hooks, the model predicts that the behavior of the bond joint under monotonic loading is determined by the strength of the concrete, the stress-strain characteristics of the bar and the lead-in length to the hook. As Figs. 80 through 83 show, the effects of the concrete strength and the stress-strain characteristics of the bar on predictions of the load-displacement curves for joints with 90 degree hooks are essentially the same as those for joints with straight bars. The effect of the lead-in length to the predicted load-displacement curves is shown in Fig. 84. A longer lead-in length, results in a greater maximum capacity and a much greater maximum



displacement. The load-displacement curves before failure are identical since in the model the degree of confinement for the hook is assumed to remain constant as the lead-in length decreases. Fig. 85 shows the correlation between the load-displacement curve and the penetration of $\tau_c$ and $\tau_{max}$ for Specimen B81. In this figure, it is shown again that bond stresses near the attack end of the bar did not reach $\tau_{max}$ until after yielding of the bar. Since the failure for joints terminating in 90 degree hooks is due to the spalling of concrete cover for the hook, the longitudinal crack is not predicted as penetrating to the hook prior to failure of the joint. As shown in Fig. 85(b), the longitudinal crack, which corresponds to $\tau_{max}$, is predicted as having penetrated to only about half way along the lead-in length at the time of failure of the joint. However, the cone-like cracking, which corresponds to $\tau_c$ and always penetrates further than the longitudinal crack, and is predicted as having penetrated to the end of the lead-in zone at the time of failure of the joint.

### 4.5.2 Cyclic Model

Comparisons between the predicted and measured load-displacement relationships for cyclic loading are shown in Figs. 86 through 126. The number of cycles, a minimum of two for each specimen cyclically loaded, were chosen at random.

For tensile half cycles, except for Fig. 102, the comparison between the predicted and measured values is good. The reason for the poor correlation in Fig. 102 is that Specimen S107 had a low concrete strength. If the concrete strength is low, the maximum bond stress $\tau_{max}$, determined by Eq. (3-9), and the local bond stress-slip relationship, discussed in Chapter 3, may not be correct and the predicted load-displacement curves are likely to be too conservative. For compressive half cycles, the predicted load-displacement curves are generally less stiff than the measured curves and the compressive peak loads predicted by the model are significantly smaller than the test results. That poor agreement for compressive half cycles is attributed to two factors: (1) the contribution of concrete outside the column steel to the bond capacity of the bar for compressive loadings is totally ignored in the cyclic load-displacement model and (2) the contraction of the steel embedded into the concrete, loaded previously into the inelastic range, and subjected to compression may be much smaller than that predicted by the cyclic stress-strain relationship, presented in Chapter 2. Thsoe relationships were developed from test results of bars without surrounding concrete. Once cracks create a cone in the concrete outside the column steel, it is obvious that for tensile loadings, there will be little stress transfer between the bar and the concrete for the portion of the bar lying outside the column steel. For compressive loadings, however, it is reasonable to expect that the wedge will be pushed back into the main body of concrete and that there will be significant stress transfer between the bar and the concrete over the length of the wedge. The wedge's contribution to the bar's bond strength decreases as the displacement increases and as the number of cycles between constant slip limits increases, as shown in the comparisons for Specimens S102, S103, S105, S106, B85 and S64 in Figs. 86, 87, 88, 89, 90, 91; 93, 94, 95; 96, 97, 98, 99; 115, 116 and 123, 124, 125. For tensile loadings, the steel strains along the bar can be predicted reasonably well by using the



stress-strain relationship for the steel. When the bar is subject to tensile loadings, the presence of the surrounding concrete does not significantly affect the elongation of the bar. However, for compressive loadings, aggregate interlock effects may force cracks in the concrete surrounding the bar to remain open and thus significantly constrict the bar's contraction. It is not unreasonable to expect that the bar's real contraction will be less than that predicted by the stress-strain model especially if the joint in which the bar is anchored is subjected to significant shearing actions. As a result it is believed that it is reasonable to find, that for compressive loadings measured peak loads are larger than predicted values and measured load-displacement curves stiffer than predicted curves.

A comparison of the measured and predicted strains along the length of the bar was made for Specimens S102, S103, S104 and S107. The variables considered in those comparisons were load history, the yield strength of the bar and the strength of the concrete. Except for Figs. 128, 129 and 136, the predicted shapes of strain distributions along the bar are essentially in good agreement with the measured shapes. Possible reasons for the poor correlations in Figs. 128, 129 and 136 are: (1) some strain gages did not work well and (2) cracking within the joint due to shear and bending effects. For example, in Fig. 129 the strain readings at the tail end of the bar are close to the yield strain of the bar. In reality, that is extremely unlikely unless shear cracking strongly affected bar strains.

From a comparison of strains along the length of the bars, it is apparent that yielding in the bars penetrated about 3 in. deeper into the specimen than values predicted by the model. In general, measured strains along the bars for tensile loadings are somewhat larger than predicted values while for compressive loadings measured strains are shomewhat smaller than predicted values. Those trends may be explained partially by the effects of cracking discussed previously and by discrepancies in the actual and predicted stress-strain relationships for the bars and local bond stress-slip relationships for the bars. In the latter case the models developed in Chapter 2 and 3 respectively were based on limited test results each involving only one size of bar and may therefore be inaccurate. However, overall the strain data suggests that the deterioration of bond stress in the tests was slightly more severe than predicted.



# CHAPTER 5

## SIGNIFICANCE OF RESULTS FOR SEISMIC CODE PROVISIONS

Test results show clearly that connections between flexural members and columns should not be assumed to be rigid for seismic-type loadings. Reinforcing bar pull-out causes rigid body rotations at the connections between flexural members and columns.

For adequate seismic resistance of concrete members in ductile moment resistant space frames designed to UBC 1979, bar strengths greater than the yield strength must be able to be achieved under reversed cyclic loadings to attack end displacements up to at least 10 times greater than those for first yielding. For all specimens used in this study, the embedment lengths provided and the development lengths required by ACI 318-77 Code, ACI-ASCE Committee 352's recommendations (38) and ACI Committee 408's recommendations (39) are listed in Table 7. It is apparent from Table 7 that Specimens S61, S62 and S63 had embedment lengths equal to or greater than the development lengths required by ACI 318-77 Code. However, those three specimens failed at displacements considerably less than 10 times those for first yielding. Thus, those results indicate that the ACI 318-77 provisions for development length in Chapter 12 are not adequately conservative for No. 6 Grade 60 straight bars subject to the types of reversed cyclic loadings likely when thsoe bars are used in hinging regions in ductile moment resistant frames.

There is no direct evidence from the test data in Table 7 to show the appropriateness of the ACI 318-77 provisions for No. 10 and No. 8 bars subject to similar reversed cyclic loadings. However, from those results it is that for No. 10 Grade 60 bars terminating in 90 degree hooks the lead-in length must be greater than 15.75 in. for adequate behavior under reversed cyclic loading and that for No. 8 Grade 60 bars the lead-in length can be less than 18.0 in. for adequate behavior under reversed cyclic loading. For reversed cyclic loadings into the inelastic range, the formulas recommended by ACI-ASCE Committee 352, which take into account the ineffectiveness of the concrete beyond the line of the column reinforcement at the loaded end of the bar and the probable force in the bar rather than the nominal yield force, result in more conservative requirements for development length than those recommended by ACI 318-77. The formulas recommended by ACI Committee 408, which tend to update the ACI 318-77 provisions for development length, can result in more conservative requirements for development length for straight bars than ACI-ASCE Committee 352's recommendations. However, for bars terminating in 90 degree hooks and subject to reversed cyclic loadings, test results and Table 7 show that the ACI Committee 408's recommendations for lead-in lengths are not appropriate.

The model presented in this thesis is capable of predicting the load-displacement curves for a wide variety of loading histories and can be used to predict the minimum anchorage length for a bar to be able to maintain its yield strengths for reversed cyclic displacements up to ten times those for first yielding. Consider for example the use of this model to predict the minimum anchorage lengths satisfying the 10 times yield displacement criteria for reversed cyclic loading for Specimens S101 and B103. For Specimen S101 subject to reversed cyclic loading, the correlation between the predicted monotonic response curve, indicated by a broken line, and the cyclic response curves, indicated by solid lines,



is shown in Fig. 137. For the cyclic loading shown, it is predicted that the maximum capacity will occur at a displacement of 0.22 in. and that for greater displacements the capacity will decrease with cycling. That maximum displacement is about 49% of that achieved for monotonic loading. The embedment length had to be increased from 24 in. to 30 in. in order that the maximum capacity was maintained up to displacements 10 times those for first yielding. The correlation between the predicted monotonic and cyclic curves for Specimen S101 with a 30 in. embedment length is shown in Fig. 138. The distinct improvement in the form of the hysteresis loops with greater embedment length is also apparent from a comparison of Figs. 137 and 138.

For Specimen B103 subject to reversed cyclic loading, the correlation between the predicted monotonic load-displacement curve and the cyclic load-displacement curves is shown in Fig. 139. For the cyclic loading shown, it is predicted that the maximum capacity will occur at a displacement of 0.17 in. and for greater displacement the capacity will decrease with cycling. The displacement corresponding to the maximum capacity is about 52% of the achieved for monotonic loading. It was found that the lead-in length had to be increased from 15.75 in. to 23 in. in order that the maximum capacity was maintained up to displacements ten times those for first yielding. The correlation between the predicted monotonic and cyclic load-displacement curves for Specimen B103 with a 23 in. lead-in length is shown in Fig. 140. From the comparison of Figs. 139 and 140, it is also apparent that Specimen B103 with a 23 in. lead-in length has distinctly better hysteresis loops than the same specimen with a 15.75 in. lead-in length.

Shown in Fig. 141 is a comparison of the result obtained in the test on specimen B85 ($f'_c$ - 3,300 psi; 18.0 in. load-in. length) and the predicted result for cyclic loading. The test result is indicated by broken lines and the predicted result by unbroken lines. The main deviation between the measured and predicted responses is where displacements are negative and the loading compressive. That deviation is due to the model not recognizing that the wedge of concrete that surrounds the bar at its attack end, Fig. 25, is partially effective for compressive loading even though it is totally ineffective for tension loading. The initial stiffness on reloading in tension is also less than that predicted by the model. The reason for that deviation is not readily apparent.

Shown in Fig. 142 is the predicted result for loading a specimen similar to B85 to failure. The predicted monotonic response curve is indicated by the broken line and the predicted cyclic load response curve by the unbroken lines. The assumed loading history was three fully reversed cycles at ductility ratios of 2.0, 4.0, 6.0, 8.0, and 10.0. Failure is predicted to occur due to bar slippage in compression at the ductility ratio of 10.0. Obviously, the model presented here can be used to predict the effects of different loading histories on anchorage length requirements and is therefore a suitable first step for developing code requirements for anchorage for seismic loadings.

# CHAPTER 6

# CONCLUSIONS

Based on the results and analysis reported here, it is concluded:

(1) It is possible to predict the load-slip characteristics of bars anchored in reinforced concrete connections by integration of the local bond-slip and stress-strain characteristics for those bars. Further studies will probably be needed to improve the models developed in this study for local bond-slip and stress-strain characteristics.

(2) The models developed in this thesis will provide reasonable predictions of load-slip characteristics for monotonically or reversed cyclically loaded bars embedded in concrete connections having properties of the type tested in this study.

(3) The assumption that beam-column joints of moment-resisting reinforced concrete frames are rigid is incorrect. The main reinforcing bars of beams can develop marked slips relative to the concrete at the interface between those beams and the columns into which they frame. The load-slip characteristics for the bars are as important as their stress-strain characteristics for predictions of the overall response of connections.

(4) Cyclic reversed loading induces a progressive deterioration of bond between concrete and reinforcing bars. The characteristics of that deterioration are a major factor determining the rotation characteristics of a connection.

(5) Bond deterioration characteristics are sensitive to load history and in particular to the maximum displacement attained in the compression half cycle compared to the displacement in the tension half

cycle.

(6) The concrete strength, the stress-strain characteristics for reinforcing bar and the embedment length for the bar are significant factors affecting the stiffness, the capacity, the rate of bond deterioration and the load-slip characteristics of the connection.

(7) For bars terminating in 90 degree hooks, the hook for reversed cyclic loading provides less contribution to the bond capacity than for monotonic loading. The effective embedment length for hooked bars under reversed cyclic loadings can be taken as the lead-in length for the bar plus the radius of the hook.

(8) Failure under reversed cyclic loading occurs at ultimate load and deformation capacities considerably less than those for monotonic loading.

(9) The appearance of the test specimens with hooks after failure suggests that, in buildings surviving an earthquake, loss of cover from behind the hook should be interpreted as a warning of the possible destruction of the anchorage for such bars.

(10) The formulas recommended in ACI 318-77 for development length are inappropriate to No. 6 Grade 60 straight bars subject to reversed cyclic loadings of the type anticipated for bars in hinging regions of ductile moment resistant frames.

(11) For No. 10 Grade 60 straight bars subject to reversed cyclic loadings of the type anticipated for bars in hinging regions of ductile moment resistant frames, ACI 318-77 provisions result in conservative requirements for development length for straight bars. However, for No. 10 Grade 60 bars terminating in 90 degree hooks, the lead-in length to



the hook as required by ACI 318-77 provisions is apparently just adequate.

(12) For reinforcing bars reversed cyclically loaded into the inelastic range, the formulas recommended by ACI-ASCE Committee 352 result in more conservative requirements for development length than those recommended by ACI 318-77.

(13) For straight bars subject to reversed cyclic loadings into the inelastic range, the formulas recommended by ACI Committee 408 can result in more conservative requirements for development length than those recommended by ACI 318-77 and ACI-ASCE Committee 352. However, ACI Committee 408's recommendations are unconservative for bars terminating in 90 degree hooks and subject to reversed cyclic loadings into the inelastic range.

TABLE 1 - PROPERTIES OF SPECIMENS USED FOR COMPARISONS BETWWEEN HASSAN'S MODEL AND SUBSEQUENT STUDIES

| Specimen No. | Type of Loading | $f'_c$ (psi) | Type of Bar |
|---|---|---|---|
| S104 | Cyclic | 3,000 | #10 - NW Grade 60 Straight |
| S61 | Cyclic | 3,450 | #6 - NW Grade 60 Straight |
| S107 | Cyclic | 2,640 | #10 - NW Grade 40 Straight |



TABLE 2 - PROPERTIES OF SPECIMENS

| Specimen No. | Concrete Strength (psi) | Type* of Rebar | Type of Loading | Dimensions (in.) |
|---|---|---|---|---|
| S101 | 2,890 | #10 Grade 60 Straight | Monotonic | 66 x 24 x 6 |
| S102 | 3,630 | #10 Grade 60 Straight | Cyclic | 66 x 24 x 6 |
| S103 | 4,100 | #10 Grade 60 Straight | Cyclic | 66 x 24 x 6 |
| S104 | 3,000 | #10 Grade 60 Straight | Cyclic | 66 x 24 x 6 |
| S105 | 5,120 | #10 Grade 60 Straight | Cyclic | 66 x 24 x 6 |
| S106 | 3,760 | #10 Grade 60 Straight | Cyclic | 66 x 24 x 6 |
| S107 | 2,640 | #10 Grade 60 Straight | Cyclic | 66 x 24 x 6 |
| B101 | 2,630 | #10 Grade 60 $90^o$ hook | Cyclic | 66 x 24 x 6 |

TABLE 2 - PROPERTIES OF SPECIMENS (CONTINUED)

| Specimen No. | Concrete Strength (psi) | Type* of Rebar | Type of Loading | Dimensions (in.) |
|---|---|---|---|---|
| B102 | 3,050 | #10 Grade 60 $90^{o}$ hook | Cyclic | 66 x 24 x 6 |
| B103 | 2,980 | #10 Grade 60 $90^{o}$ hook | Cyclic | 66 x 24 x 6 |
| B104 | 4,110 | #10 Grade 60 $90^{o}$ hook | Cyclic | 66 x 24 x 6 |
| B81 | 3,280 | #8 Grade 60 $90^{o}$ hook | Monotonic | 66 x 24 x 8 |
| B82 | 3,760 | #8 Grade 60 $90^{o}$ hook | Cyclic | 66 x 24 x 8 |
| B83 | 3,080 | #8 Grade 60 $90^{o}$ hook | Cyclic | 66 x 24 x 8 |
| B84 | 2,780 | #8 Grade 60 $90^{o}$ hook | Cyclic | 66 x 24 x 8 |



TABLE 2 - PROPERTIES OF SPECIMENS (CONTINUED)

| Specimen No. | Concrete Strength (psi) | Type* of Rebar | Type of Loading | Dimensions (in.) |
|---|---|---|---|---|
| B85 | 3,300 | #8 Grade 60 $90^{o}$ hook | Cyclic | 66 x 24 x 8 |
| S61 | 3,450 | #6 Grade 60 Straight | Cyclic | 66 x 16 x 6 |
| S62 | 3,400 | #6 Grade 60 Straight | Cyclic | 66 x 16 x 6 |
| S63 | 2,760 | #6 Grade 60 Straight | Cyclic | 66 x 16 x 6 |
| S64 | 4,170 | #6 Grade 60 Straight | Monotonic | 66 x 24 x 6 |
| S65 | 5,070 | #6 Grade 60 Straight | Cyclic | 66 x 24 x 6 |
| S66 | 3,880 | #6 Grade 60 Straight | Cyclic | 66 x 24 x 6 |

* All bars were manufactured by Northwest Rolling Mills

89

TABLE 4 - PROPERTIES OF LOCAL BOND SPECIMENS

| Specimen No. | Concrete Strength (psi) | Type of Loading | Bonded Length (in.) | Dimensions (in.) |
|---|---|---|---|---|
| LM1 | 3,270 | Monotonic | 1.64 | 12 x 12 x 7 |
| LC1 | 3,270 | Cyclic | 1.64 | 12 x 12 x 7 |
| LM2 | 3,980 | Monotonic | 1.64 | 12 x 12 x 7 |
| LC2 | 3,980 | Cyclic | 1.64 | 12 x 12 x 7 |
| LM3 | 4,470 | Monotonic | 1.64 | 12 x 12 x 7 |
| LC3 | 4,470 | Cyclic | 1.64 | 12 x 12 x 7 |

88

TABLE 3 - PROPERTIES OF TEST BARS

| Type of Bar | $f_y$ (ksi) | $E_s$ (ksi) | $\varepsilon_{sh}$ | $E_{sh}$ (ksi) | $\varepsilon_{su}$ | $f_{su}$ (ksi) | Nominal Diameter d (in.) | Asperity Slope, d Side 1 | Side 2 | Provided (in.) Lug Spacing | Asperity Height | ASTM A615 (in.) Max. Lug Spacing | Min. Asperity Height |
|---|---|---|---|---|---|---|---|---|---|---|---|---|---|
| #10 Grade 60 | 60 | 29600 | 0.006 | 715 | 0.185 | 95.9 | 1.27 | 44 | 55 | 0.82 | 0.085 | 0.889 | 0.064 |
| #10 Grade 40 | 47 | 29600 | 0.010 | 550 | 0.215 | 79.5 | 1.27 | 44 | 55 | 0.82 | 0.085 | 0.889 | 0.064 |
| #8 Grade 60 | 68 | 29000 | 0.0024 | 880 | 0.164 | 122.5 | 1.0 | 45 | 63 | 0.67 | 0.065 | 0.7 | 0.05 |
| #6 Grade 60 | 63 | 29000 | 0.003 | 900 | 0.152 | 112.5 | 0.75 | 35 | 44 | 0.5 | 0.048 | 0.525 | 0.038 |

TABLE 6 - COMPARISONS BETWEEN MORITA'S AND LIN'S CYCLIC BOND-SLIP MODELS

| Model Proposed by | $k_4$ (Kip/in$^3$) | $\alpha$ | $\beta$ | $f'_c$ (psi) |
|---|---|---|---|---|
| Morita and Kaku | 1,442 | 0.18 | 0.9 for $S_x^* < 0.002$ in.<br>$0.9 - 11.11(S_x - 0.002)$ for $0.002 \text{ in.} < S_x < 0.02$ in. | 4,300 – 5,000 |
| Lin | 3,000 | 0.15 | 0.9 for the loading direction for which $\lvert\tau\rvert$ has never been greater than $\tau_c$<br>$0.9 \geqslant \beta = 0.9 - 15\Delta S \geqslant 0.75$ for the loading direction for which $\lvert\tau\rvert$ has been greater than $\tau_c$ | 3,000 – 4,500 |

$S_x$ - the slip value of the point from which unloading is started



TABLE 5 - COMPARISONS BETWEEN MORITA'S AND LIN'S MONOTONIC BOND-SLIP MODELS

| Model Proposed by | $k_1$ (Kip/in$^3$) | $k_2$ (Kip/in$^3$) | $k_3$ (Kip/in$^3$) | $f'_c$ (psi) |
|---|---|---|---|---|
| Morita and Kaku | 721 $(10.6\sqrt{f'_c})$ | 39.7 $(\frac{f'_c}{1360})^3$ | — | 4,300 – 5,000 |
| Lin | $5\sqrt{f'_c}$ | $(\frac{f'_c}{1400})^3$ | 4.0 | 3,000 – 4,500 |

TABLE 7 - DEVELOPMENT LENGTHS FOR SPECIMENS (CONTINUED)

| Specimen No. | Concrete Strength (psi) | Type of Rebar | Development Lengths (in.) Provided | Required by ACI 318-77 | Required by Committee 352 | Required by Committee 408 | Displacement at Maximum Load / Displacement at First Yielding |
|---|---|---|---|---|---|---|---|
| S107 Cyclic | 2,640 | #10 Grade 40 | 24.0 | 29.2 | 38.4 | 41.8 | 2.8 |
| B101 Cyclic | 2,630 | #10 Grade 60 | 90° hook + 15.75 | 90° hook + 25.8 | 90° hook + 30.6 | 90° hook + 14.5 | 2.8 |
| B102 Cyclic | 3,050 | #10 Grade 60 | 90° hook + 15.75 | 90° hook + 22.7 | 90° hook + 27.1 | 90° hook + 13.1 | 3.1 |
| B103 Cyclic | 2,980 | #10 Grade 60 | 90° hook + 15.75 | 90° hook + 23.2 | 90° hook + 27.7 | 90° hook + 13.3 | 2.9 |
| B104 Cyclic | 4,110 | #10 Grade 60 | 90° hook + 15.75 | 90° hook + 17.0 | 90° hook + 20.9 | 90° hook + 10.4 | 4.5 |





TABLE 7 - DEVELOPMENT LENGTHS FOR SPECIMENS

| Specimen No. | Concrete Strength (psi) | Type of Rebar | Development Lengths (in.) Provided | Required by ACI 318-77 | Required by Committee 352 | Required by Committee 408 | Displacement at Maximum Load / Displacement at First Yielding |
|---|---|---|---|---|---|---|---|
| S101 Monotonic | 2,890 | #10 Grade 60 | 24.0 | 41.8 | 54.2 | 59.9 | 9.4 |
| S102 Cyclic | 3,630 | #10 Grade 60 | 24.0 | 37.3 | 48.6 | 53.4 | 3.0 |
| S103 Cyclic | 4,100 | #10 Grade 60 | 24.0 | 35.1 | 45.9 | 50.3 | 4.0 |
| S104 Cyclic | 3,000 | #10 Grade 60 | 24.0 | 41.0 | 53.3 | 58.7 | 1.9 |
| S105 Cyclic | 5,120 | #10 Grade 60 | 24.0 | 31.4 | 41.2 | 45.0 | 5.5 |
| S106 Cyclic | 3,760 | #10 Grade 60 | 24.0 | 36.6 | 47.8 | 52.5 | 4.4 |

TABLE 7 - DEVELOPMENT LENGTHS FOR SPECIMENS (CONTINUED)

| Specimen No. | Concrete Strength (psi) | Type of Rebar | Development Lengths (in.) Provided | Required by ACI 318-77 | Required by Committee 352 | Required by Committee 408 | Displacement at Maximum Load / Displacement at First Yielding |
|---|---|---|---|---|---|---|---|
| S61 Cyclic | 3,450 | #6 Grade 60 | 16.0 | 14.4 | 19.5 | 21.6 | 2.5 |
| S62 Cyclic | 3,400 | #6 Grade 60 | 16.0 | 14.5 | 19.6 | 21.6 | 6.3 |
| S63 Cyclic | 2,760 | #6 Grade 60 | 16.0 | 16.1 | 21.6 | 25.6 | 2.4 |
| S64 Monotonic | 4,170 | #6 Grade 60 | 24.0 | 14.4 | 19.5 | 21.6 | 4.1 |
| S65 Cyclic | 5,070 | #6 Grade 60 | 24.0 | 14.4 | 19.5 | 21.6 | 5.7 |
| S66 Cyclic | 3,880 | #6 Grade 60 | 24.0 | 14.4 | 19.5 | 21.6 | 16.1 |





TABLE 7 - DEVELOPMENT LENGTHS FOR SPECIMENS (CONTINUED)

| Specimen No. | Concrete Strength (psi) | Type of Rebar | Development Lengths (in.) Provided | Required by ACI 318-77 | Required by Committee 352 | Required by Committee 408 | Displacement at Maximum Load / Displacement at First Yielding |
|---|---|---|---|---|---|---|---|
| B81 Monotonic | 3,280 | #8 Grade 60 | $90^\circ$ hook + 18.0 | $90^\circ$ hook + 11.4 | $90^\circ$ hook + 14.5 | $90^\circ$ hook + 10.7 | 12.9 |
| B82 Cyclic | 3,760 | #8 Grade 60 | $90^\circ$ hook + 18.0 | $90^\circ$ hook + 9.8 | $90^\circ$ hook + 12.7 | $90^\circ$ hook + 9.7 | 2.8 |
| B83 Cyclic | 3,080 | #8 Grade 60 | $90^\circ$ hook + 18.0 | $90^\circ$ hook + 12.1 | $90^\circ$ hook + 15.3 | $90^\circ$ hook + 11.1 | 4.9 |
| B84 Cyclic | 2,780 | #8 Grade 60 | $90^\circ$ hook + 18.0 | $90^\circ$ hook + 13.4 | $90^\circ$ hook + 16.7 | $90^\circ$ hook + 11.9 | 6.5 |
| B85 Cyclic | 3,300 | #8 Grade 60 | $90^\circ$ hook + 18.0 | $90^\circ$ hook + 11.3 | $90^\circ$ hook + 14.4 | $90^\circ$ hook + 10.6 | 8.1 |

## REFERENCES


1. Earthquake Engineering Research, National Academy of Sciences, Washington D.C., 1969.

2. Anchorage and the Alaska Earthquake, American Iron and Steel Institute, New York, 1964.

3. The Venezuela Earthquake, July 29, 1967, American Iron and Steel Institute, New York, 1969.

4. ACI Standard Building Code Requirements for Reinforced Concrete (ACI 318-77), American Concrete Institute, Detroit, Michigan, 1977.

5. ASCE-ACI Committee 426, "The Shear Strength of Reinforced Concrete Members," Journal of the Structural Division, ASCE, Vol. 99, No. ST6, June 1973 and Vol. 100, No. ST8, August 1974.

6. Bertero, V. V. and Popov, E. P., "Hysteretic Behavior of Reinforced Concrete Flexural Members with Special Web Reinforcement," Proceedings of U.S. National Conference on Earthquake Engineering, Ann Arbor, Michigan, June 1975.

7. Hassan, F. M., "Bond Deterioration Under Simulated Seismic Loading," Ph.D dissertation, University of Washington, Seattle, Washington, 1973.

8. Nordby, G. M., "Fatigue of Concrete - A Review of Research," ACI Journal, Vol. 55, No. 2, August, 1958, pp. 191-220.

9. Bresler, B. and Bertero, V., "Behavior of Reinforced Concrete under Repeated Loading," Journal of the Structural Division, ASCE, Vol. 94, No. ST6, June 1968, pp. 1,567-1,590.

10. Brown, C. B., "Bond Failure Between Steel and Concrete," Journal of Franklin Institute, Vol. 282, No. 5, November, 1966.

11. Perry, E. S. and Nabil, Jundi, "Pullout Bond Stress Distribution under Static and Dynamic Repeated Loadings," ACI Journal, Proc. Vol. 66, May, 1969, pp. 377-380.

12. Goto, Y., "Cracks Formed in Concrete Around Deformed Tension Bars," ACI Journal, Vol. 68, No. 4, April 1971, pp. 245-251.

13. Okamura, H. and Takahashi, M., "Bond of Lightweight Aggregate Concrete to Deformed Reinforcing Bars," Report No. 7106, 24th General Meeting, The Cement Association of Japan, May, 1970.

14. Ismail, M. A. F., "The Effect of Cyclic Loads on Bond," M. Sc. Thesis, Rice University, Houston, Texas, March, 1968.





15. Ismail, M. A. F., "Bond Deterioration in Reinforced Concrete Under Cyclic Loading," Ph.D Thesis, Rice University, Houston, Texas, February, 1970.

16. Ismail, M. A. F. and Jirsa, J. O., "Behavior of Anchored Bars Under Low Cycle Overloads Producing Inelastic Strains," ACI Journal, Proceedings, Vol. 69, July, 1972, pp. 433-438.

17. Ismail, M. A. F. and Jirsa, J. O., "Bond Deterioration in Reinforced Concrete Subject to Low Cycle Loads," ACI Journal, Proceedings, Vol. 69, June, 1972, pp. 334-343.

18. Carpenter et al., "Structural Walls in Earthquake Resistant Structures," Experimental Program, Progress Report, Portland Cement Association, Skokie, Ill., August, 1975.

19. Yamazaki, J. and Hawkins, N. M., "Shear and Moment Transfer Between Reinforced Concrete Flat Plates and Columns," Report SM 75-2, Department of Civil Engineering, University of Washington, Seattle, WA, September, 1975.

20. Hanna, S. N., Mitchell, D. and Hawkins, N. M., "Slab-Column Connections Containing Shear Reinforcement and Transferring High Intensity Reversed Moments," Report SM 75-1, Department of Civil Engineering, University of Washington, Seattle, WA, August, 1975.

21. Hassan, F. M. and Hawkins, N. M., "Anchorage of Reinforcing Bars for Seismic Forces," Reinforced Concrete in Earthquake Zones, SP-53, American Concrete Institute, Detroit, 1977.

22. Hawkins, N. M., Kobayashi, A. S. and Fourney, M. E., "Reversed Cyclic Loading Bond Deterioration Tests," Report SM 75-5, Department of Civil Engineering, University of Washington, Seattle, Nov., 1975.

23. Hawkins, N. M., Kobayashi, A. S., Chan, Y-L. A. and Lin, I-J., "Bond Deterioration under Seismic Loading," SM 79-1, Department of Civil Engineering, University of Washington, Seattle, WA, May, 1979.

24. Aminian, K., "Effect of Cyclic Loading on Bond Deterioration of Number 6 Reinforcing Bars," M.S.C.E. Thesis, University of Washington, Seattle, WA, 1977.

25. Popov, E. P., Bertero, V. V., Cowell, A. D. and Viwathanatepa, S., "Reinforcing Steel Bond Under Monotonic and Cyclic Loadings," SEAOC Conference, Lake Tahoe, Sept. 29, 1978.

26. Viwathanatepa, S., Popov, E. P. and Bertero, V. V., "Effects of Generalized Loadings on Bond of Reinforcing Bars Embedded in Confined Concrete Blocks," Report No. UCB/EERC-79/22, Earthquake Engineering Research Center, University of California, Berkeley, August, 1979.

27. Hawkins, N. M., Wong, C. F. and Yang, C. H., "Slab-Edge Column Connections Transferring High Intensity Reversing Moments Normal to the Edge of the Slab," Report SM 78-1, Department of Civil Engineering, University of Washington, May, 1978.

28. Hawkins, N. M. and Lin, I. J., "Bond Characteristics of Reinforcing Bars for Seismic Loadings," Third Canadian Conference on Earthquake Engineering, Proceedings, Volume 2, Montreal, 1979.

29. Su, T. L., "Behavior of Reinforcing Bars Under Inelastic Cyclic Reversed Loadings," M.S.C.E. Thesis, University of Washington, Seattle, WA, 1979.

30. Liu, Y. H., "Local Bond Strength of Concrete Under Cyclic Loading," M.S.C.E. Report, University of Washington, Seattle, WA, 1978.

31. Jeang, F. L., "Local Bond Strength of Concrete Under Cyclic Reversed Loadings," M.S.C.E. Thesis, University of Washington, Seattle, WA, 1980.

32. Popov, E. P., "Mechanical Characteristics and Bond of Reinforcing Steel Under Seismic Conditions," Workshop on Earthquake-Resistant R/C Building Construction, University of California, Berkeley, July, 1977.

33. Morita, S. and Kaku, T., "Local Bond Stress-Slip Relationship Under Repeated Loading," Preliminary Report, LABSE Symposium, Lisbon, 1973.

34. Morita, S. and Kaku, T., "Cracking and Deformation of Reinforced Concrete Prisms Subjected to Tension," Preliminary Report, LIEGE, 1975.

35. Clough, R. W. and Johnston, S. B., "Effect of Stiffness Degeneration on Earthquake Ductility Requirements," proceedings, Japan Earthquake Symposium, October, 1966, pp. 227-232.

36. PCI Design Handbook, Prestressed Concrete Institute, Chicago, 1971.

37. Marques, J. L. G. and Jirsa, J. O., "A Study of Hooked Bar Anchorages in Beam-Column Joints," ACI Journal, Proceedings, V. 72, No. 5, May, 1975, pp. 198-209.

38. ACI-ASCE Committee 352, "Recommendations for Design of Beam-Column Joints in Monolithic Reinforced Concrete Structures," ACI Journal, Vol. 73, No. 7, July 1976.

39. ACI Committee 408, "Suggested Development, Splice, and Standard Hook Provisions for Deformed Bars in Tension," ACI Journal, Vol. 1, No. 7, July, 1979.




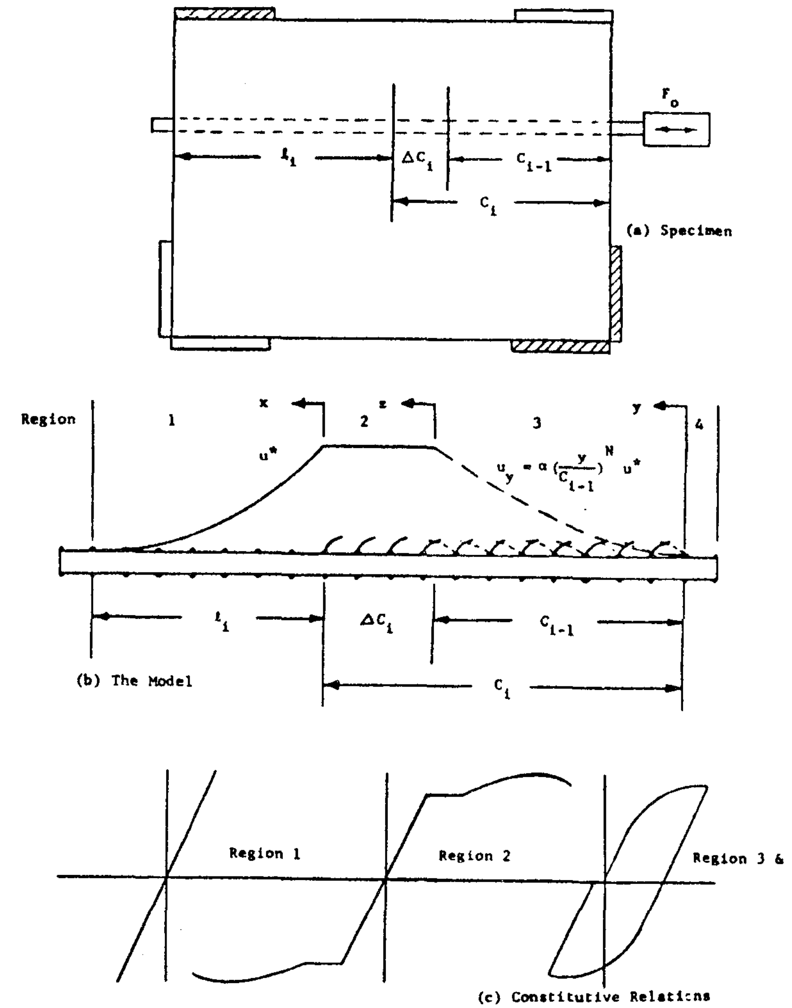


FIG. 1 HASSAN'S CYCLIC MODEL IDEALIZATION

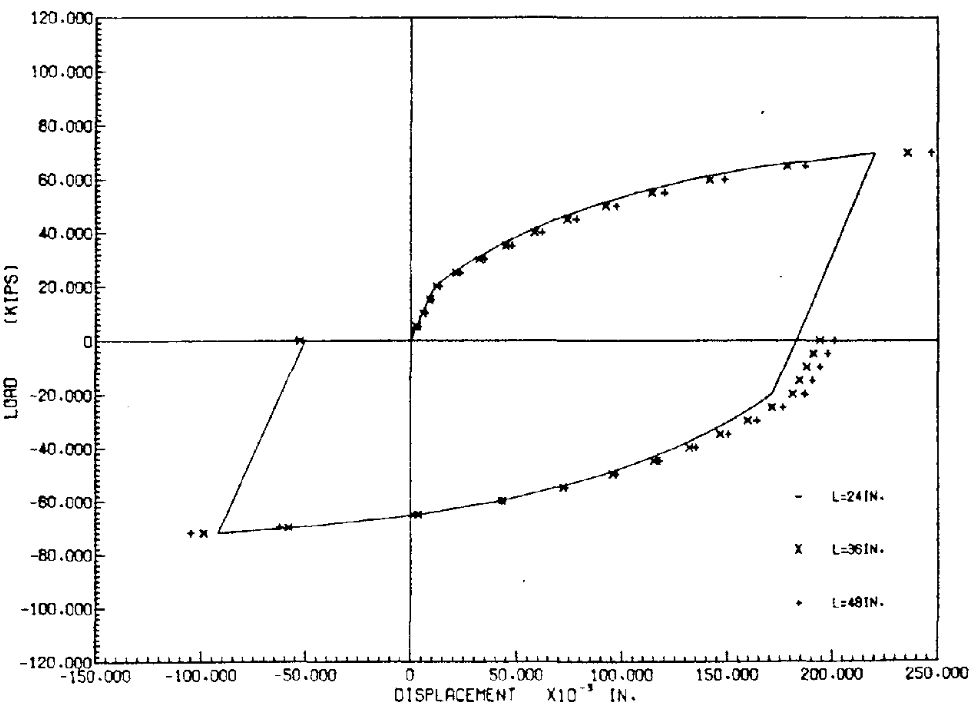


FIG. 2 LENGTH OF EMBEDMENT EFFECTS PREDICTED BY HASSAN'S MODEL

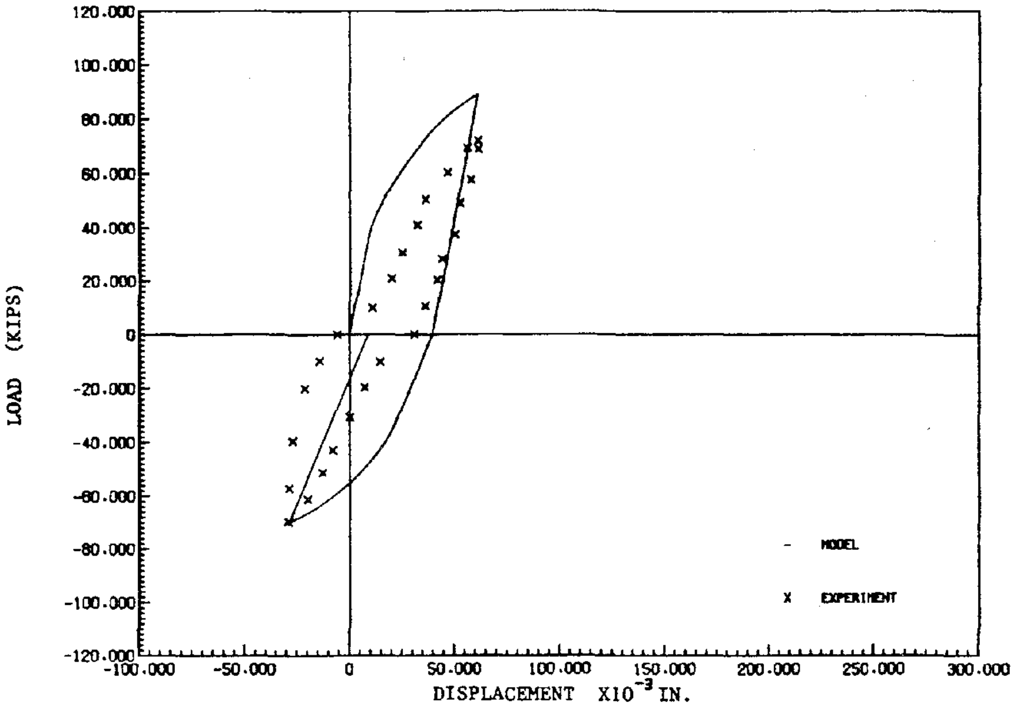


FIG. 3 COMPARISON OF PREDICTIONS OF HASSAN'S CYCLIC MODEL AND EXPERIMENT, SPECIMEN S104, CYCLE 2

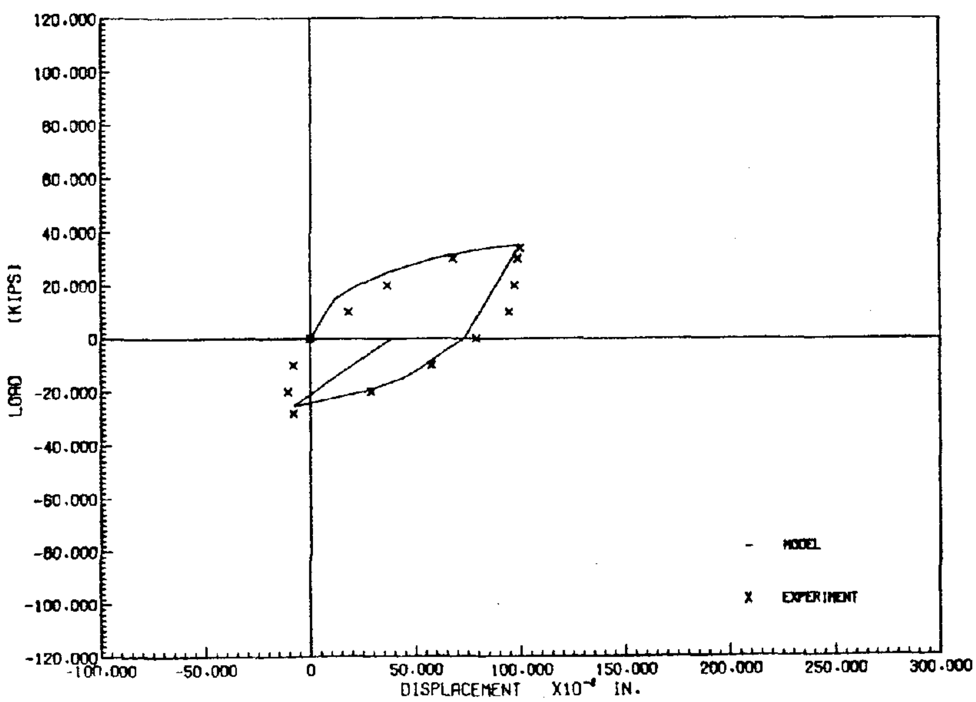


FIG. 4 COMPARISON OF PREDICTIONS OF HASSAN'S CYCLIC MODEL AND EXPERIMENT, SPECIMEN S61, CYCLE 3

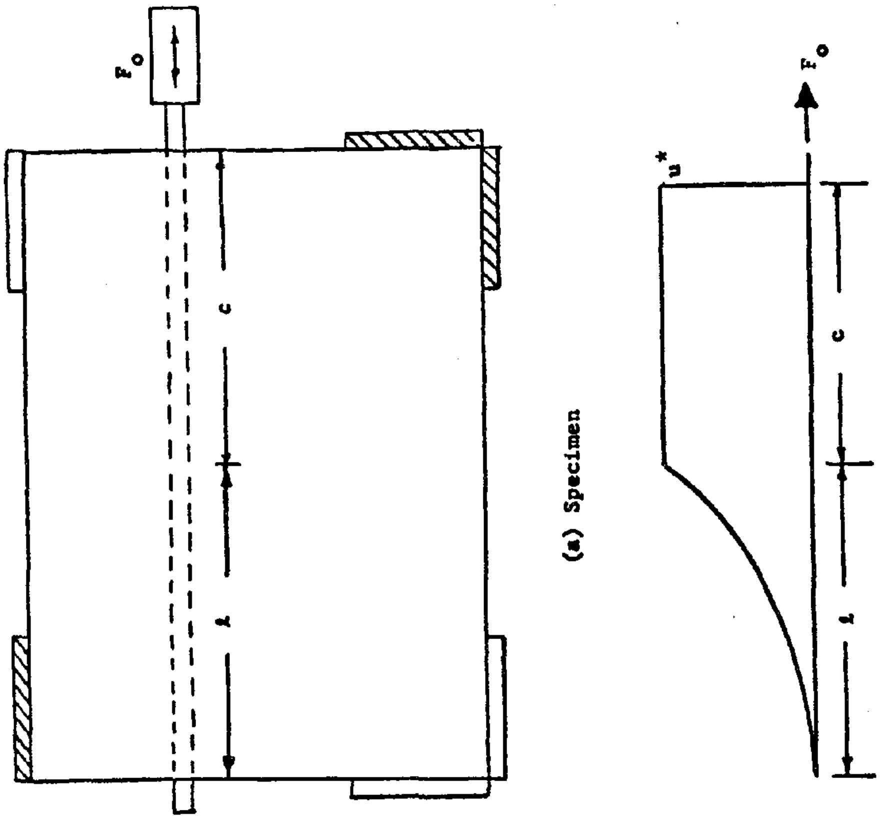


FIG. 6 IDEALIZATION FOR HASSAN'S MONOTONIC MODEL

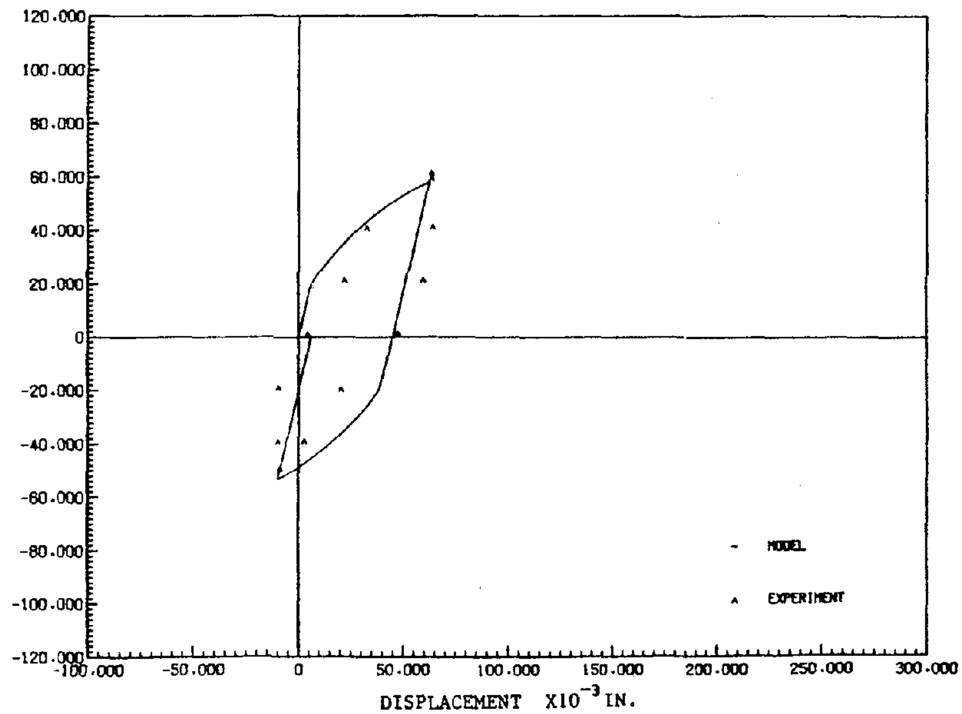


FIG. 5 COMPARISON OF PREDICTIONS OF HASSAN'S CYCLIC MODEL AND EXPERIMENT, SPECIMEN S107, CYCLE 3

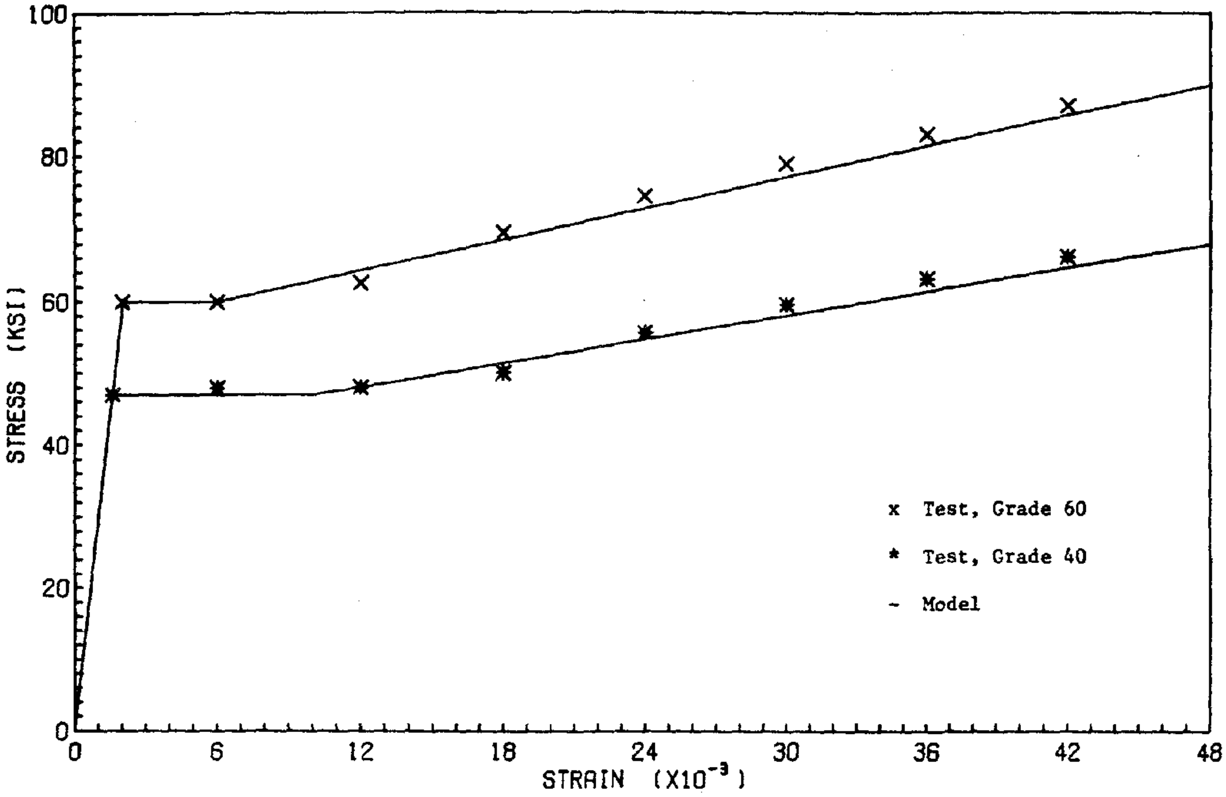


FIG. 8 MONOTONIC STRESS-STRAIN RELATIONSHIPS FOR NO. 10 BAR

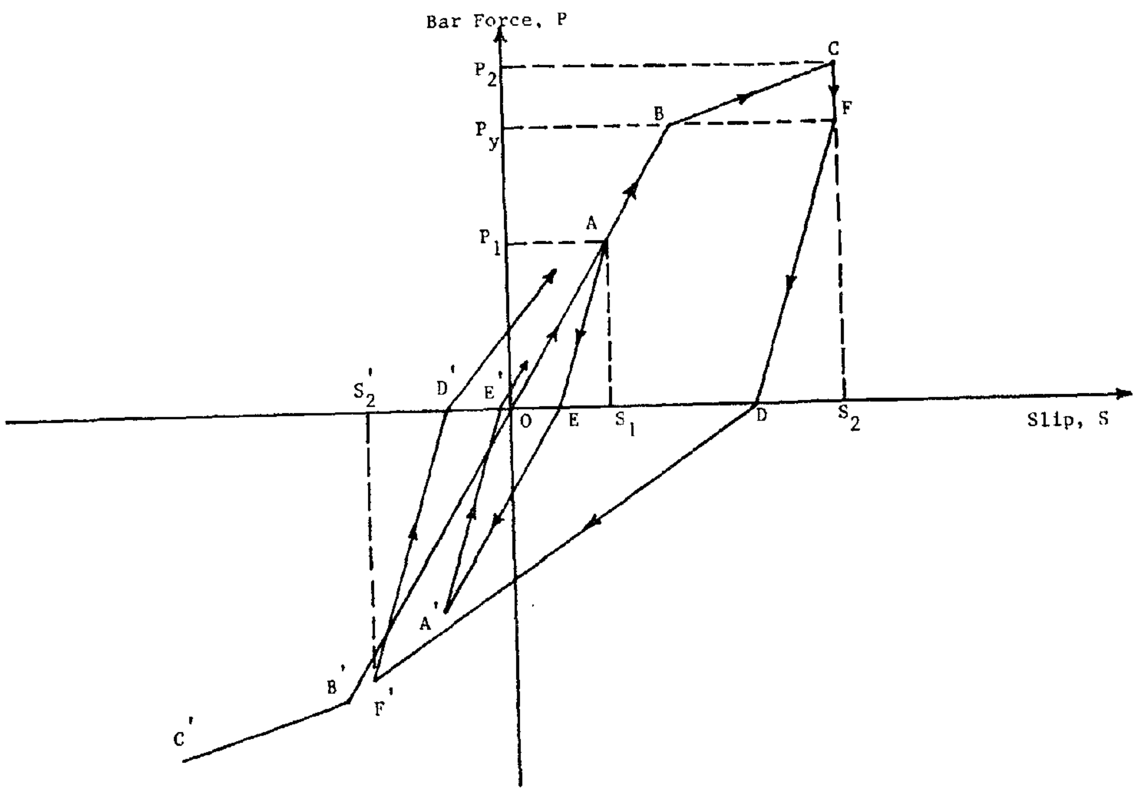


FIG. 7 BAR FORCE-SLIP RELATIONSHIP FOR CYCLIC LOADING (27, 28)

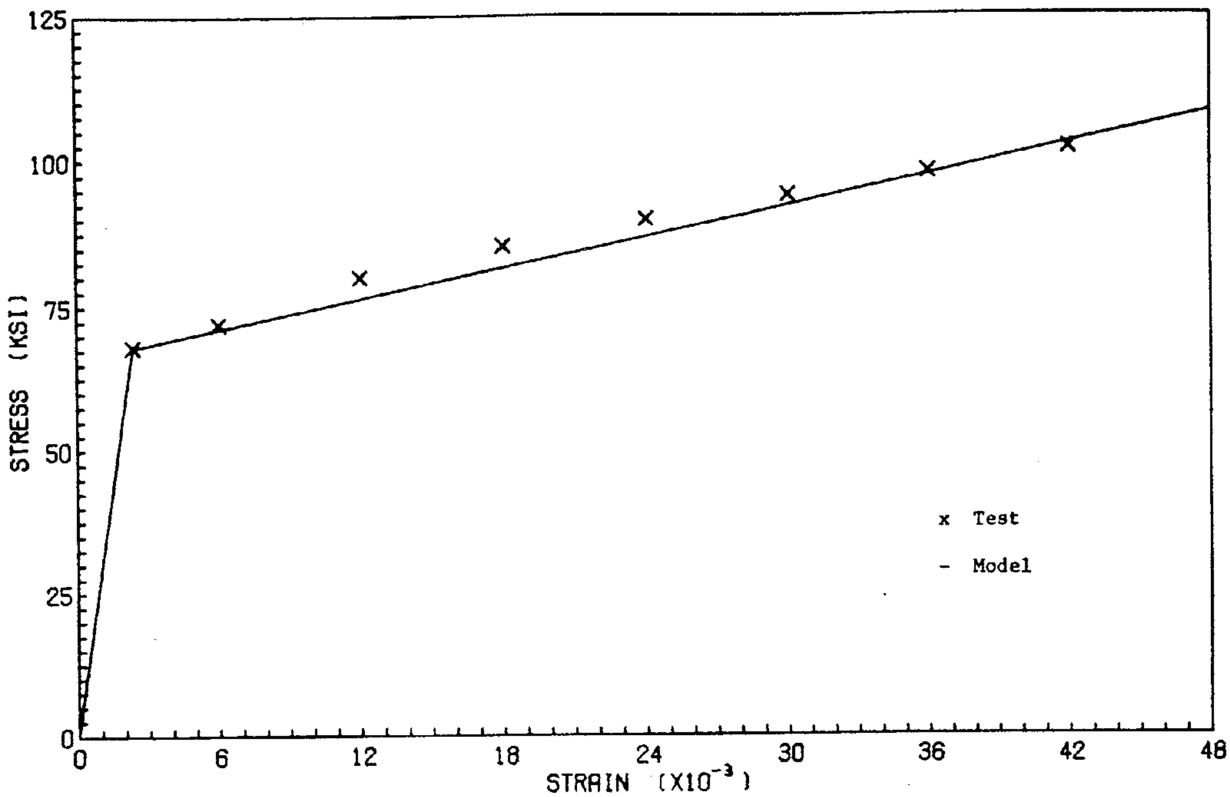


FIG. 9 MONOTONIC STRESS-STRAIN RELATIONSHIPS FOR NO. 8 BAR

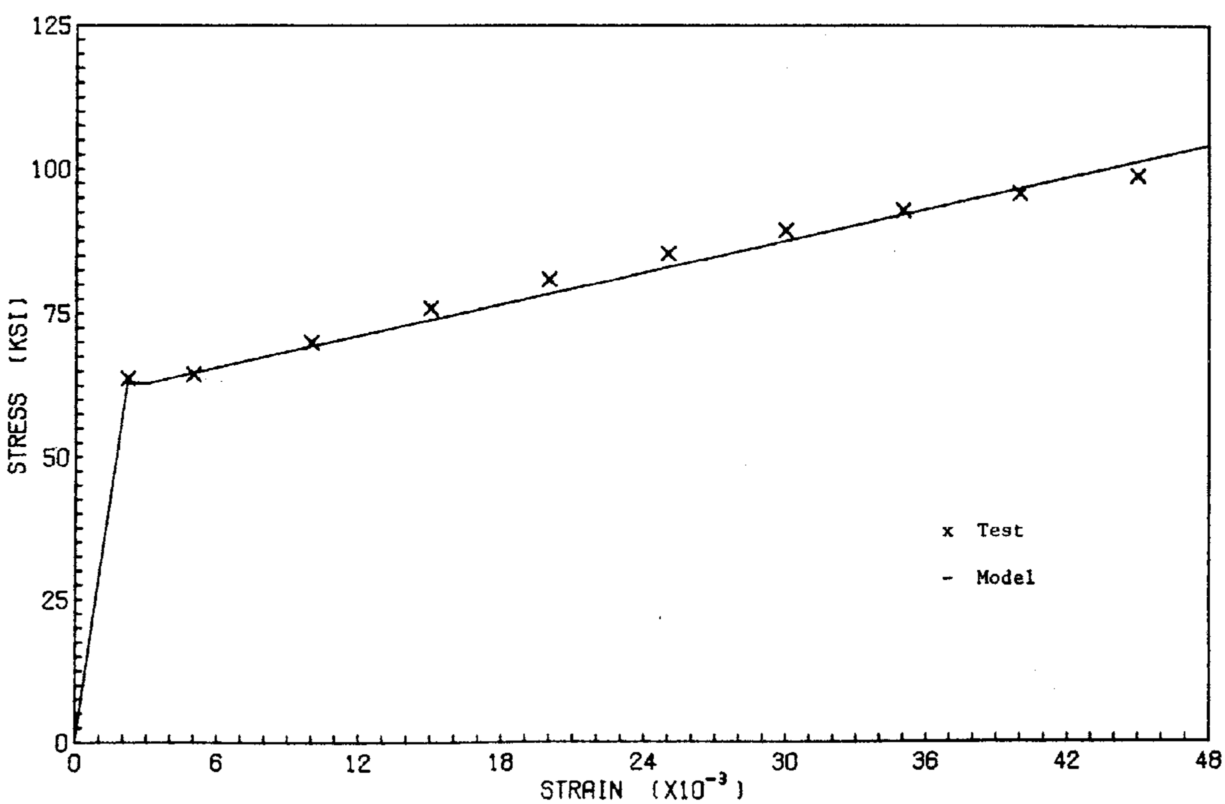


FIG. 10 MONOTONIC STRESS-STRAIN RELATIONSHIPS FOR NO. 6 BAR

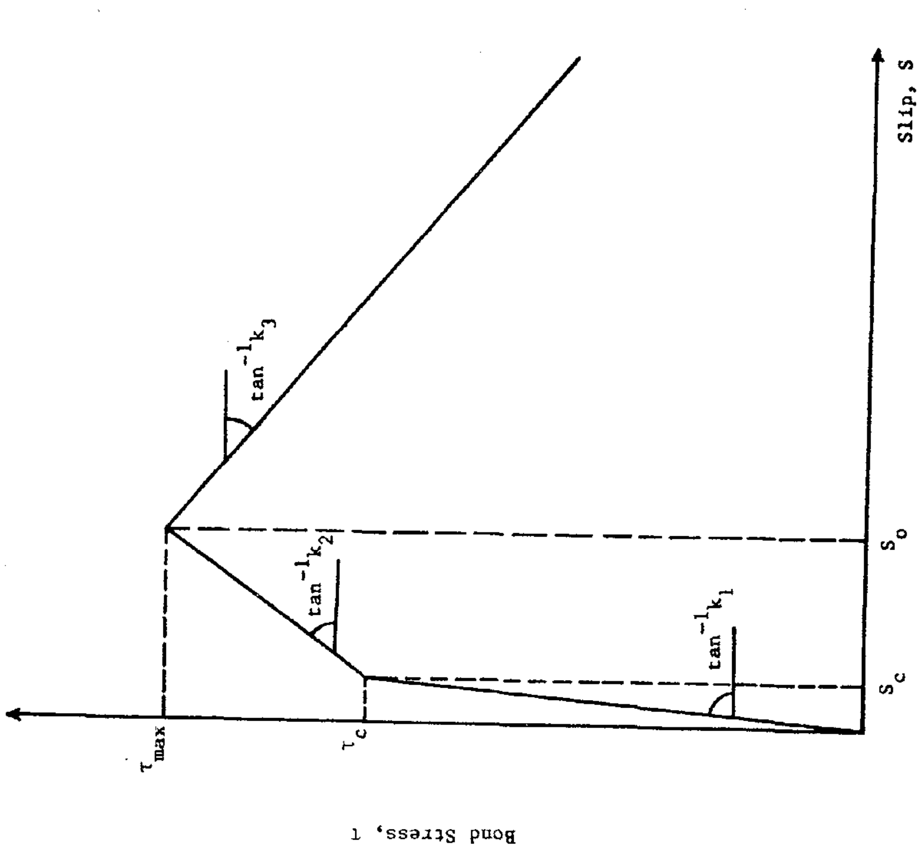


FIG. 12 SIMPLIFIED MODEL FOR MONOTONIC LOCAL BOND STRESS-SLIP CURVE

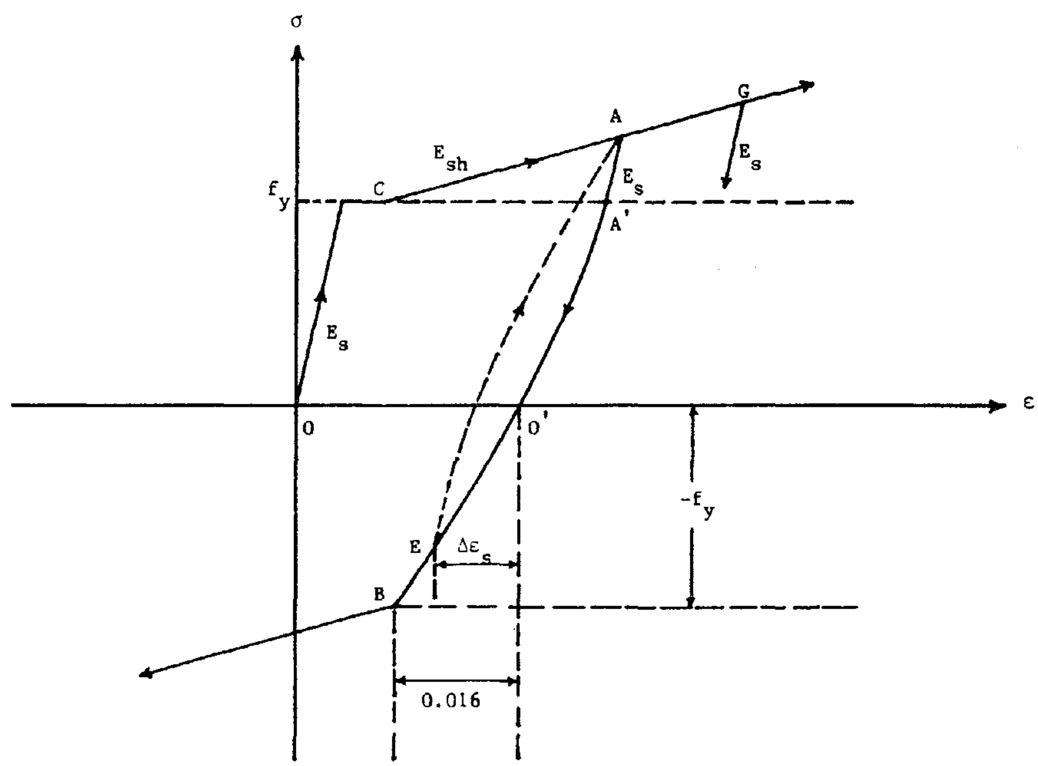


FIG. 11 CONSTRUCTION OF HYSTERETIC STRESS-STRAIN RELATIONSHIPS FOR REINFORCING STEEL

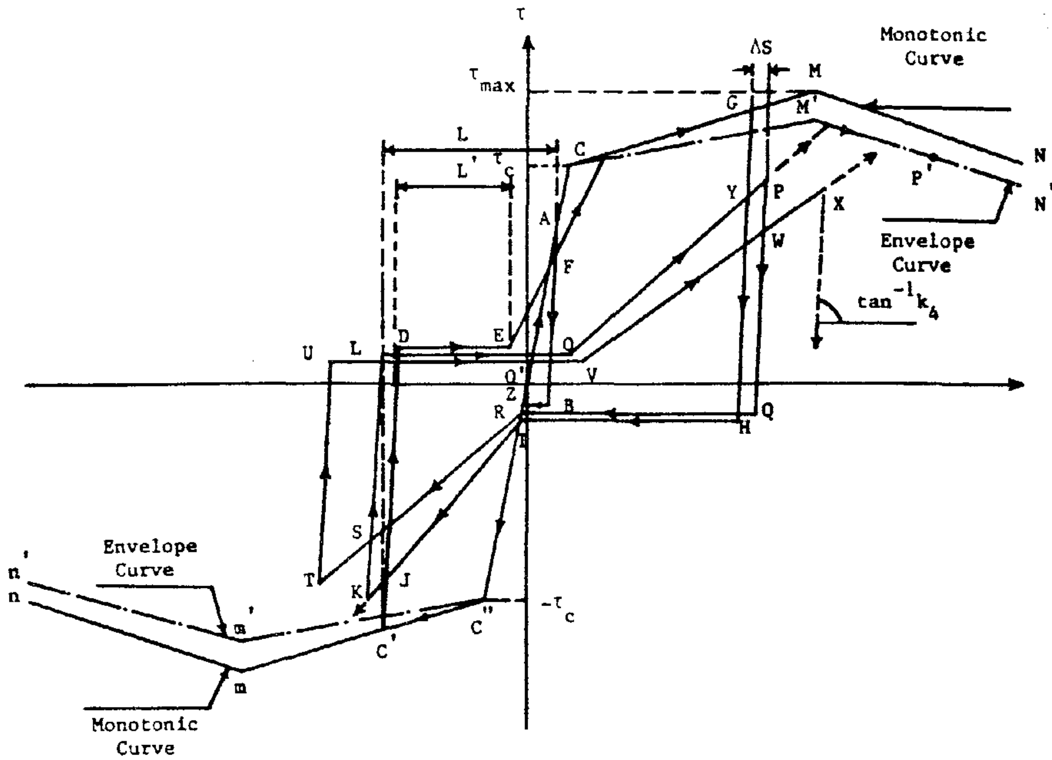


FIG. 16 LOCAL BOND STRESS-SLIP RELATIONSHIPS FOR CYCLIC LOADING

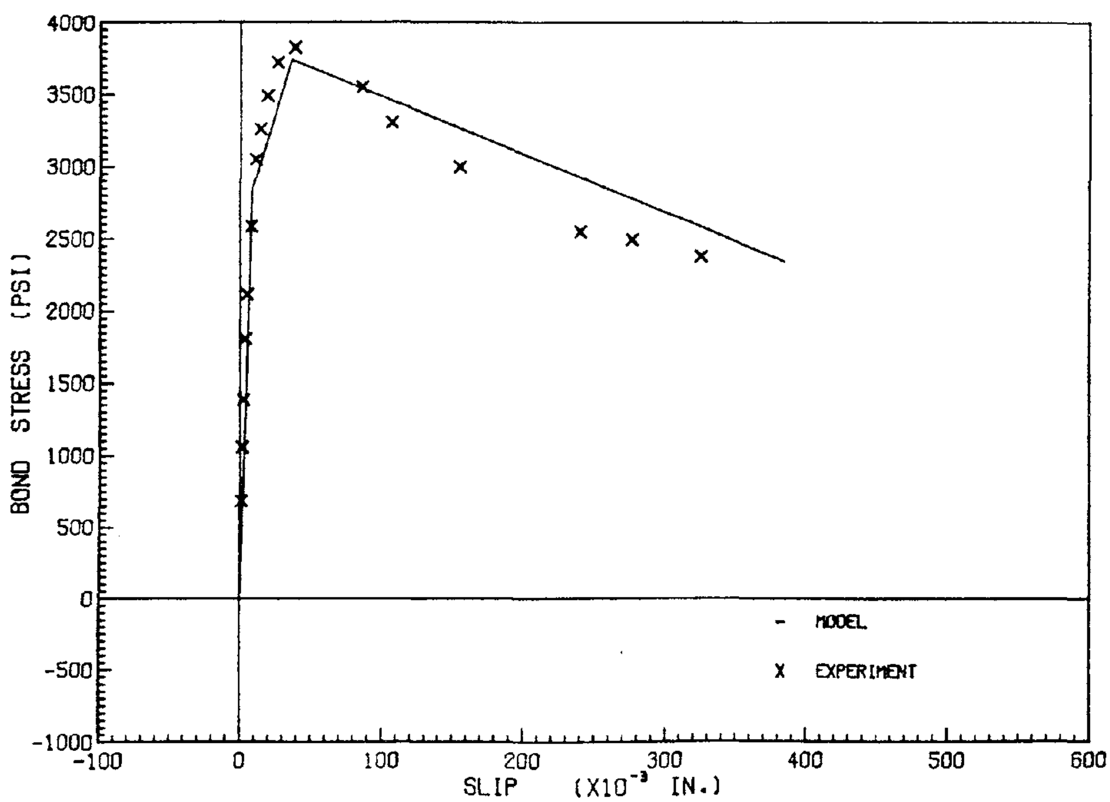


FIG. 15 COMPARISON OF MEASURED AND PREDICTED BOND STRESS-SLIP CURVES, SPECIMEN LM3

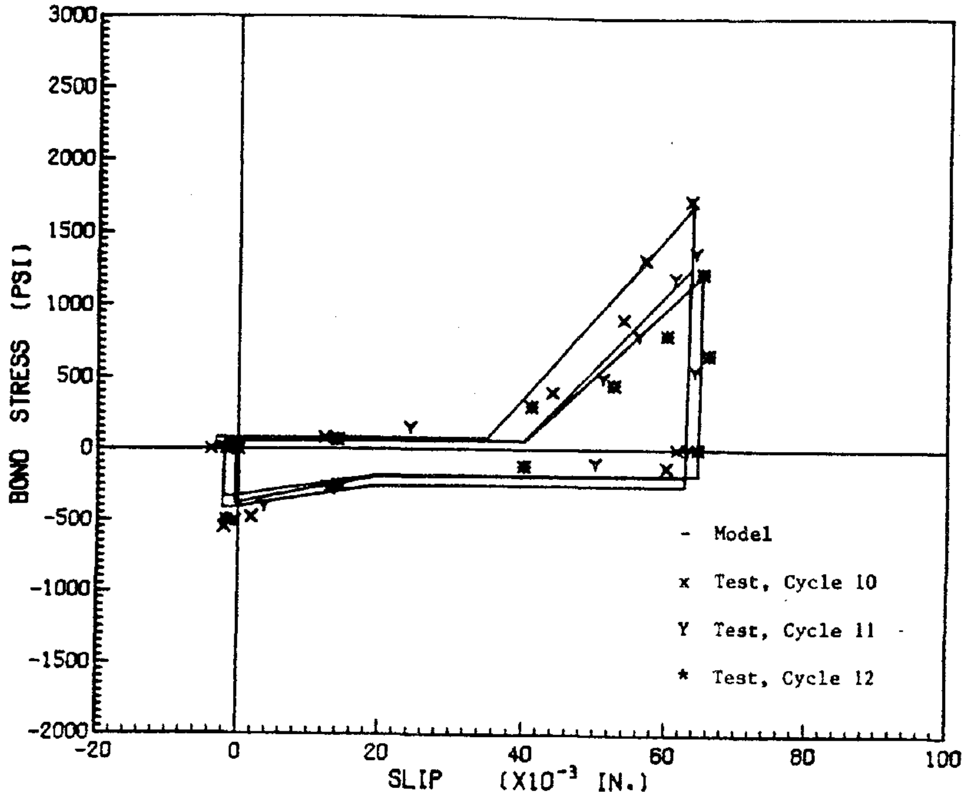


FIG. 18 COMPARISON OF MEASURED AND PREDICTED BOND STRESS-SLIP CURVES, SPECIMEN LC1, CYCLES 10, 11 AND 12

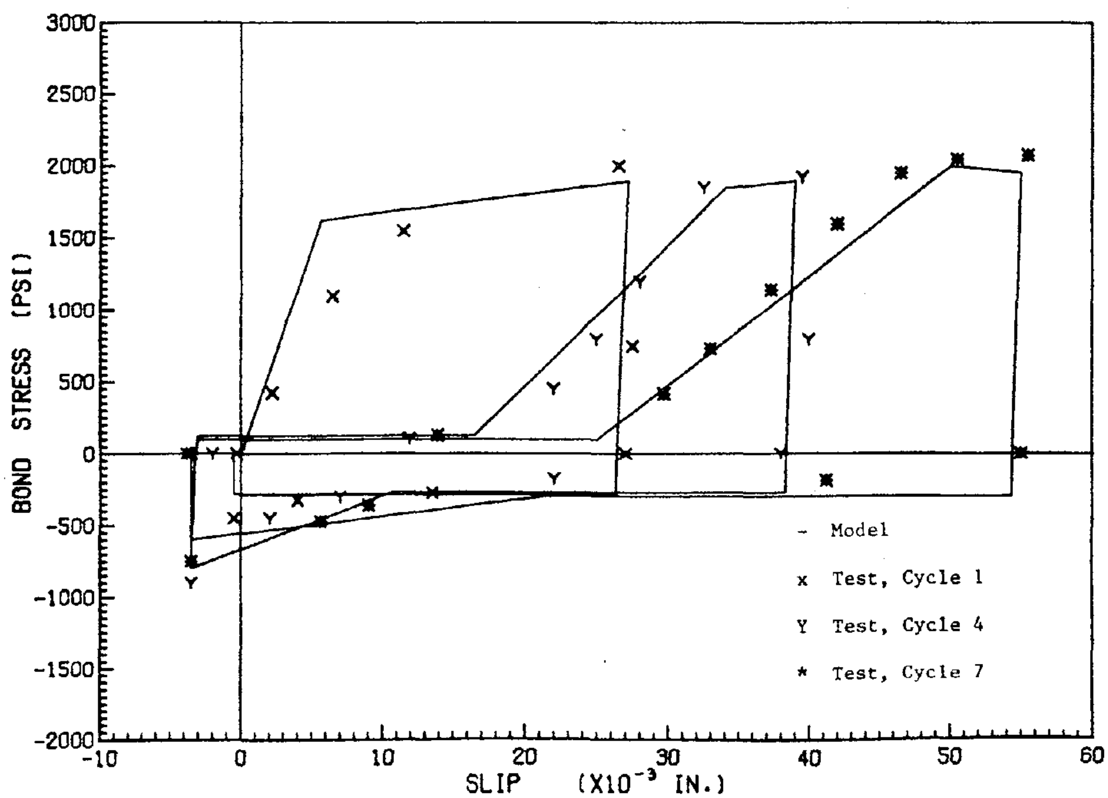


FIG. 17 COMPARISON OF MEASURED AND PREDICTED BOND STRESS-SLIP CURVES, SPECIMEN LC1, CYCLES 1, 4 AND 7

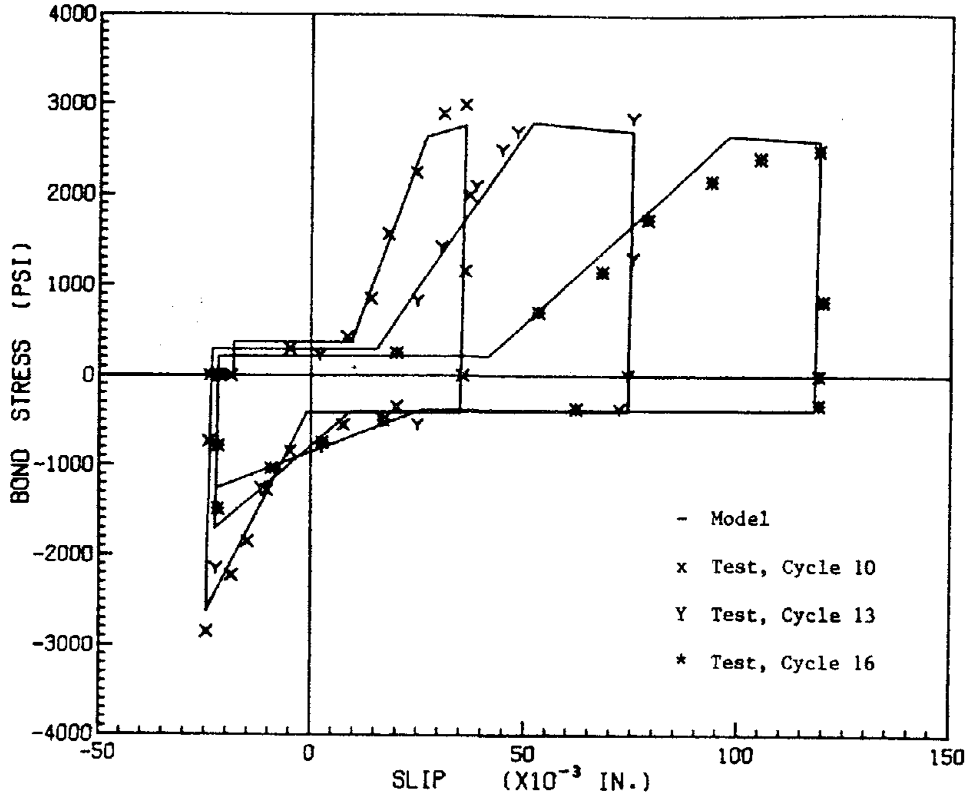


FIG. 20 COMPARISON OF MEASURED AND PREDICTED BOND STRESS-SLIP CURVES, SPECIMEN LC2, CYCLES 10, 13 AND 16

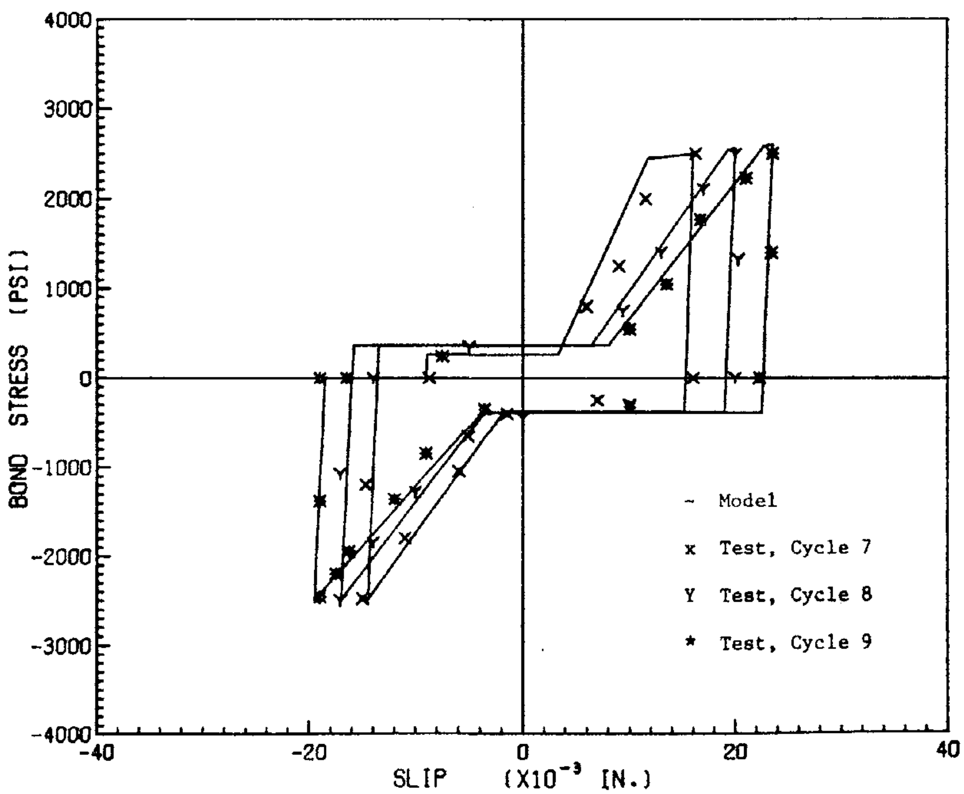


FIG. 19 COMPARISON OF MEASURED AND PREDICTED BOND STRESS-SLIP CURVES, SPECIMEN LC2, CYCLES 7, 8 AND 9

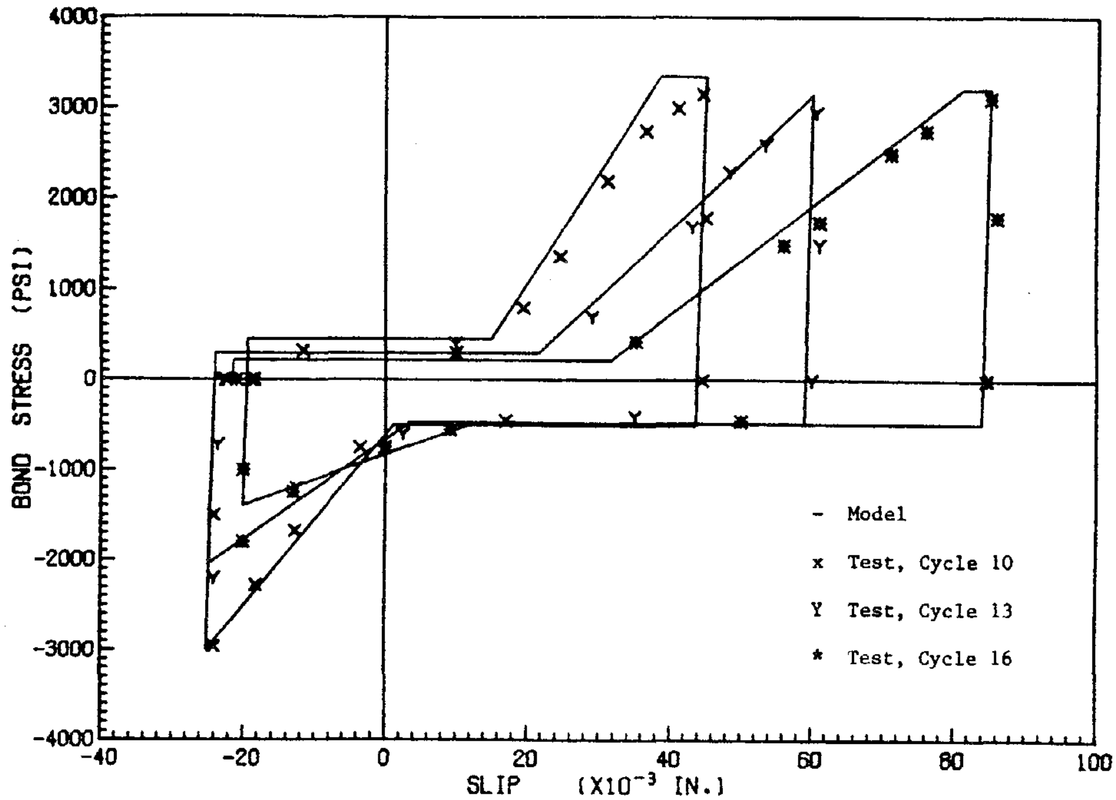


FIG. 22 COMPARISON OF MEASURED AND PREDICTED BOND STRESS-SLIP CURVES, SPECIMEN LC3, CYCLES 10, 13 AND 16

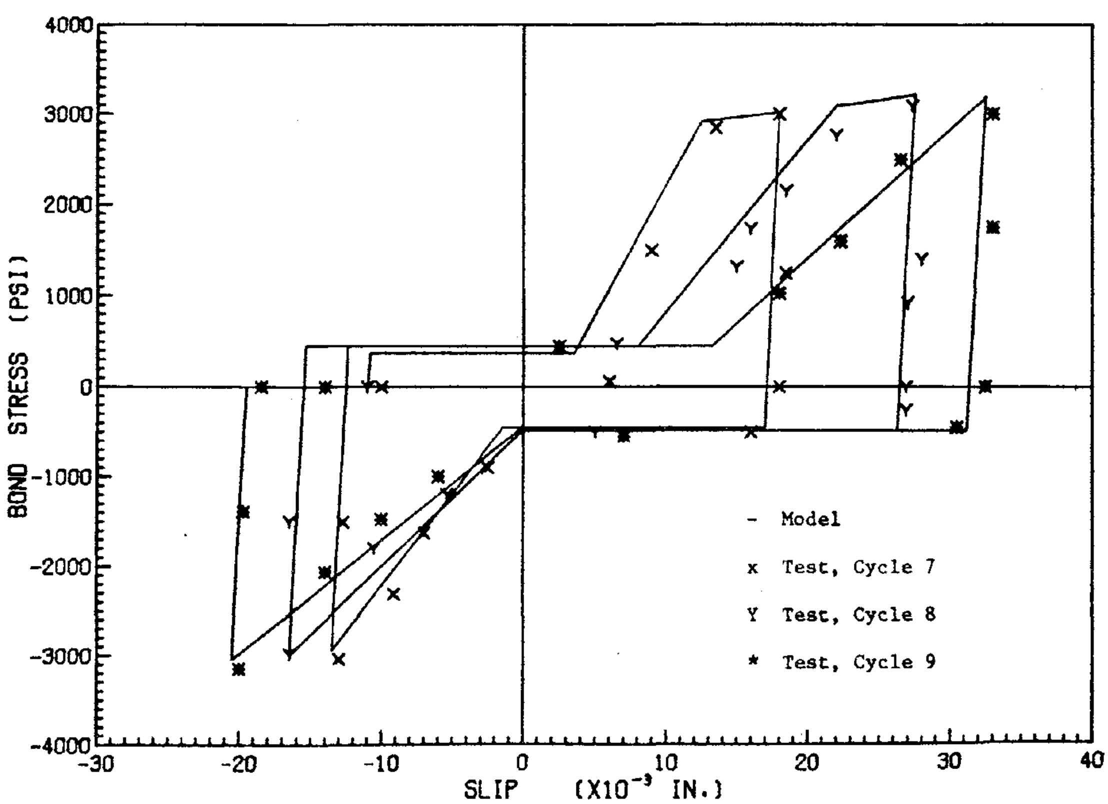


FIG. 21 COMPARISON OF MEASURED AND PREDICTED BOND STRESS-SLIP CURVES, SPECIMEN LC3, CYCLES 7, 8 AND 9

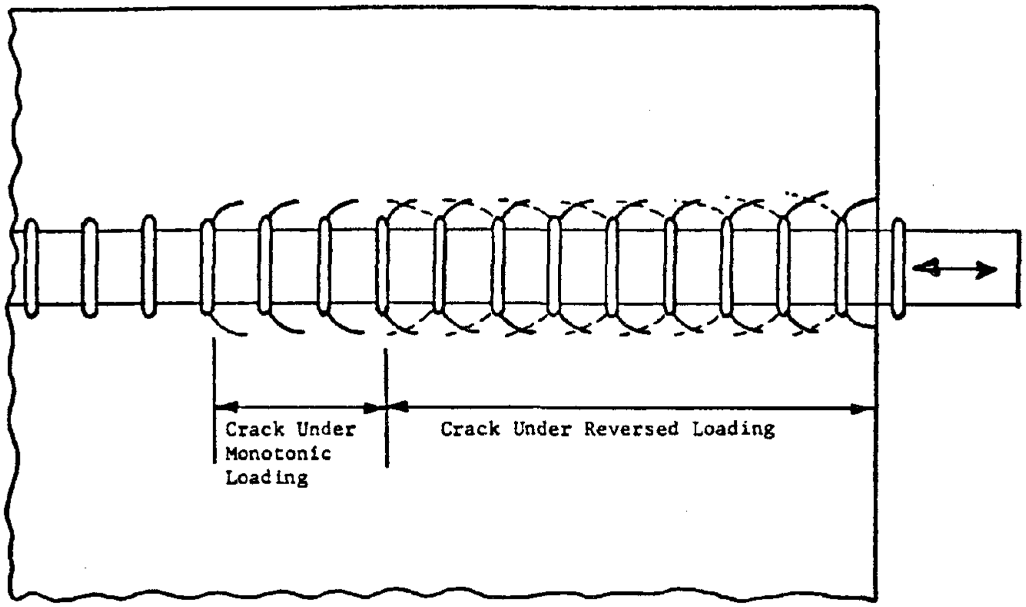


FIG. 23 CRACK PATTERN UNDER REVERSED AND MONOTONIC LOADING

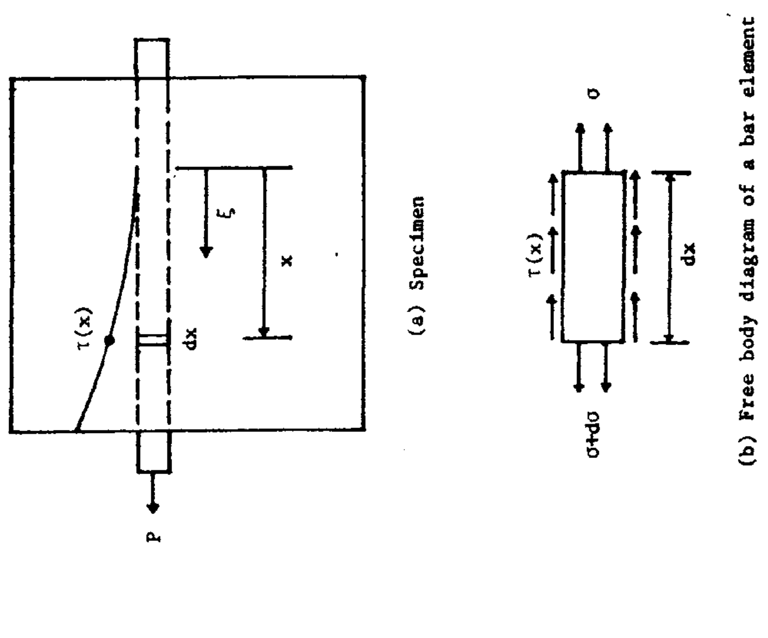


FIG. 24 DIAGRAMS FOR DERIVATION OF EQUILIBRIUM EQUATION

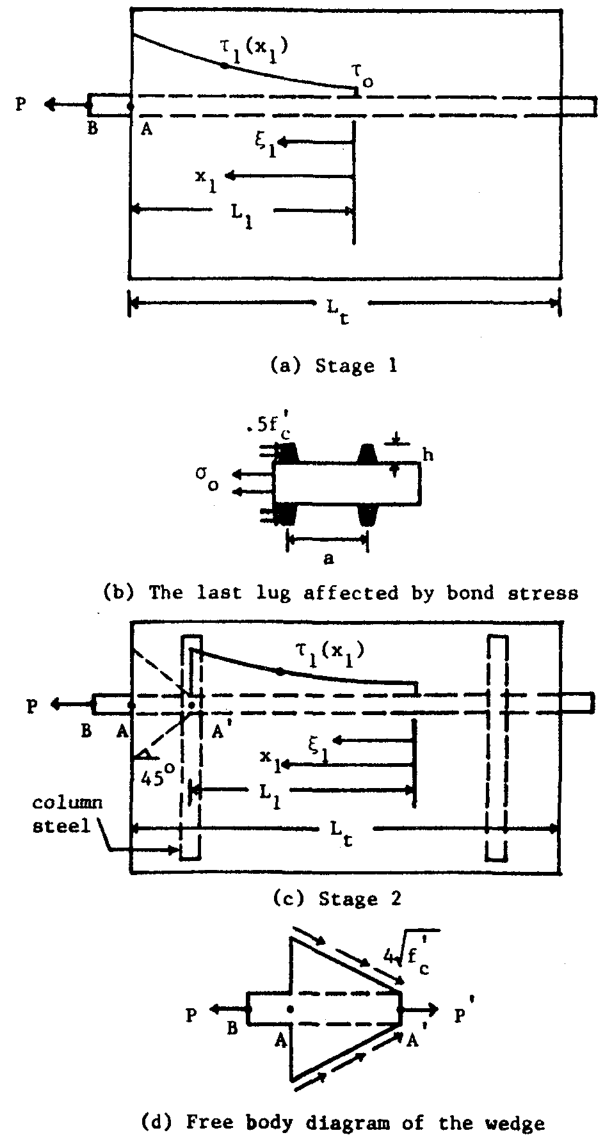


FIG. 25 THE VARIATION OF BOND STRESS DISTRIBUTION FOR SPECIMEN S101, STAGES 1 - 2

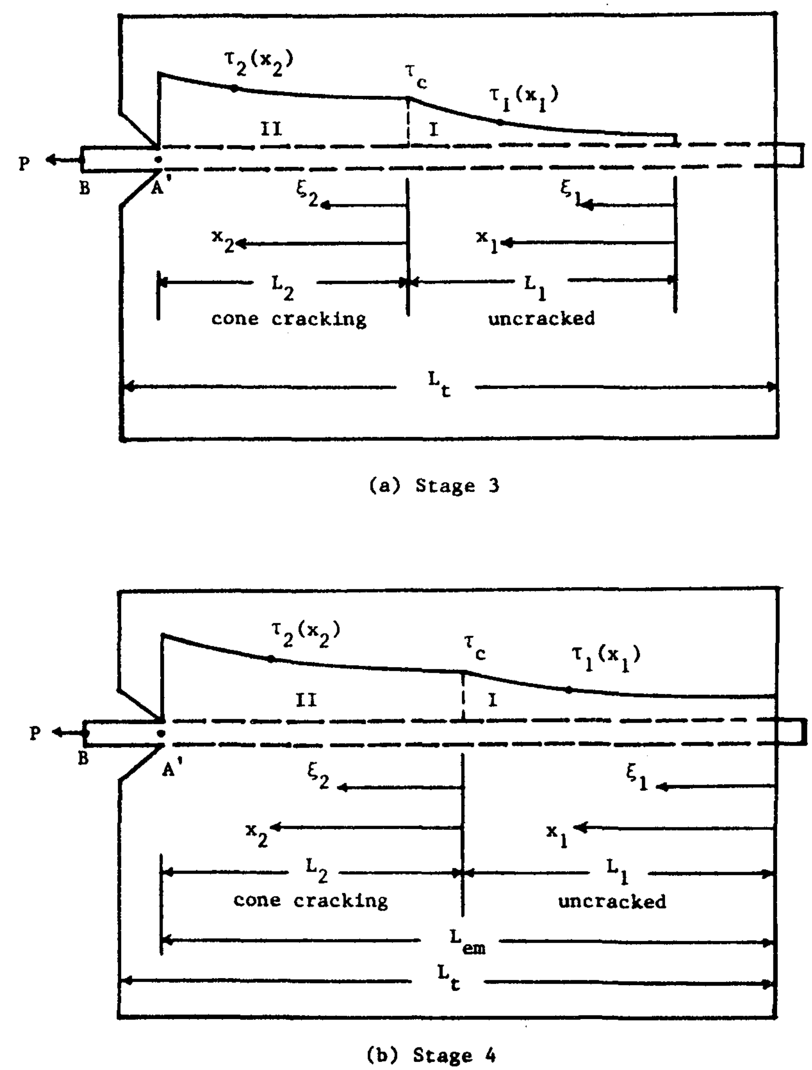


FIG. 26 THE VARIATION OF BOND STRESS DISTRIBUTION FOR SPECIMEN S101, STAGES 3 - 4

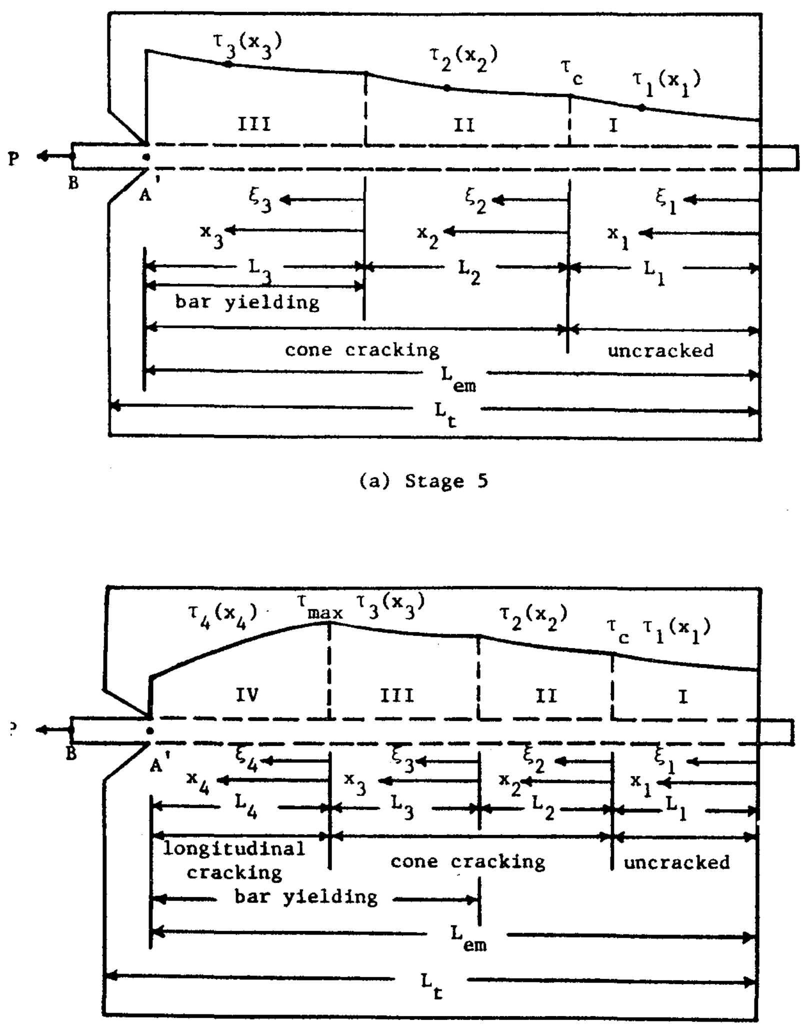


(a) Stage 5

(b) Stage 6

[G. 27 THE VARIATION OF BOND STRESS DISTRIBUTION FOR SPECIMEN S101,
STAGES 5 - 6

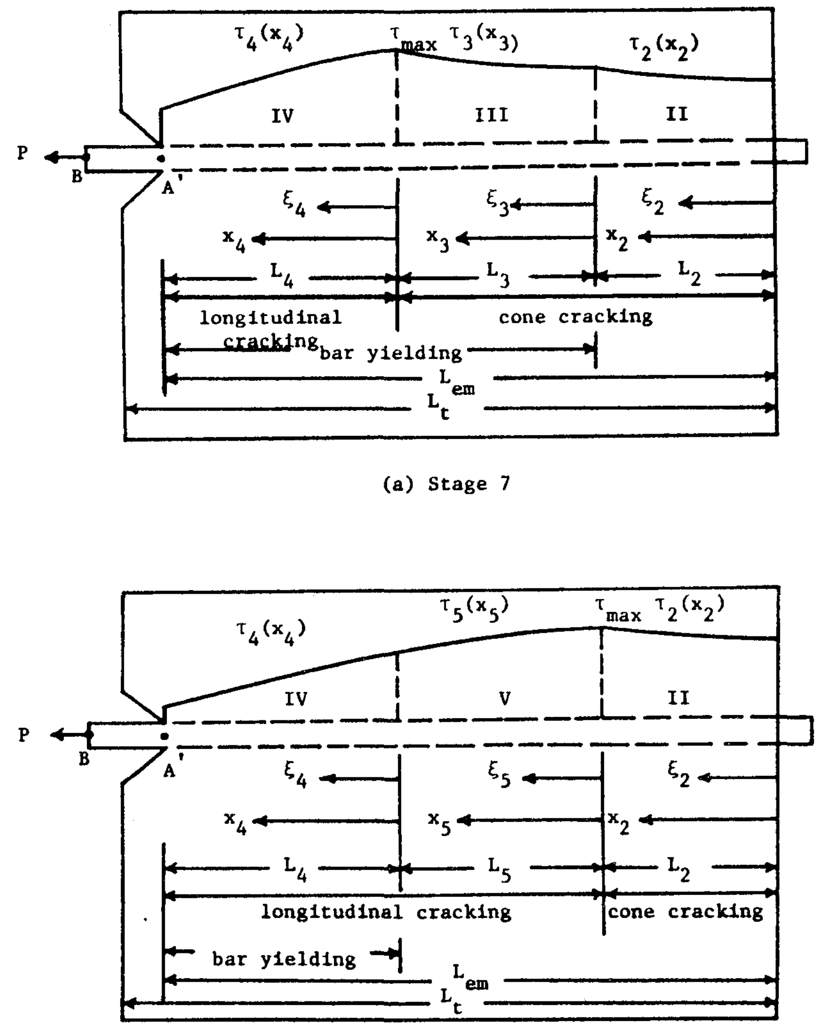


(a) Stage 7

(d) Stage 8

FIG. 28 THE VARIATION OF BOND STRESS DISTRIBUTION FOR SPECIMEN S101,
STAGES 7 - 8

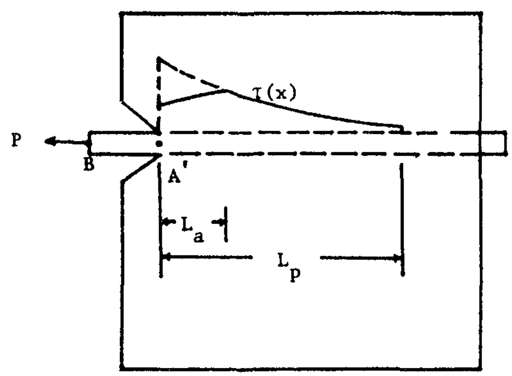


(a) Bond Stress Distribution

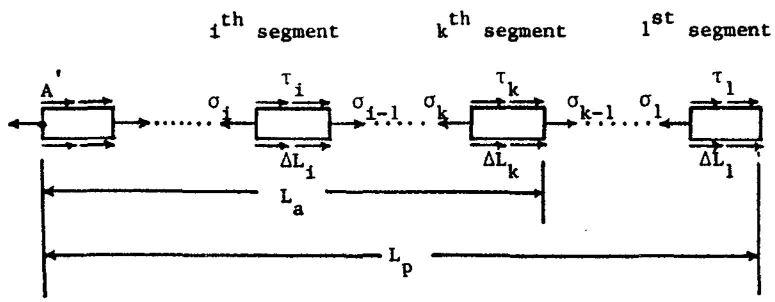


(b) Free Body Diagram

FIG. 29 THE VARIATION OF BOND STRESS DISTRIBUTION UNDER LOAD REVERSALS, CASE 1

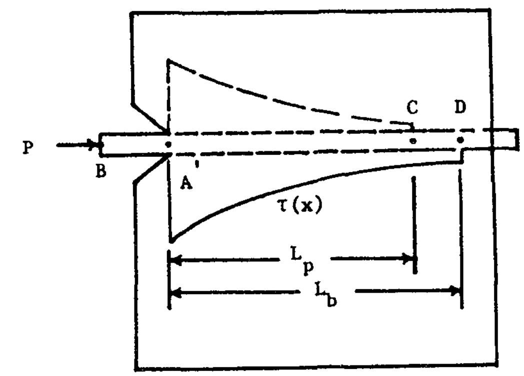


(a) Bond Stress Distribution

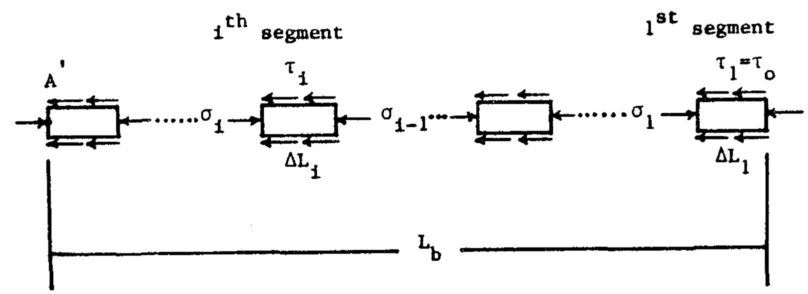


(b) Free Body Diagram

FIG. 30 THE VARIATION OF BOND STRESS DISTRIBUTION UNDER LOAD REVERSALS, CASE 2

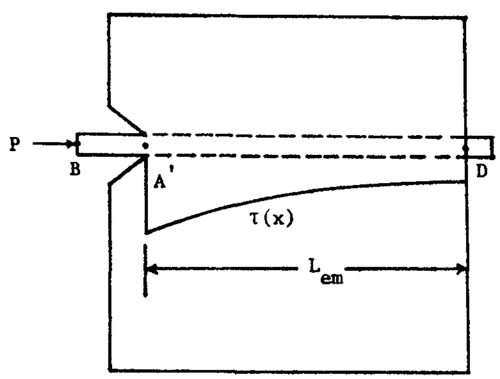


(a) Bond Stress Distribution

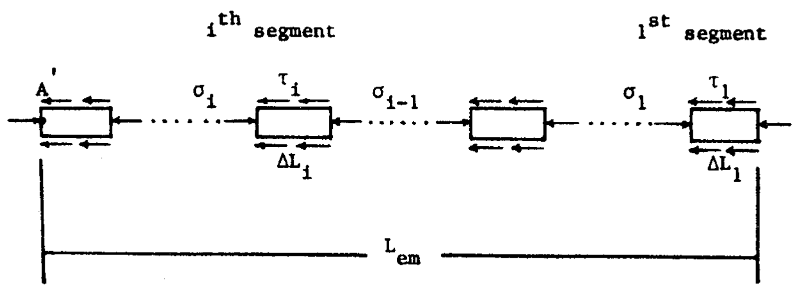


(b) Free Body Diagram

FIG. 31 THE VARIATION OF BOND STRESS DISTRIBUTION UNDER LOAD REVERSALS, CASE3

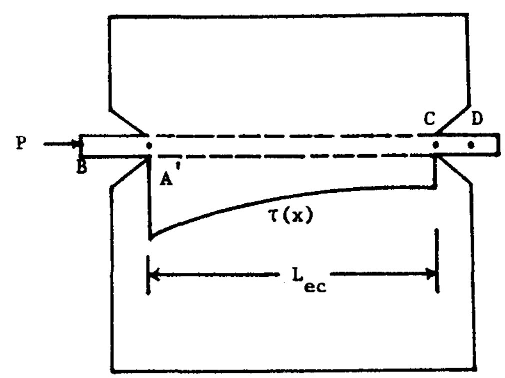


(a) Bond Stress Distribution

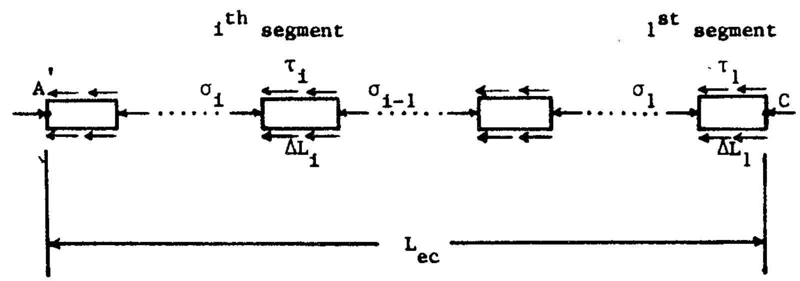


(b) Free Body Diagram

FIG. 32 THE VARIATION OF BOND STRESS DISTRIBUTION UNDER LOAD REVERSALS, CASE 4

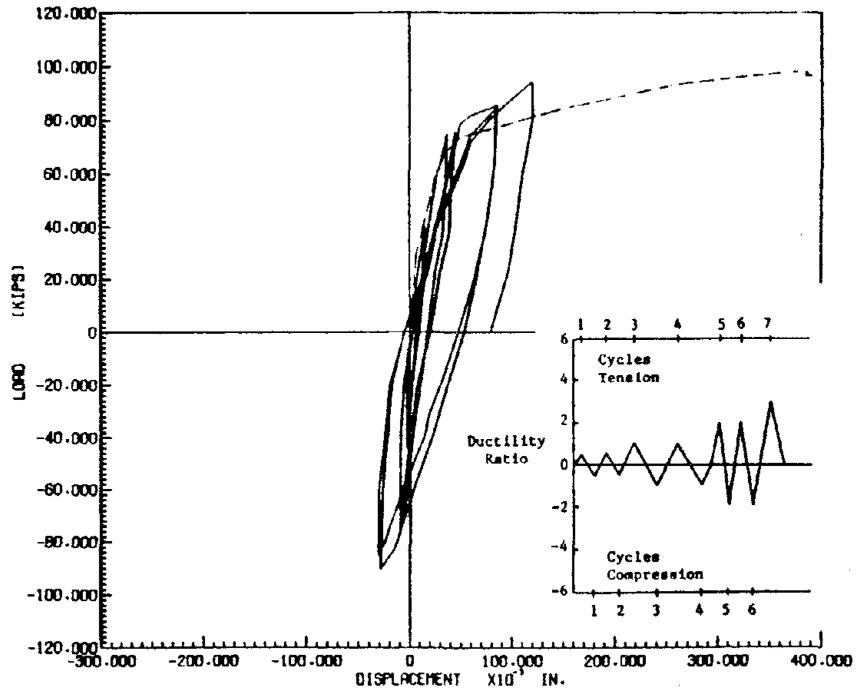


FIG. 34 LOAD-DISPLACEMENT CURVE, SPECIMEN S102

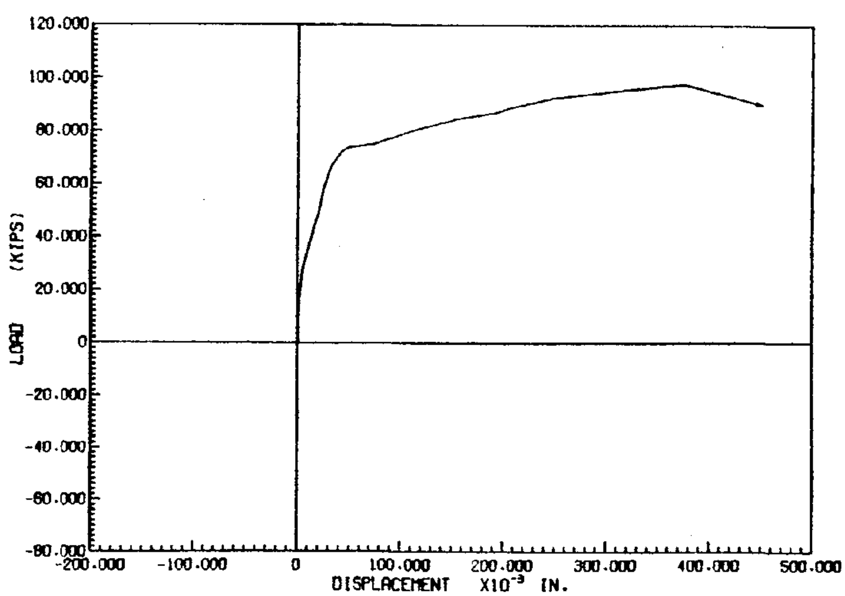


FIG. 33 LOAD-DISPLACEMENT CURVE, SPECIMEN S101

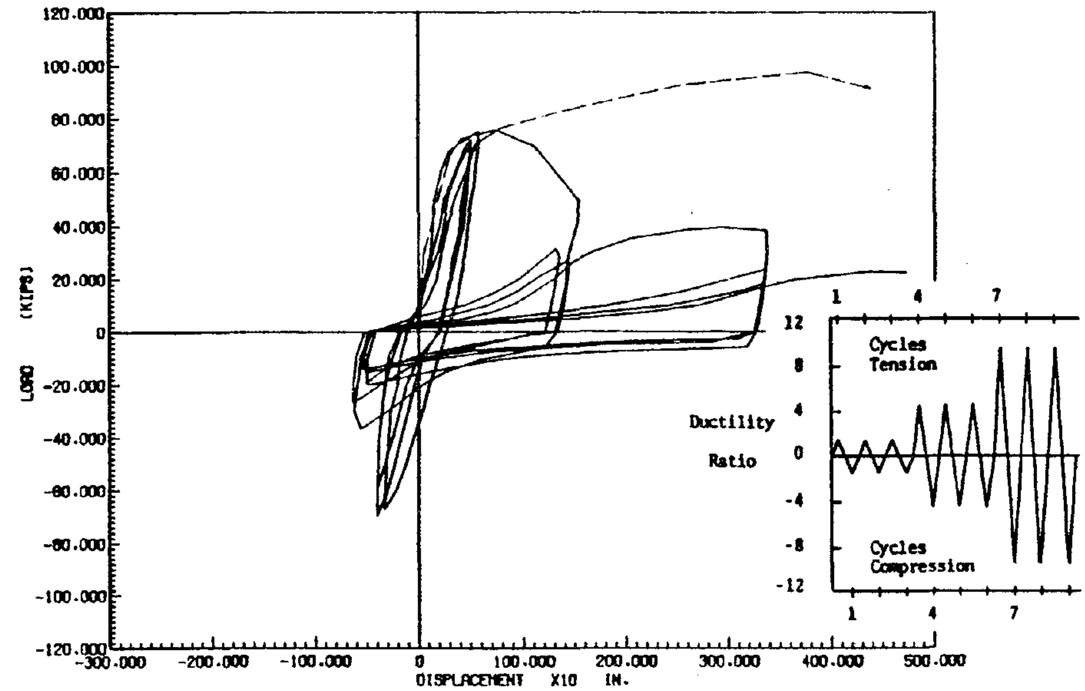


FIG. 36 LOAD-DISPLACEMENT CURVE, SPECIMEN S104

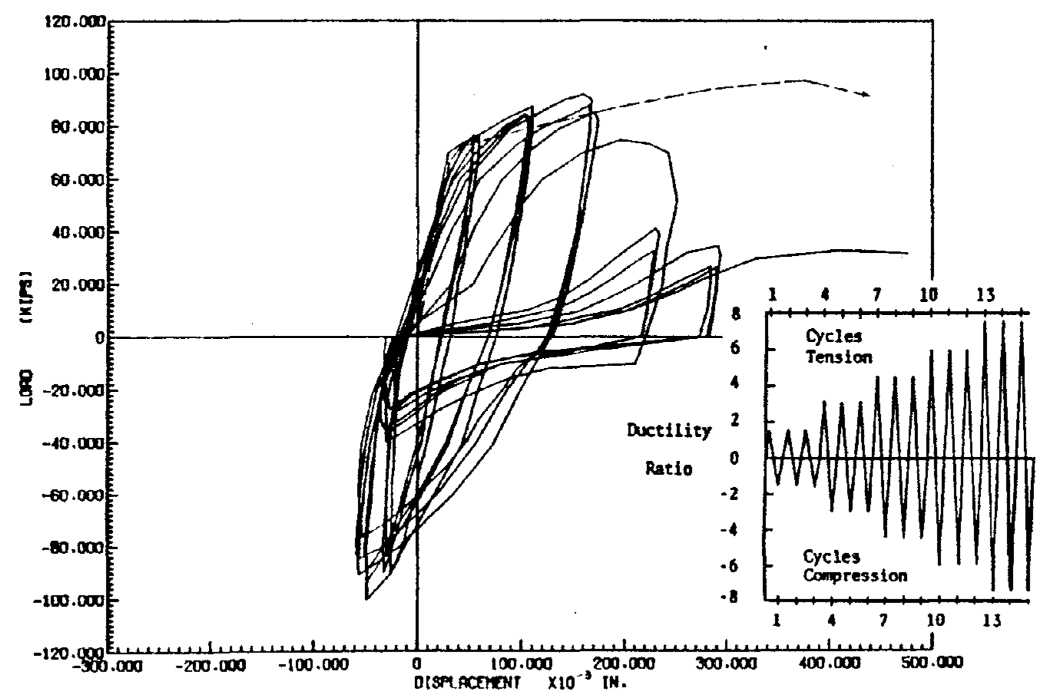


FIG. 35 LOAD-DISPLACEMENT CURVE, SPECIMEN S103

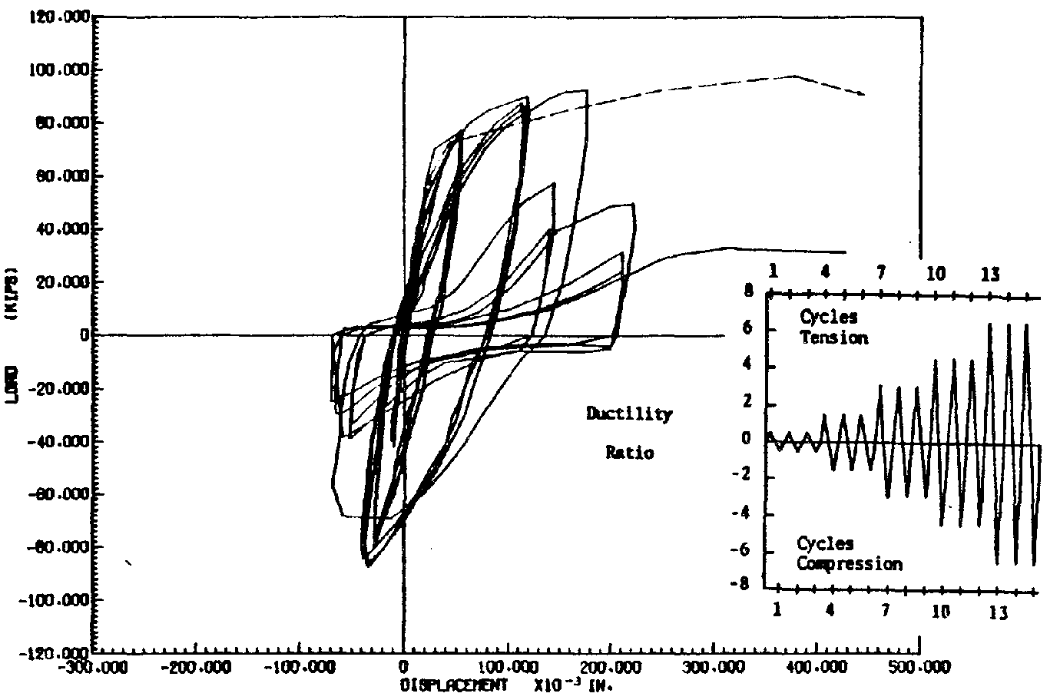


FIG. 38 LOAD-DISPLACEMENT CURVE, SPECIMEN S106

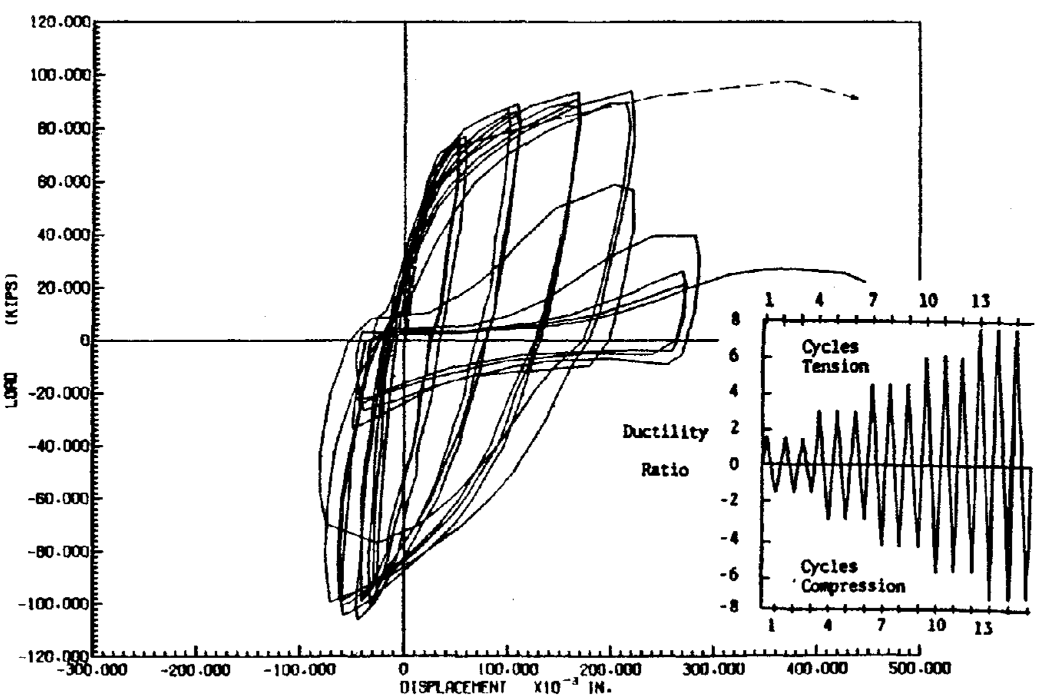


FIG. 37 LOAD-DISPLACEMENT CURVE, SPECIMEN S105

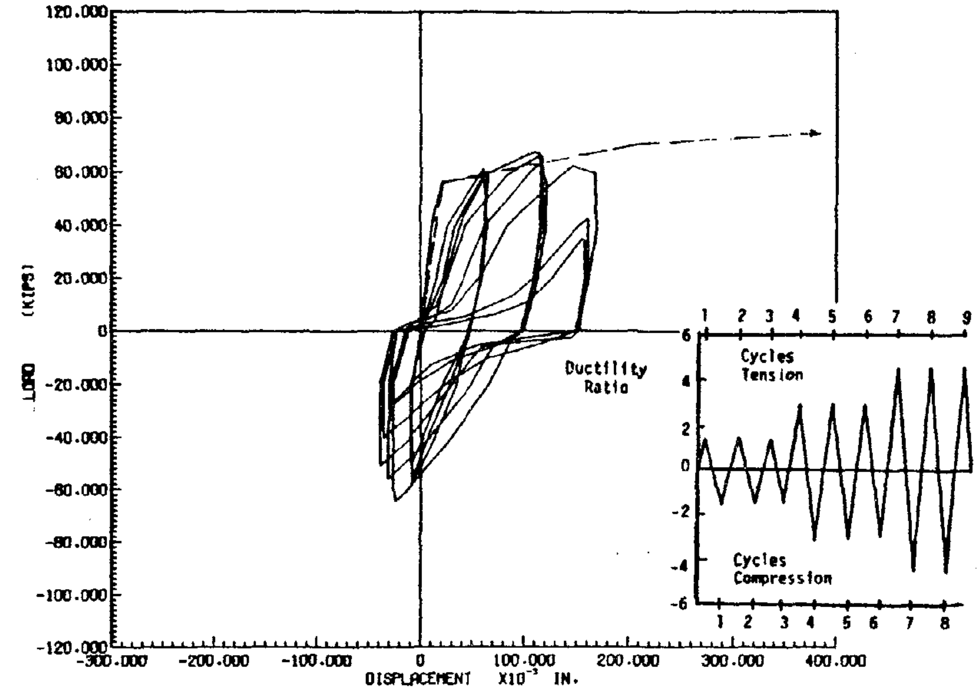


FIG. 39 LOAD-DISPLACEMENT CURVE, SPECIMEN S107

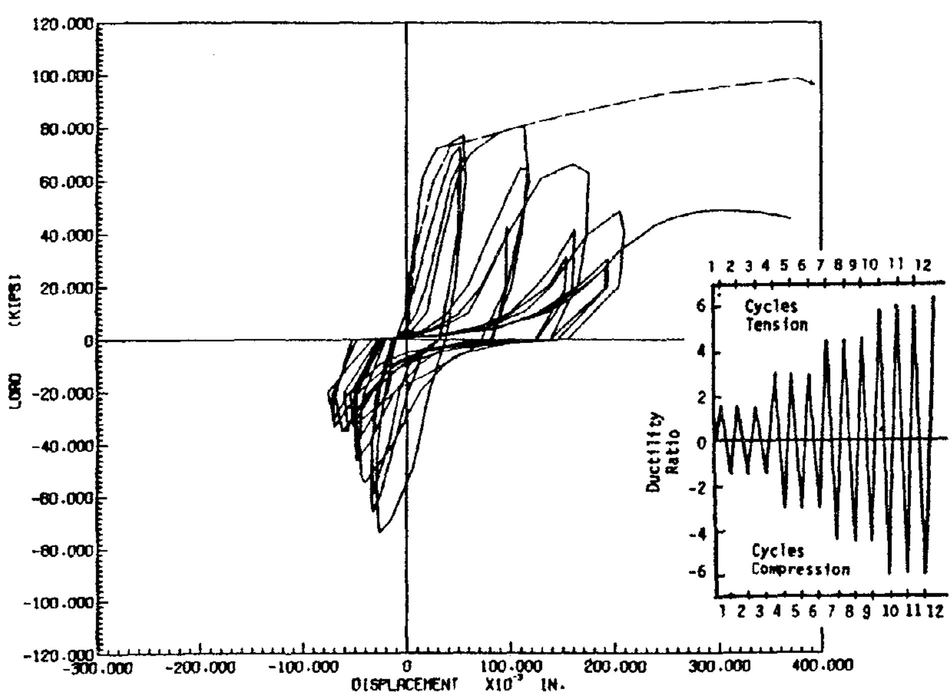


FIG. 40 LOAD-DISPLACEMENT CURVE, SPECIMEN B101

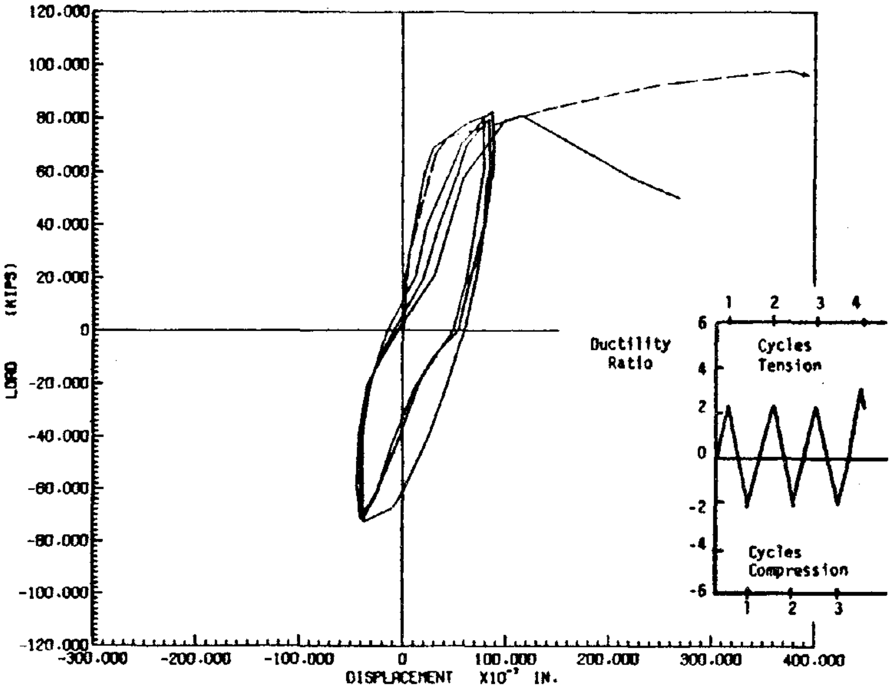


FIG. 42 LOAD-DISPLACEMENT CURVE, SPECIMEN B103

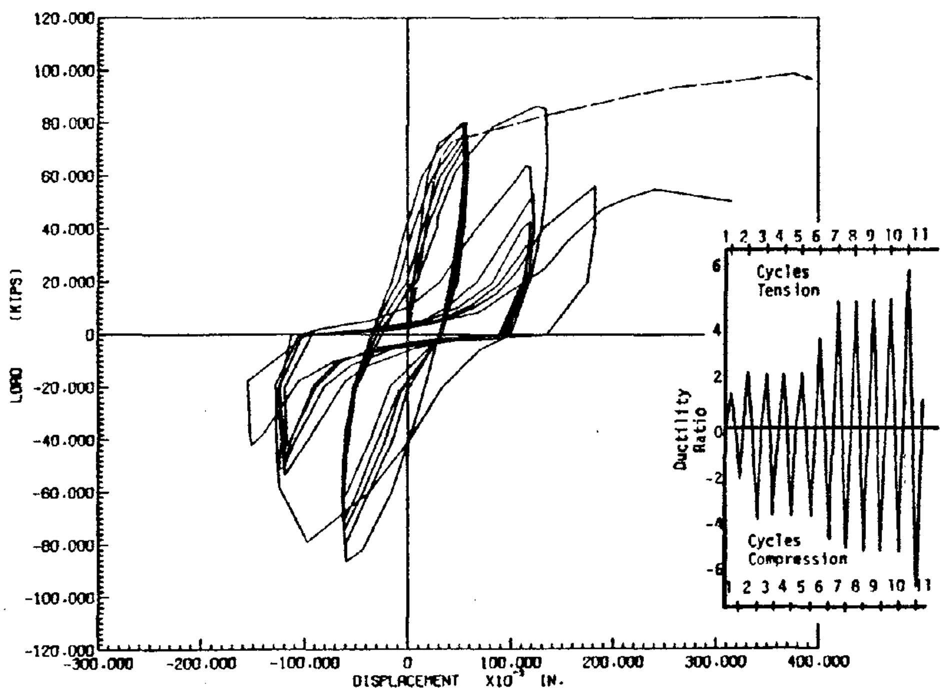


FIG. 41 LOAD-DISPLACEMENT CURVE, SPECIMEN B102

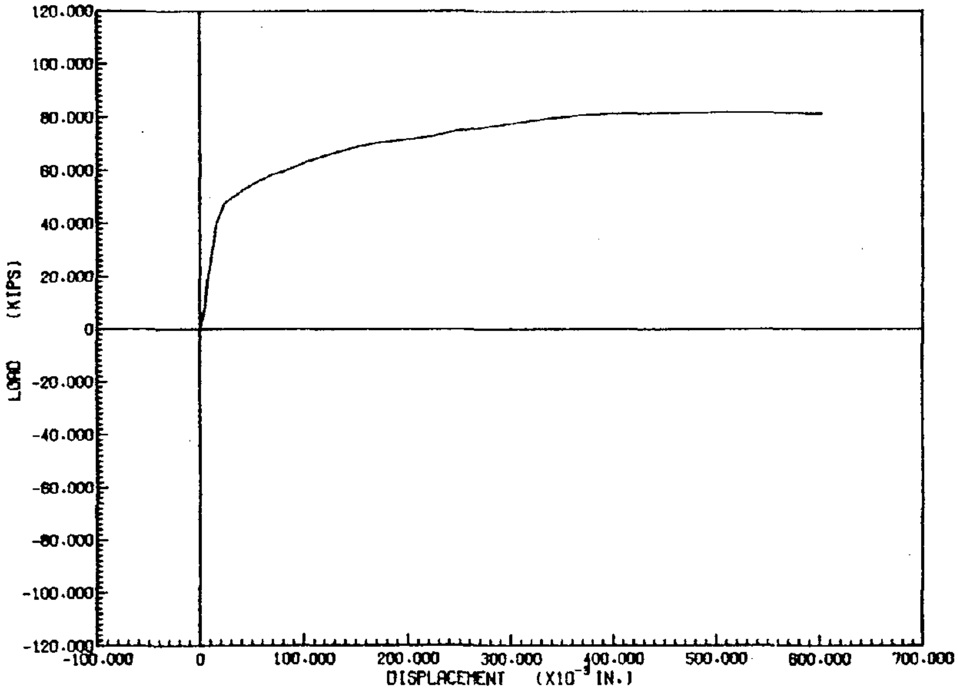


FIG. 44 LOAD-DISPLACEMENT CURVE, SPECIMEN B81

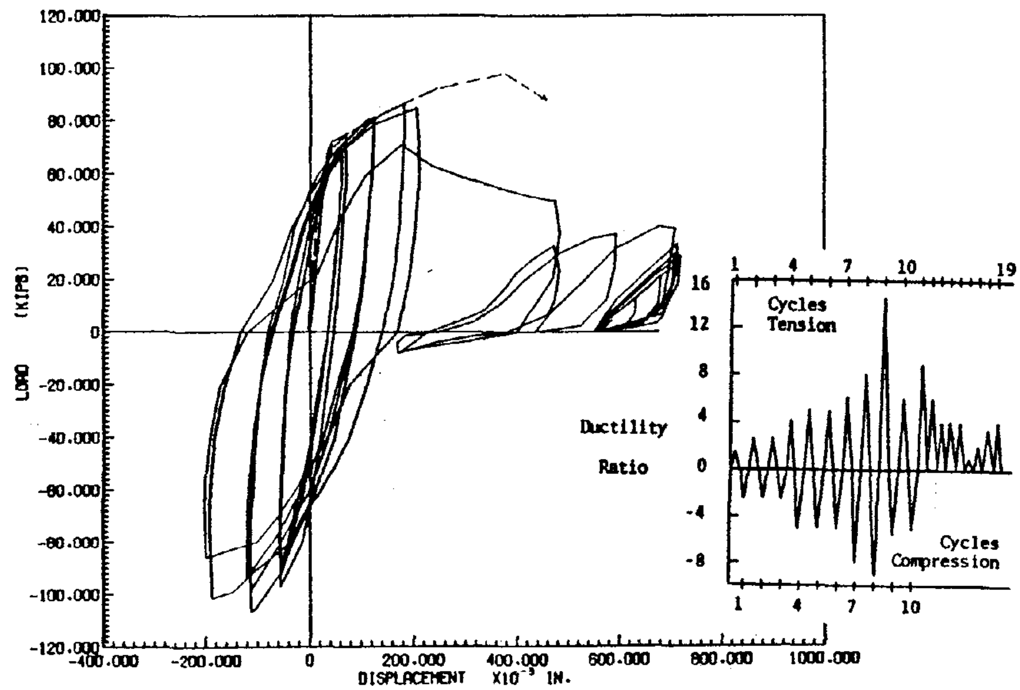


FIG. 43 LOAD-DISPLACEMENT CURVE, SPECIMEN B104

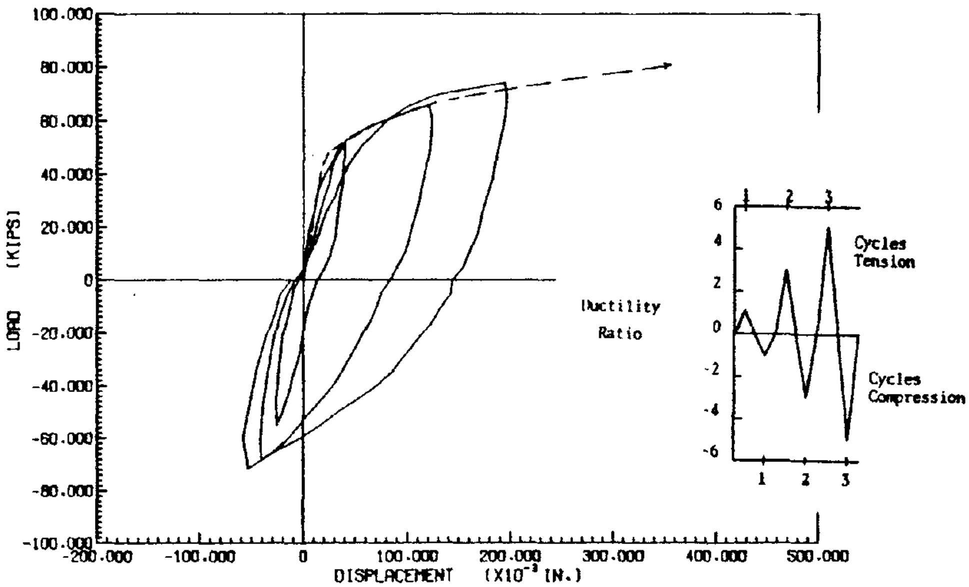


FIG. 46 LOAD-DISPLACEMENT CURVE, SPECIMEN B83

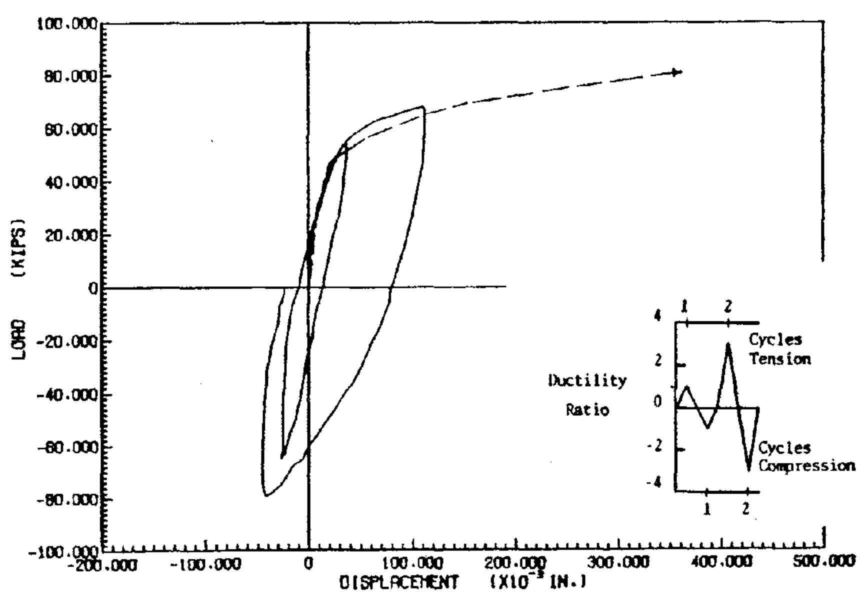


FIG. 45 LOAD-DISPLACEMENT CURVE, SPECIMEN B82

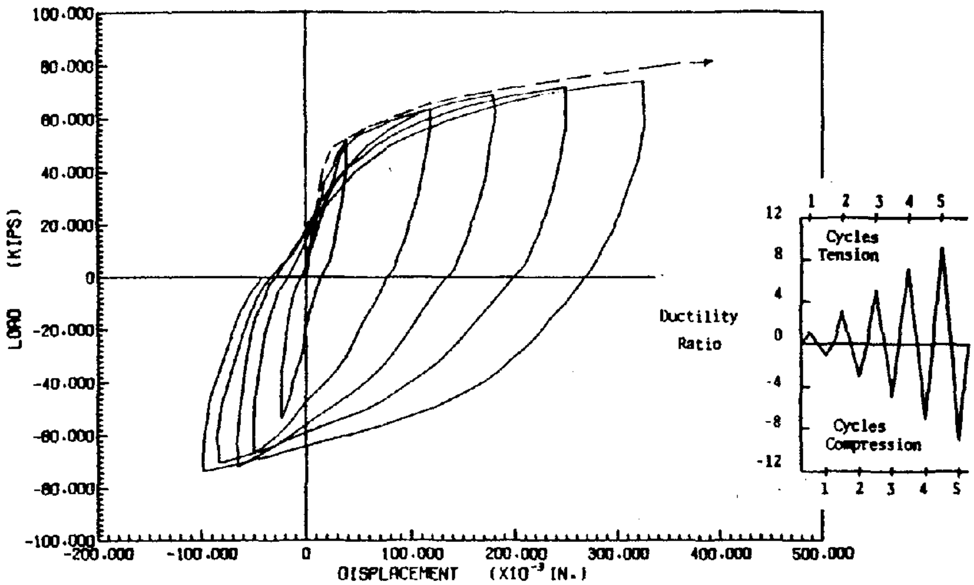


FIG. 48 LOAD-DISPLACEMENT CURVE, SPECIMEN B85

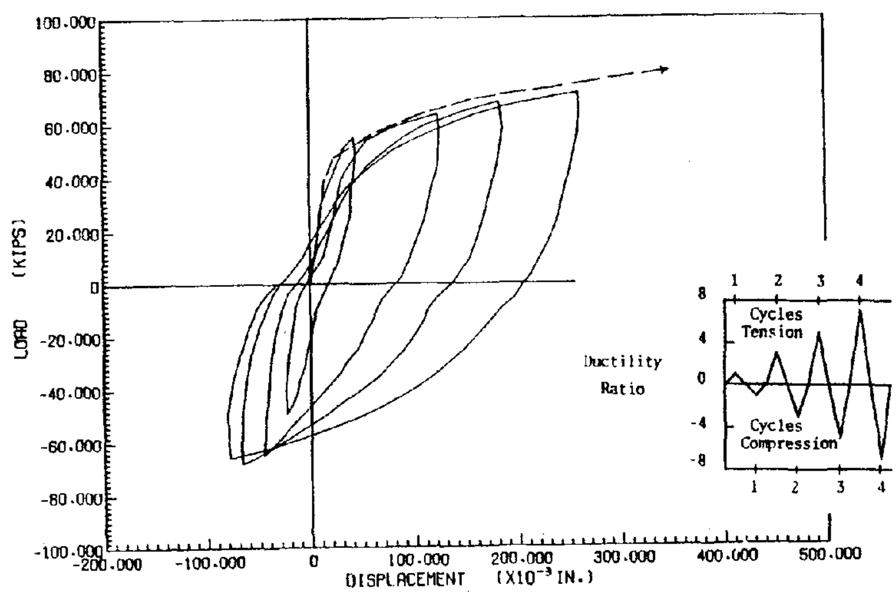


FIG. 47 LOAD-DISPLACEMENT CURVE, SPECIMEN B84

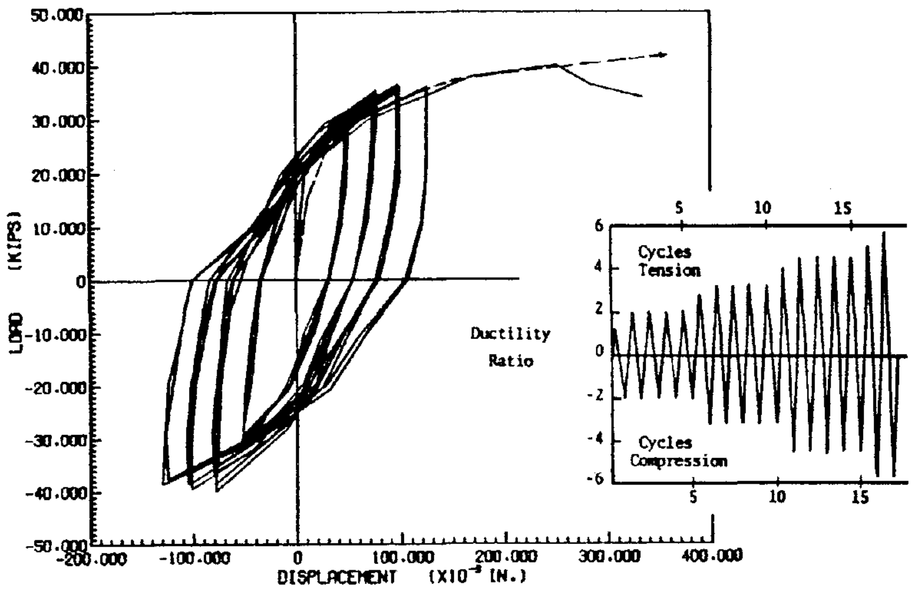


FIG. 50 LOAD-DISPLACEMENT CURVE, SPECIMEN S62

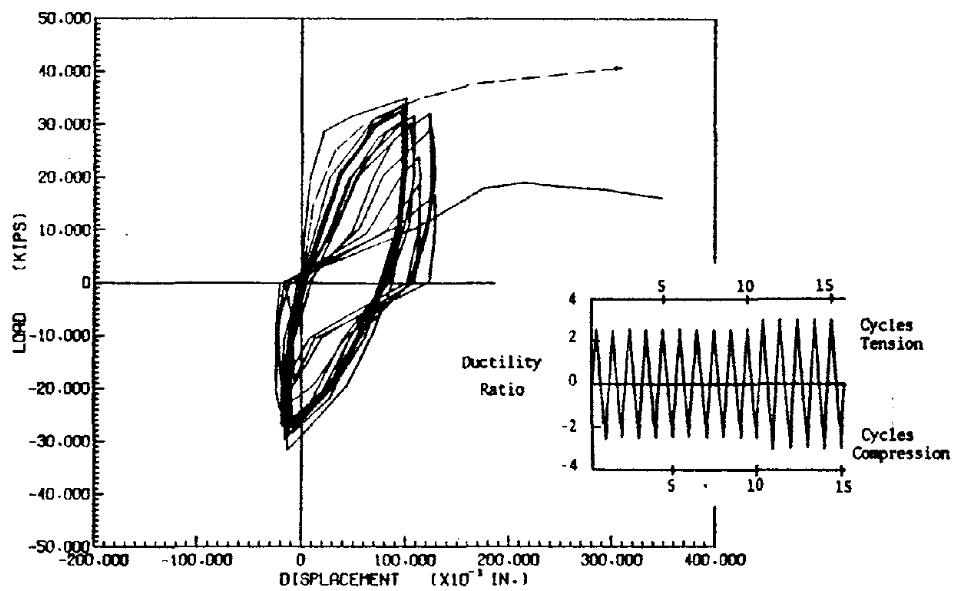


FIG. 49 LOAD-DISPLACEMENT CURVE, SPECIMEN S61

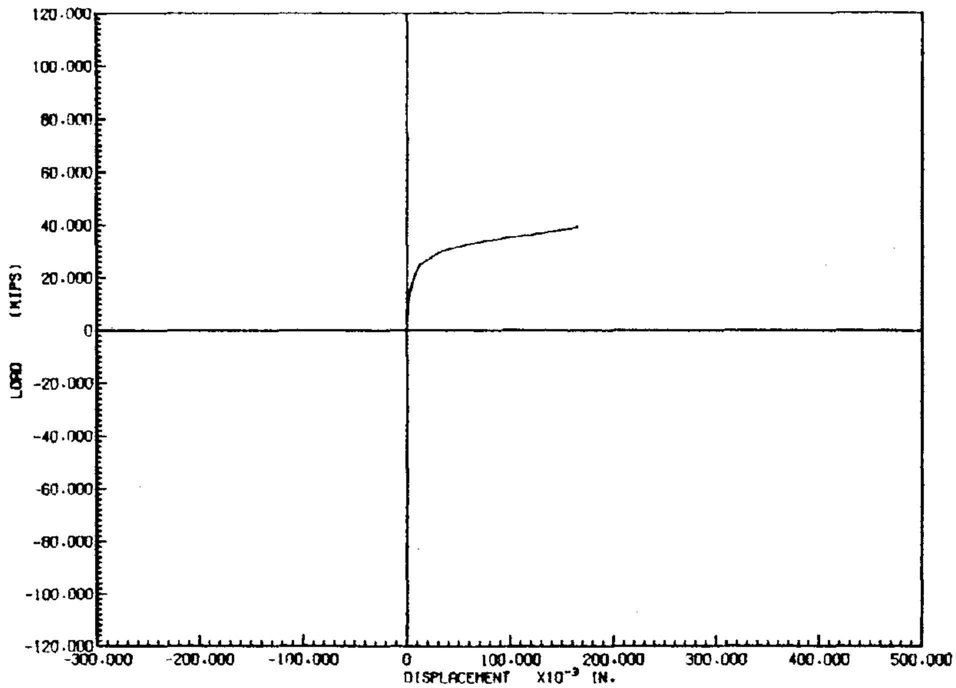


FIG. 52 LOAD-DISPLACEMENT CURVE, SPECIMEN S64

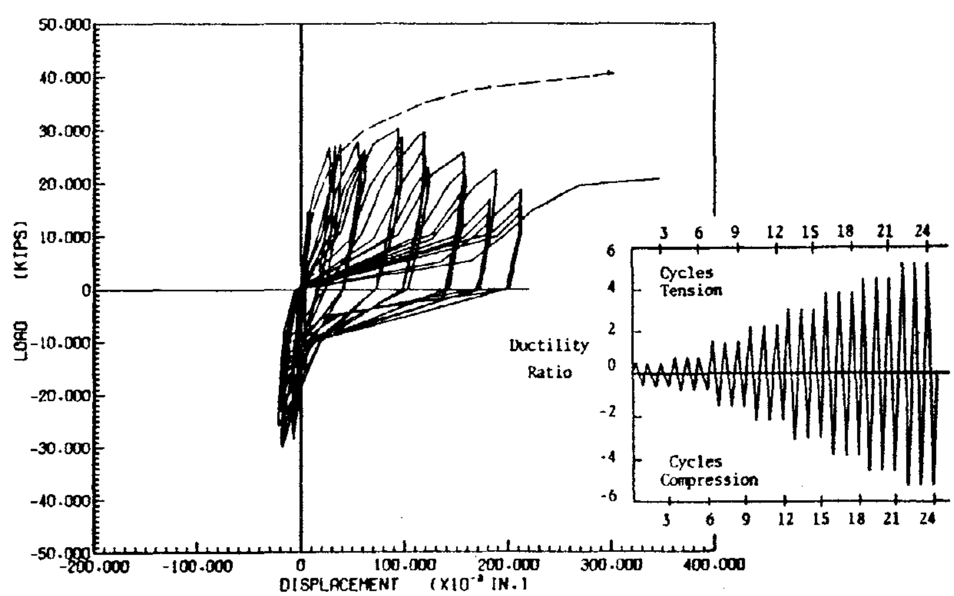


FIG. 51 LOAD-DISPLACEMENT CURVE, SPECIMEN S63

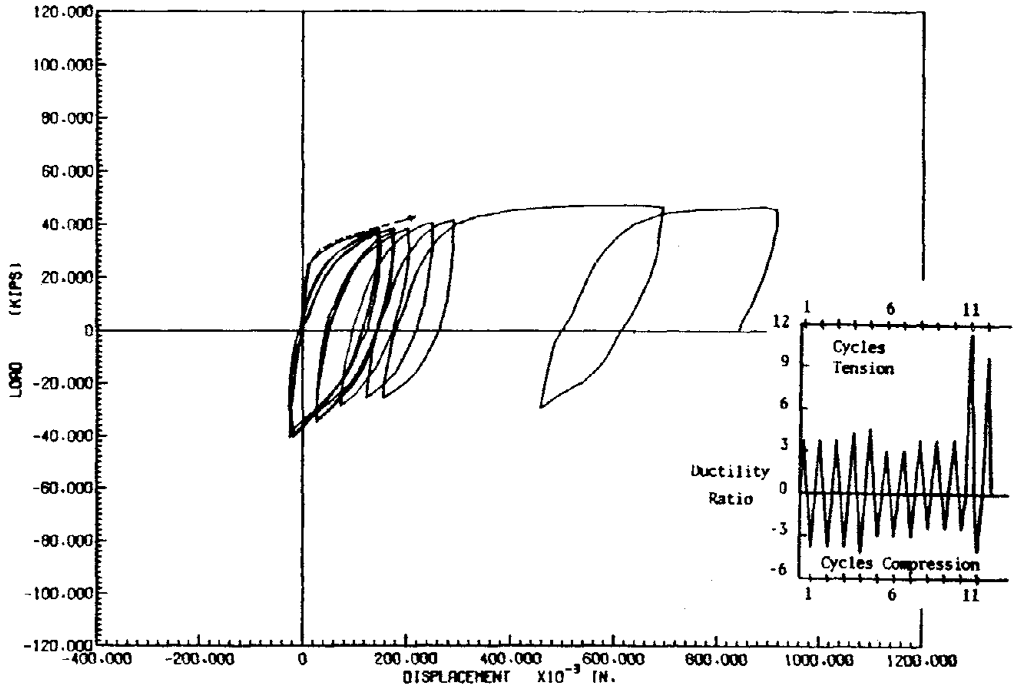


FIG. 54 LOAD-DISPLACEMENT CURVE, SPECIMEN S66

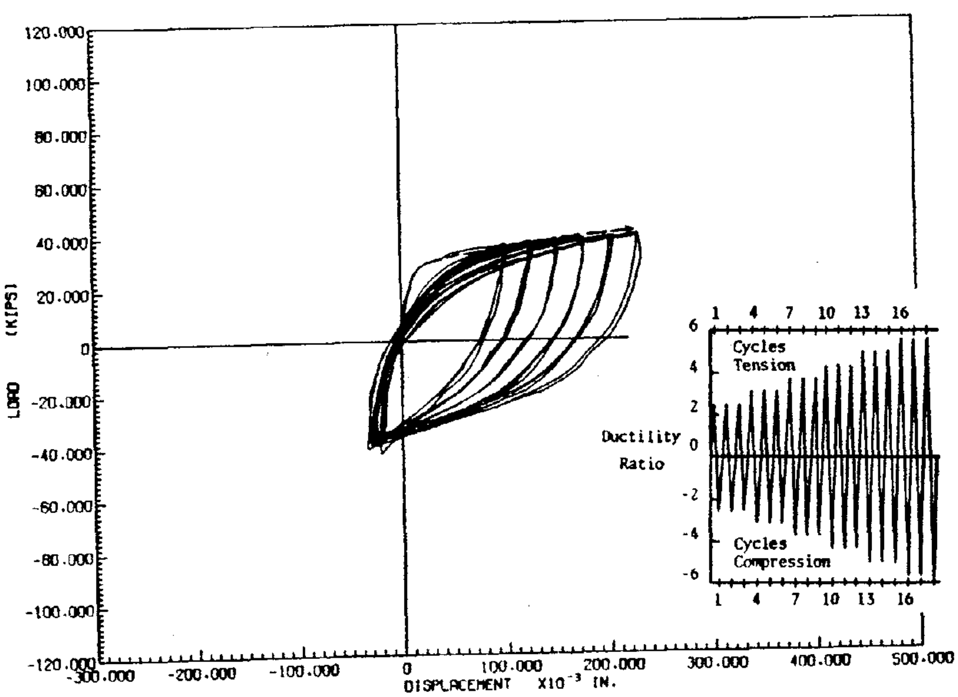


FIG. 53 LOAD-DISPLACEMENT CURVE, SPECIMEN S65

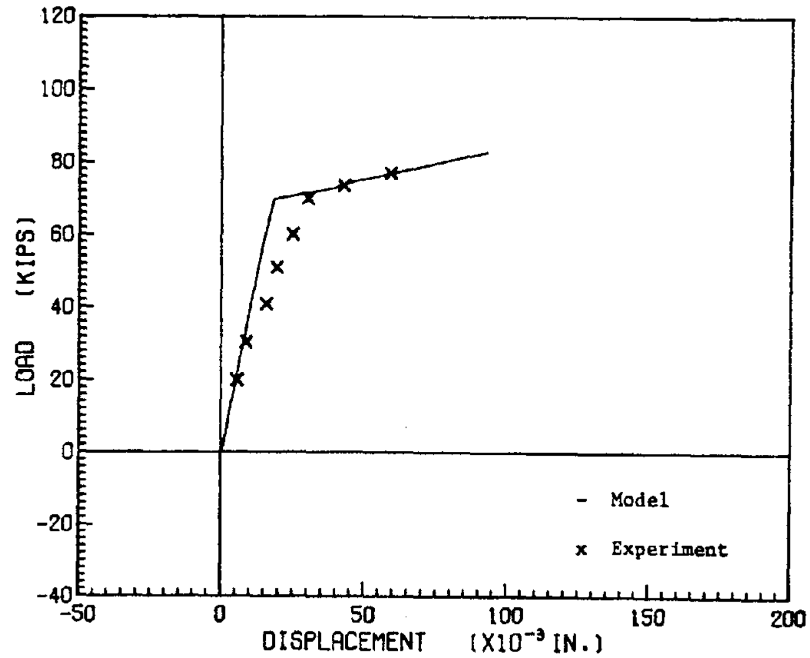


FIG. 56 COMPARISON OF MONOTONIC MODEL AND EXPERIMENT, SPECIMEN S103

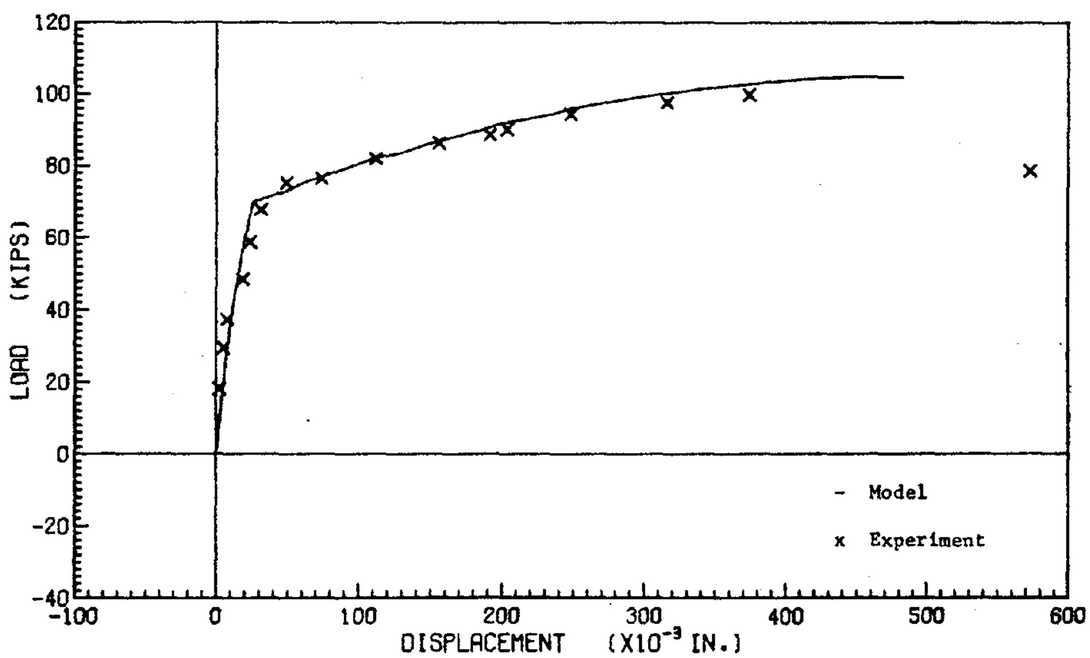


FIG. 55 COMPARISON OF MONOTONIC MODEL AND EXPERIMENT, SPECIMEN S101

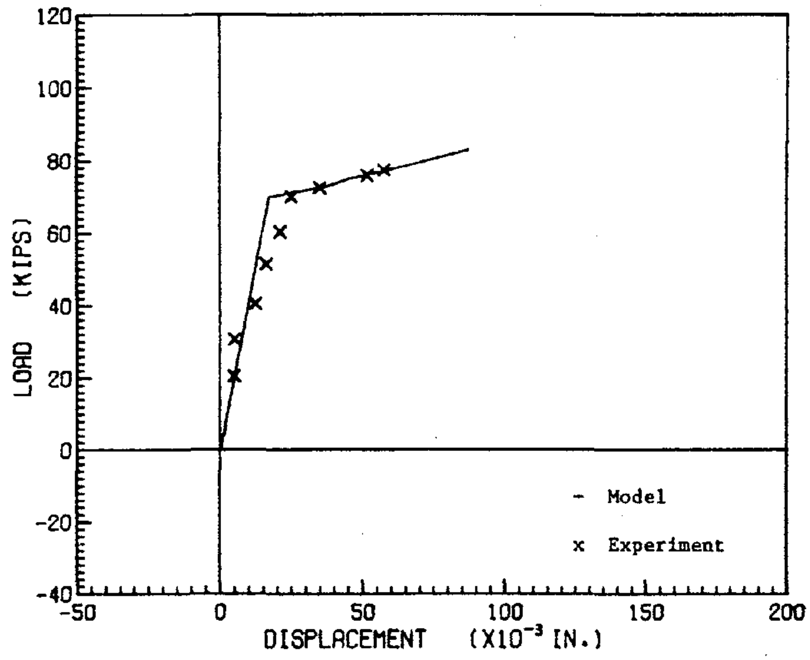


FIG. 58 COMPARISON OF MONOTONIC MODEL AND EXPERIMENT, SPECIMEN S105

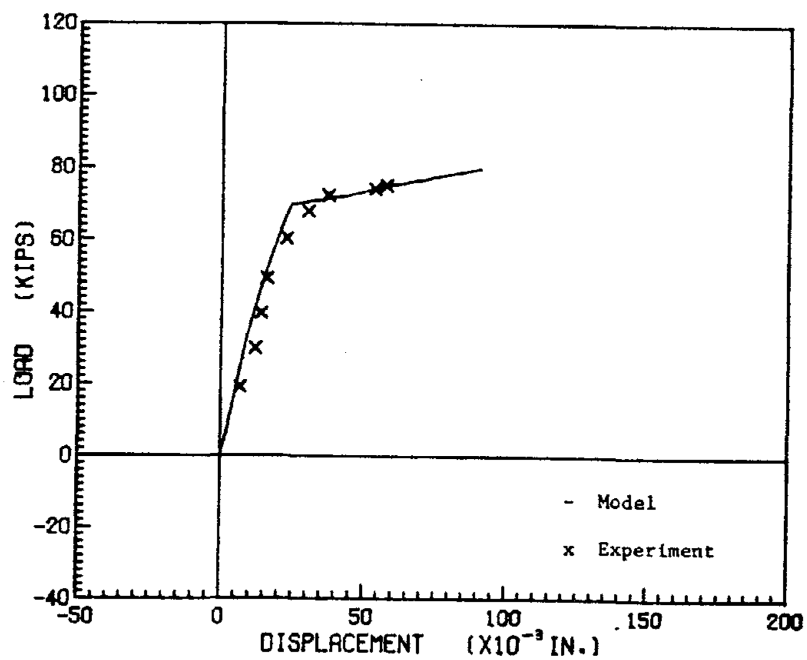


FIG. 57 COMPARISON OF MONOTONIC MODEL AND EXPERIMENT, SPECIMEN S104

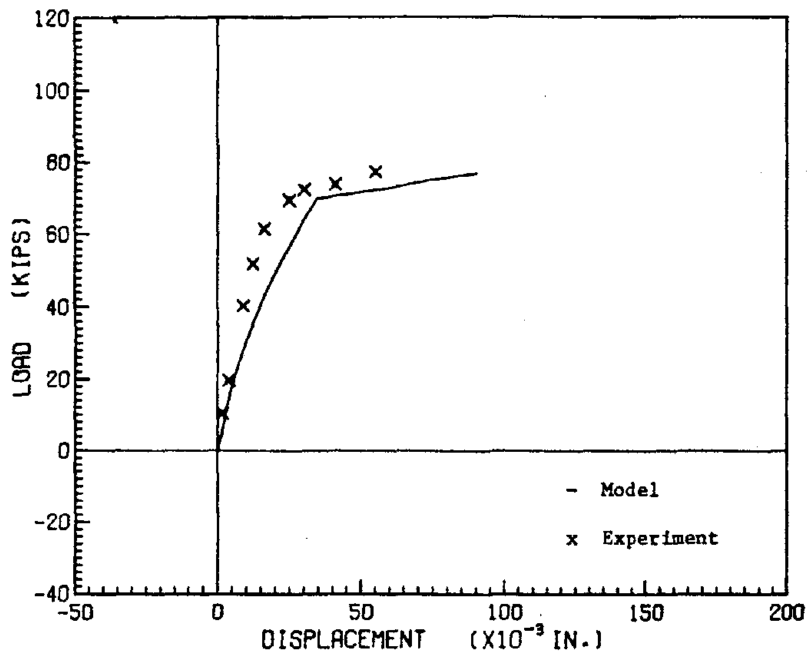


FIG. 60 COMPARISON OF MONOTONIC MODEL AND EXPERIMENT, SPECIMEN B101

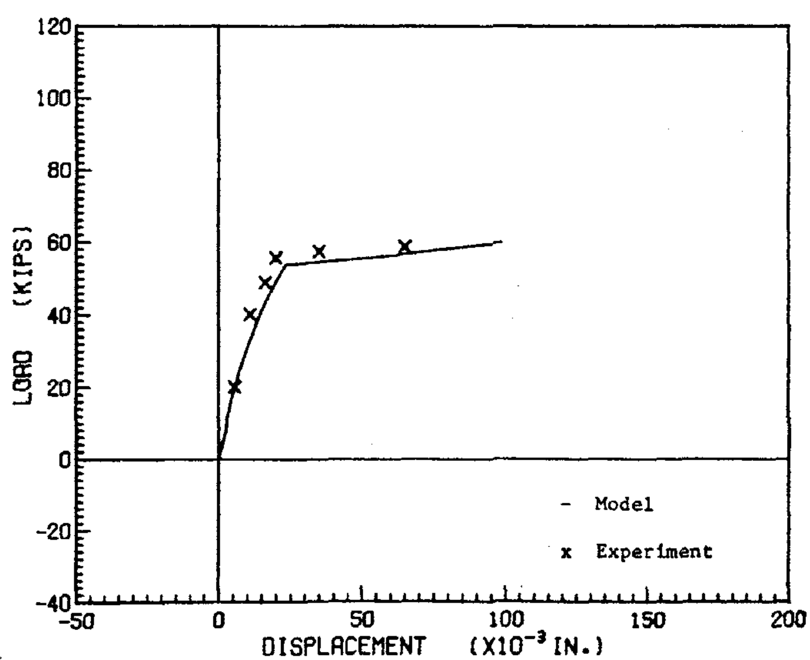


FIG. 59 COMPARISON OF MONOTONIC MODEL AND EXPERIMENT, SPECIMEN S107

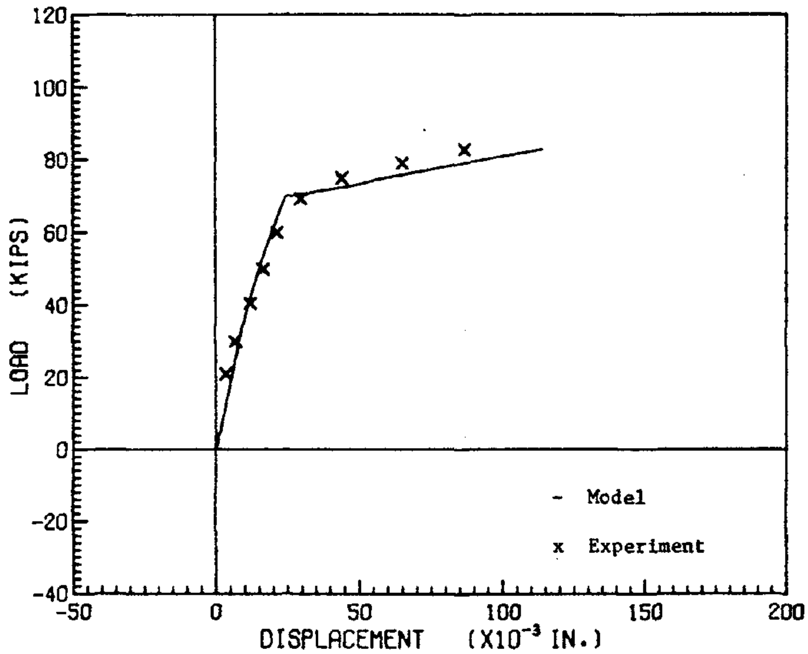


FIG. 62 COMPARISON OF MONOTONIC MODEL AND EXPERIMENT, SPECIMEN B103

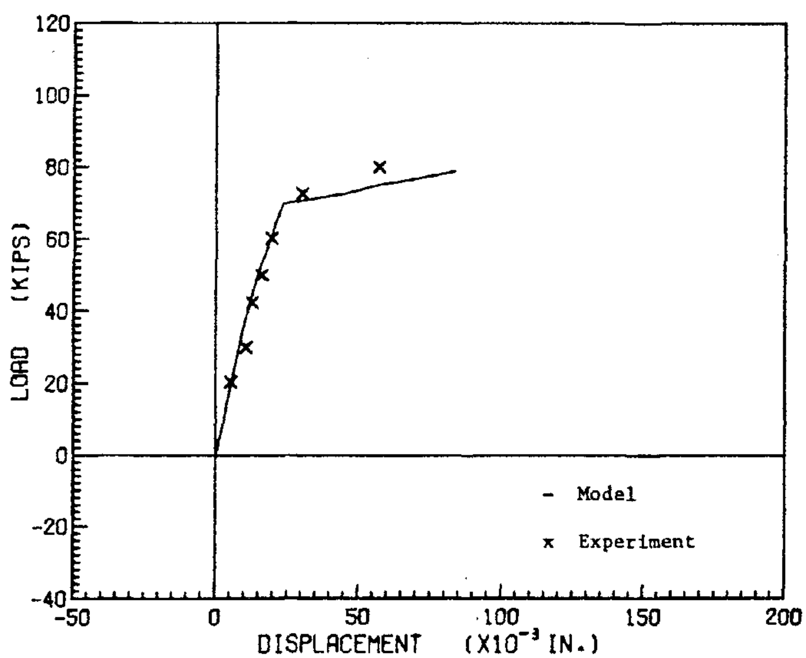


FIG. 61 COMPARISON OF MONOTONIC MODEL AND EXPERIMENT, SPECIMEN B102

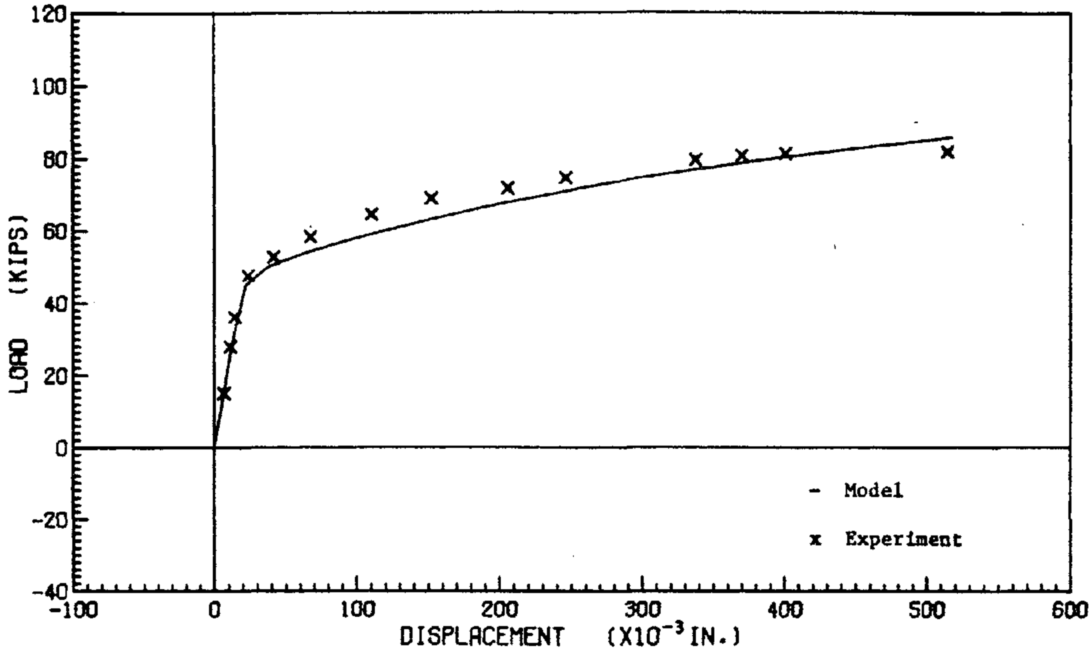


FIG. 64 COMPARISON OF MONOTONIC MODEL AND EXPERIMENT, SPECIMEN B81

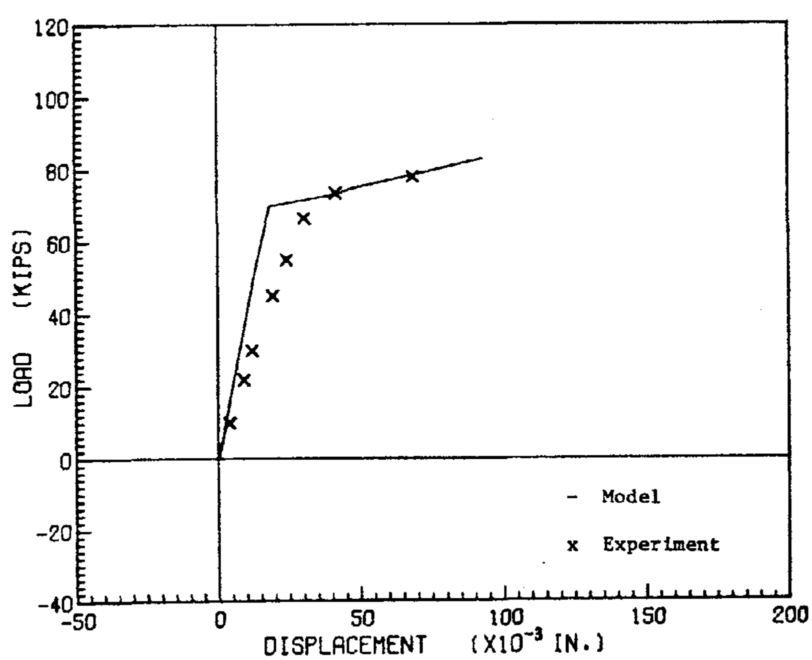


FIG. 63 COMPARISON OF MONOTONIC MODEL AND EXPERIMENT, SPECIMEN B104

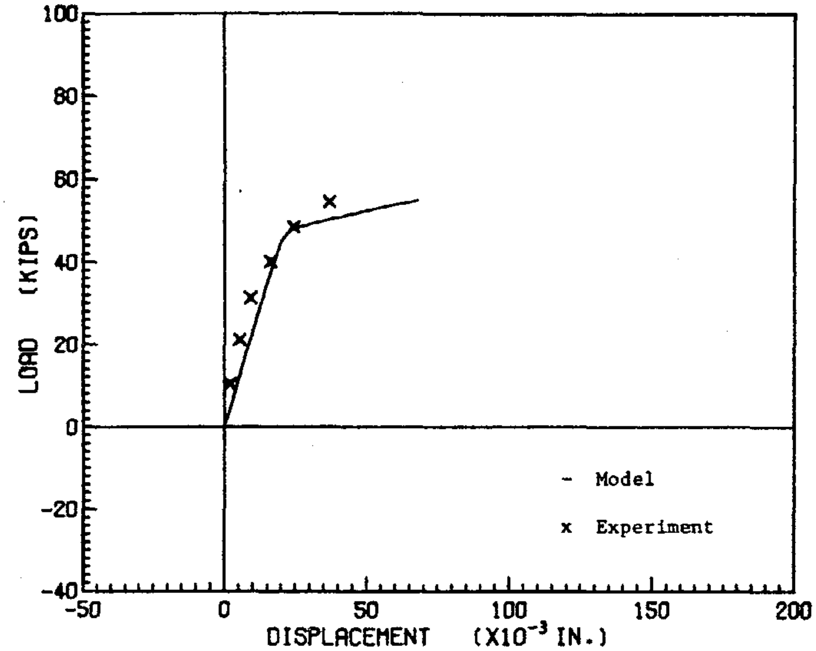


FIG. 65 COMPARISON OF MONOTONIC MODEL AND EXPERIMENT, SPECIMEN B82

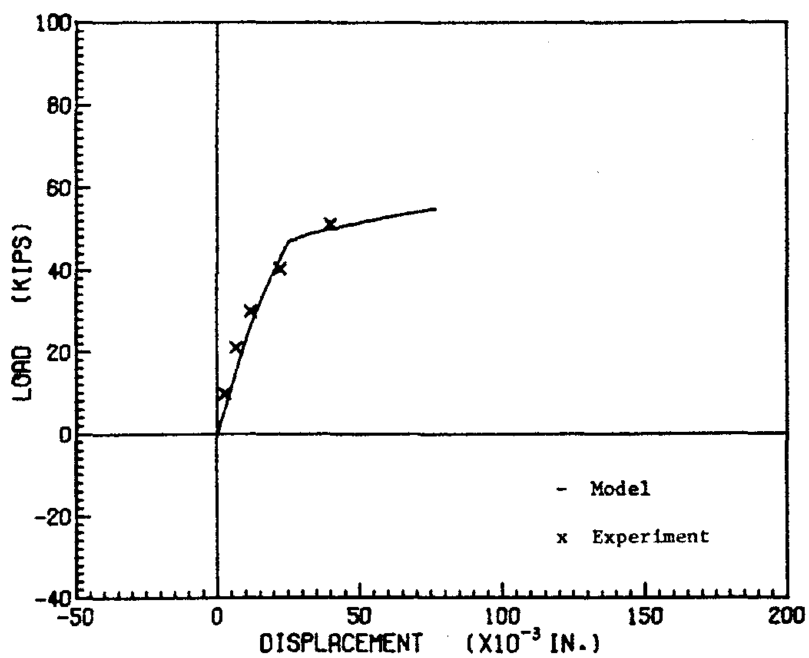


FIG. 66 COMPARISON OF MONOTONIC MODEL AND EXPERIMENT, SPECIMEN B83

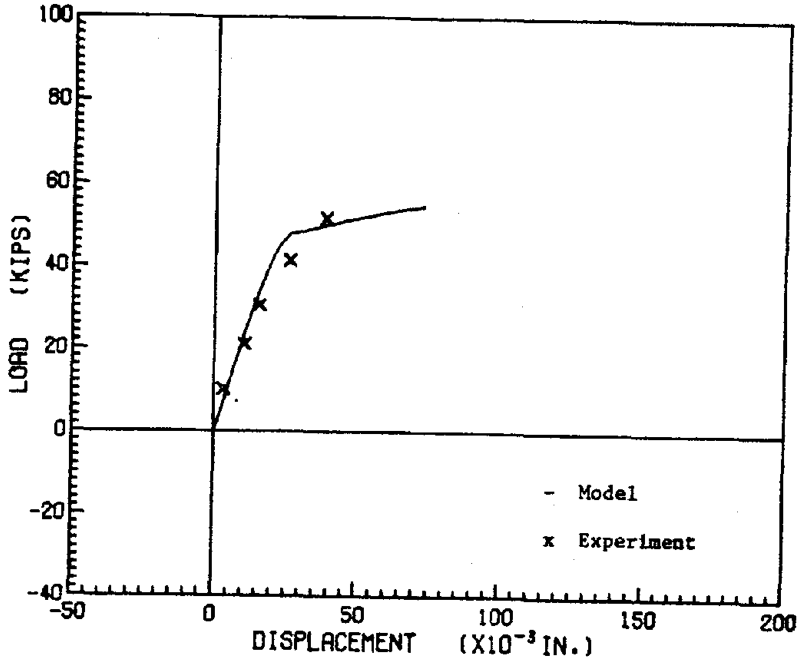


FIG. 68 COMPARISON OF MONOTONIC MODEL AND EXPERIMENT, SPECIMEN B85

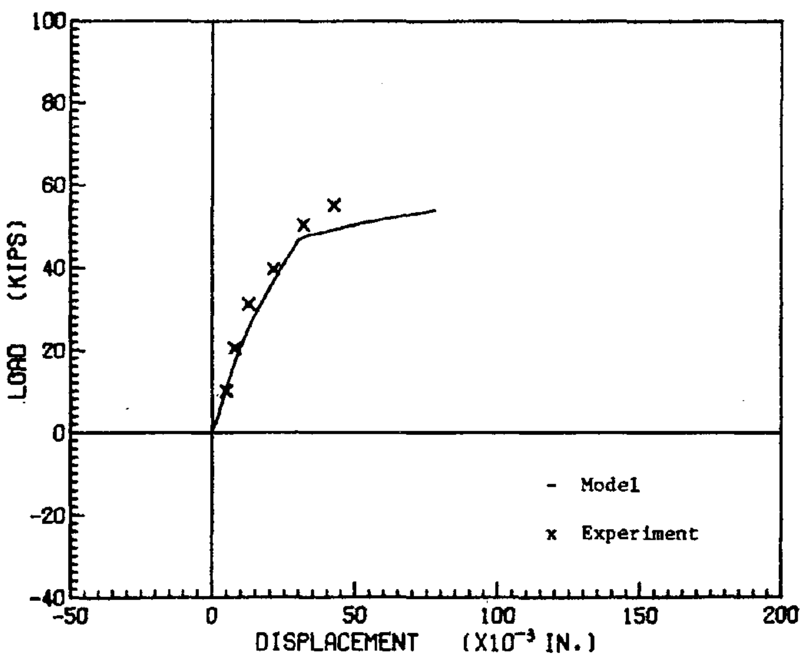


FIG. 67 COMPARISON OF MONOTONIC MODEL AND EXPERIMENT, SPECIMEN B84

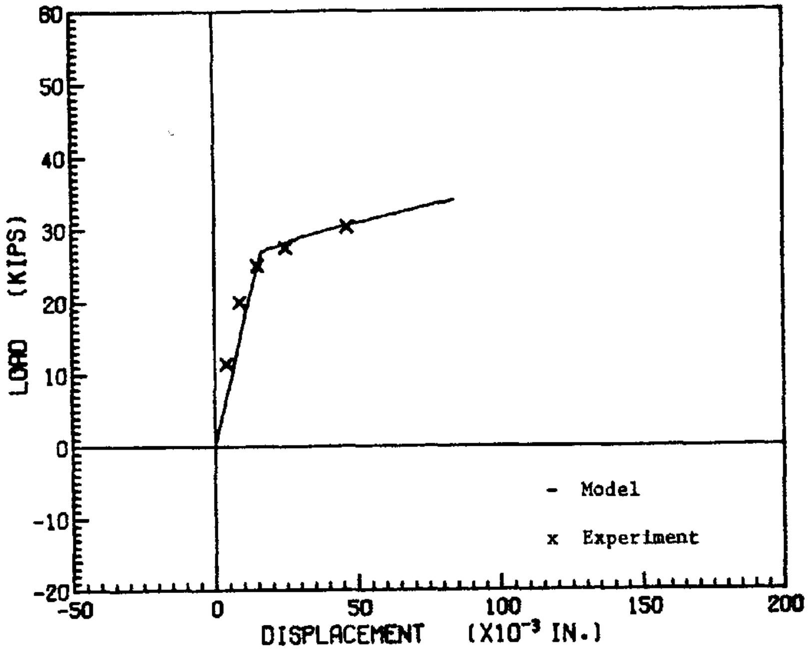


FIG. 70 COMPARISON OF MONOTONIC MODEL AND EXPERIMENT, SPECIMEN S62

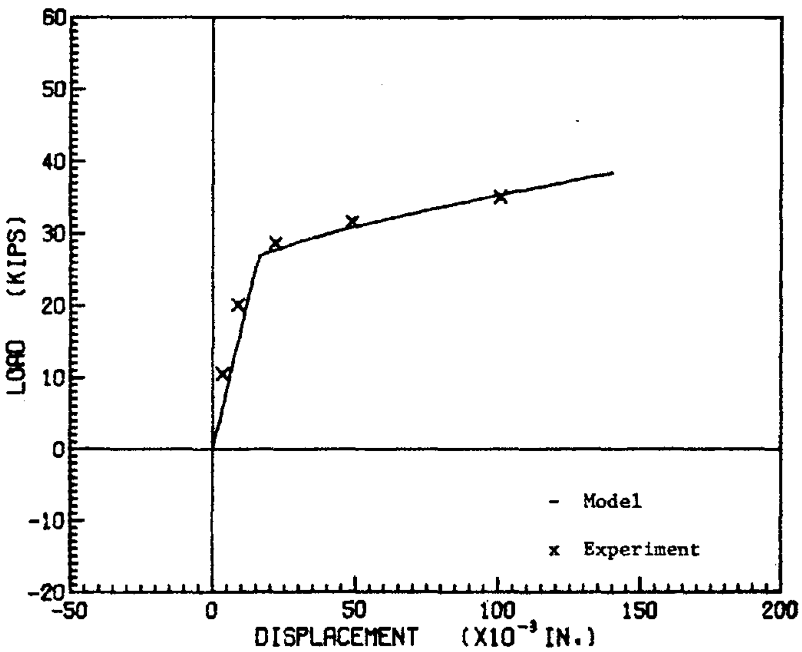


FIG. 69 COMPARISON OF MONOTONIC MODEL AND EXPERIMENT, SPECIMEN S61

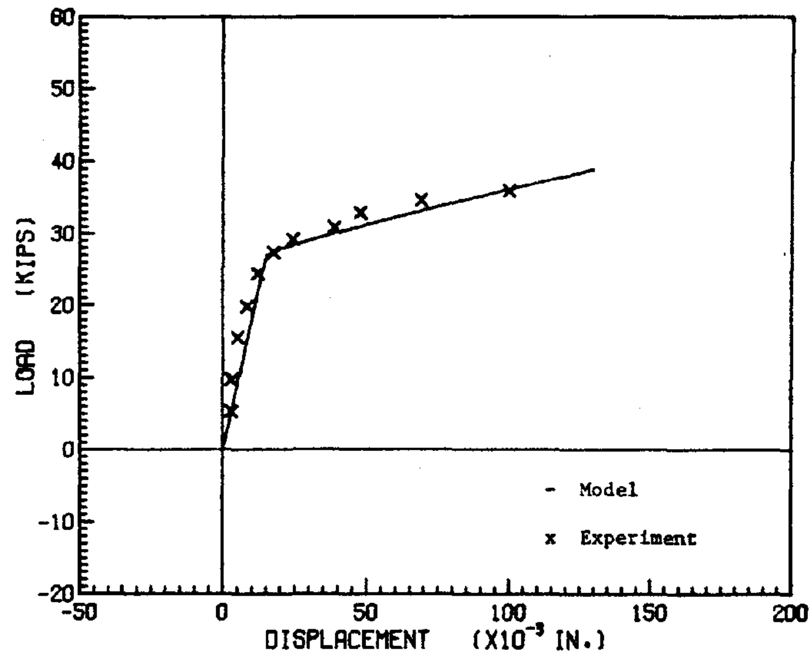


FIG. 72 COMPARISON OF MONOTONIC MODEL AND EXPERIMENT, SPECIMEN S65

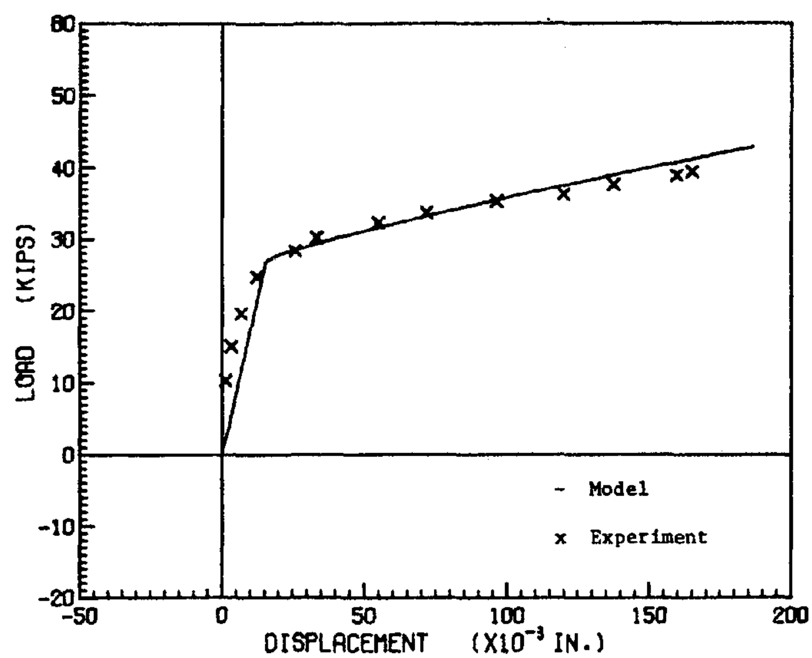


FIG. 71 COMPARISON OF MONOTONIC MODEL AND EXPERIMENT, SPECIMEN S64

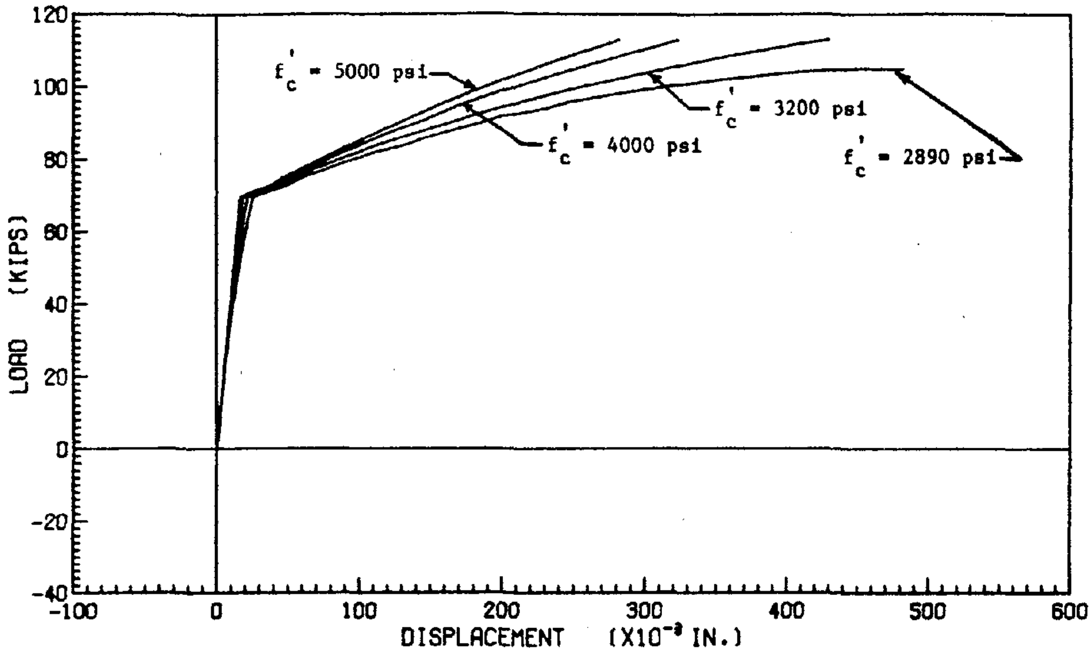


FIG. 74 EFFECT OF THE CONCRETE STRENGTH TO THE PREDICTION OF LOAD-DISPLACEMENT CURVES FOR JOINTS WITH STRAIGHT BARS

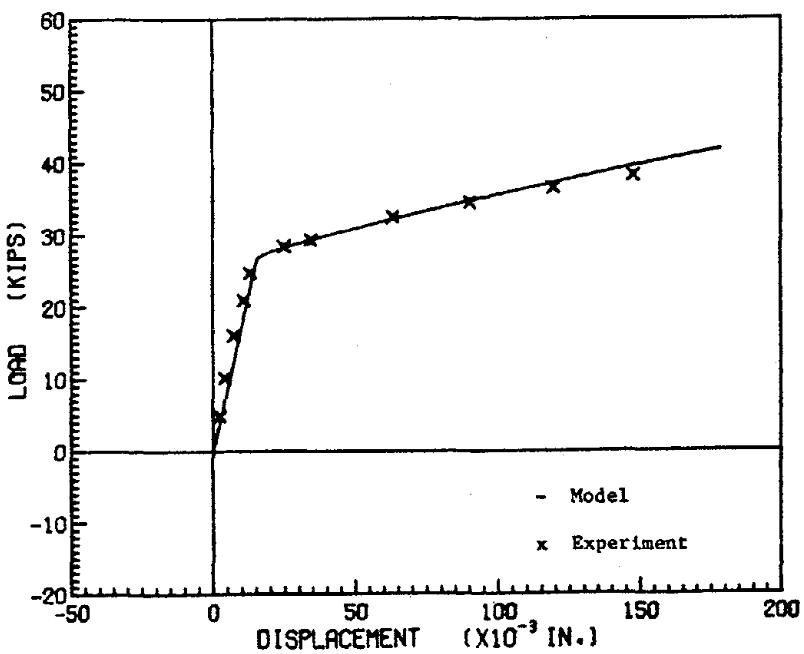


FIG. 73 COMPARISON OF MONOTONIC MODEL AND EXPERIMENT, SPECIMEN S66

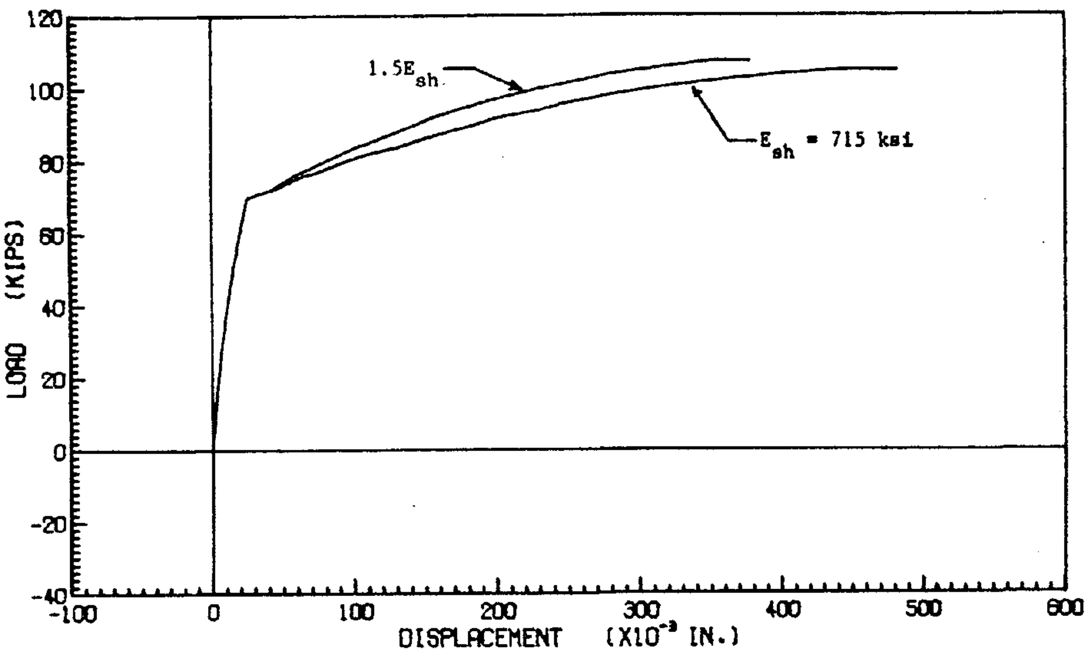


FIG. 76 EFFECT OF THE STRAIN HARDENING MODULUS TO THE PREDICTION OF LOAD-DISPLACEMENT CURVES FOR JOINTS WITH STRAIGHT BARS

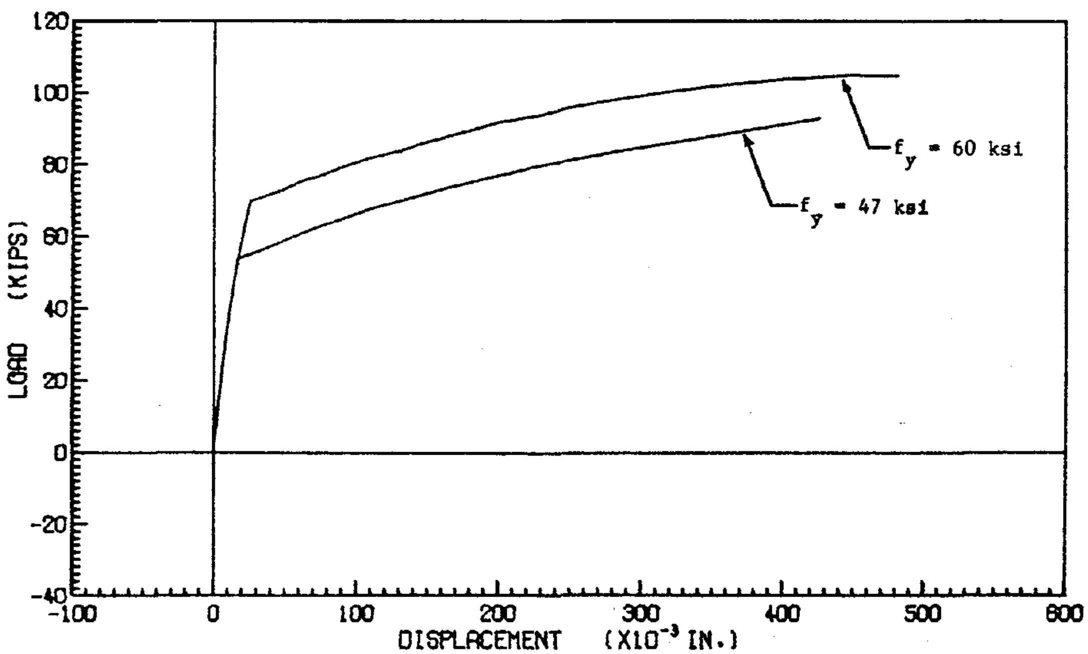


FIG. 75 EFFECT OF THE BAR'S YIELD STRENGTH TO THE PREDICTION OF LOAD-DISPLACEMENT CURVES FOR JOINTS WITH STRAIGHT BARS

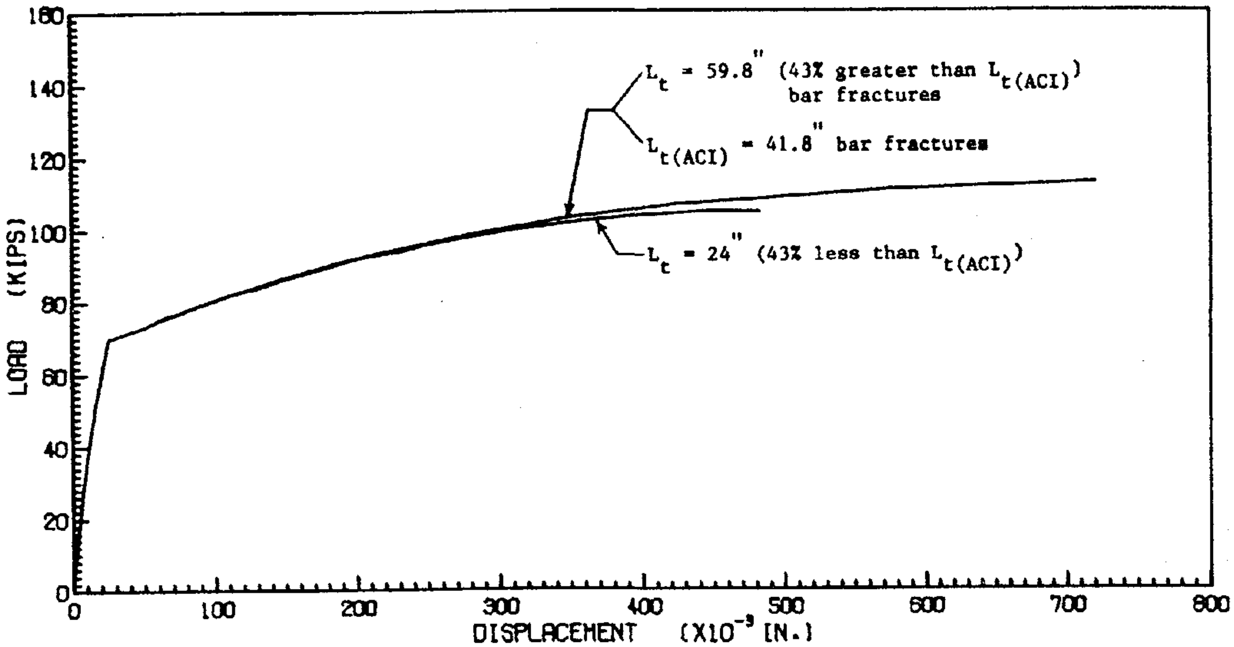


FIG. 78 EFFECT OF THE EMBEDMENT LENGTH TO THE PREDICTION OF LOAD-DISPLACEMENT CURVES FOR JOINTS WITH STRAIGHT BARS

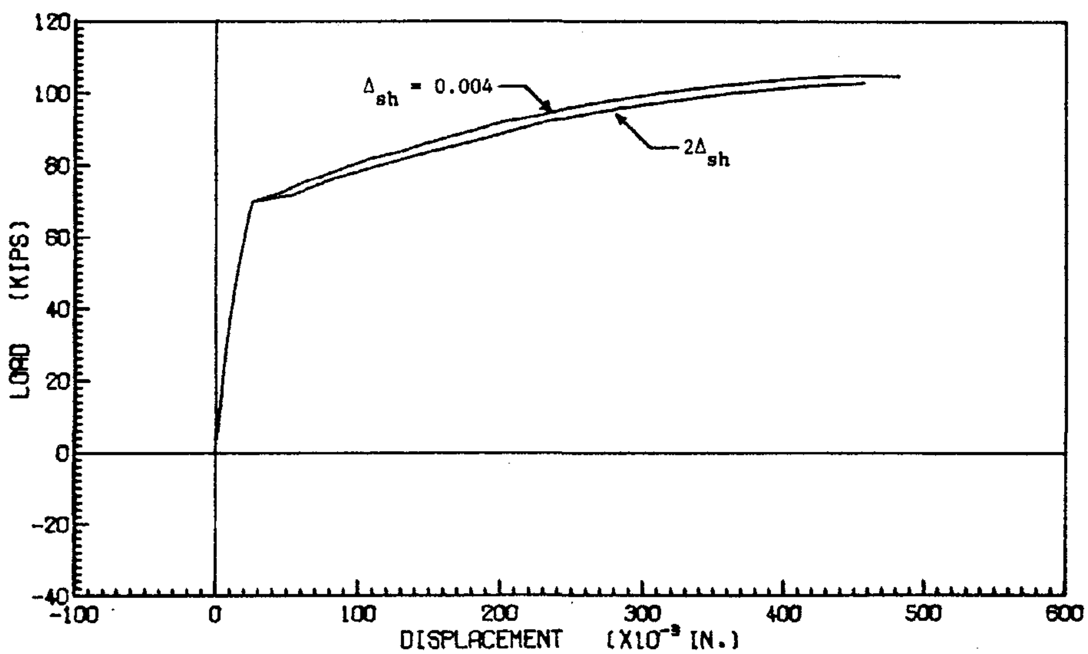


FIG. 77 EFFECT OF THE LENGTH OF YIELD PLATEAU TO THE PREDICTION OF LOAD-DISPLACEMENT CURVES FOR JOINTS WITH STRAIGHT BARS

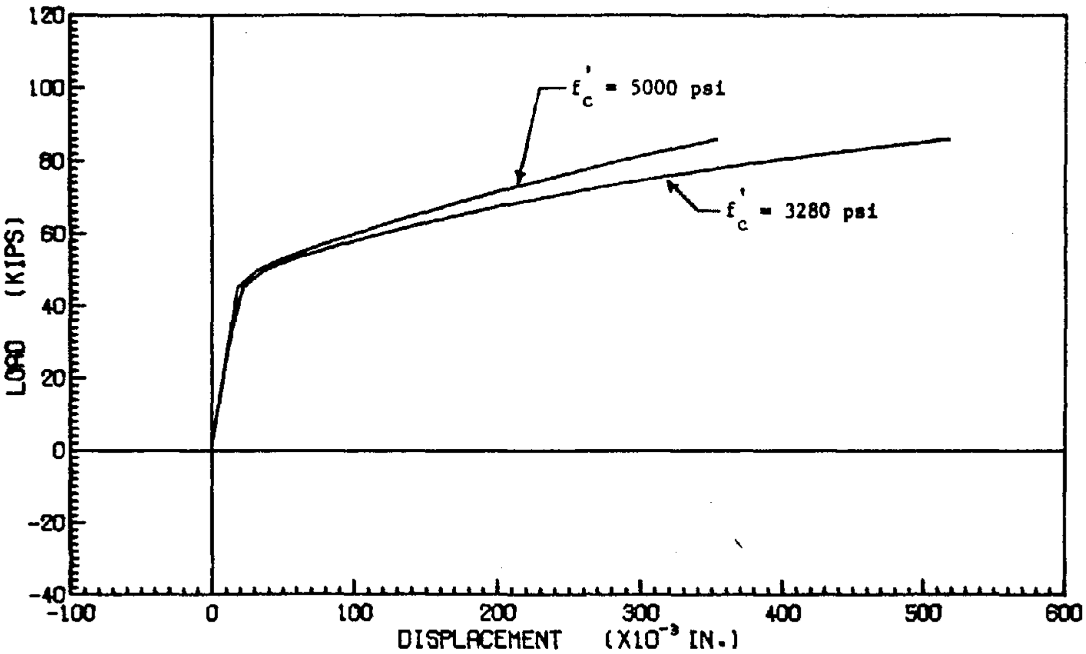


FIG. 80 EFFECT OF THE CONCRETE STRENGTH TO THE PREDICTION OF LOAD-DISPLACEMENT CURVES FOR JOINTS WITH 90 DEGREE HOOKED BARS

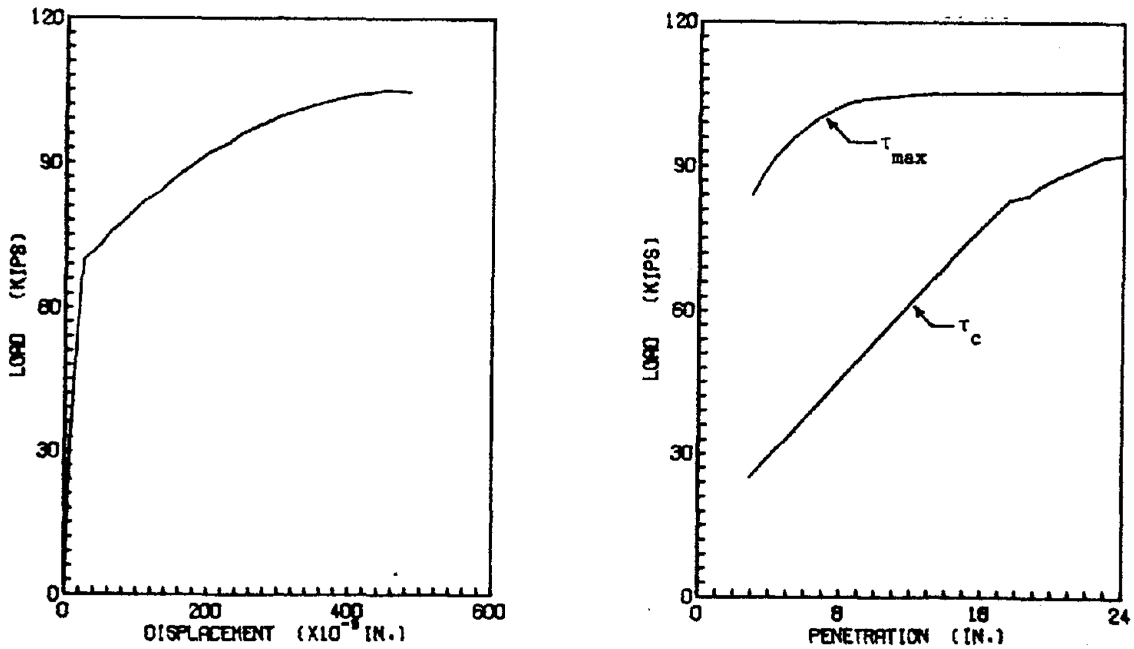


(a) Load-Displacement Curve

(b) Penetration of $\tau_c$ and $\tau_{max}$

FIG. 79 CORRELATION BETWEEN THE LOAD-DISPLACEMENT CURVE AND THE PENETRATION OF $\tau_c$ AND $\tau_{max}$, SPECIMEN S101

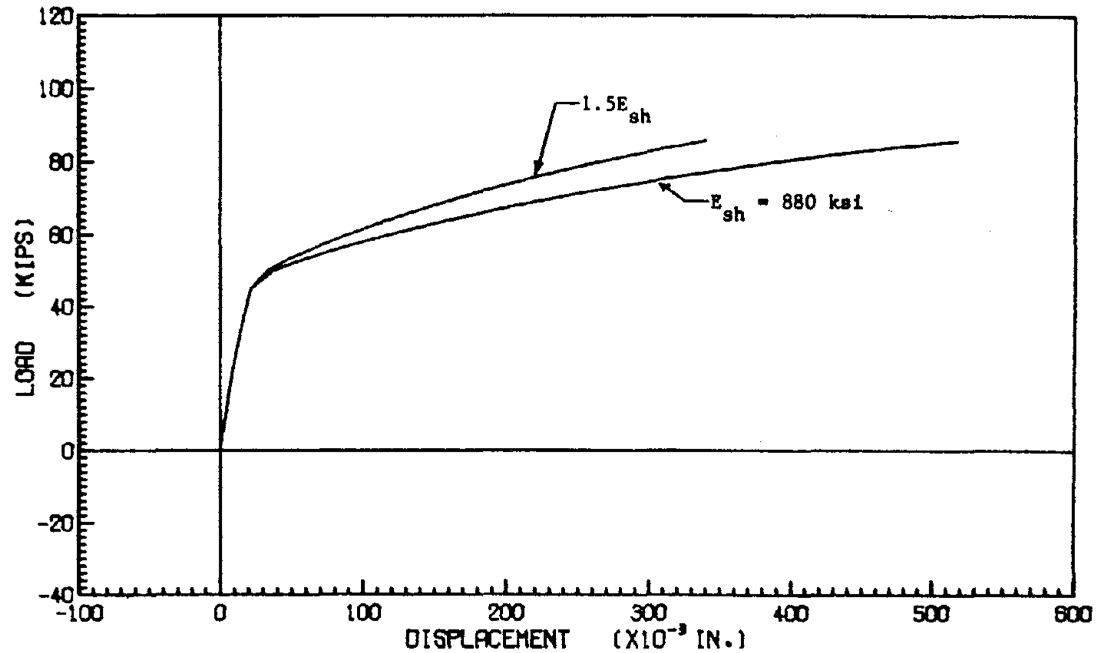


FIG. 82 EFFECT OF THE STRAIN HARDENING MODULUS TO THE PREDICTION OF LOAD-DISPLACEMENT CURVES FOR JOINTS WITH 90 DEGREE HOOKED BARS

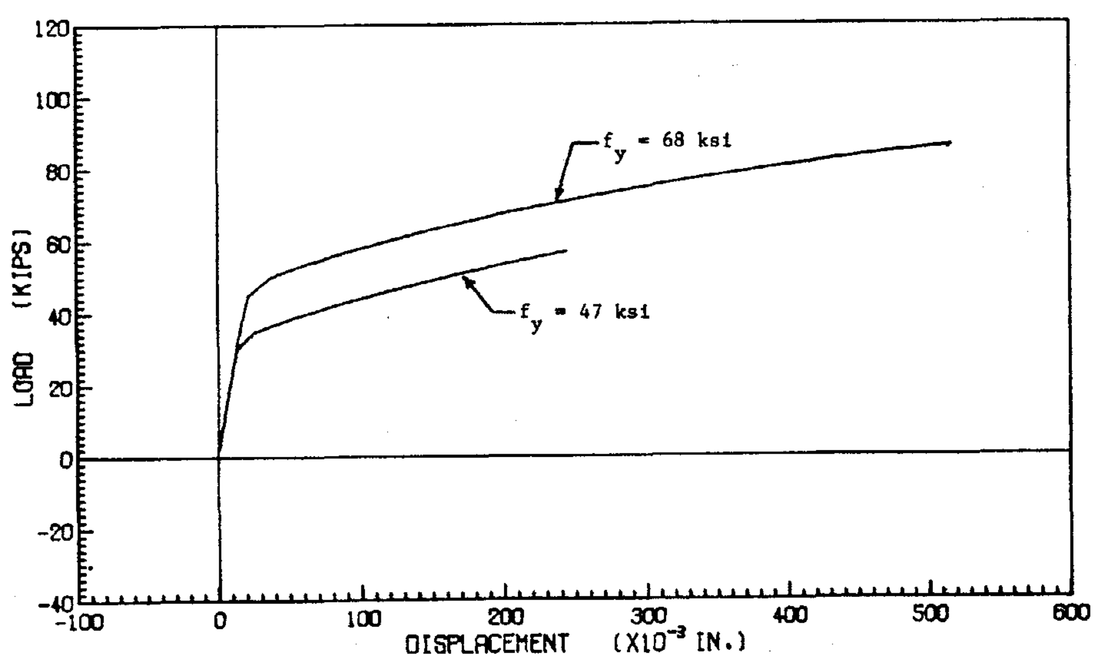


FIG. 81 EFFECT OF THE YIELD STRENGTH TO THE PREDICTION OF LOAD-DISPLACEMENT CURVES FOR JOINTS WITH 90 DEGREE HOOKED BARS

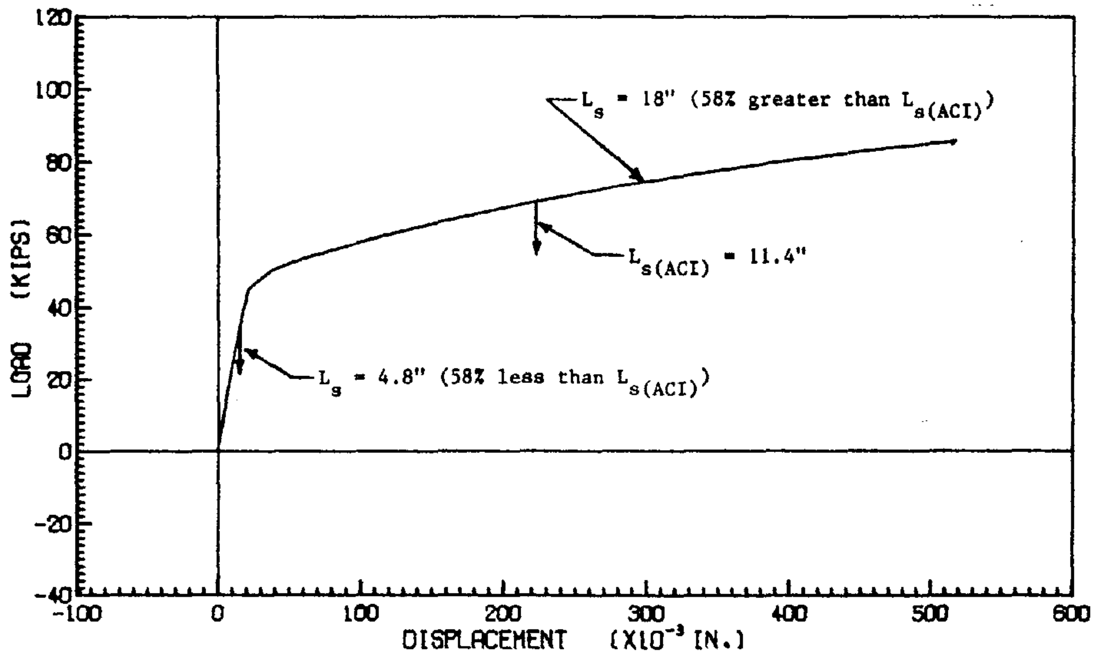


FIG. 84 EFFECT OF THE LEAD-IN LENGTH TO THE PREDICTION OF LOAD-DISPLACEMENT CURVES FOR JOINTS WITH 90 DEGREE HOOKED BARS

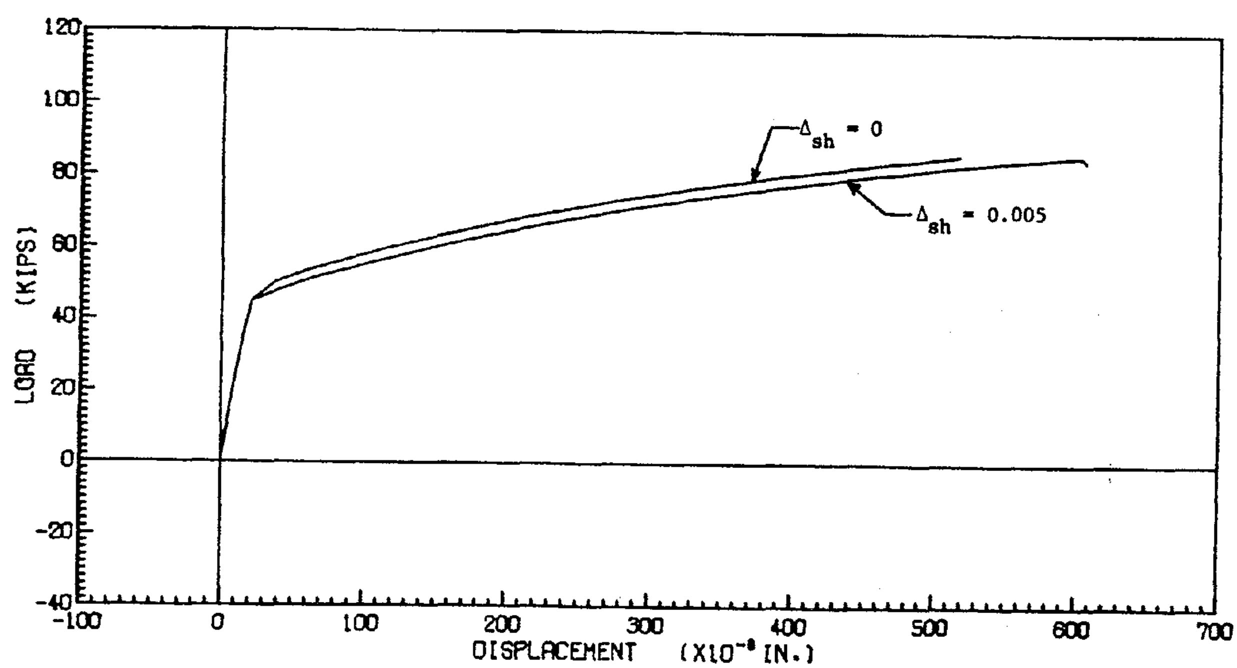


FIG. 83 EFFECT OF THE LENGTH OF THE YIELD PLATEAU TO THE PREDICTION OF LOAD-DISPLACEMENT CURVES FOR JOINTS WITH 90 DEGREE HOOKED BARS

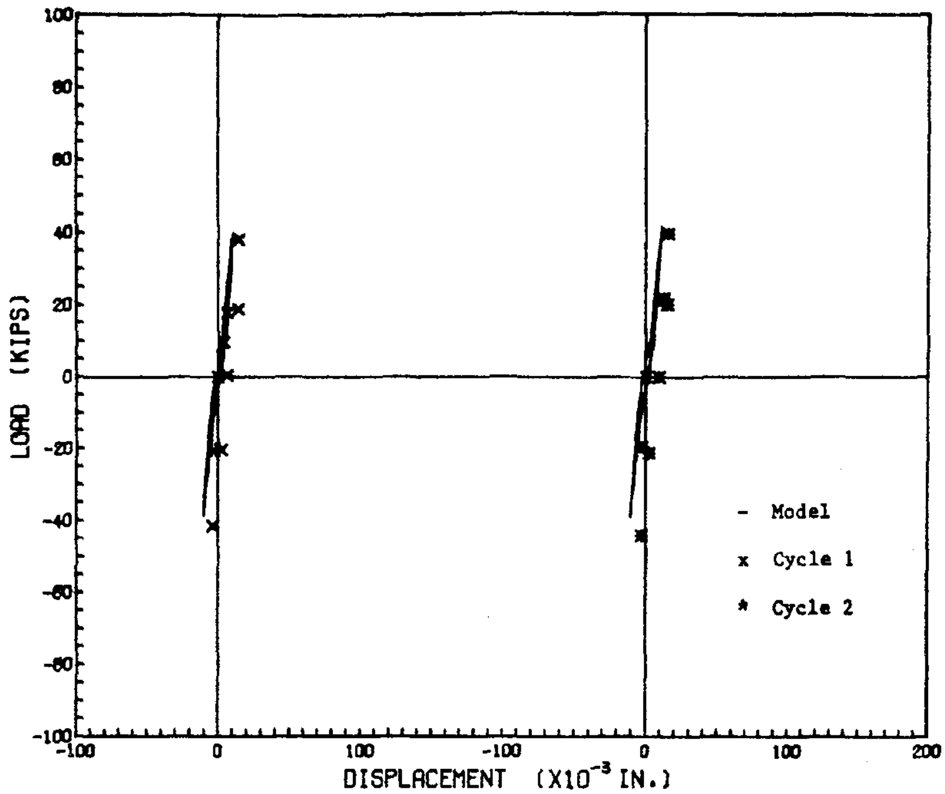


FIG. 86 COMPARISON OF CYCLIC MODEL AND EXPERIMENT, SPECIMEN S102, CYCLES 1 - 2

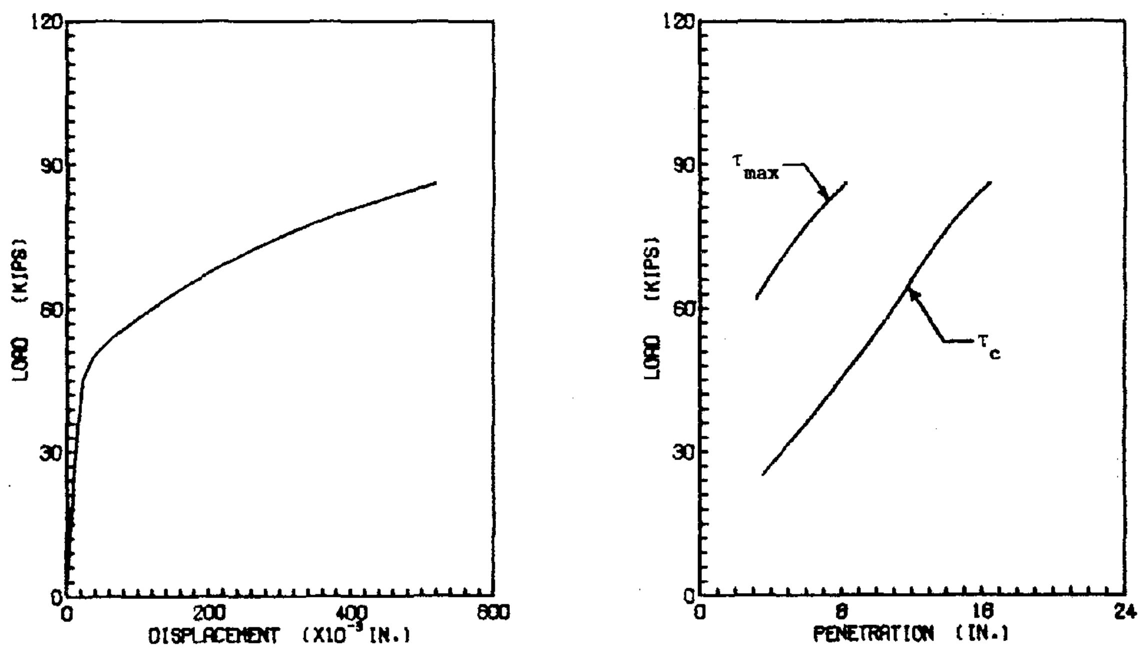


(a) Load-Displacement Curve

(b) Penetration of $\tau_c$ and $\tau_{max}$

FIG. 85 CORRELATION BETWEEN THE LOAD-DISPLACEMENT CURVE AND THE PENETRATION OF $\tau_c$ AND $\tau_{max}$, SPECIMEN B81

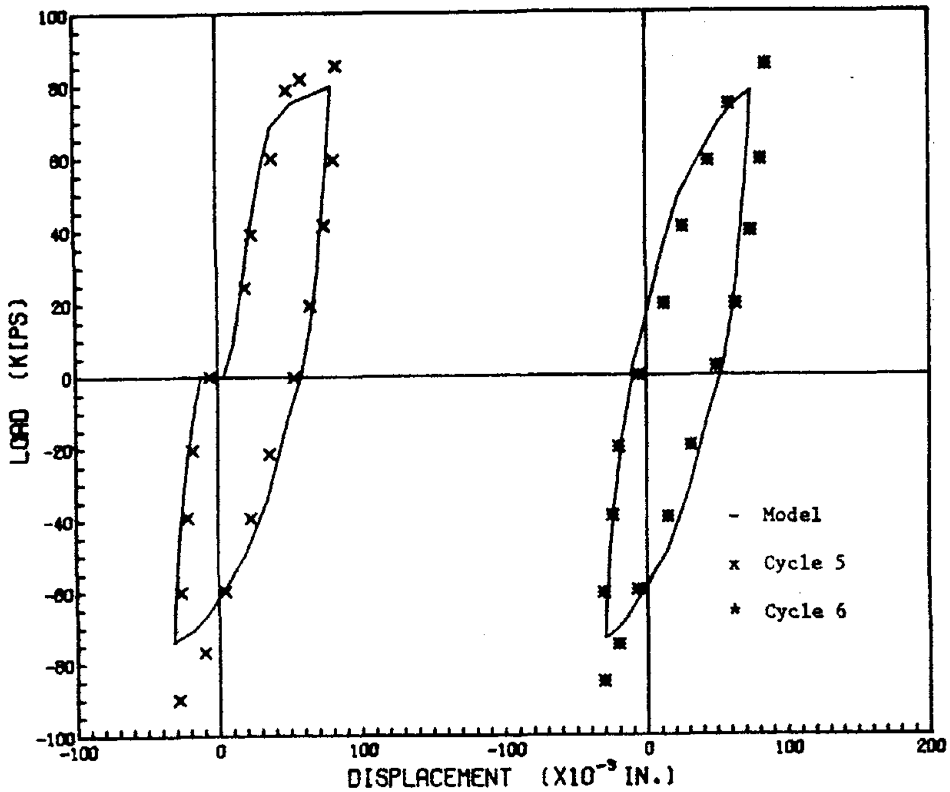


FIG. 88 COMPARISON OF CYCLIC MODEL AND EXPERIMENT, SPECIMEN S102, CYCLES 5 - 6

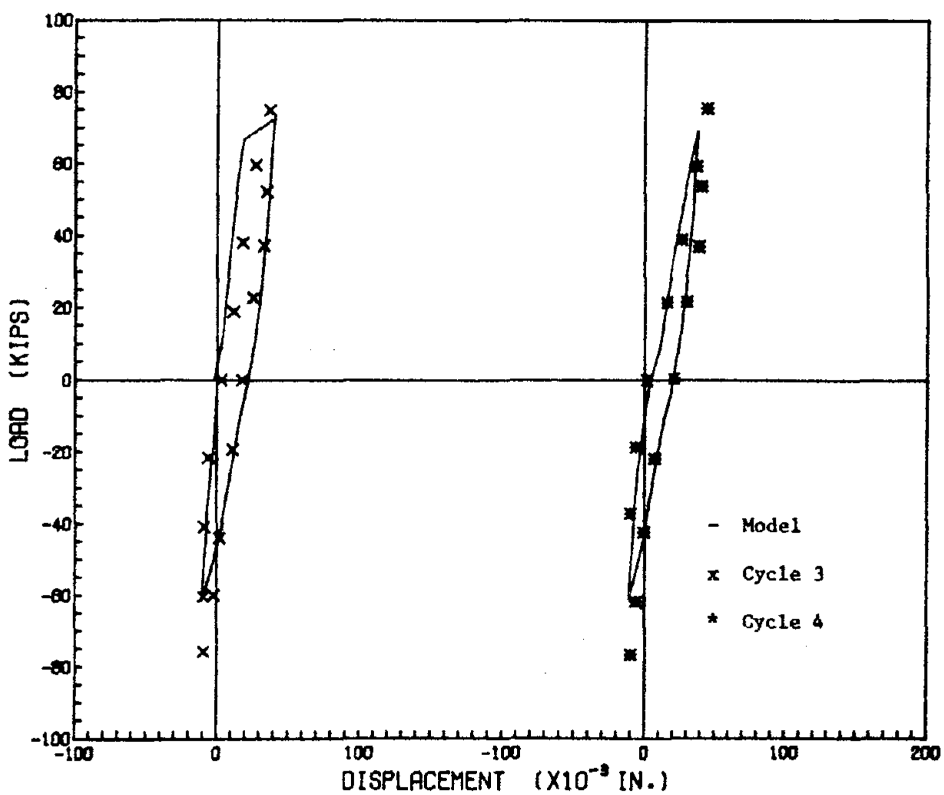


FIG. 87 COMPARISON OF CYCLIC MODEL AND EXPERIMENT, SPECIMEN S102, CYCLES 3 - 4

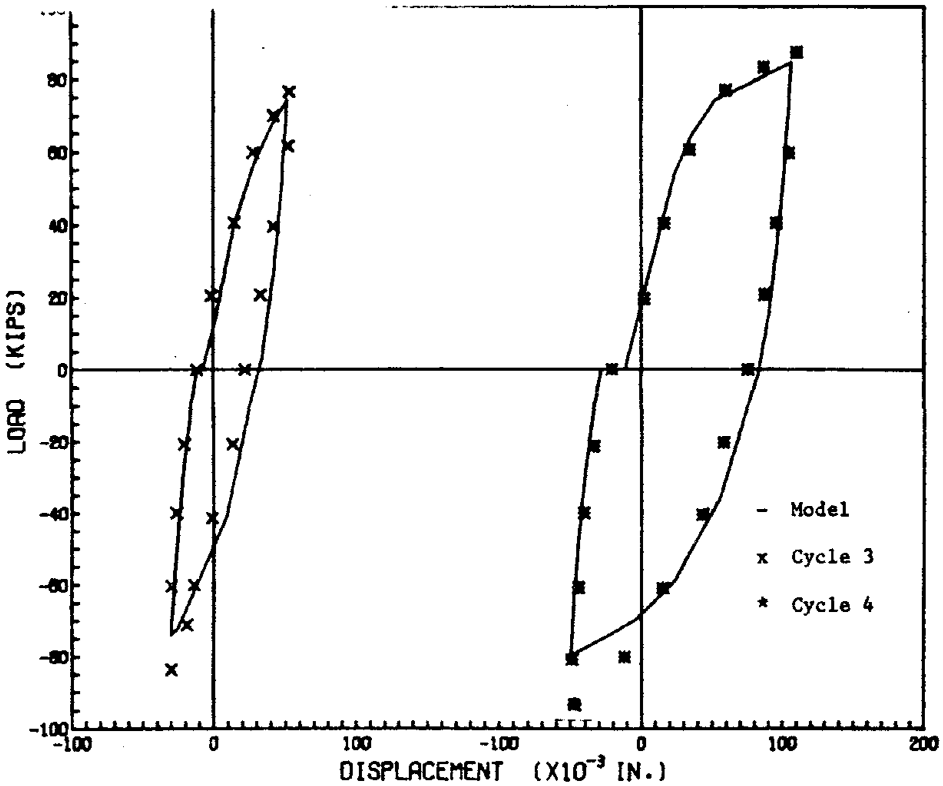


FIG. 90 COMPARISON OF CYCLIC MODEL AND EXPERIMENT, SPECIMEN S103, CYCLES 3 - 4

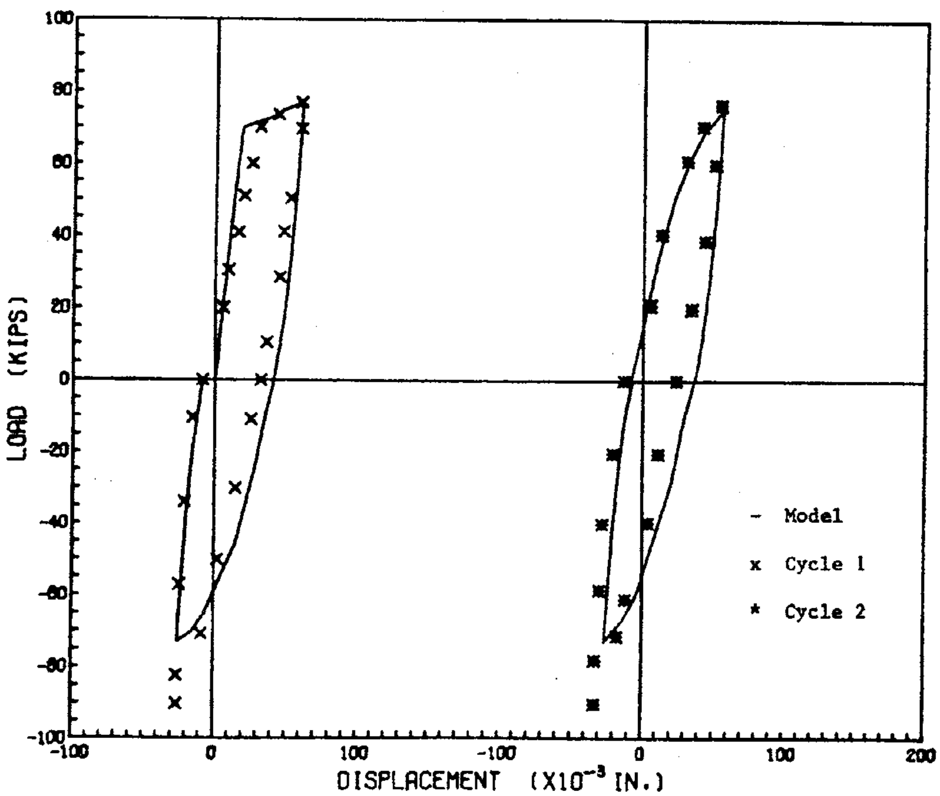


FIG. 89 COMPARISON OF CYCLIC MODEL AND EXPERIMENT, SPECIMEN S103, CYCLES 1 - 2

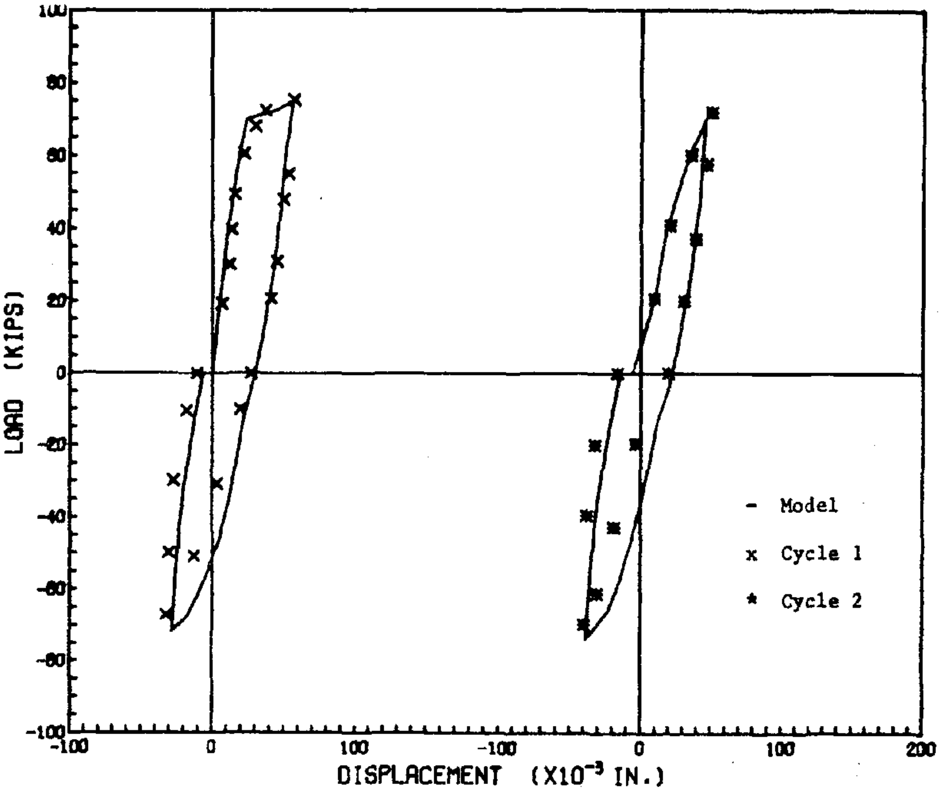


FIG. 92 COMPARISON OF CYCLIC MODEL AND EXPERIMENT, SPECIMEN S104, CYCLES 1 - 2

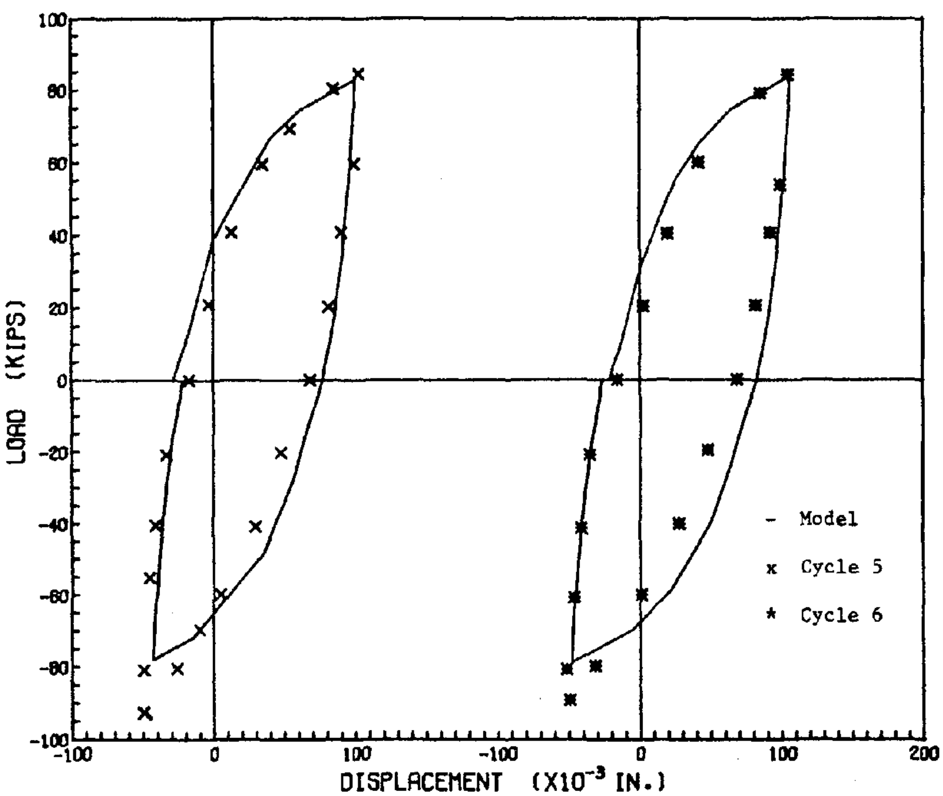


FIG. 91 COMPARISON OF CYCLIC MODEL AND EXPERIMENT, SPECIMEN S103, CYCLES 5 - 6

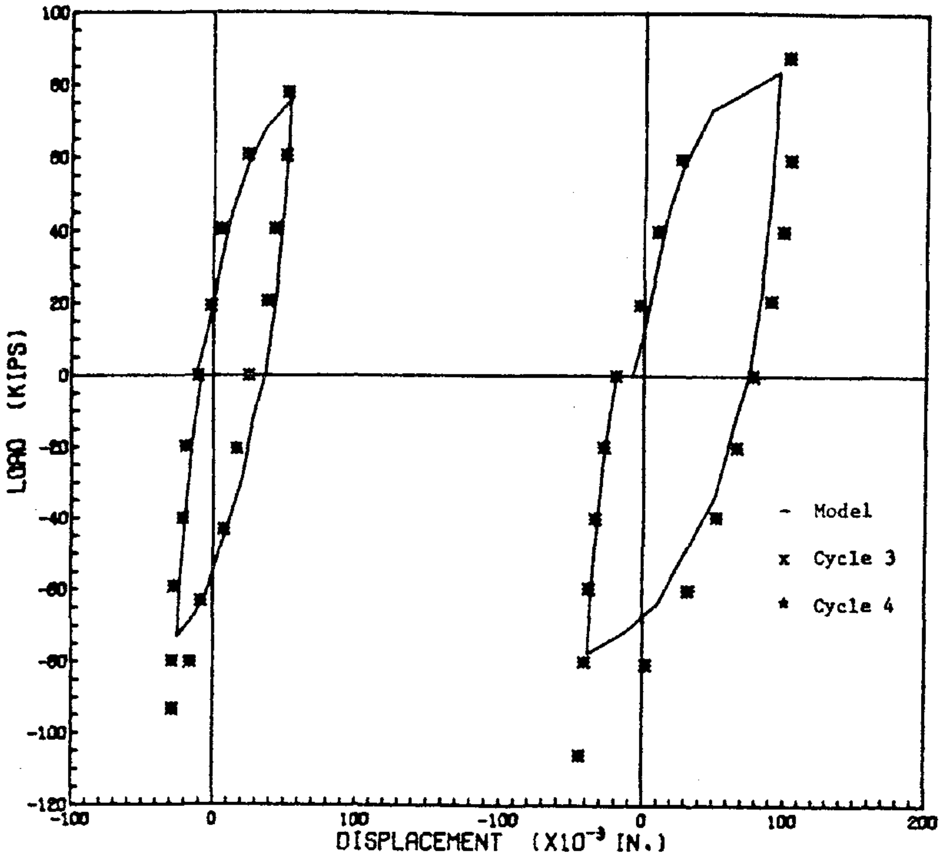

FIG. 94 COMPARISON OF CYCLIC MODEL AND EXPERIMENT, SPECIMEN S105, CYCLES 3 - 4

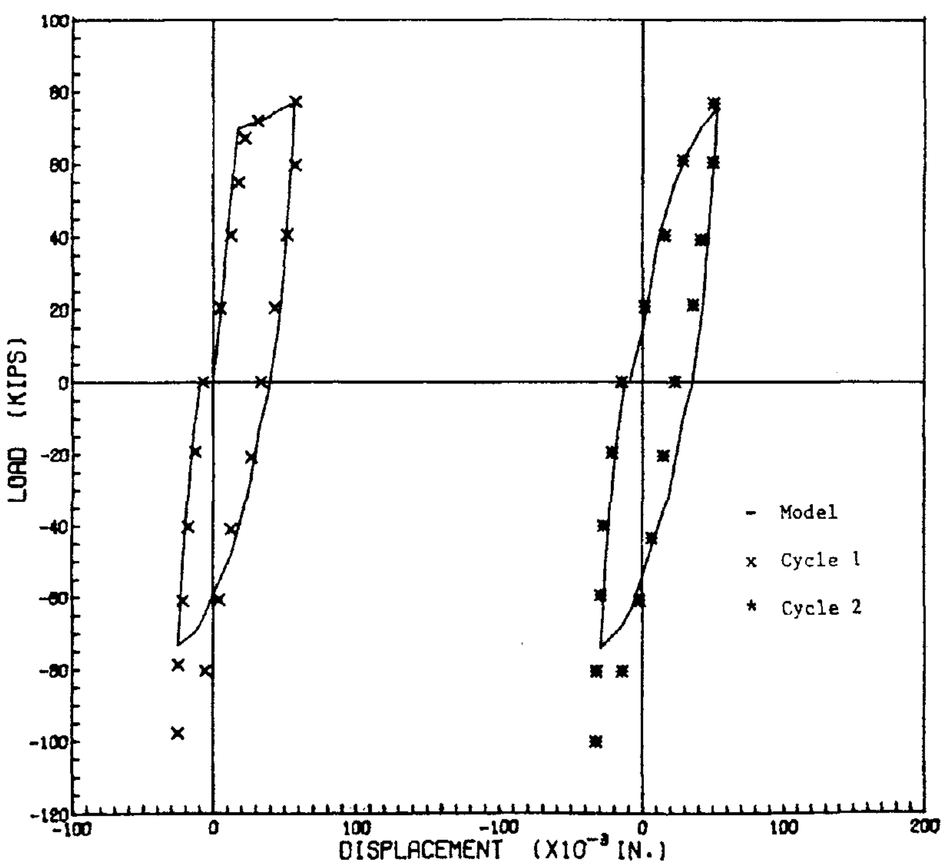

FIG. 93 COMPARISON OF CYCLIC MODEL AND EXPERIMENT, SPECIMEN S105, CYCLES 1 - 2

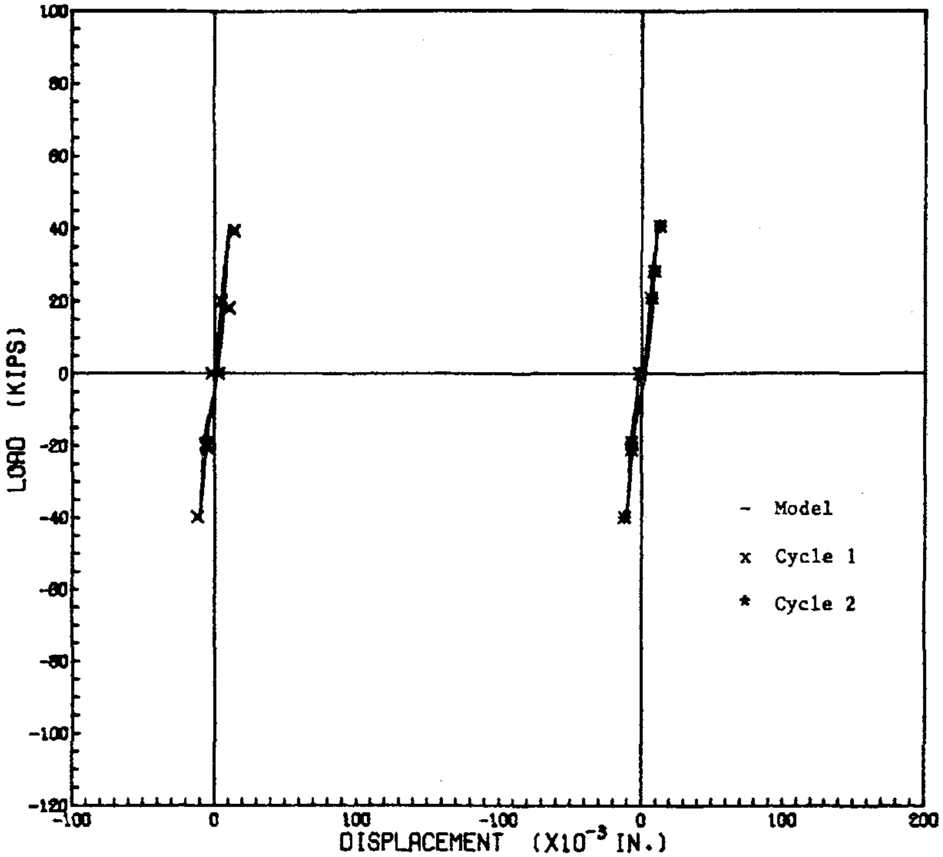

FIG. 96 COMPARISON OF CYCLIC MODEL AND EXPERIMENT, SPECIMEN S106, CYCLES 1 - 2

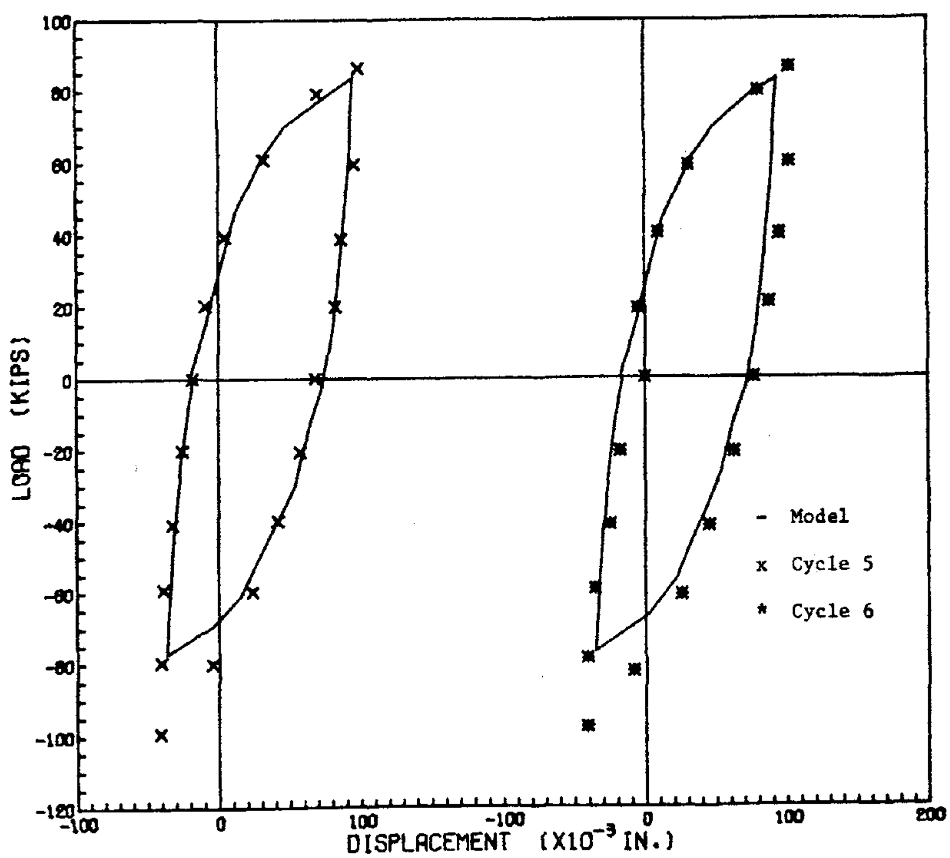

FIG. 95 COMPARISON OF CYCLIC MODEL AND EXPERIMENT, SPECIMEN S105, CYCLES 5 - 6

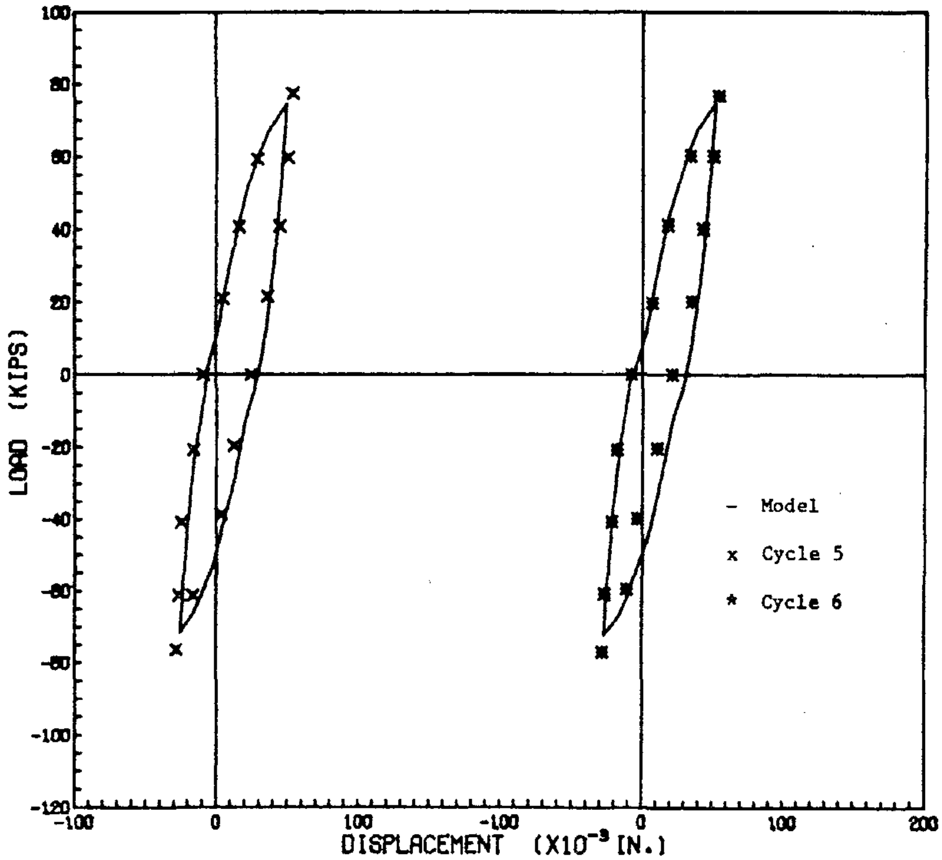


FIG. 98 COMPARISON OF CYCLIC MODEL AND EXPERIMENT, SPECIMEN S106, CYCLES 5 - 6

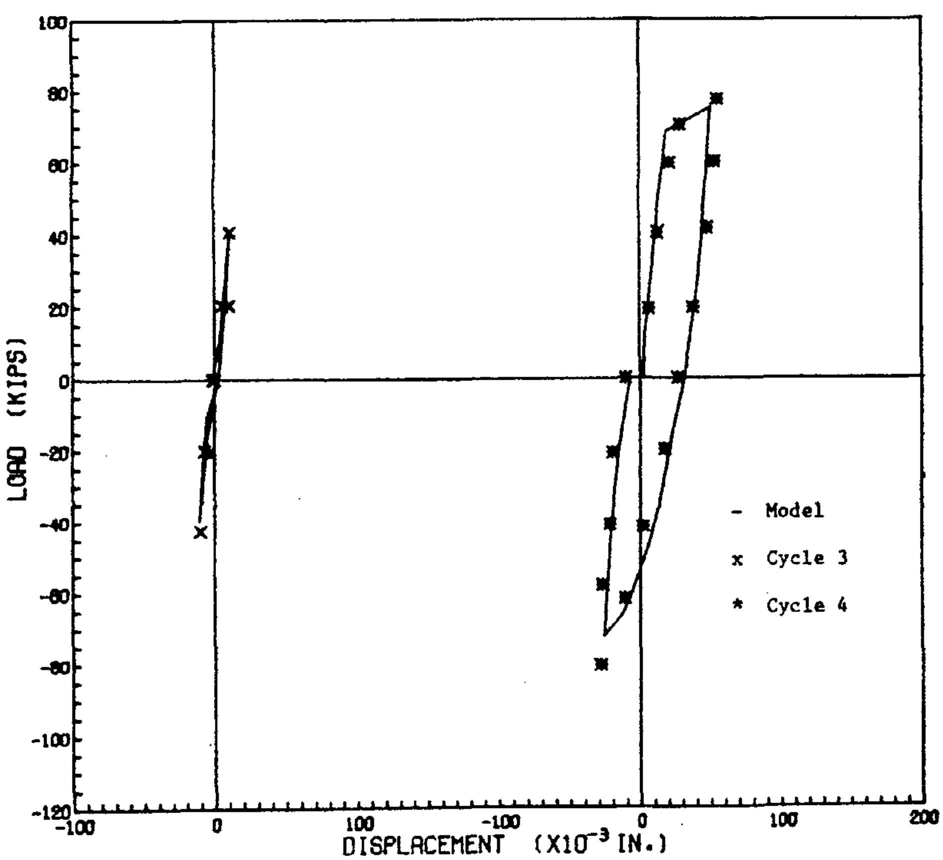


FIG. 97 COMPARISON OF CYCLIC MODEL AND EXPERIMENT, SPECIMEN S106, CYCLES 3 - 4

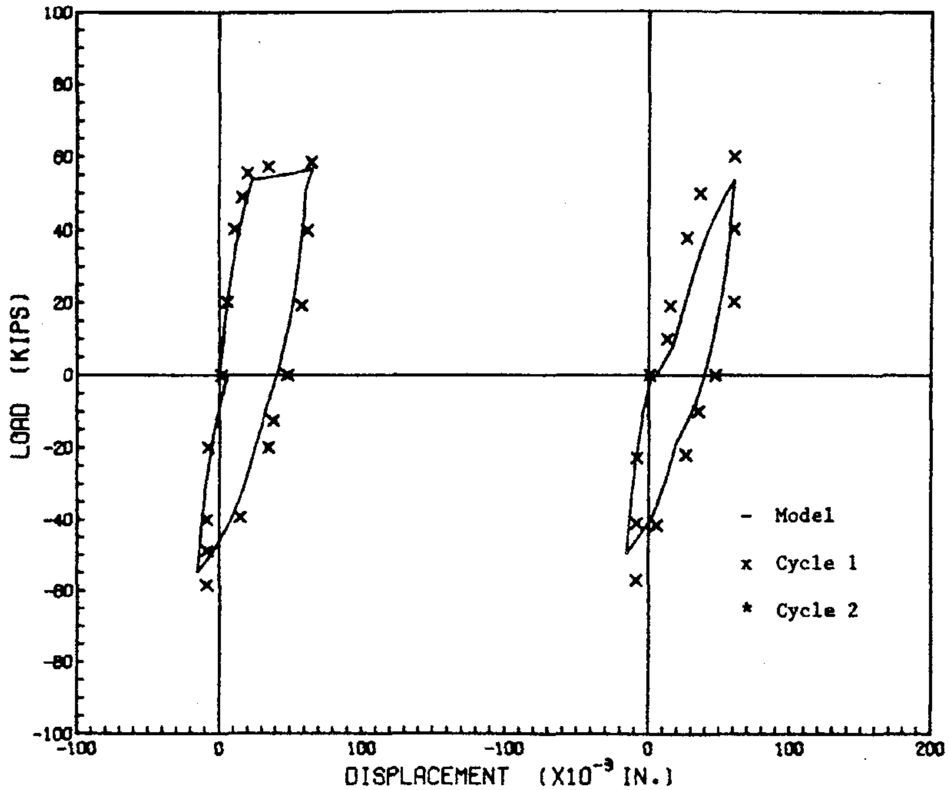


FIG. 100 COMPARISON OF CYCLIC MODEL AND EXPERIMENT, SPECIMEN S107, CYCLES 1 - 2

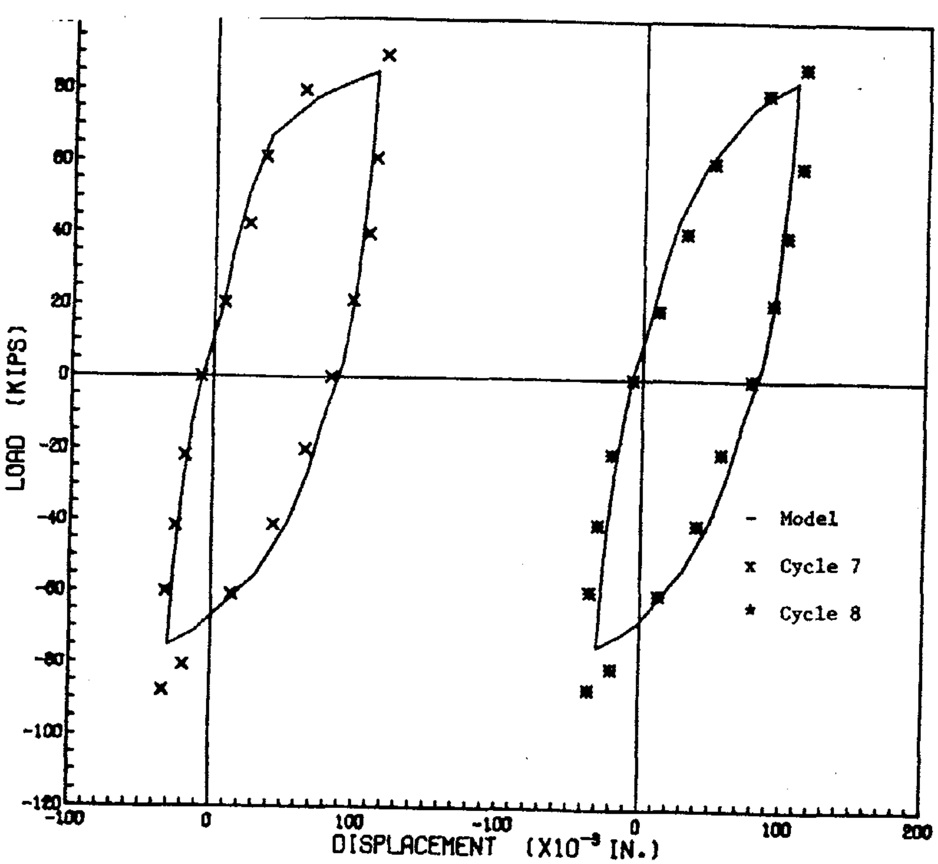


FIG. 99 COMPARISON OF CYCLIC MODEL AND EXPERIMENT, SPECIMEN S106, CYCLES 7 - 8

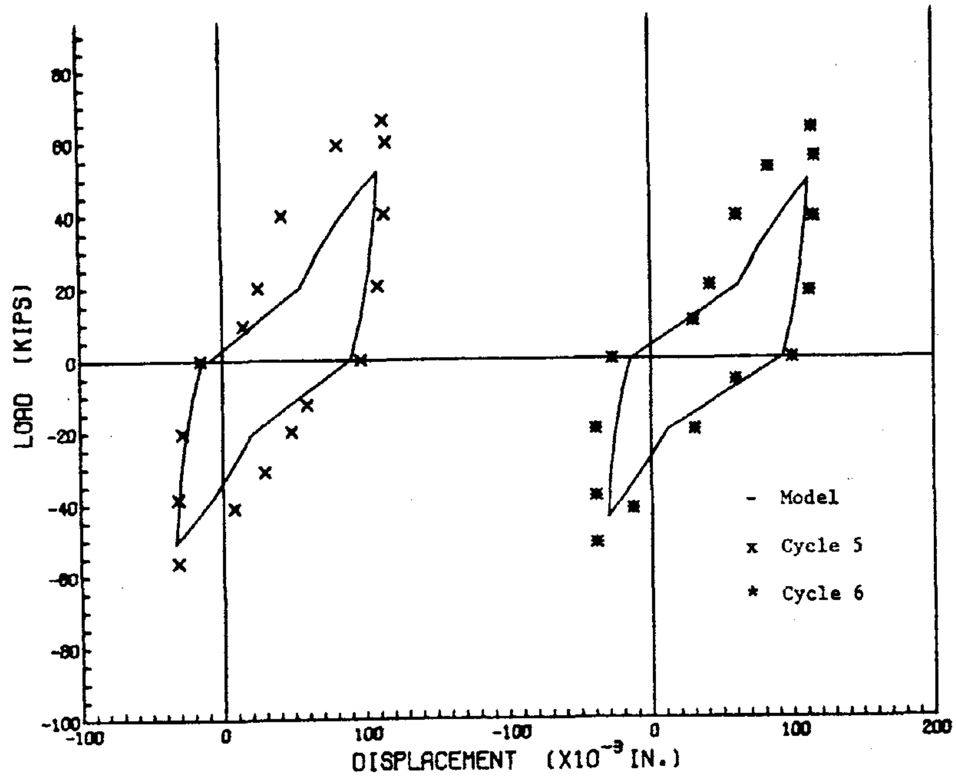


FIG. 102 COMPARISON OF CYCLIC MODEL AND EXPERIMENT, SPECIMEN S107, CYCLES 5 - 6

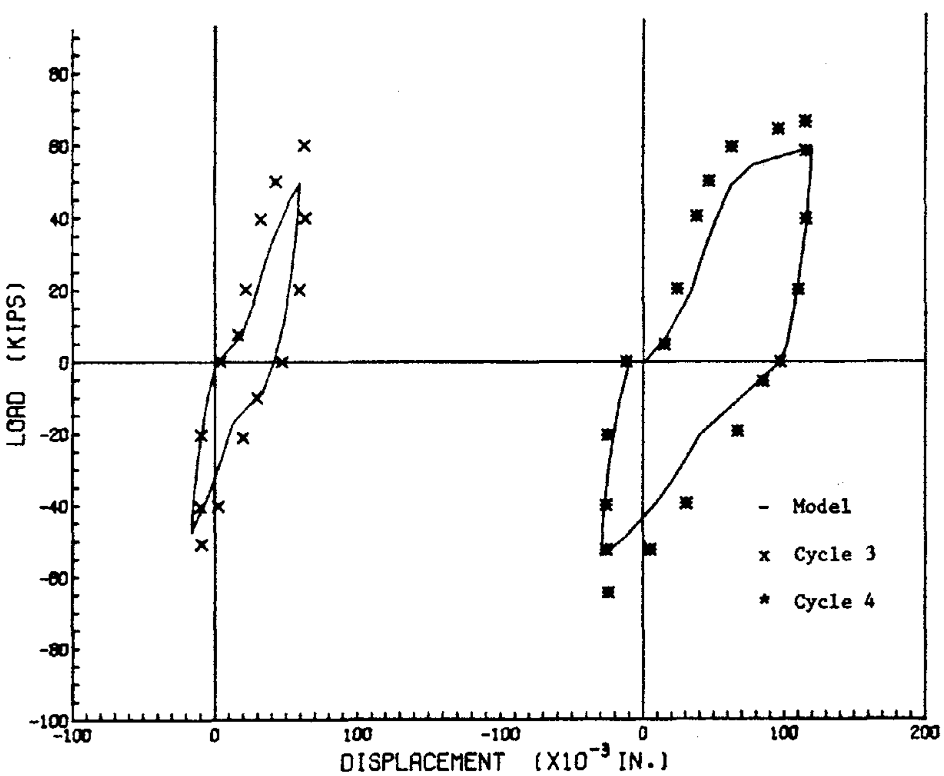


FIG. 101 COMPARISON OF CYCLIC MODEL AND EXPERIMENT, SPECIMEN S107, CYCLES 3 - 4

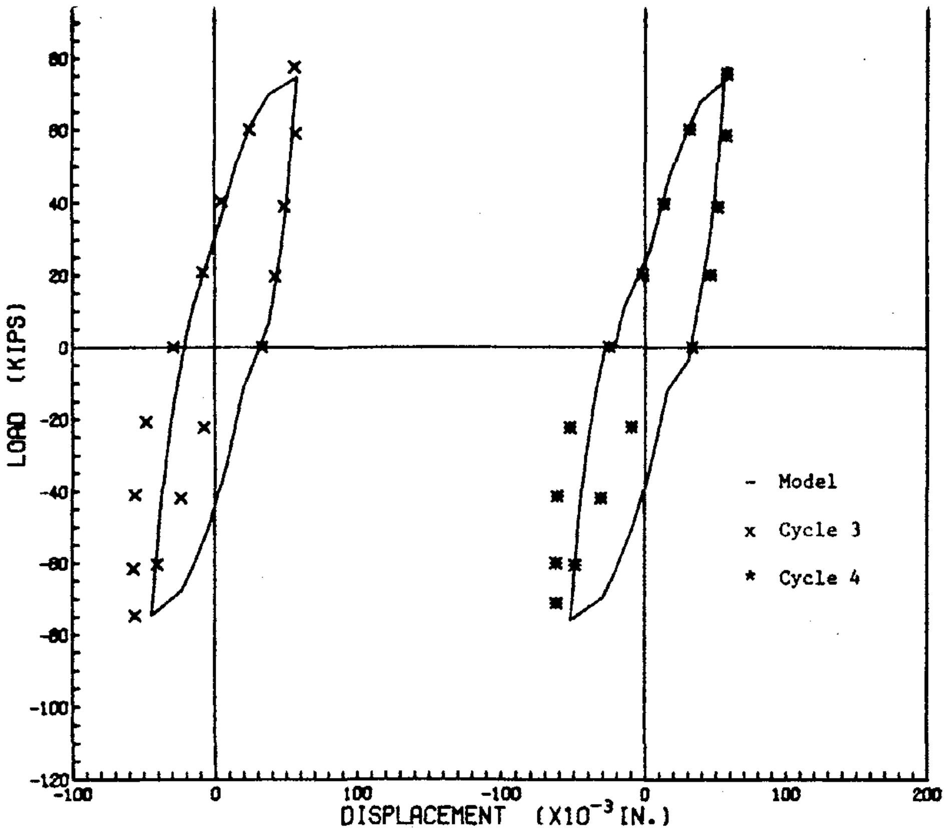


FIG. 104 COMPARISON OF CYCLIC MODEL AND EXPERIMENT, SPECIMEN B102, CYCLES 3 - 4

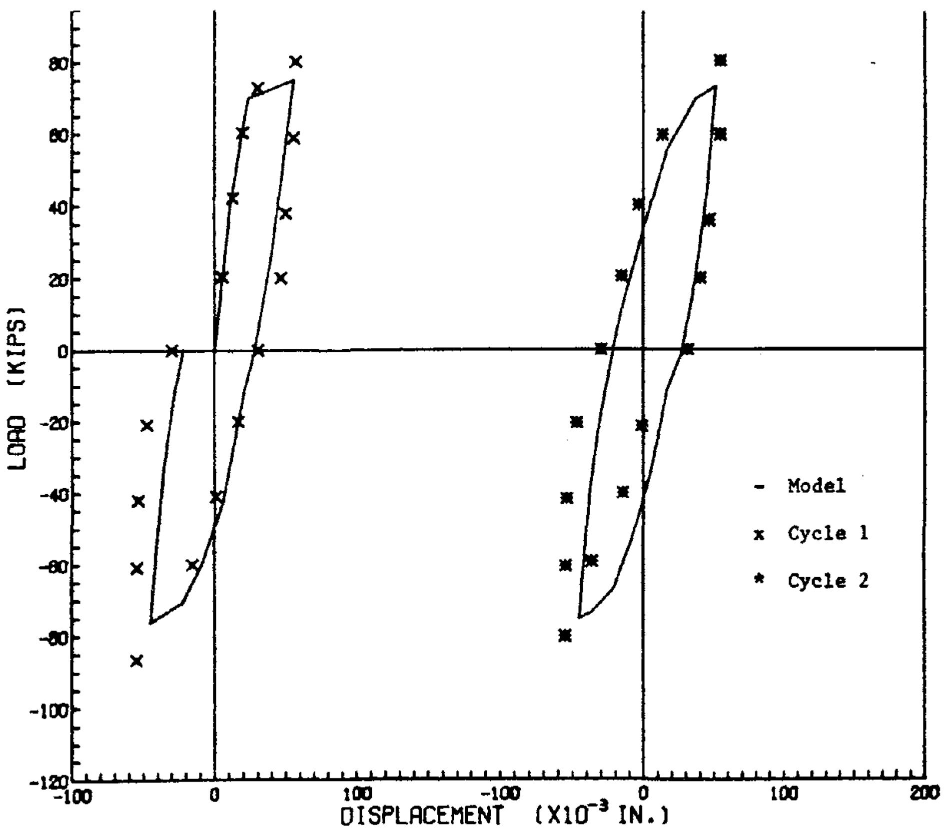


FIG. 103 COMPARISON OF CYCLIC MODEL AND EXPERIMENT, SPECIMEN B102, CYCLES 1 - 2

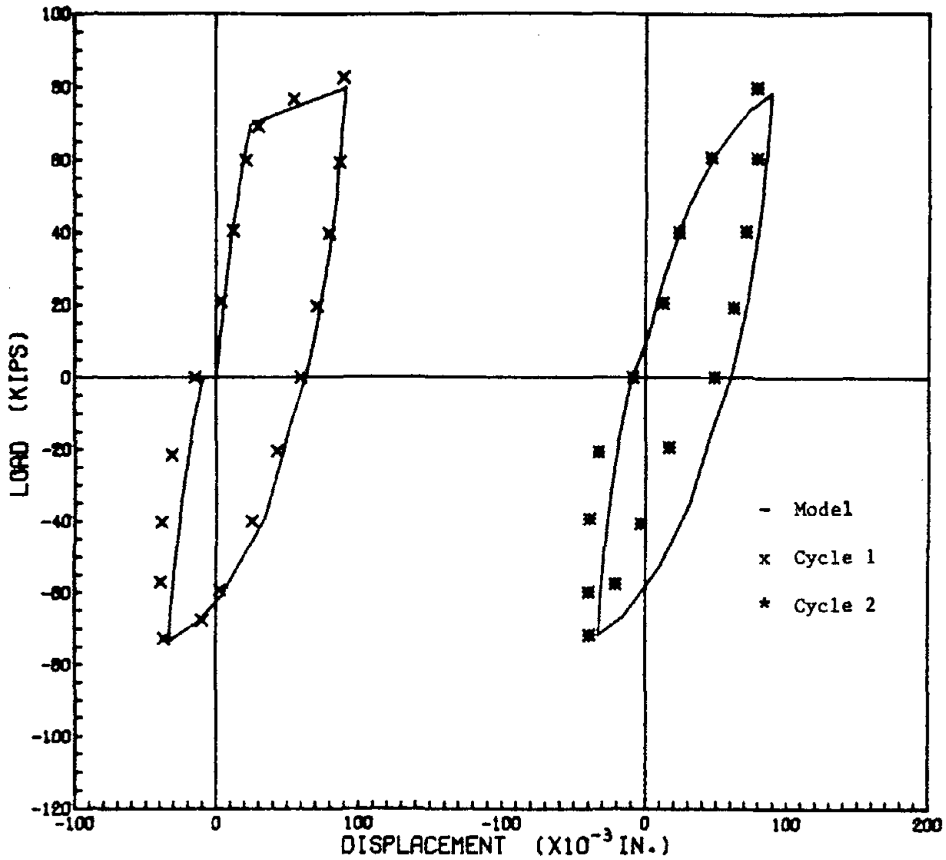

FIG. 106 COMPARISON OF CYCLIC MODEL AND EXPERIMENT, SPECIMEN B103, CYCLES 1 - 2

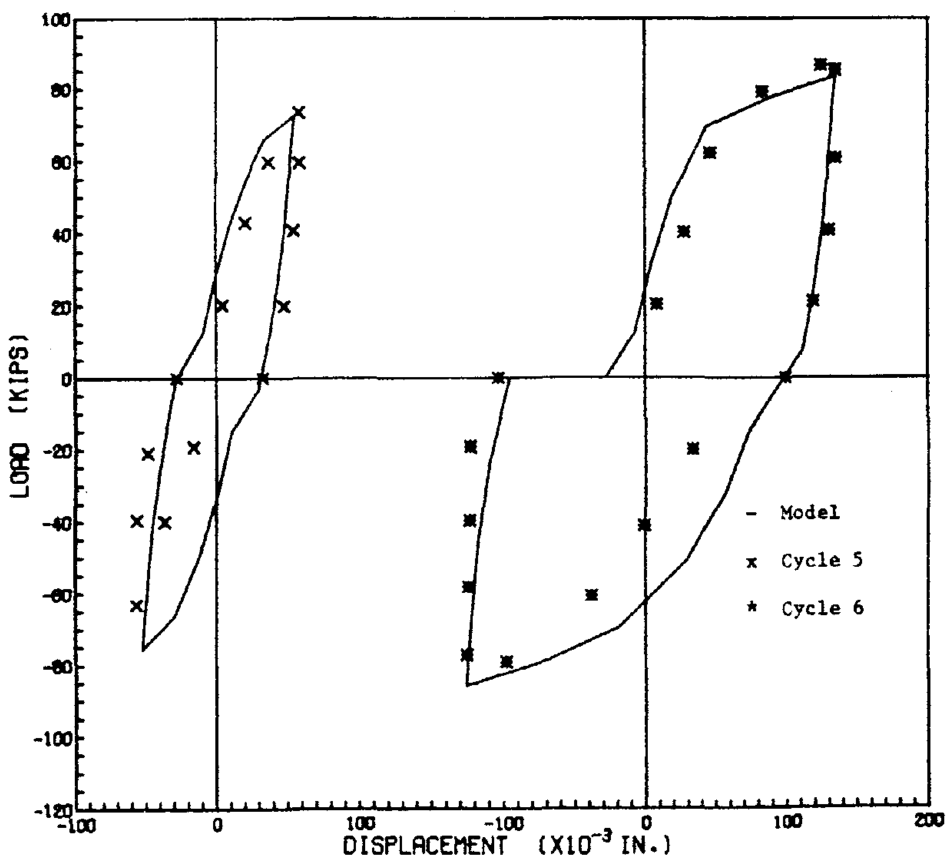

FIG. 105 COMPARISON OF CYCLIC MODEL AND EXPERIMENT, SPECIMEN B102, CYCLES 5 - 6

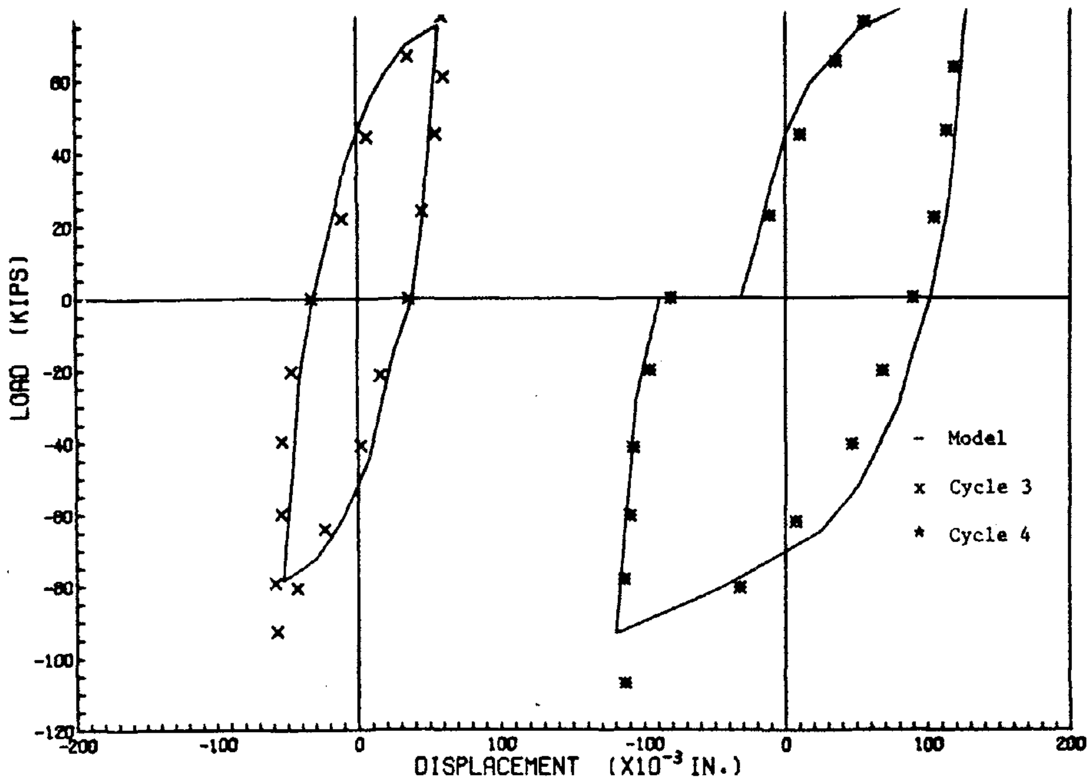


FIG. 108 COMPARISON OF CYCLIC MODEL AND EXPERIMENT, SPECIMEN B104, CYCLES 3 - 4

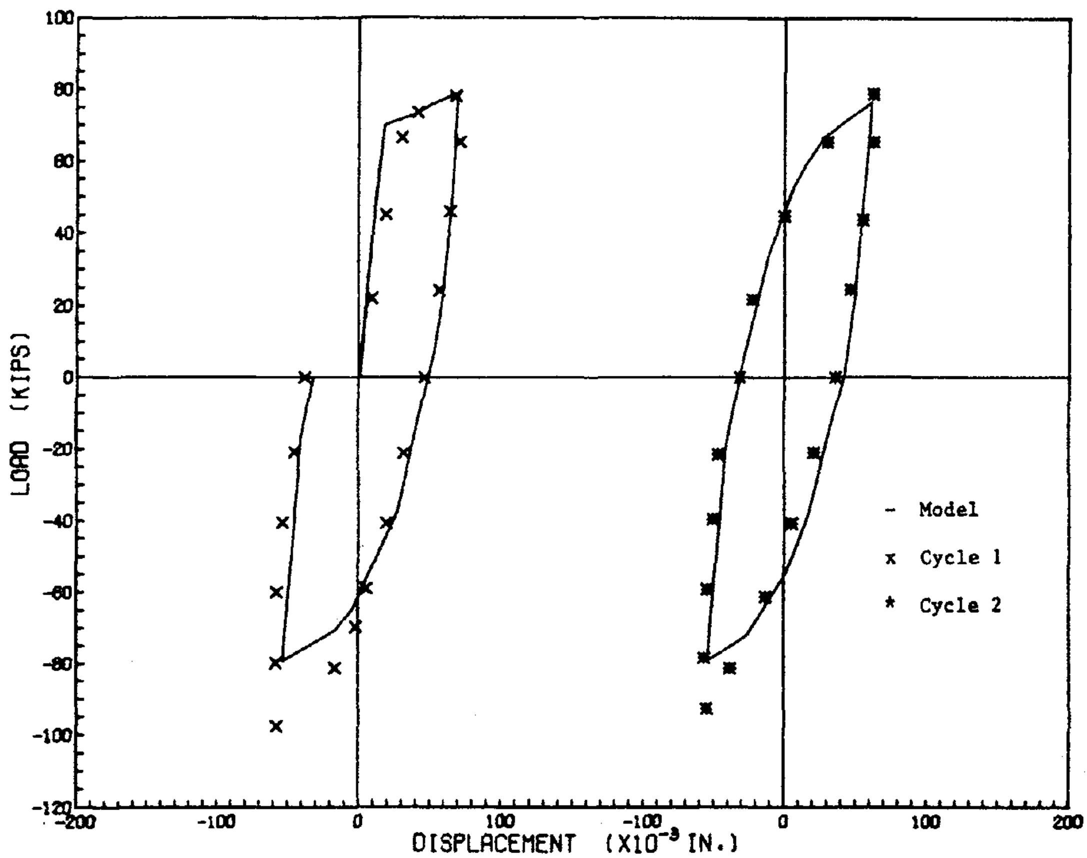


FIG. 107 COMPARISON OF CYCLIC MODEL AND EXPERIMENT, SPECIMEN B104, CYCLES 1 - 2

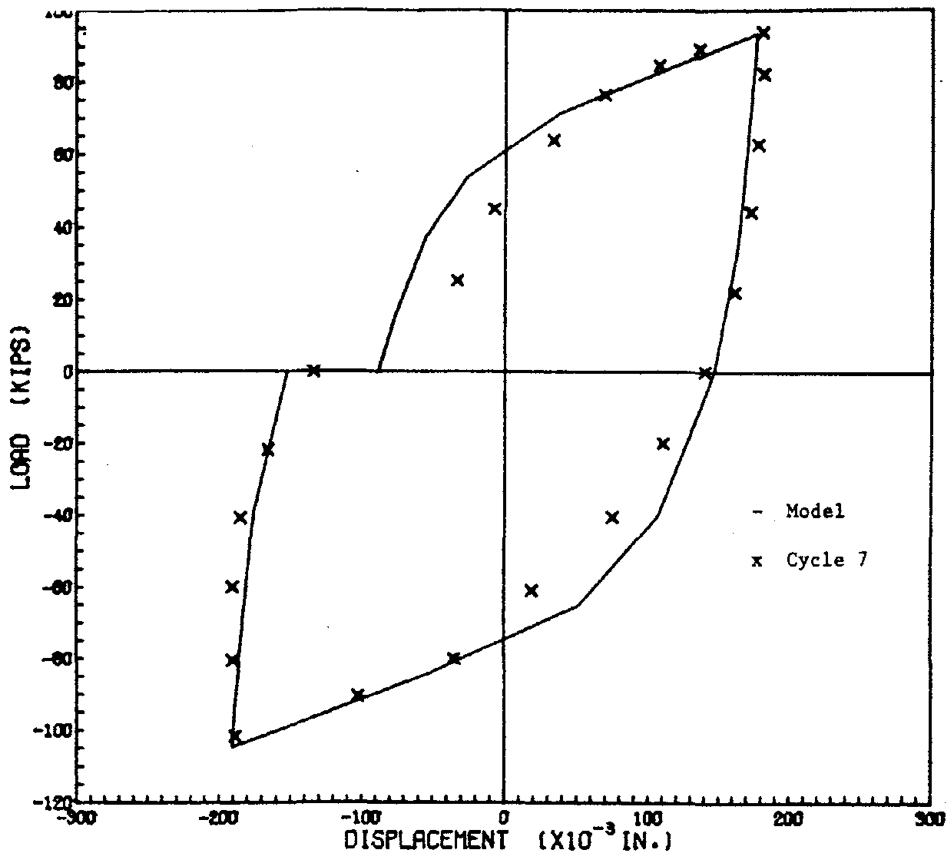

FIG. 110 COMPARISON OF CYCLIC MODEL AND EXPERIMENT, SPECIMEN B104, CYCLE 7

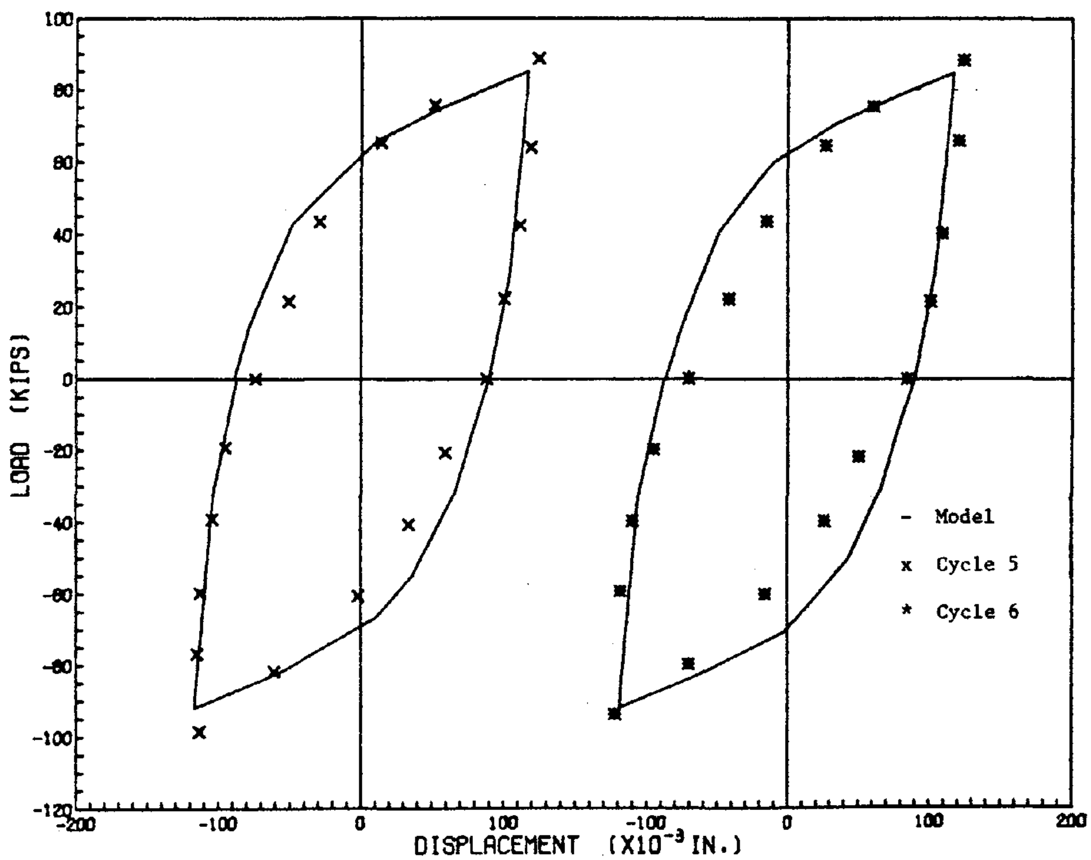

FIG. 109 COMPARISON OF CYCLIC MODEL AND EXPERIMENT, SPECIMEN B104, CYCLES 5 - 6

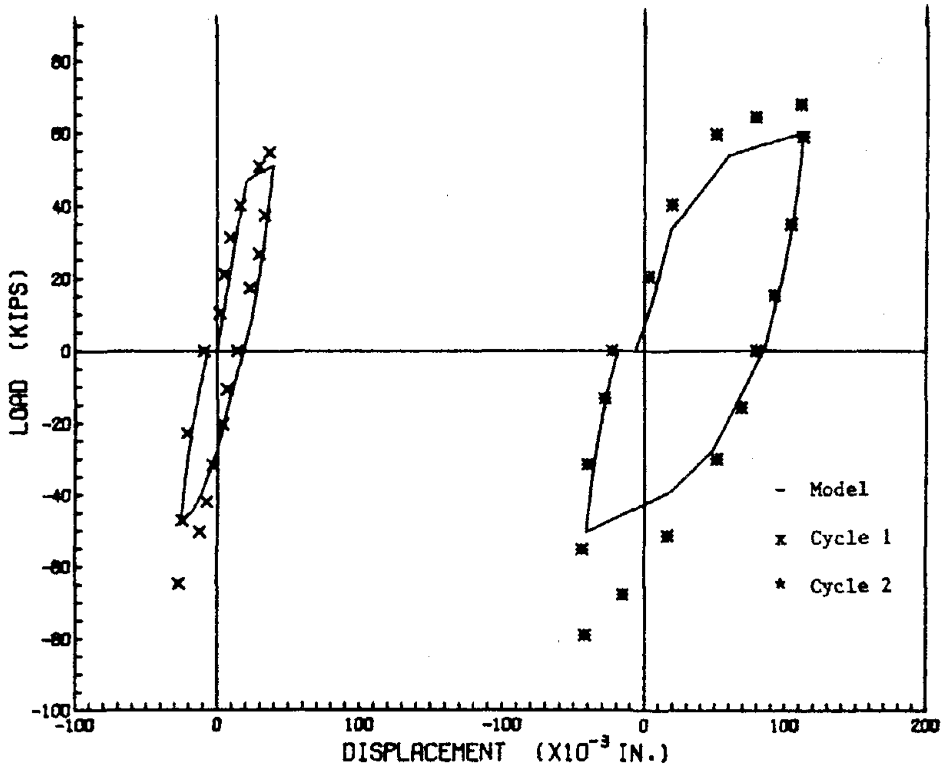


FIG. 112 COMPARISON OF CYCLIC MODEL AND EXPERIMENT, SPECIMEN B82, CYCLES 1 - 2

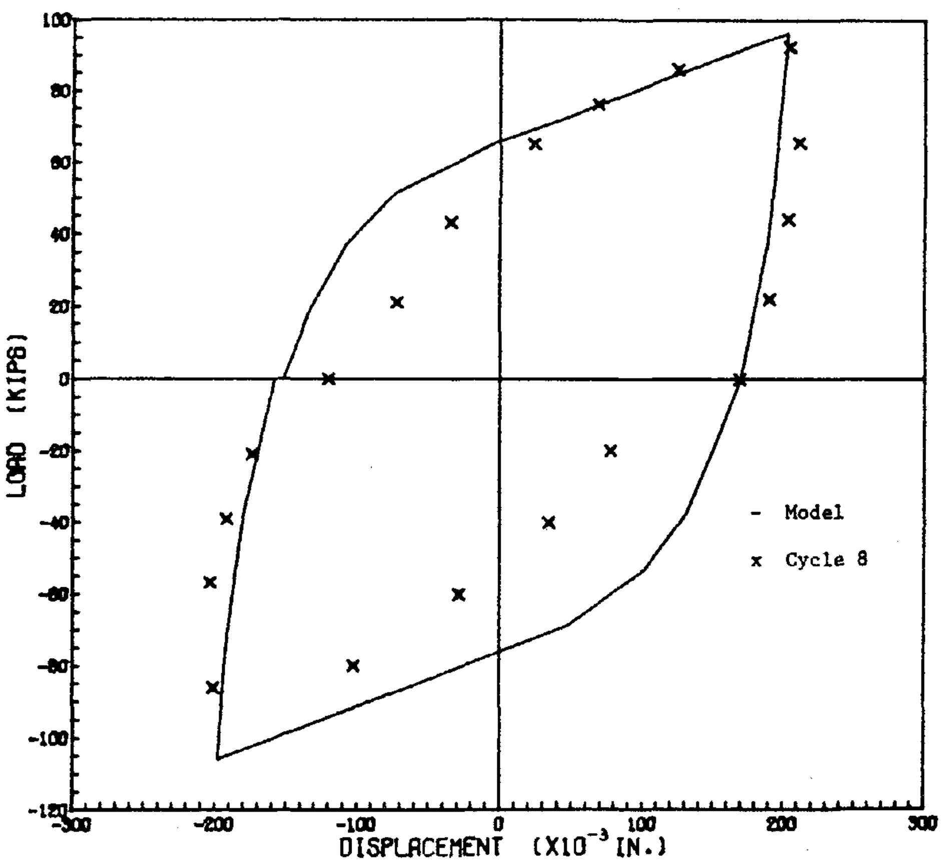


FIG. 111 COMPARISON OF CYCLIC MODEL AND EXPERIMENT, SPECIMEN B104, CYCLE 8

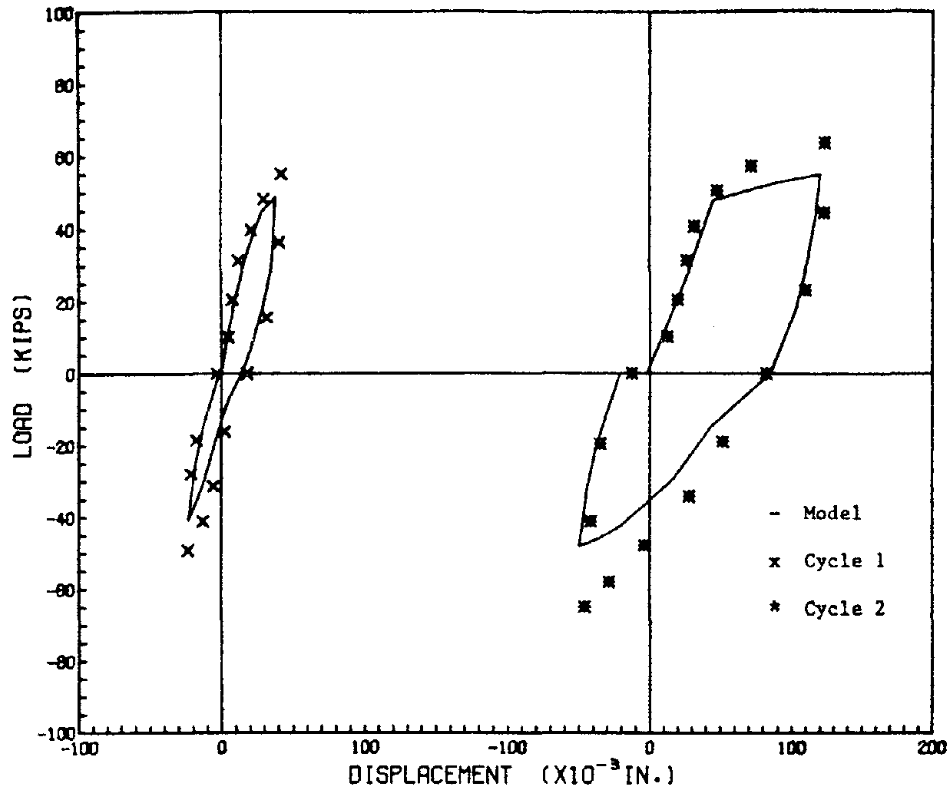


FIG. 114 COMPARISON OF CYCLIC MODEL AND EXPERIMENT, SPECIMEN B84, CYCLES 1 - 2

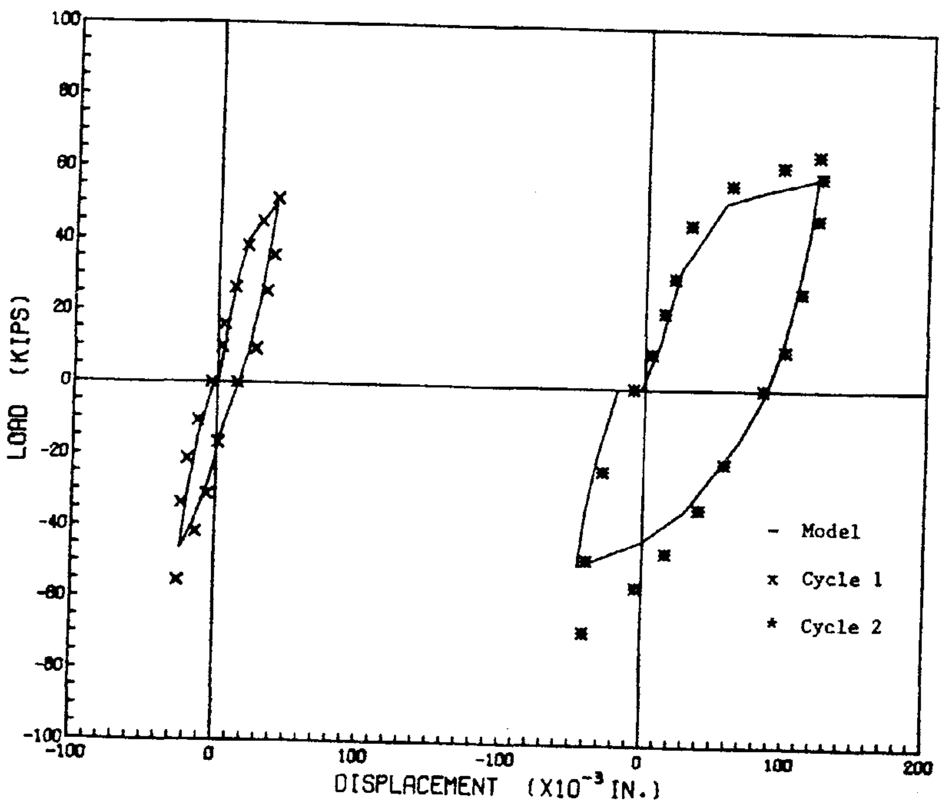


FIG. 113 COMPARISON OF CYCLIC MODEL AND EXPERIMENT, SPECIMEN B83, CYCLES 1 - 2

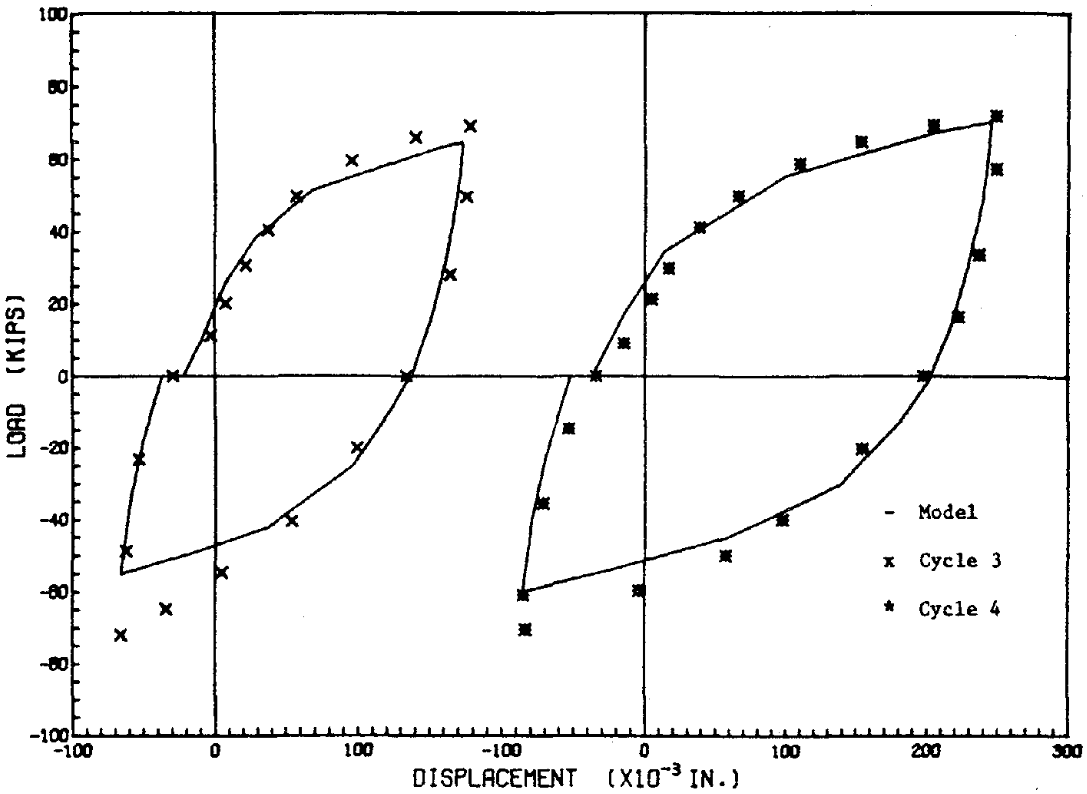


FIG. 116 COMPARISON OF CYCLIC MODEL AND EXPERIMENT, SPECIMEN B85, CYCLES 3 - 4

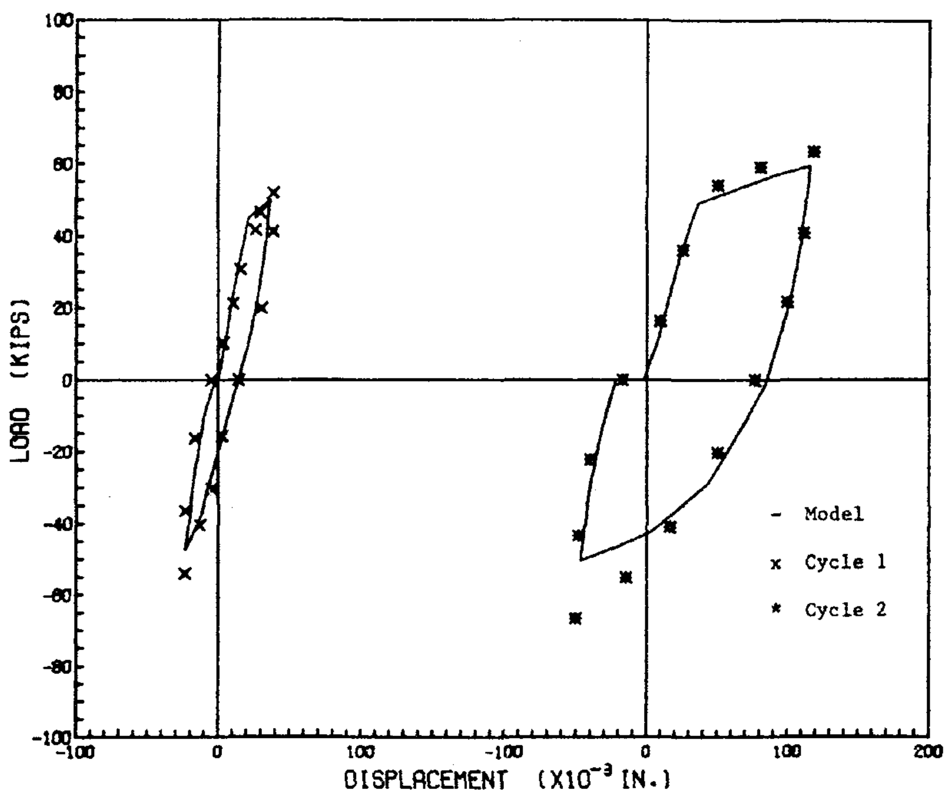


FIG. 115 COMPARISON OF CYCLIC MODEL AND EXPERIMENT, SPECIMEN B85, CYCLES 1 - 2

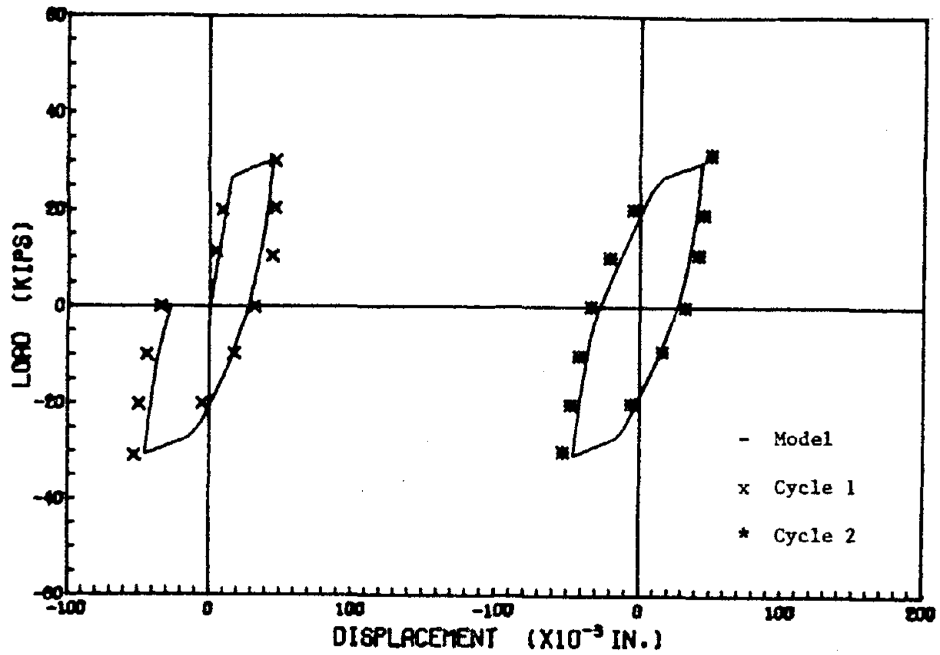


FIG. 118 COMPARISON OF CYCLIC MODEL AND EXPERIMENT, SPECIMEN S62, CYCLES 1 - 2

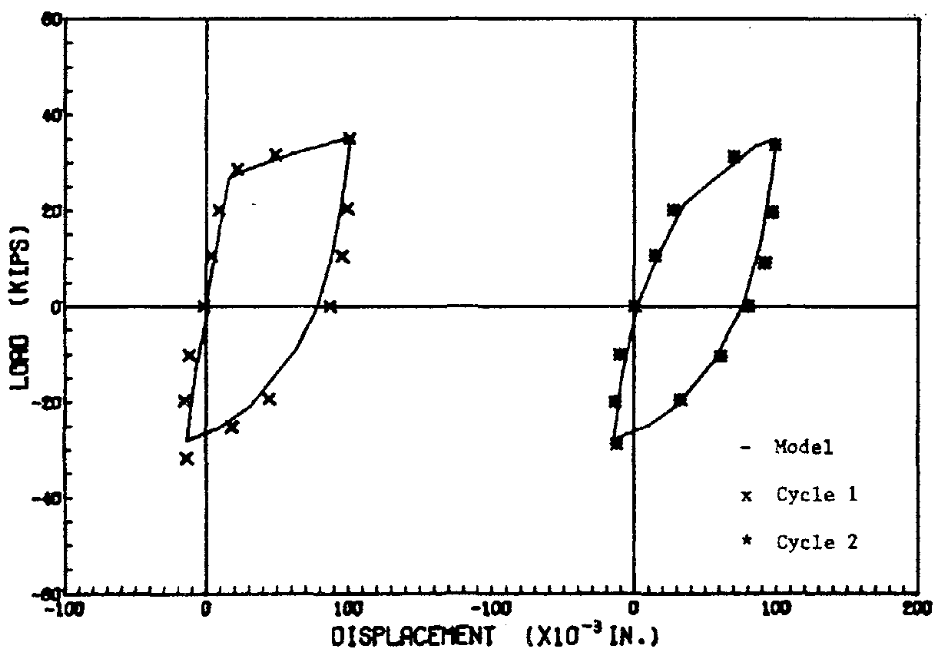


FIG. 117 COMPARISON OF CYCLIC MODEL AND EXPERIMENT, SPECIMEN S61, CYCLES 1 - 2

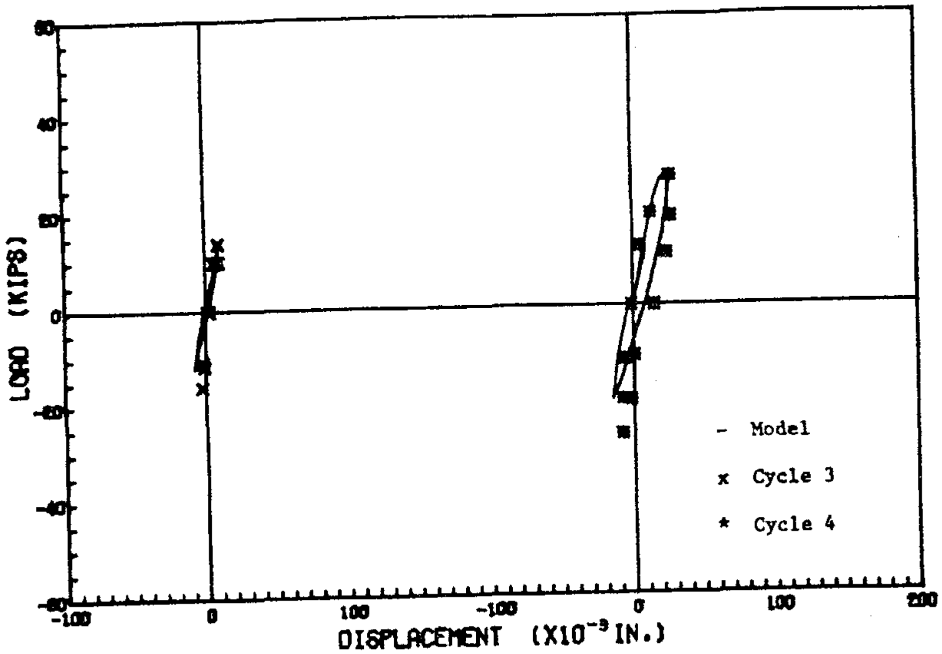


FIG. 120 COMPARISON OF CYCLIC MODEL AND EXPERIMENT, SPECIMEN S63, CYCLES 3 - 4

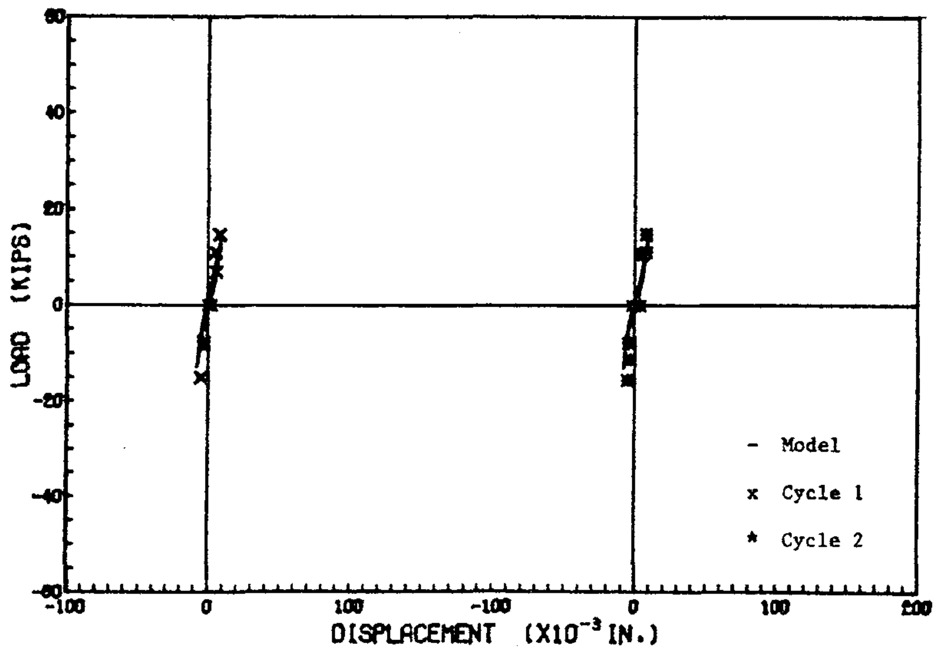


FIG. 119 COMPARISON OF CYCLIC MODEL AND EXPERIMENT, SPECIMEN S63, CYCLES 1 - 2

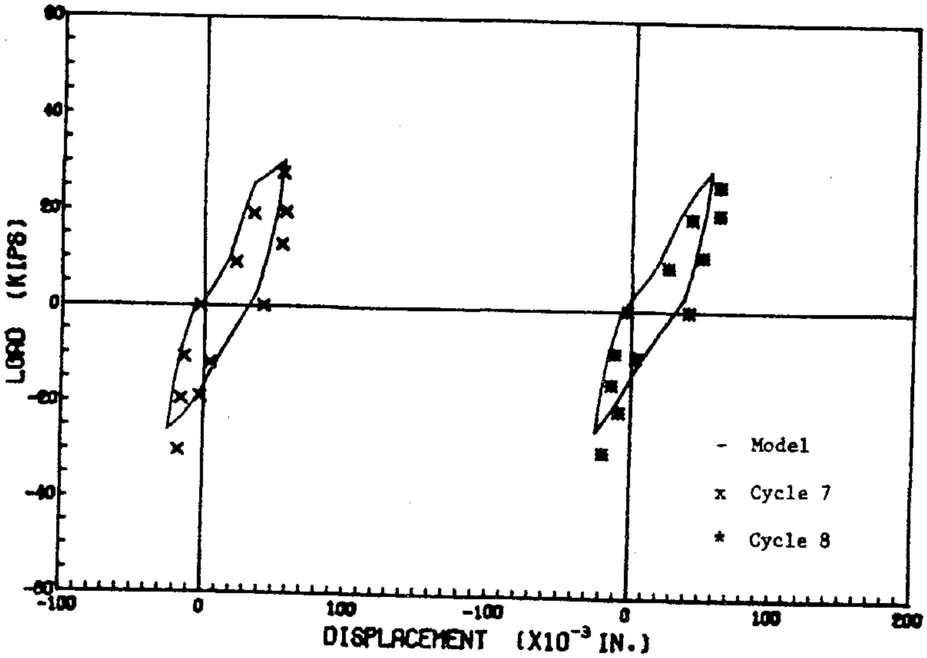


FIG. 122 COMPARISON OF CYCLIC MODEL AND EXPERIMENT, SPECIMEN S63, CYCLES 7 - 8

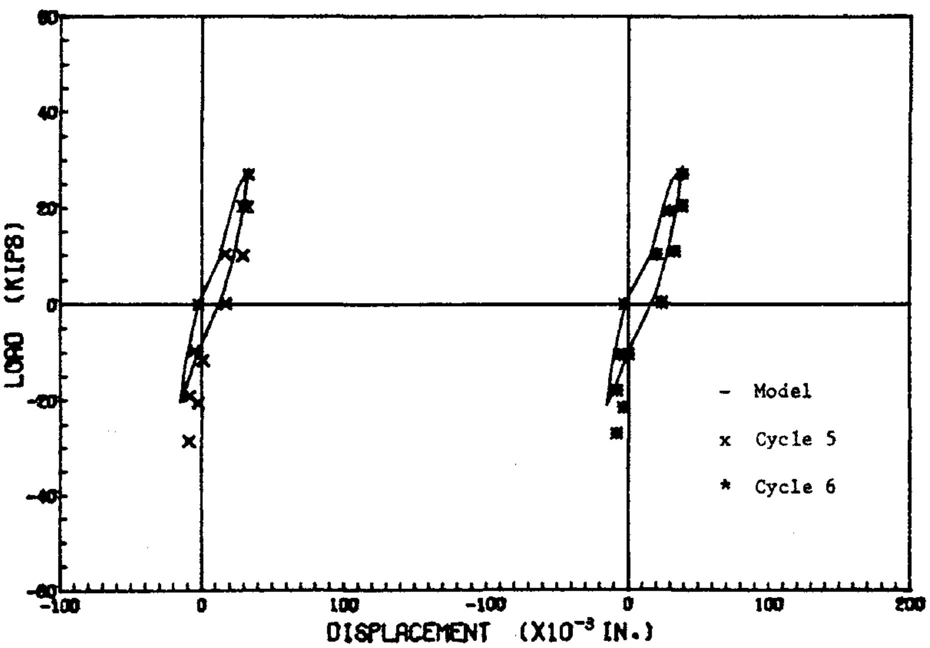


FIG. 121 COMPARISON OF CYCLIC MODEL AND EXPERIMENT, SPECIMEN S63, CYCLES 5 - 6

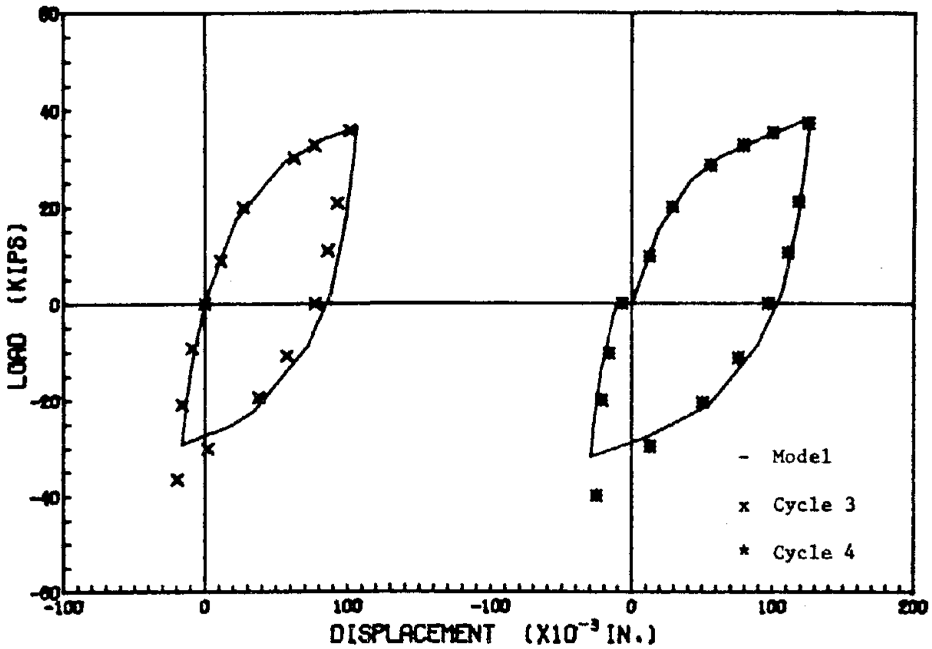


FIG. 124 COMPARISON OF CYCLIC MODEL AND EXPERIMENT, SPECIMEN S65, CYCLES 3 - 4

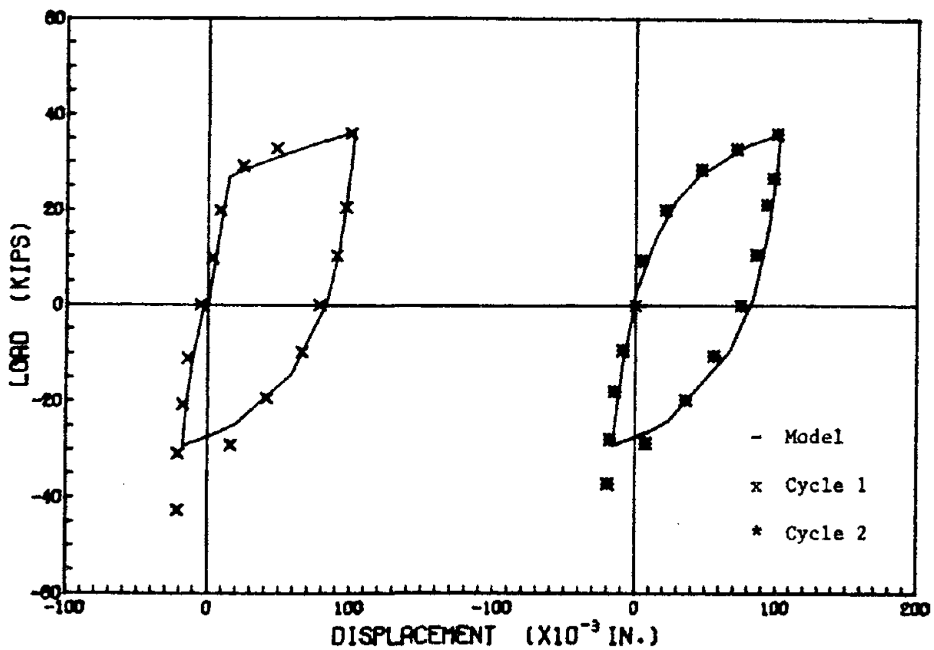


FIG. 123 COMPARISON OF CYCLIC MODEL AND EXPERIMENT, SPECIMEN S65, CYCLES 1 - 2

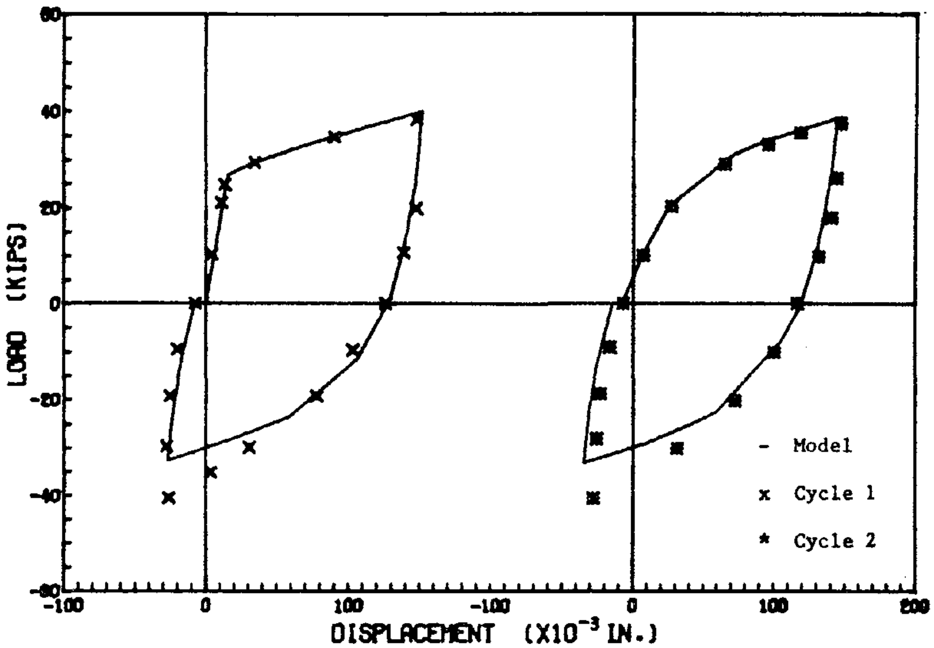


FIG. 126 COMPARISON OF CYCLIC MODEL AND EXPERIMENT, SPECIMEN S66, CYCLES 1 - 2

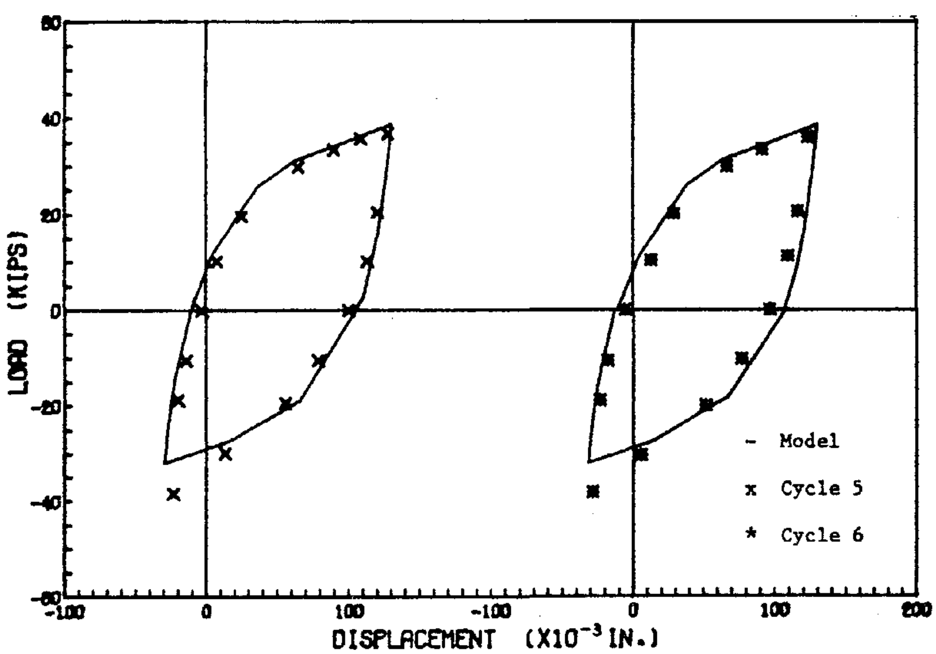


FIG. 125 COMPARISON OF CYCLIC MODEL AND EXPERIMENT, SPECIMEN S65, CYCLES 5 - 6

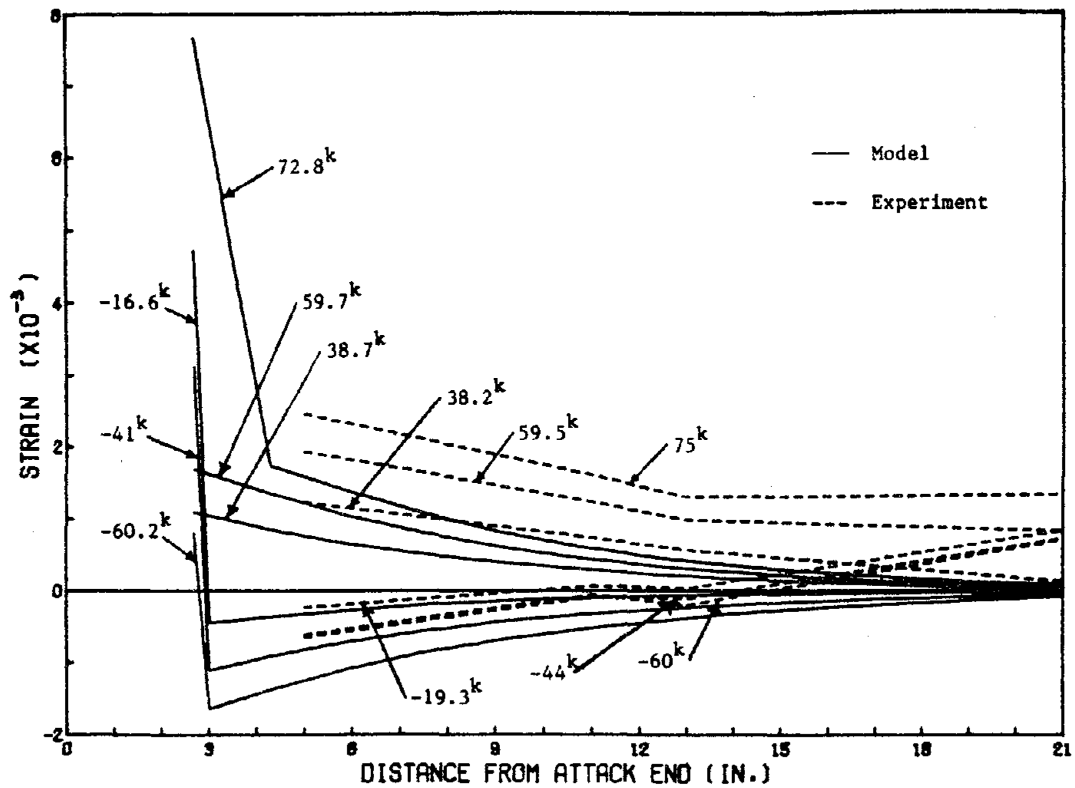


FIG. 128 COMPARISON OF STRAINS ALONG BAR, SPECIMEN S102, CYCLE 3

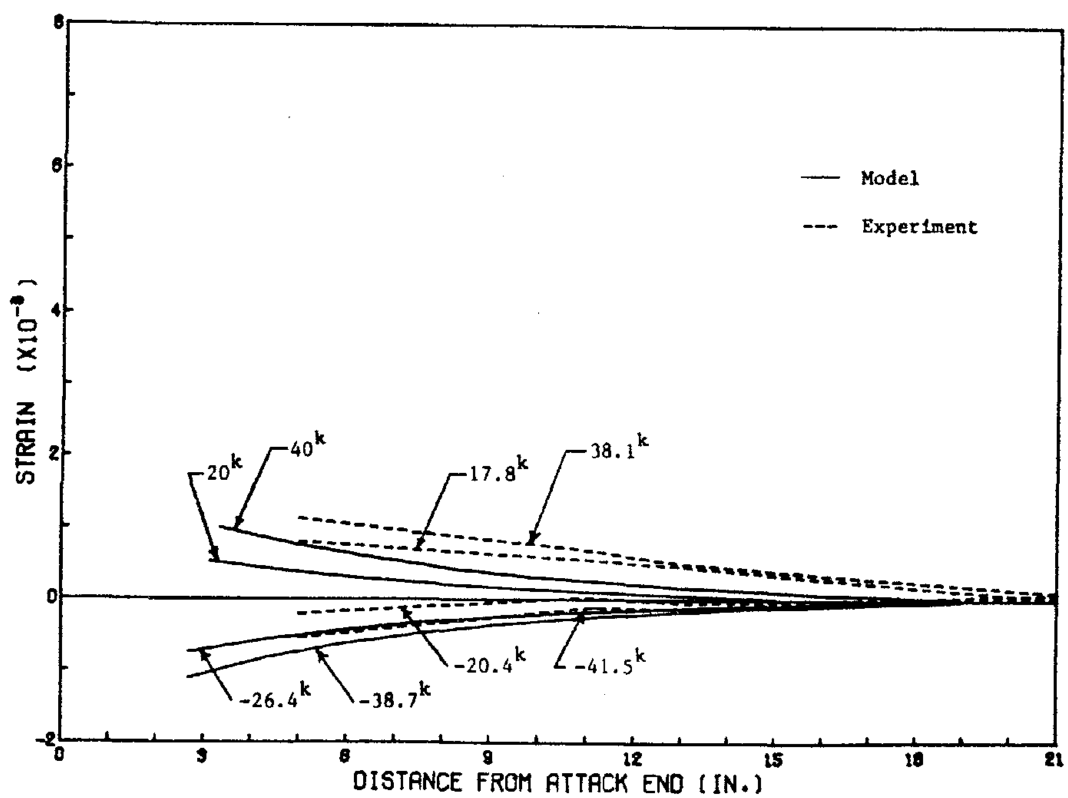


FIG. 127 COMPARISON OF STRAINS ALONG BAR, SPECIMEN S102, CYCLE 1

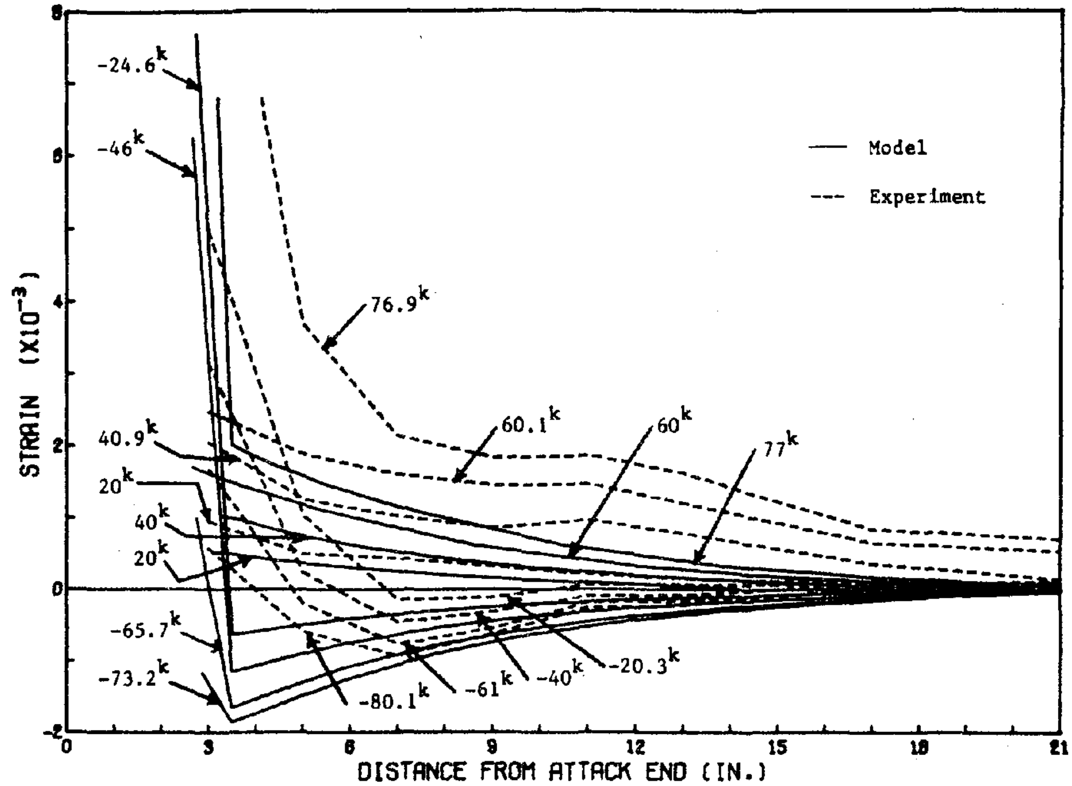


FIG. 130 COMPARISON OF STRAINS ALONG BAR, SPECIMEN S103, CYCLE 1

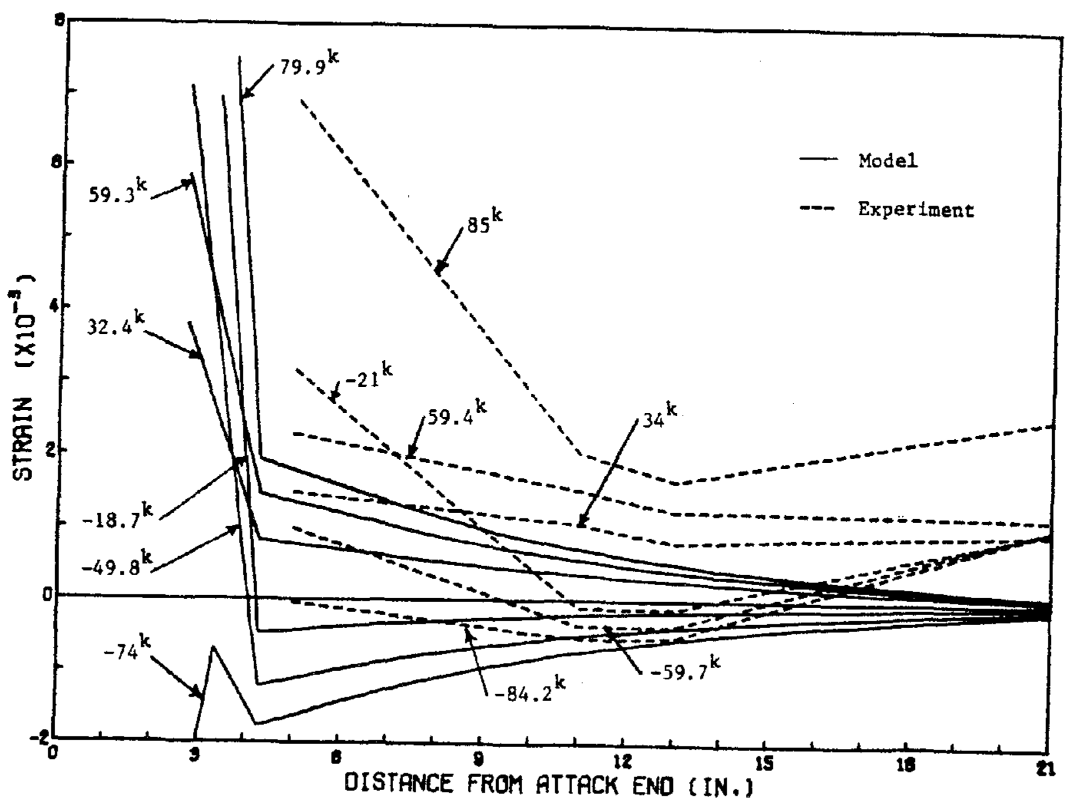


FIG. 129 COMPARISON OF STRAINS ALONG BAR, SPECIMEN S102, CYCLE 5

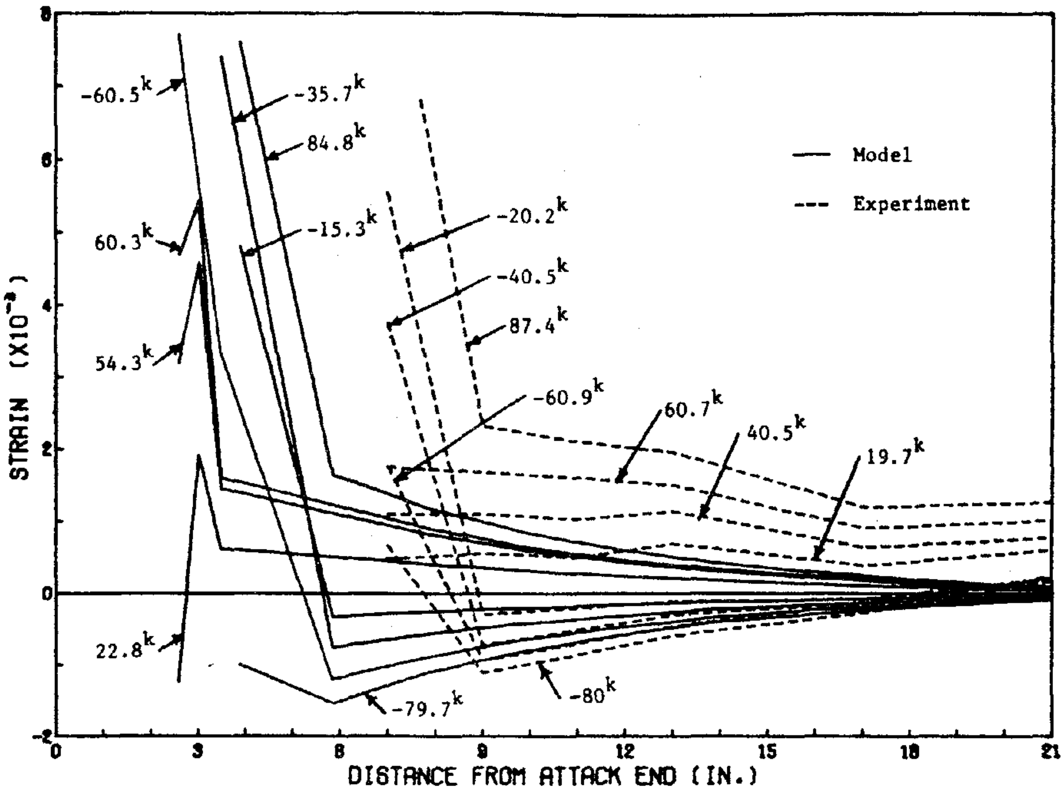


FIG. 131 COMPARISON OF STRAINS ALONG BAR, SPECIMEN S103, CYCLE 4

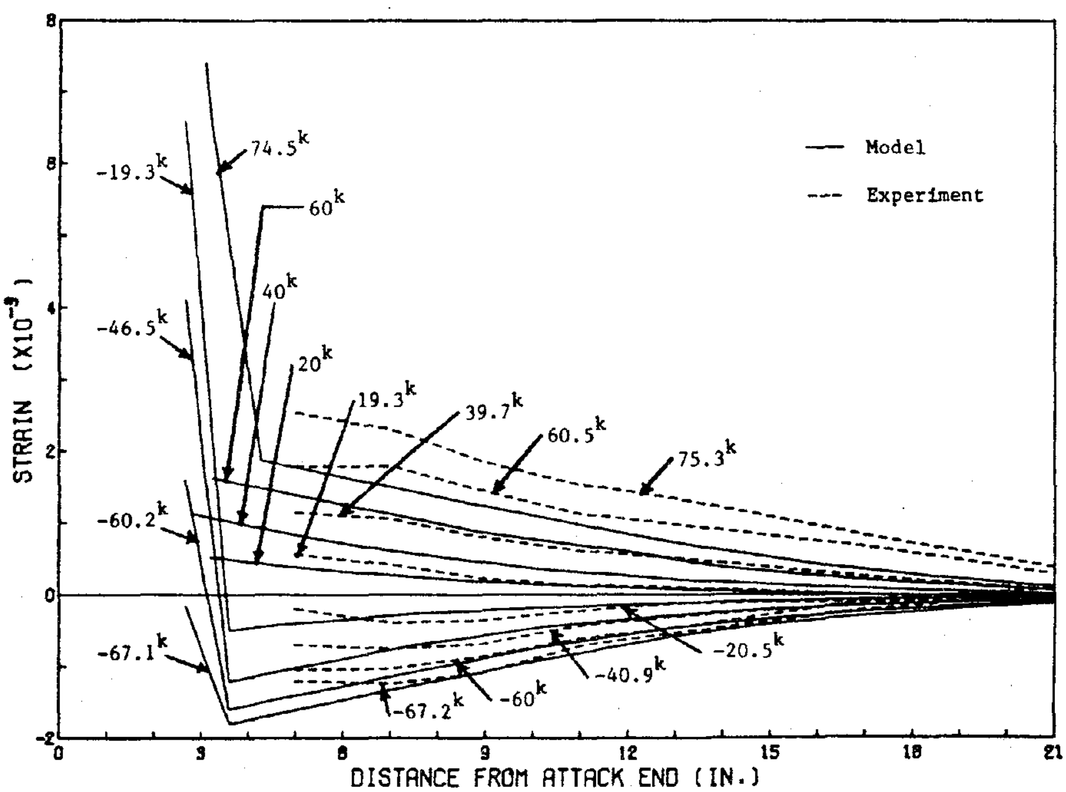


FIG. 132 COMPARISON OF STRAINS ALONG BAR, SPECIMEN S104, CYCLE 1

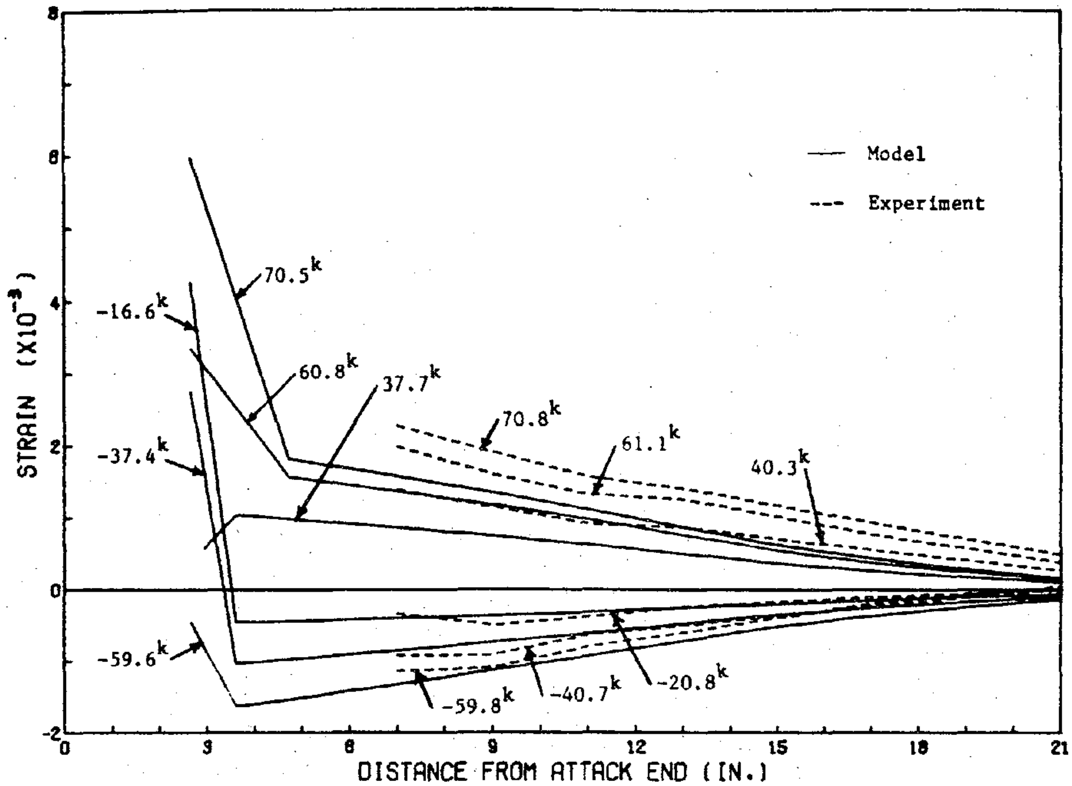


FIG. 134 COMPARISON OF STRAINS ALONG BAR, SPECIMEN S104, CYCLE 3

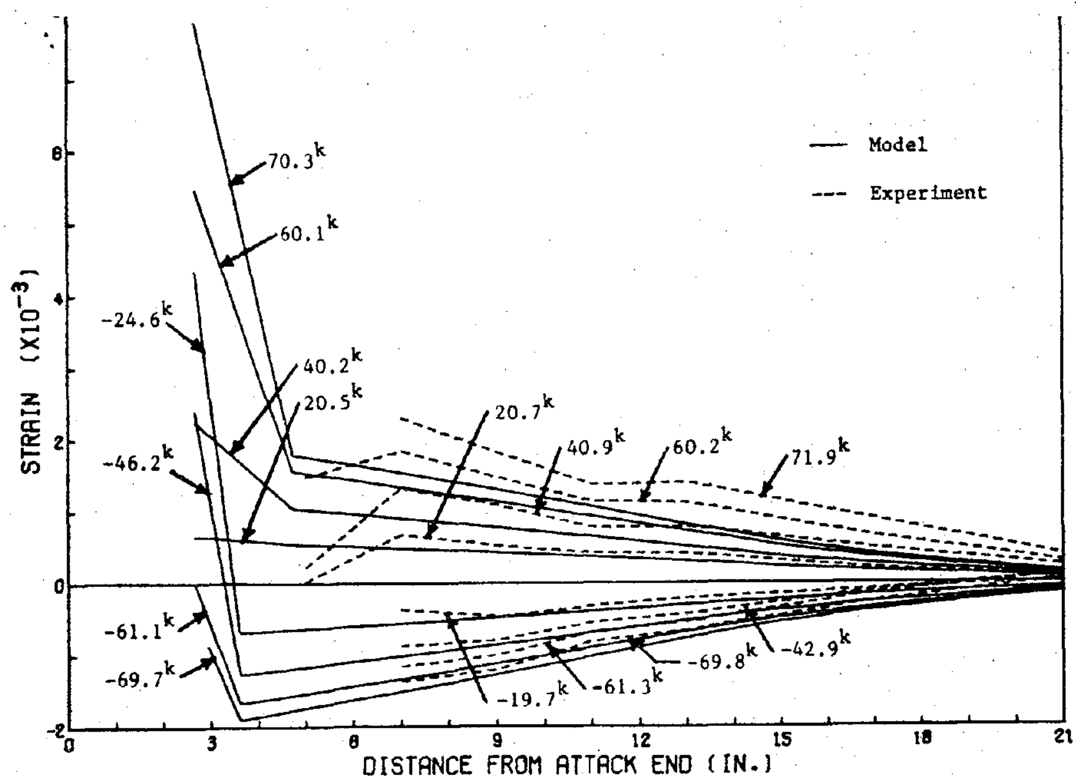


FIG. 133 COMPARISON OF STRAINS ALONG BAR, SPECIMEN S104, CYCLE 2

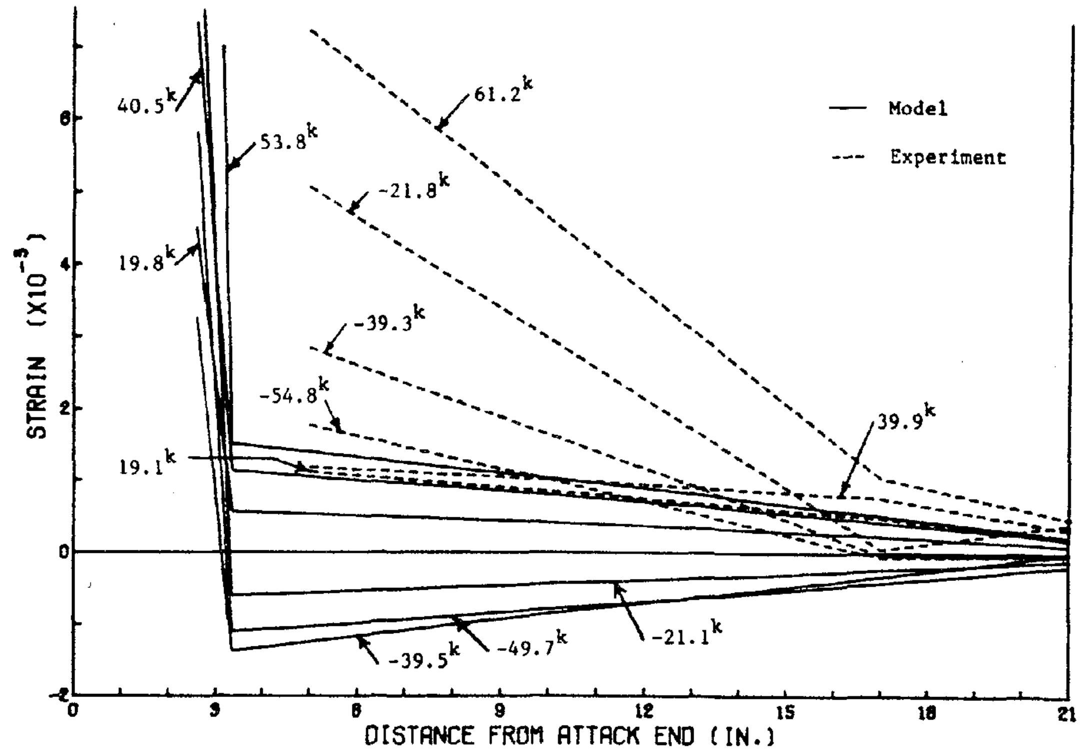


FIG. 136 COMPARISON OF STRAINS ALONG BAR, SPECIMEN S107, CYCLE 2

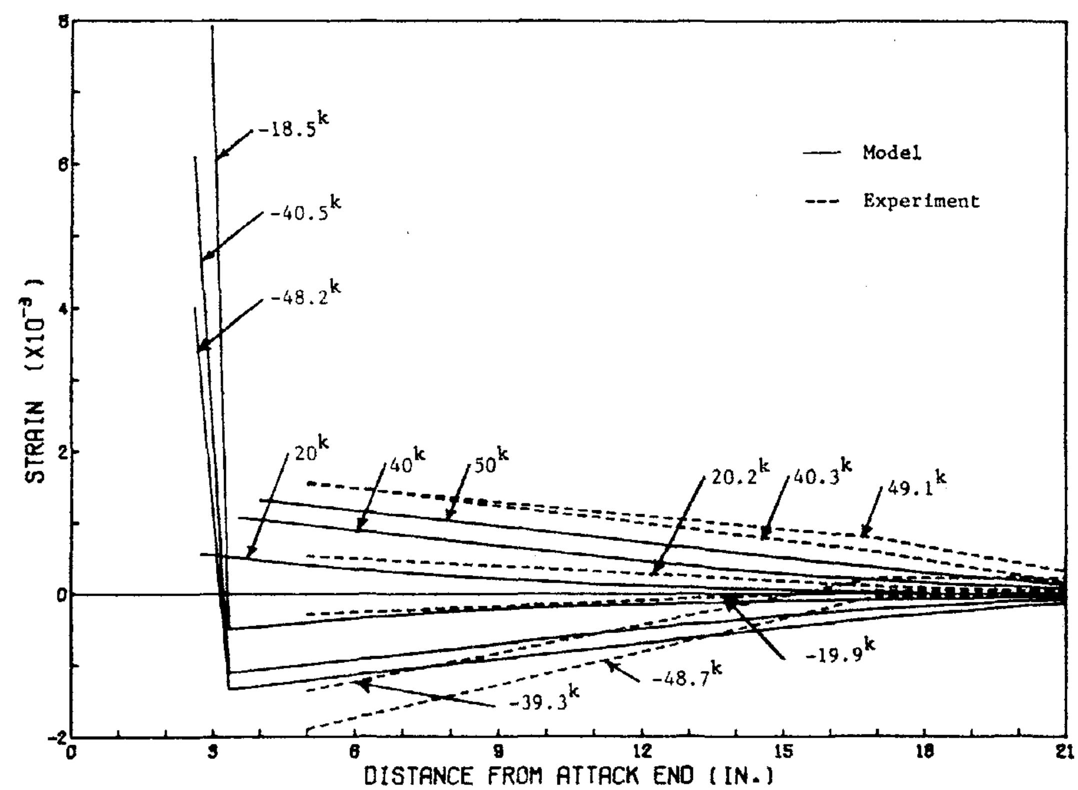


FIG. 135 COMPARISON OF STRAINS ALONG BAR, SPECIMEN S107, CYCLE 1

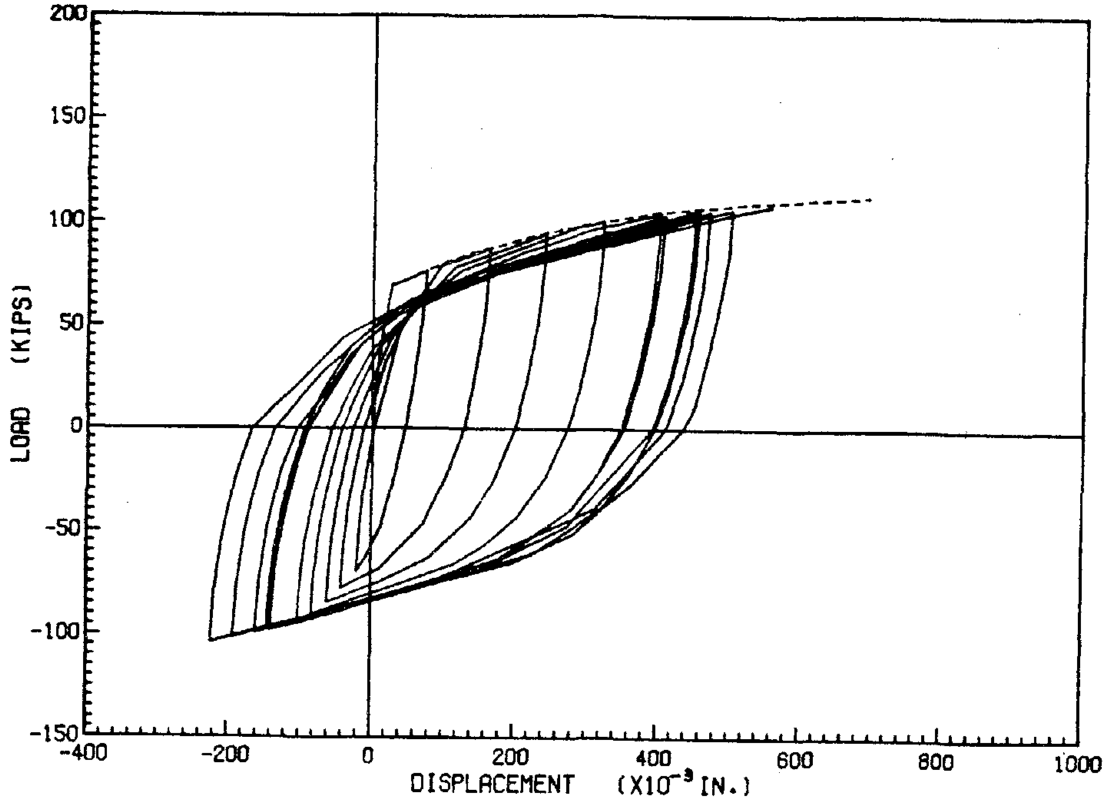


FIG. 138 CORRELATION BETWEEN THE PREDICTED MONOTONIC AND CYCLIC CURVES, SPECIMEN S101, $L_t$ = 30 IN.

233

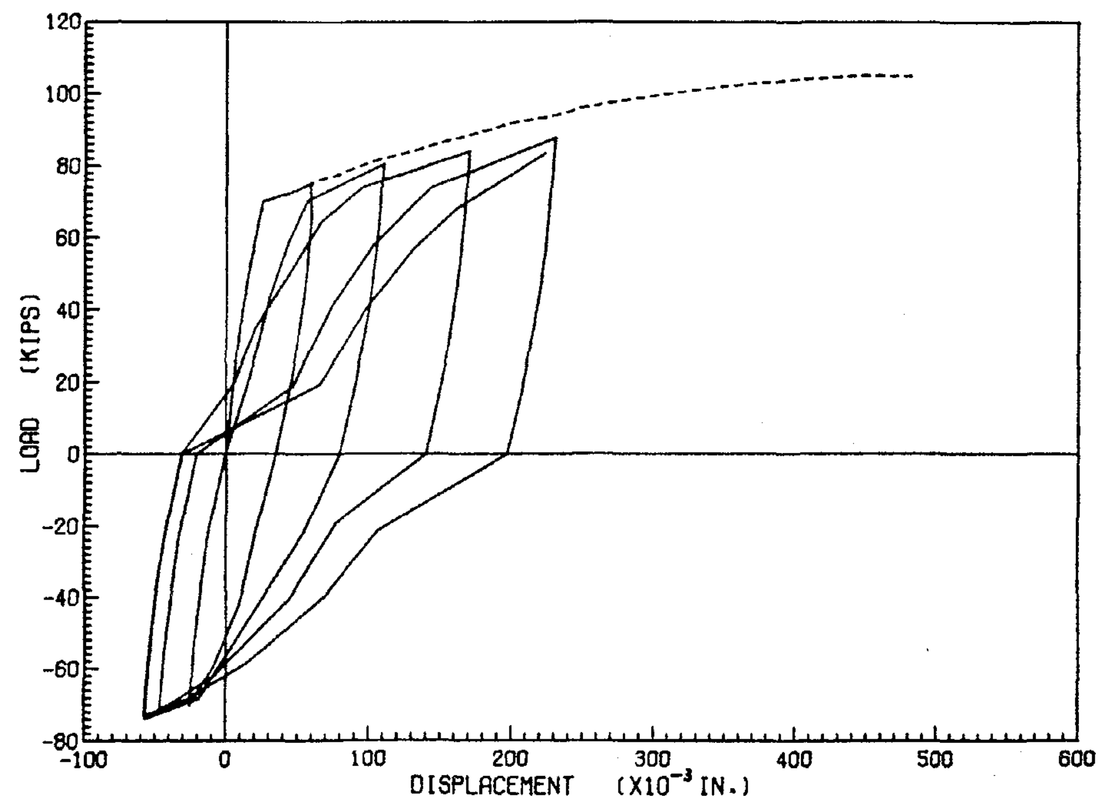


FIG. 137 CORRELATION BETWEEN THE PREDICTED MONOTONIC AND CYCLIC CURVES, SPECIMEN S101, $L_t$ = 24 IN.

232

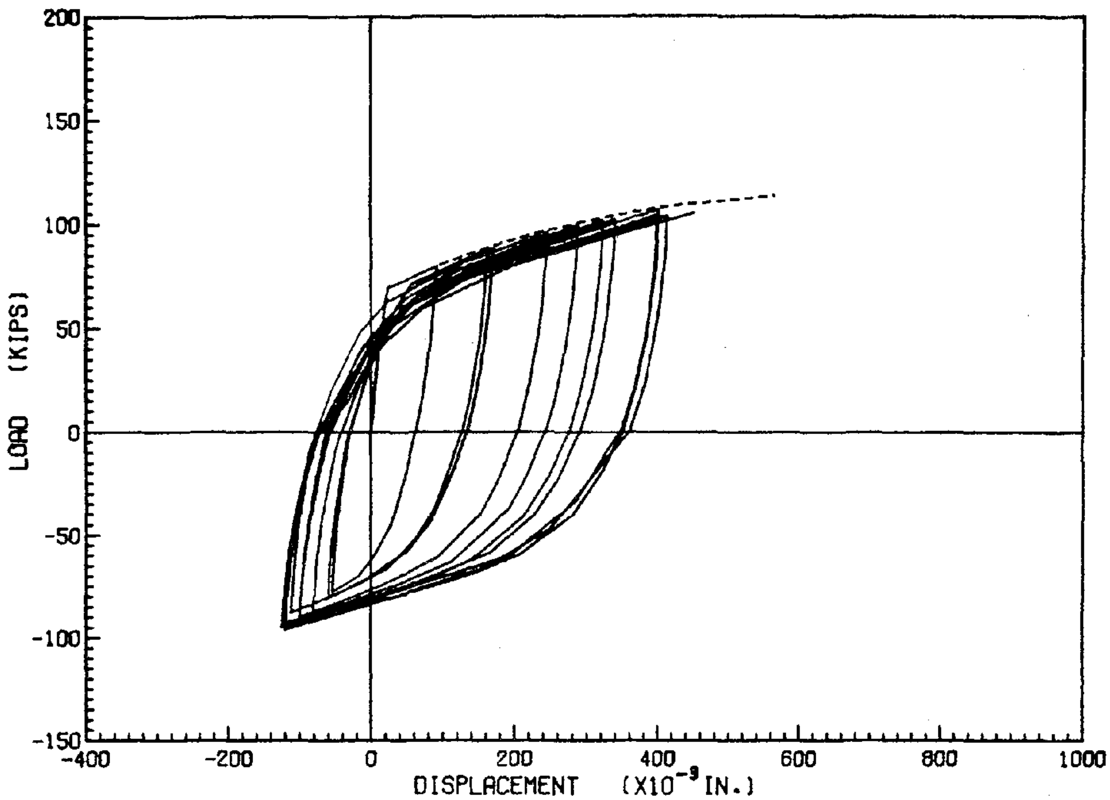


FIG. 140 CORRELATION BETWEEN THE PREDICTED MONOTONIC AND CYCLIC CURVES, SPECIMEN B103, $L_s$ = 23 IN.



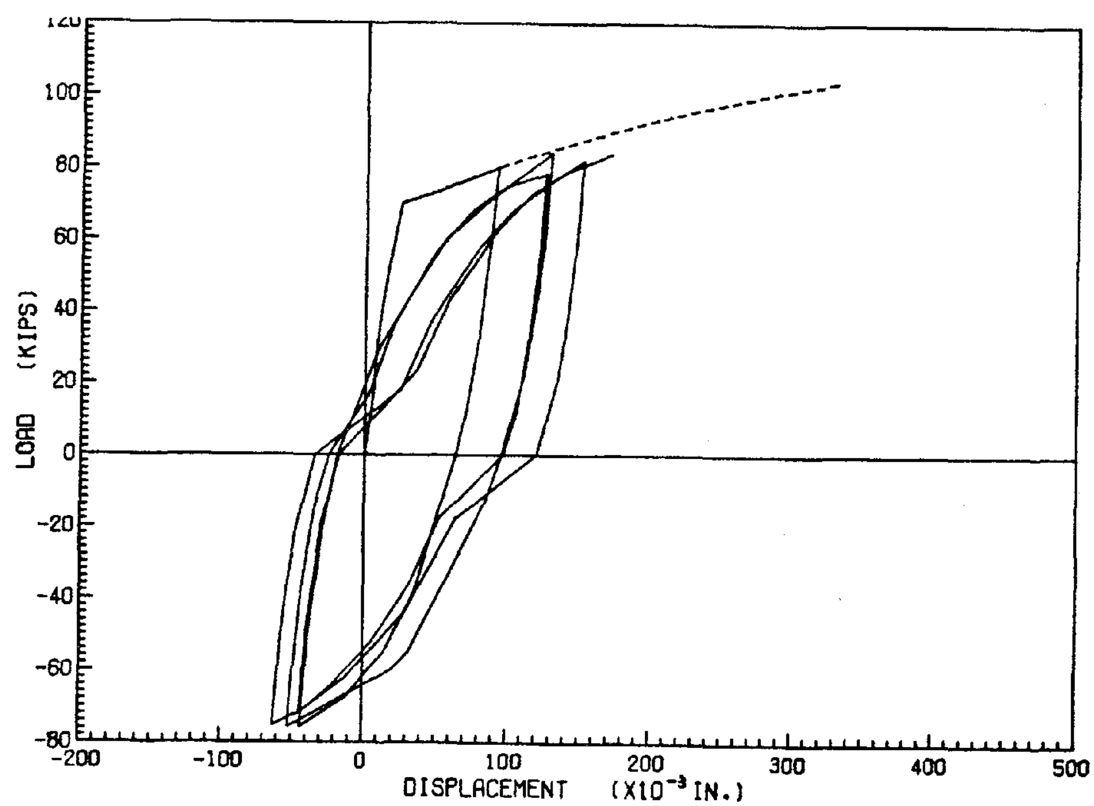


FIG. 139 CORRELATION BETWEEN THE PREDICTED MONOTONIC AND CYCLIC CURVES, SPECIMEN B103, $L_s$ = 15.75 IN.

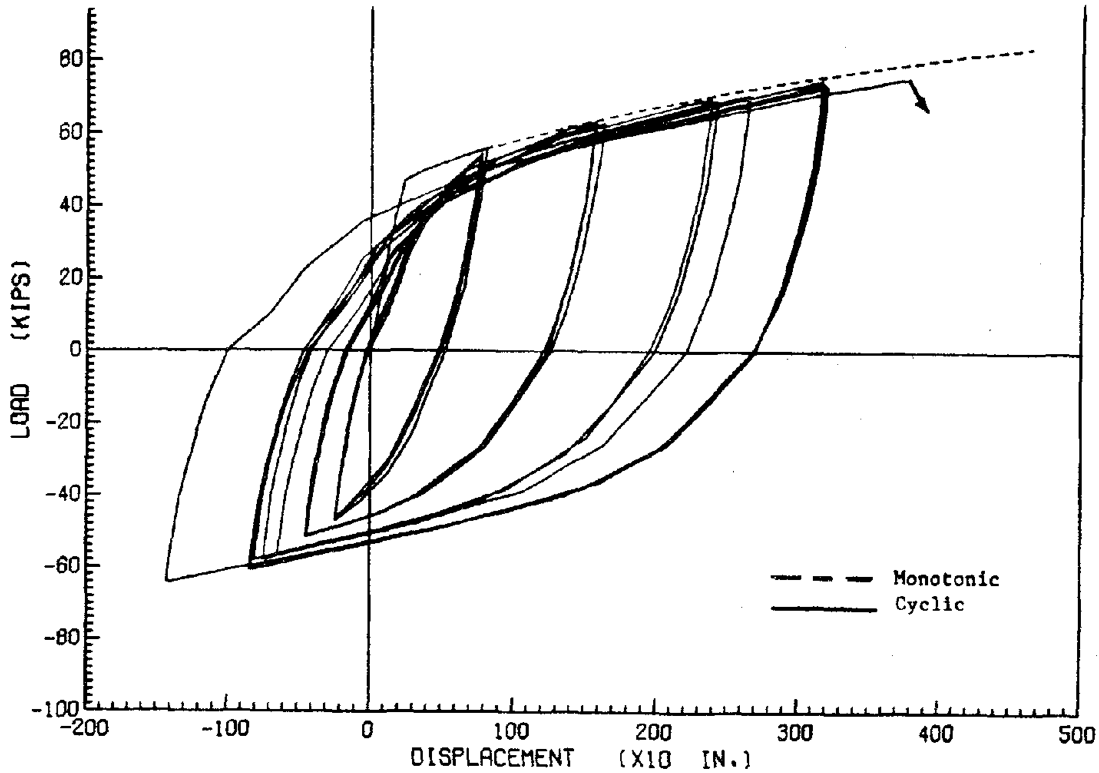


FIG. 142 CORRELATION BETWEEN THE PREDICTED MONOTONIC AND CYCLIC CURVES, SPECIMEN B85 LOADED TO FAILURE.



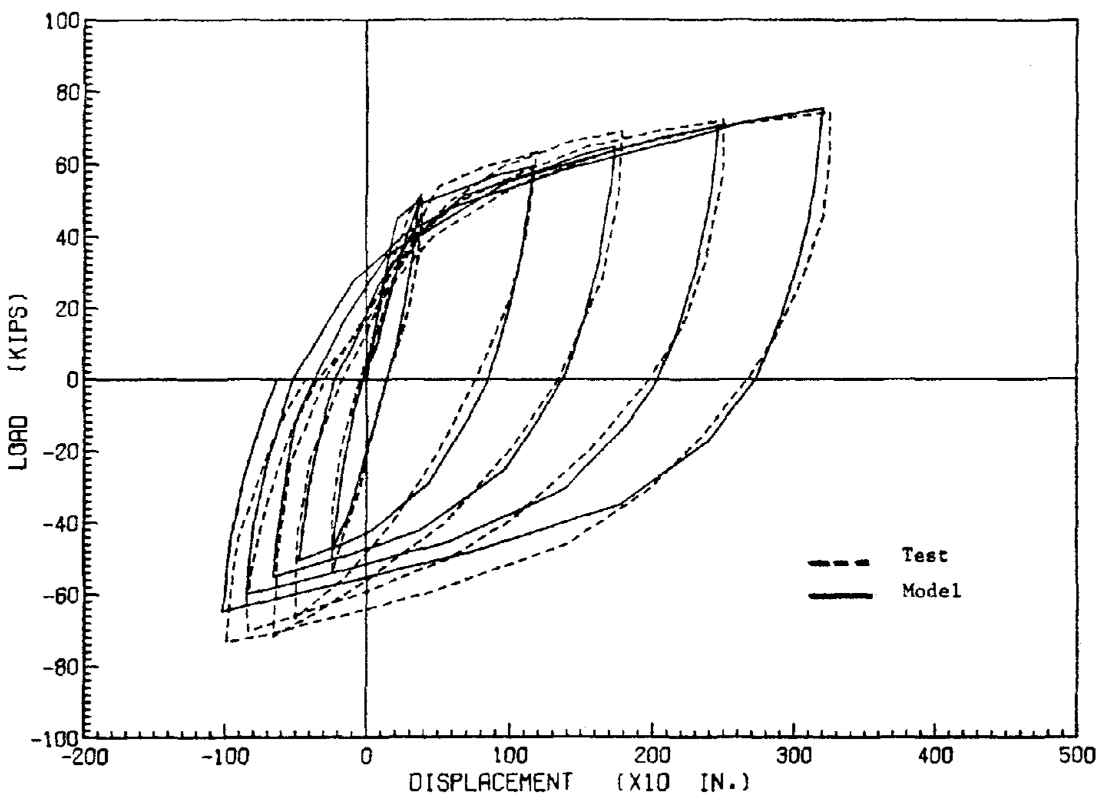


FIG. 141 CORRELATION BETWEEN THE PREDICTED AND MEASURED CYCLIC CURVES, SPECIMEN B85

# APPENDIX A

## COMPUTER PROGRAM FOR PREDICTION OF THE MONOTONIC LOAD-DISPLACEMENT CURVE FOR SPECIMEN S101

```
      PROGRAM LIN(INPUT,OUTPUT,TAPE5=INPUT,TAPE6=OUTPUT)
      REAL L,KK1,KK2,KK3,K1,K2,K3,K4,KKK1,KKK2,LL,L1,L2,L3,L4,KKK3,KKK4
      COMMON/LO/FC,KK1,KK2,KK3,K1,K2,K3,K4,SIGMAY,D,A,AA,PERI,SPACE,H,E1
     $,E2,L,TMAX,SO,SC,TC,LL,SIGEND,PY,L1,L2,L3,L4,EPSILOY,EPSISH,TEND,T
     $TMAX,TTC,TL,TLL,UL1,UL2
C     FC - CONCRETE STRENGTH (PSI)
C     KK1, KK2, KK3 - STIFFNESS ON LOCAL BOND STRESS - SLIP CURVE
C     THE UNIT FOR KK1,KK2,KK3 IS KIP/IN**3
C     K1,K2,K3,K4 ARE CONSTANTS USED IN DE
C     SIGMAY - YIELD STRESS OF STEEL (KSI)
C     D - NOMINAL DIAMETER OF BAR (IN.)
C     AA - NOMINAL AREA OF BAR      (IN.**2)
C     A - REDUCED AREA OF BAR (IN.**2)
C     PERI - EFFECTIVE PERIMETER OF BAR (IN.)
C     SPACE - LUG SPACING OF BAR (IN.)
C     H - HEIGHT OF LUG (IN.)
C     E1 - MODULUS OF ELASTICITY BEFORE YIELDING OF BAR (KSI)
C     E2 - MODULUS OF ELASTICITY AFTER  YIELDING OF BAR (KSI)
C     LL - BONDED LENGTH (IN.)
C     L - EFFECTIVE BONDED LENGTH (IN.)
C     UL1 - DEPTH OF THE WEDGE AT THE ATTACK END
C     UL2 - LENGTH OF THE BAR OUTSIDE THE CONCRETE
C     SIGEND - STEEL STRESS WHICH WILL DROP TO ZERO WITHIN ONE LUG
C     SPACING (KSI)
C     SIGENOL - DISTANCE WHERE CUTOFF IS MADE ,MEASURED FROM DEAD END
C     PENEL - DISTANCE FOR PENETRATION OF BOND STRESS, MEASURED FROM
C     ATTACK END (IN.)
C     TMAX - MAXIMUM LOCAL BOND STRESS (KSI)
C     SO - LOCAL SLIP CORRESPONDING TO TMAX (IN.)
C     TC - LOCAL BOND STRESS WHICH CAUSES DIAGONAL CRACKING (KSI)
C     SC - LOCAL SLIP CORRESPONDING TO TC (IN.)
C     P - APPLIED FORCE AT ATTACK END (KIPS)
C     PY - YIELD LOAD OF BAR
C     EPSILOY - STRAIN AT YIELD STRESS OF BAR
      READ(5,1)FC,KK3,SIGMAY,E1,E2,D,A,AA,PERI,H,LL,SPACE,EPSISH,UL1,UL2
    1 FORMAT(8F10.4)
```

```
      KKK1=(KK1*PERI)/(A*E1)
      K1=SQRT(KKK1)
      KKK2=(KK2*PERI)/(A*E1)
      K2=SQRT(KKK2)
      TMAX=((FC-2300.)/300.)**0.666667
      SO=160./FC
      SC=(TMAX-KK2*SO)/(KK1-KK2)
      TC=KK1*SC
      SIGEND=H*22./14.*D*FC/A/1000.
      TEND=SIGEND*A/SPACE/PERI
      PY=SIGMAY*A
      EPSILOY=SIGMAY/E1
      TTMAX=TMAX-0.03
      TTC=TC-0.05
      WRITE(6,5)
    5 FORMAT(1H1,4X,*DATA FOR LOCAL BOND STRESS - SLIP CURVE OF SPECIMEN
     1 L5*,//)
      WRITE(6,3)
    3 FORMAT(14X,2HFC,10X,3HKK1,10X,3HKK2,10X,2HK1,10X,2HK2,10X,4HTMAX,1
     10X,2HSO,10X,2HTC,10X,2HSC,/)
      WRITE(6,2)FC,KK1,KK2,K1,K2,TMAX,SO,TC,SC
    2 FORMAT(10X,2(F10.4,3X),7(F10.5,2X),////)
      WRITE(6,16)
   16 FORMAT(4X,*THE FOLLOWING ARE THEORETICAL RESULTS FOR SPECIMEN L5*
     1,//)
      P=5.
      CALL CASE1(P)
      CALL CASE2(P)
      CALL CASE3(P)
      CALL CASE3B(P)
      CALL CASE3B1(P)
      CALL CASE3B3(P)
      CALL CASE3A3(P)
```

241

242

END
STOP

171

```
      GO TO 13
   11 RETURN
      END
```

244

```
      SUBROUTINE CASE1(P)
      REAL L,KK1,KK2,KK3,K1,K2,K3,K4,KKK1,KKK2,LL,L1,L2,L3,L4,KKK3,KKK4
      COMMON/LO/FC,KK1,KK2,KK3,K1,K2,K3,K4,SIGMAY,D,A,AA,PERI,SPACE,H,E1
     $,E2,L,TMAX,SO,SC,TC,LL,SIGEND,PY,L1,L2,L3,L4,EPSILOY,EPSISH,TEND,T
     $TMAX,TTC,TL,TLL,UL1,UL2
      COMMON T1(20),ST1(20),X(20)
C     T1 - BOND STRESS IN SEGMENT 1       ST1 - STEEL STRESS IN SEGMENT 1
   13 E=P/A
      A1=.5*(SIGEND+TEND*PERI/A/K1)
      B1=.5*(SIGEND-TEND*PERI/A/K1)
      R1=(E**2)-4*A1*B1
      RR1=(E+SQRT(R1))/2./A1
      L1=ALOG(RR1)/K1
      X(1)=0
      N=10
      M=N+1
      DO 12 I=1,M
      T1(I)=A*K1/PERI*(A1*EXP(K1*X(I))-B1*EXP(-K1*X(I)))
      ST1(I)=A1*EXP(K1*X(I))+B1*EXP(-K1*X(I))
      X(I+1)=X(I)+L1/N
   12 CONTINUE
      IF(T1(M).GT.TC)GO TO 11
      DELTA=T1(M)/KK1+P/A/E1*UL1+P/AA/E1*UL2
      PENEL=L1+UL1+SPACE
      WRITE(6,14)P,DELTA,PENEL,A1,B1,L1,(X(I),I=1,M),(T1(I),I=1,M),(ST1(
     1I),I=1,M)
   14 FORMAT(4X,4H****,2X,8HFORCE = ,F6.2/
     110X,15HDISPLACEMENT = ,F6.4/
     810X,8HPENEL = ,F5.2/
     210X,5HA1 = ,F8.4/
     310X,5HB1 = ,F8.4/
     410X,14HZONE LENGTH = ,F5.2/
     510X,5HX1 = ,4X,11F8.3/
     610X,9HT1(X1) = ,11F8.3/
     710X,9HST1(X1)= ,11F8.3/)
      P=P+5.
```

243

```
      SUBROUTINE CASE2(P)
      REAL L,KK1,KK2,KK3,K1,K2,K3,K4,KKK1,KKK2,LL,L1,L2,L3,L4,KKK3,KKK4
      COMMON/LO/FC,KK1,KK2,KK3,K1,K2,K3,K4,SIGMAY,D,A,AA,PERI,SPACE,H,E1
     $,E2,L,TMAX,SO,SC,TC,LL,SIGEND,PY,L1,L2,L3,L4,EPSILOY,EPSISH,TEND,T
     $TMAX,TTC,TL,TLL,UL1,UL2
      COMMON T1(10),ST1(10),T2(10),ST2(10),X1(10),X2(10)
   25 E=P/A
      IF(P.GT.PY)GO TO 29
      A1=.5*(SIGEND+TEND*PERI/A/K1)
      B1=.5*(SIGEND-TEND*PERI/A/K1)
      R1=(TC*PERI/A/K1)**2+4.*A1*B1
      RR1=((TC*PERI/A/K1)+SQRT(R1))/2./A1
      L1=ALOG(RR1)/K1
      A2=.5*(A1*EXP(K1*L1)+B1*EXP(-K1*L1)+TC*PERI/A/K2)
      B2=.5*(A1*EXP(K1*L1)+B1*EXP(-K1*L1)-TC*PERI/A/K2)
      R2=E**2-4.*A2*B2
      RR2=(E+SQRT(R2))/2./A2
      L2=ALOG(RR2)/K2
      TL=L1+L2
      TLL=L-SPACE
      IF(TL.GT.TLL)GO TO 29
      N=5
      M=N+1
      X1(1)=0
      DO 23 I=1,M
      T1(I)=A*K1/PERI*(A1*EXP(K1*X1(I))-B1*EXP(-K1*X1(I)))
      ST1(I)=A1*EXP(K1*X1(I))+B1*EXP(-K1*X1(I))
      X1(I+1)=X1(I)+L1/N
   23 CONTINUE
      X2(1)=0
      DO 24 I=1,M
      T2(I)=A*K2/PERI*(A2*EXP(K2*X2(I))-B2*EXP(-K2*X2(I)))
      ST2(I)=A2*EXP(K2*X2(I))+B2*EXP(-K2*X2(I))
      X2(I+1)=X2(I)+L2/N
   24 CONTINUE
      DELTA=(T2(M)-TC)/KK2+SC+P/A/E1*UL1+P/AA/E1*UL2
```



```
      PENEL=TL+UL1+SPACE
      WRITE(6,14)P,DELTA,PENEL,A1,B1,L1,(X1(I),I=1,M),(T1(I),I=1,M),(ST1
     1(I),I=1,M),A2,B2,L2,(X2(I),I=1,M),(T2(I),I=1,M),(ST2(I),I=1,M)
   14 FORMAT(4X,4H****,2X,8HFORCE = ,F6.2/
     110X,15HDISPLACEMENT = ,F6.4/
     810X,8HPENEL = ,F5.2/
     210X,5HA1 = ,F8.4/
     310X,5HB1 = ,F8.4/
     110X,19HLENGTH OF ZONE 1 = ,F5.2/
     110X,5HX1 = ,4X,6F8.3/
     110X,9HT1(X1) = ,6F8.3/
     110X,9HST1(X1)= ,6F8.3/
     110X,5HA2 = ,F8.4/
     110X,5HB2 = ,F8.4/
     110X,19HLENGTH OF ZONE 2 = ,F5.2/
     110X,5HX2 = ,4X,6F8.3/
     110X,9HT2(X2) = ,6F8.3/
     110X,9HST2(X2)= ,6F8.3/)
      PPY=PY-5.
      IF(P.GE.PPY)26,27
   26 P=P+1.
      GO TO 25
   27 P=P+5.
      GO TO 25
   29 RETURN
      END
```

```
      PENEL=LL
      WRITE(6,14)P,DELTA,PENEL,A1,B1,L1,(X1(I),I=1,M),(T1(I),I=1,M),(ST1
     1(I),I=1,M),A2,B2,L2,(X2(I),I=1,M),(T2(I),I=1,M),(ST2(I),I=1,M)
   14 FORMAT(4X,4H****,2X,8HFORCE = ,F6.2/
     110X,15HDISPLACEMENT = ,F6.4/
     810X,8HPENEL = ,F5.2/
     210X,5HA1 = ,F8.4/
     310X,5HB1 = ,F8.4/
     110X,19HLENGTH OF ZONE 1 = ,F5.2/
     110X,5HX1 = ,4X,6F8.3/
     110X,9HT1(X1) = ,6F8.3/
     110X,9HST1(X1)= ,6F8.3/
     110X,5HA2 = ,F8.4/
     110X,5HB2 = ,F8.4/
     110X,19HLENGTH OF ZONE 2 = ,F5.2/
     110X,5HX2 = ,4X,6F8.3/
     110X,9HT2(X2) = ,6F8.3/
     110X,9HST2(X2)= ,6F8.3/)
      PPY=PY-5.
      IF(P.GE.PPY)26,27
   26 P=P+1.
      GO TO 25
   27 P=P+5.
      GO TO 25
   29 RETURN
      END
```



```
      SUBROUTINE CASE3(P)
      REAL L,KK1,KK2,KK3,K1,K2,K3,K4,KKK1,KKK2,LL,L1,L2,L3,L4,KKK3,KKK4
      COMMON/LO/FC,KK1,KK2,KK3,K1,K2,K3,K4,SIGMAY,D,A,AA,PERI,SPACE,H,E1
     $,E2,L,TMAX,SO,SC,TC,LL,SIGEND,PY,L1,L2,L3,L4,EPSILOY,EPSISH,TEND,T
     $TMAX,TTC,TL,TLL,UL1,UL2
      COMMON T1(10),ST1(10),T2(10),ST2(10),X1(10),X2(10)
      L1=L
   25 IF(P.GT.PY)GO TO 29
   21 L1=L1-0.01
      L2=L-L1
      E=P/A
      A1=TC*PERI/A/K1/(EXP(K1*L1)+EXP(-K1*L1))
      B1=-A1
      A2=.5*(A1*EXP(K1*L1)+B1*EXP(-K1*L1)+TC*PERI/A/K2)
      B2=.5*(A1*EXP(K1*L1)+B1*EXP(-K1*L1)-TC*PERI/A/K2)
      F=A2*EXP(K2*L2)+B2*EXP(-K2*L2)
      DIFF=(E-F)/E
      DIFFA=ABS(DIFF)
      IF(DIFFA.LE.0.005)GO TO 22
      GO TO 21
   22 N=5
      M=N+1
      X1(1)=0
      DO 23 I=1,M
      T1(I)=A*K1/PERI*(A1*EXP(K1*X1(I))-B1*EXP(-K1*X1(I)))
      ST1(I)=A1*EXP(K1*X1(I))+B1*EXP(-K1*X1(I))
      X1(I+1)=X1(I)+L1/N
   23 CONTINUE
      X2(1)=0
      DO 24 I=1,M
      T2(I)=A*K2/PERI*(A2*EXP(K2*X2(I))-B2*EXP(-K2*X2(I)))
      ST2(I)=A2*EXP(K2*X2(I))+B2*EXP(-K2*X2(I))
      X2(I+1)=X2(I)+L2/N
   24 CONTINUE
      IF(T2(M).GT.1.5.OR.T1(1).GE.0.9)GO TO 29
      DELTA=(T2(M)-TC)/KK2+SC+P/A/E1*UL1+P/AA/E1*UL2
```

```
      SUBROUTINE CASE3B(P)
      REAL L,KK1,KK2,KK3,K1,K2,K3,K4,KKK1,KKK2,LL,L1,L2,L3,L4,KKK3,KKK4
      COMMON/LO/FC,KK1,KK2,KK3,K1,K2,K3,K4,SIGMAY,D,A,AA,PERI,SPACE,H,E1
     $,E2,L,TMAX,SO,SC,TC,LL,SIGEND,PY,L1,L2,L3,L4,EPSILOY,EPSISH,TEND,T
     $TMAX,TTC,TL,TLL,UL1,UL2
      COMMON T1(10),ST1(10),T2(10),ST2(10),T3(10),ST3(10),X1(10),X2(10),
     $X3(10)
      KKK3=KK2*PERI/A/E2
      K3=SQRT(KKK3)
      L1=L1+SPACE
   30 E=P/A
      L1=L1-0.01
      DL=L2+2.
      DDL=L2-1.
   34 L2=DDL
   33 IF(L2.GE.DL)GO TO 35
      A1=TC*PERI/A/K1/(EXP(K1*L1)+EXP(-K1*L1))
      B1=-A1
      A2=.5*(A1*EXP(K1*L1)+B1*EXP(-K1*L1)+TC*PERI/A/K2)
      B2=.5*(A1*EXP(K1*L1)+B1*EXP(-K1*L1)-TC*PERI/A/K2)
      EE1=A2*EXP(K2*L2)+B2*EXP(-K2*L2)
      DIFF1=(SIGMAY-EE1)/SIGMAY
      DIFF1A=ABS(DIFF1)
      IF(DIFF1A.LE.0.005)GO TO 31
      L2=L2+0.01
      GO TO 33
   31 L3=L-L1-L2
      A3=.5*(EPSISH*E2+K2/K3*(A2*EXP(K2*L2)-B2*EXP(-K2*L2)))
      B3=.5*(EPSISH*E2-K2/K3*(A2*EXP(K2*L2)-B2*EXP(-K2*L2)))
      EE2=A3*EXP(K3*L3)+B3*EXP(-K3*L3)+(SIGMAY-E2*EPSISH)
      DIFF2=(E-EE2)/E
      DIFF2A=ABS(DIFF2)
      IF(DIFF2A.LE.0.005)GO TO 32
      L2=L2+0.01
      GO TO 33
   35 L1=L1-0.01
```



```
      GO TO 34
   32 N=5
      M=N+1
      X1(1)=0
      DO 23 I=1,M
      T1(I)=A*K1/PERI*(A1*EXP(K1*X1(I))-B1*EXP(-K1*X1(I)))
      ST1(I)=A1*EXP(K1*X1(I))+B1*EXP(-K1*X1(I))
      X1(I+1)=X1(I)+L1/N
   23 CONTINUE
      X2(1)=0
      DO 24 I=1,M
      T2(I)=A*K2/PERI*(A2*EXP(K2*X2(I))-B2*EXP(-K2*X2(I)))
      ST2(I)=A2*EXP(K2*X2(I))+B2*EXP(-K2*X2(I))
      X2(I+1)=X2(I)+L2/N
   24 CONTINUE
      X3(1)=0
      DO 25 I=1,M
      T3(I)=A*K3/PERI*(A3*EXP(K3*X3(I))-B3*EXP(-K3*X3(I)))
      ST3(I)=A3*EXP(K3*X3(I))+B3*EXP(-K3*X3(I))+(SIGMAY-E2*EPSISH)
      X3(I+1)=X3(I)+L3/N
   25 CONTINUE
      SIGMA=P/AA
      IF(SIGMA.GT.SIGMAY)37,36
   36 DELTA=(T3(M)-TC)/KK2+SC+((P/A-SIGMAY)/E2+EPSISH)*UL1+P/AA/E1*UL2
      GO TO 38
   37 DELTA=(T3(M)-TC)/KK2+SC+((P/A-SIGMAY)/E2+EPSISH)*UL1+((P/AA-SIGMAY
     1)/E2+EPSISH)*UL2
   38 WRITE(6,14)P,DELTA,A1,B1,L1,(X1(I),I=1,M),(T1(I),I=1,M),(ST1(I),I=
     11,M),A2,B2,L2,(X2(I),I=1,M),(T2(I),I=1,M),(ST2(I),I=1,M),A3,B3,L3,
     1(X3(I),I=1,M),(T3(I),I=1,M),(ST3(I),I=1,M)
   14 FORMAT(4X,4H****,2X,8HFORCE = ,F6.2/
     110X,15HDISPLACEMENT = ,F6.4/
     210X,5HA1 = ,F8.4/
     310X,5HB1 = ,F8.4/
     110X,19HLENGTH OF ZONE 1 = ,F5.2/
     110X,5HX1 = ,4X,6F8.3/
```

```
      SUBROUTINE CASE3B1(P)
      REAL L,KK1,KK2,KK3,K1,K2,K3,K4,KKK1,KKK2,LL,L1,L2,L3,L4,KKK3,KKK4
      COMMON/LO/FC,KK1,KK2,KK3,K1,K2,K3,K4,SIGMAY,D,A,AA,PERI,SPACE,H,E1
     $,E2,L,TMAX,SO,SC,TC,LL,SIGENO,PY,L1,L2,L3,L4,EPSILOY,EPSISH,TEND,T
     $TMAX,TTC,TL,TLL,UL1,UL2
      COMMON T1(10),ST1(10),T2(10),ST2(10),T3(10),ST3(10),X1(10),X2(10),
     $X3(10),T4(10),ST4(10),X4(10)
      KKK3=KK2*PERI/A/E2
      K3=SQRT(KKK3)
      KKK4=KK3*PERI/A/E2
      K4=SQRT(KKK4)
      EE=TMAX*PERI/A/K3
   45 E=P/A
      L1=L1-2.0
      L1=L1+0.1
      DL1=L2+1.0
      DDL1=L2-0.5
      DL2=L3+1.0
      DDL2=L3-0.5
   34 L2=DDL1
   33 IF(L2.GE.DL1)GO TO 35
      A1=TC*PERI/A/K1/(EXP(K1*L1)+EXP(-K1*L1))
      B1=-A1
      A2=.5*(A1*EXP(K1*L1)+B1*EXP(-K1*L1)+TC*PERI/A/K2)
      B2=.5*(A1*EXP(K1*L1)+B1*EXP(-K1*L1)-TC*PERI/A/K2)
      EE1=A2*EXP(K2*L2)+B2*EXP(-K2*L2)
      DIFF1=(SIGMAY-EE1)/SIGMAY
      DIFF1A=ABS(DIFF1)
      IF(DIFF1A.LE.0.01)GO TO 30
   41 L2=L2+0.1
      GO TO 33
   30 L3=DDL2
   31 IF(L3.GE.DL2)GO TO 41
      A3=.5*(EPSISH*E2+K2/K3*(A2*EXP(K2*L2)-B2*EXP(-K2*L2)))
      B3=.5*(EPSISH*E2-K2/K3*(A2*EXP(K2*L2)-B2*EXP(-K2*L2)))
      EE2=A3*EXP(K3*L3)-B3*EXP(-K3*L3)
```

252

```
     110X,9HT1(X1) = ,6F8.3/
     110X,9HST1(X1)= ,6F8.3/
     110X,5HA2 = ,F8.4/
     110X,5HB2 = ,F8.4/
     110X,19HLENGTH OF ZONE 2 = ,F5.2/
     110X,5HX2 = ,4X,6F8.3/
     110X,9HT2(X2) = ,6F8.3/
     110X,9HST2(X2)= ,6F8.3/
     110X,5HA3 = ,F8.4/
     110X,5HB3 = ,F8.4/
     110X,19HLENGTH OF ZONE 3 = ,F5.2/
     110X,5HX3 = ,4X,6F8.3/
     110X,9HT3(X3) = ,6F8.3/
     110X,9HST3(X3)= ,6F8.3/)
      P=P+1.
      IF(T3(M).GT.TTMAX.OR.T1(1).GE.TTC)GO TO 39
      GO TO 30
   39 RETURN
      END
```

251

```
      DIFF2A=ABS(DIFF2)
      IF(DIFF2A.LE.0.01)GO TO 32
      L3=L3+0.1
      GO TO 31
   32 L4=L-L1-L2-L3
      A4=TMAX*PERI/A/K4
      B4=A3*EXP(K3*L3)+B3*EXP(-K3*L3)
      EE3=A4*SIN(K4*L4)+B4*COS(K4*L4)+SIGMAY-E2*EPSISH
      DIFF3=(E-EE3)/E
      DIFF3A=ABS(DIFF3)
      IF(DIFF3A.LE.0.01)GO TO 42
      L3=L3+0.1
      GO TO 31
   35 L1=L1+0.1
      GO TO 34
   42 N=5
      M=N+1
      X1(1)=0
      DO 23 I=1,M
      T1(I)=A*K1/PERI*(A1*EXP(K1*X1(I))-B1*EXP(-K1*X1(I)))
      ST1(I)=A1*EXP(K1*X1(I))+B1*EXP(-K1*X1(I))
      X1(I+1)=X1(I)+L1/N
   23 CONTINUE
      X2(1)=0
      DO 24 I=1,M
      T2(I)=A*K2/PERI*(A2*EXP(K2*X2(I))-B2*EXP(-K2*X2(I)))
      ST2(I)=A2*EXP(K2*X2(I))+B2*EXP(-K2*X2(I))
      X2(I+1)=X2(I)+L2/N
   24 CONTINUE
      X3(1)=0
      DO 25 I=1,M
      T3(I)=A*K3/PERI*(A3*EXP(K3*X3(I))-B3*EXP(-K3*X3(I)))
      ST3(I)=A3*EXP(K3*X3(I))+B3*EXP(-K3*X3(I))+SIGMAY-E2*EPSISH
      X3(I+1)=X3(I)+L3/N
   25 CONTINUE
```



```
      X4(1)=0
      DO 26 I=1,M
      T4(I)=A*K4/PERI*(A4*COS(K4*X4(I))-B4*SIN(K4*X4(I)))
      ST4(I)=A4*SIN(K4*X4(I))+B4*COS(K4*X4(I))+SIGMAY-E2*EPSISH
      X4(I+1)=X4(I)+L4/N
   26 CONTINUE
      DELTA=(TMAX-T4(M))/KK3+SO+((P/A-SIGMAY)/E2+EPSISH)*UL1+((P/AA-SIGM
     1AY)/E2+EPSISH)*UL2
      WRITE(6,14)P,DELTA,A1,B1,L1,(X1(I),I=1,M),(T1(I),I=1,M),(ST1(I),I=
     11,M),A2,B2,L2,(X2(I),I=1,M),(T2(I),I=1,M),(ST2(I),I=1,M),A3,B3,L3,
     1(X3(I),I=1,M),(T3(I),I=1,M),(ST3(I),I=1,M),A4,B4,L4,(X4(I),I=1,M),
     1(T4(I),I=1,M),(ST4(I),I=1,M)
   14 FORMAT(10X,8HFORCE = ,F6.2/
     110X,15HDISPLACEMENT = ,F6.4/
     210X,5HA1 = ,F8.4/,10X,5HB1 = ,F8.4/
     110X,19HLENGTH OF ZONE 1 = ,F5.2/
     110X,5HX1 = ,4X,6F8.3/,10X,9HT1(X1) = ,6F8.3/,10X,9HST1(X1)=,6F8.3/
     110X,5HA2 = ,F8.4/,10X,5HB2 = ,F8.4/
     110X,19HLENGTH OF ZONE 2 = ,F5.2/
     110X,5HX2 = ,4X,6F8.3/
     110X,9HT2(X2) = ,6F8.3/,10X,9HST2(X2)= ,6F8.3/
     110X,5HA3 = ,F8.4/,10X,5HB3 = ,F8.4/
     110X,19HLENGTH OF ZONE 3 = ,F5.2/
     110X,5HX3 = ,4X,6F8.3/
     110X,9HT3(X3) = ,6F8.3/
     110X,9HST3(X3)= ,6F8.3/
     210X,5HA4 = ,F8.4/
     310X,5HB4 = ,F8.4/
     110X,19HLENGTH OF ZONE 4 = ,F5.2/
     110X,5HX4 = ,4X,6F8.3/
     110X,9HT4(X4) = ,6F8.3/
     110X,9HST4(X4)= ,6F8.3/)
      P=P+2.0
      IF(T1(1).GE.TTC.OR.L3.LE.0.02)GO TO 49
      GO TO 45
   49 RETURN
```

```
      REAL L,KK1,KK2,KK3,K1,K2,K3,K4,KKK1,KKK2,LL,L1,L2,L3,L4,KKK3,KKK4
      COMMON/LO/FC,KK1,KK2,KK3,K1,K2,K3,K4,SIGMAY,D,A,AA,PERI,SPACE,H,E1
     $,E2,L,TMAX,SO,SC,TC,LL,SIGEND,PY,L1,L2,L3,L4,EPSILOY,EPSISH,TEND,T
     $TMAX,TTC,TL,TLL,UL1,UL2
      COMMON T1(10),ST1(10),T2(10),ST2(10),T3(10),ST3(10),X1(10),X2(10),
     $X3(10),T4(10),ST4(10),X4(10)
      KKK3=KK2*PERI/A/E2
      K3=SQRT(KKK3)
      KKK4=KK3*PERI/A/E2
      K4=SQRT(KKK4)
      EE=TMAX*PERI/A/K3
      L2=L2+1.
   45 E=P/A
      L2=L2-0.01
      DL=L3+2.
      DDL=L3-2.
   34 L3=DDL
   33 IF(L3.GE.DL)GO TO 35
      A2=SIGMAY/(EXP(K2*L2)-EXP(-K2*L2))
      B2=-A2
      A3=0.5*(E2*EPSISH+K2/K3*(A2*EXP(K2*L2)-B2*EXP(-K2*L2)))
      B3=0.5*(E2*EPSISH-K2/K3*(A2*EXP(K2*L2)-B2*EXP(-K2*L2)))
      EE1=A3*EXP(K3*L3)-B3*EXP(-K3*L3)
      DIFF1=(EE1-EE)/EE
      DIFF1A=ABS(DIFF1)
      IF(DIFF1A.LE.0.005)GO TO 31
      L3=L3+0.01
      GO TO 33
   31 L4=L-L2-L3
      A4=TMAX*PERI/A/K4
      B4=A3*EXP(K3*L3)+B3*EXP(-K3*L3)
      EE2=A4*SIN(K4*L4)+B4*COS(K4*L4)+SIGMAY-E2*EPSISH
      DIFF2=(EE2-E)/E
      DIFF2A=ABS(DIFF2)
      IF(DIFF2A.LE.0.005)GO TO 22
```

```
 110X,9HST2(X2)= ,6F8.3/
 110X,5HA3 = ,F8.4/
 110X,5HB3 = ,F8.4/
 110X,19HLENGTH OF ZONE 3 = ,F5.2/
 110X,5HX3 = ,4X,6F8.3/
 110X,9HT3(X3) = ,6F8.3/
 110X,9HST3(X3)= ,6F8.3/
 210X,5HA4 = ,F8.4/
 310X,5HB4 = ,F8.4/
 110X,19HLENGTH OF ZONE 4 = ,F5.2/
 110X,5HX4 = ,4X,6F8.3/
 110X,9HT4(X4) = ,6F8.3/
 110X,9HST4(X4)= ,6F8.3/)
  P=P+1.
  IF(L3.LE.0.8)GO TO 49
  GO TO 45
49 RETURN
  END
```

258

```
   L3=L3+0.01
   GO TO 33
35 L2=L2-0.01
   GO TO 34
22 N=5
   M=N+1
   X2(1)=0
   DO 24 I=1,M
   T2(I)=A*K2/PERI*(A2*EXP(K2*X2(I))-B2*EXP(-K2*X2(I)))
   ST2(I)=A2*EXP(K2*X2(I))+B2*EXP(-K2*X2(I))
   X2(I+1)=X2(I)+L2/N
24 CONTINUE
   X3(1)=0
   DO 25 I=1,M
   T3(I)=A*K3/PERI*(A3*EXP(K3*X3(I))-B3*EXP(-K3*X3(I)))
   ST3(I)=A3*EXP(K3*X3(I))+B3*EXP(-K3*X3(I))+(SIGMAY-E2*EPSISH)
   X3(I+1)=X3(I)+L3/N
25 CONTINUE
   X4(1)=0
   DO 26 I=1,M
   T4(I)=A*K4/PERI*(A4*COS(K4*X4(I))-B4*SIN(K4*X4(I)))
   ST4(I)=A4*SIN(K4*X4(I))+B4*COS(K4*X4(I))+SIGMAY-E2*EPSISH
   X4(I+1)=X4(I)+L4/N
26 CONTINUE
   DELTA=(TMAX-T4(M))/KK3+SO+((P/A-SIGMAY)/E2+EPSISH)*UL1+((P/AA-SIGM
  1AY)/E2+EPSISH)*UL2
   WRITE(6,14)P,DELTA,A2,B2,L2,(X2(I),I=1,M),(T2(I),I=1,M),(ST2(I),I=
  11,M),A3,B3,L3,(X3(I),I=1,M),(T3(I),I=1,M),(ST3(I),I=1,M),A4,B4,L4,
  1(X4(I),I=1,M),(T4(I),I=1,M),(ST4(I),I=1,M)
14 FORMAT(4X,4H****,2X,8HFORCE = ,F6.2/
  110X,15HDISPLACEMENT = ,F6.4/
  110X,5HA2 = ,F8.4/
  110X,5HB2 = ,F8.4/
  110X,19HLENGTH OF ZONE 2 = ,F5.2/
  110X,5HX2 = ,4X,6F8.3/
  110X,9HT2(X2) = ,6F8.3/
```

257

```
      SUBROUTINE CASE3A3(P)
      REAL L,KK1,KK2,KK3,K1,K2,K3,K4,KKK1,KKK2,LL,L1,L2,L3,L4,KKK3,KKK4
      COMMON/LD/FC,KK1,KK2,KK3,K1,K2,K3,K4,SIGMAY,D,A,AA,PERI,SPACE,H,E1
     $,E2,L,TMAX,SO,SC,TC,LL,SIGEND,PY,L1,L2,L3,L4,EPSILOY,EPSISH,TEND,T
     $TMAX,TTC,TL,TLL,UL1,UL2
      COMMON T1(10),ST1(10),T2(10),ST2(10),T3(10),ST3(10),X1(10),X2(10),
     $X3(10),T4(10),ST4(10),X4(10)
      KKK3=KK3*PERI/A/E1
      K3=SQRT(KKK3)
      KKK4=KK3*PERI/A/E2
      K4=SQRT(KKK4)
   45 E=P/A
      L2=L2-0.01
      DL=L3+2.
      DDL=0.
   34 L3=DDL
   33 IF(L3.GE.DL)GO TO 35
      A2=TMAX*PERI/(A*K2*(EXP(K2*L2)+EXP(-K2*L2)))
      B2=-A2
      A3=TMAX*PERI/A/K3
      B3=A2*EXP(K2*L2)+B2*EXP(-K2*L2)
      EE1=A3*SIN(K3*L3)+B3*COS(K3*L3)
      DIFF1=(SIGMAY-EE1)/SIGMAY
      DIFF1A=ABS(DIFF1)
      IF(DIFF1A.LE.0.005)GO TO 31
      L3=L3+0.01
      GO TO 33
   31 L4=L-L2-L3
      A4=K3/K4*(A3*COS(K3*L3)-B3*SIN(K3*L3))
      B4=E2*EPSISH
      EE2=A4*SIN(K4*L4)+B4*COS(K4*L4)+SIGMAY-E2*EPSISH
      DIFF2=(EE2-E)/E
      DIFF2A=ABS(DIFF2)
      IF(DIFF2A.LE.0.005)GO TO 22
      L3=L3+0.01
      GO TO 33
```

259

```
   35 L2=L2-0.01
      GO TO 34
   22 N=5
      M=N+1
      X2(1)=0
      DO 24 I=1,M
      T2(I)=A*K2/PERI*(A2*EXP(K2*X2(I))-B2*EXP(-K2*X2(I)))
      ST2(I)=A2*EXP(K2*X2(I))+B2*EXP(-K2*X2(I))
      X2(I+1)=X2(I)+L2/N
   24 CONTINUE
      X3(1)=0
      DO 25 I=1,M
      T3(I)=A*K3/PERI*(A3*COS(K3*X3(I))-B3*SIN(K3*X3(I)))
      ST3(I)=A3*SIN(K3*X3(I))+B3*COS(K3*X3(I))
      X3(I+1)=X3(I)+L3/N
   25 CONTINUE
      X4(1)=0
      DO 26 I=1,M
      T4(I)=A*K4/PERI*(A4*COS(K4*X4(I))-B4*SIN(K4*X4(I)))
      ST4(I)=A4*SIN(K4*X4(I))+B4*COS(K4*X4(I))+SIGMAY-E2*EPSISH
      X4(I+1)=X4(I)+L4/N
   26 CONTINUE
      DELTA=(TMAX-T4(M))/KK3+SO+((P/A-SIGMAY)/E2+EPSISH)*UL1+((P/AA-SIGM
     1AY)/E2+EPSISH)*UL2
      WRITE(6,14)P,DELTA,A2,B2,L2,(X2(I),I=1,M),(T2(I),I=1,M),(ST2(I),I=
     11,M),A3,B3,L3,(X3(I),I=1,M),(T3(I),I=1,M),(ST3(I),I=1,M),A4,B4,L4,
     1(X4(I),I=1,M),(T4(I),I=1,M),(ST4(I),I=1,M)
   14 FORMAT(4X,4H****,2X,8HFORCE = ,F6.2/
     110X,15HDISPLACEMENT = ,F6.4/
     110X,5HA2 = ,F8.4/
     110X,5HB2 = ,F8.4/
     110X,19HLENGTH OF ZONE 2 = ,F5.2/
     110X,5HX2 = ,4X,6F8.3/
     110X,9HT2(X2) = ,6F8.3/
     110X,9HST2(X2)= ,6F8.3/
     110X,5HA3 = ,F8.4/
```

260

```
     110X,5HB3 = ,F8.4/
     110X,19HLENGTH OF ZONE 3 = ,F5.2/
     110X,5HX3 = ,4X,6F8.3/
     110X,9HT3(X3) = ,6F8.3/
     110X,9HST3(X3)= ,6F8.3/
     210X,5HA4 = ,F8.4/
     310X,5HB4 = ,F8.4/
     110X,19HLENGTH OF ZONE 4 = ,F5.2/
     110X,5HX4 = ,4X,6F8.3/
     110X,9HT4(X4) = ,6F8.3/
     110X,9HST4(X4)= ,6F8.3/)
      PD=TMAX-T2(1)
      IF(PD.LE.0.1)GO TO 49
      P=P+0.1
      GO TO 45
   49 PP=P+(T4(M)-T2(1))*0.1*3.49
      X=L4+0.1
      T=A*K4/PERI*(A4*COS(K4*X)-B4*SIN(K4*X))
      DELTA1=(TMAX-T)/KK3+SO+((PP/A-SIGMAY)/E2+EPSISH)*3.2+((PP/AA-SIGMA
     1Y)/E2+EPSISH)*11./16.
      WRITE(6,70)PP,DELTA1
   70 FORMAT(2F10.5)
      RETURN
      END
```

| | | | | | | | |
|---|---|---|---|---|---|---|---|
| 2890. | 4. | 60. | 29600. | 715. | 1.27 | 1.17 | 1.27 |
| 3.49 | 0.085 | 24. | 0.82 | 0.006 | 2.53 | 0.688 | |

## APPENDIX B

## COMPUTER PROGRAM FOR THE PREDICTION OF CYCLIC LOAD-DISPLACEMENT CURVES

```
      PROGRAM CYCLIC(INPUT,OUTPUT,TAPE5=INPUT,TAPE6=OUTPUT,TAPE2)
      REAL KK1,KK2,KK3,KK4,KK5,KK6,K1,K2,K3,L1,L2,L3,L
      COMMON/BOND/SIGMA(25,100),DL(100),ATCRACK,TL,MR,MP,NNN,L1,L2,L3,L,
     $SPACE,PERI,A,AA,UL1,UL2,FC,P,ADISP,DISP1,DISP2,DISP3,DISP4,DISP5,D
     $ISP6,DISP7,DISP8,AADISP1,AADISP2,AADISP3,AADISP4,AADISP5,AADISP6,A
     $ADISP7,AADISP8,D,DISP9,DISP10,AADISP9,ADISP10,JC,JC1,JC2,JC3,JC4,J
     $C5,PC1,PC2,PC3,PT1,PT2,PT3
      COMMON/LB/AT(25,100),AS(25,100),SMAX1(100),SMAX2(100),SMIN1(100),S
     $MIN2(100),KK1,KK2,KK3,KK4,KK5,KK6,AALPH,BBETA,TO,TC,SC,TMAX,SMAX,T
     $TMAX
      COMMON/STRAIN/FY,E1,E2,EPSILOY,EPSISH,ASIGMA(25,100),EPSILO(25,100
     $),SIGMAA(100),EPSILOA(100),SIGMAT(100),EPSILOT(100),EPSA(100),BETA
     $(100),ALPH(100),DSIG1(100),DSIG2(100),SIGMAT1(100),SIGMAT2(100),SI
     $GMAT3(100),SIGMAT4(100),SIGMAT5(100)
      COMMON/MONO/X(100),T(100),ST(100),T1(100),SIGMA1(100),ASIGMA1(100
     $),EPSILO1(100),AT1(100),AS1(100),K1,K2,K3
C     SIGMA : STEEL STRESS AT NODE POINT
C     D : BAR DIAMETER
C     DL : LENGTH OF SEGMENT
C     ATCRACK : AVERAGE BOND STRESS WHEN WEDGE FORMS
C     TL : PENETRATION OF BOND STRESS
C     NNN : NO OF NODE POINT
C     MP : NO OF SEGMENT
C     L : EFFECTIVE LENGTH
C     L1,L2,L3 : LENGTHS OF SEGMENTS AFTER MONOTONIC LOADING
C     SPACE : LUG SPACE
C     PERI : PERIMETER
C     A : EFFECTIVE BAR AREA
C     AA : GROSS BAR AREA
C     UL1 : LENGTH OF THE BAR OUTSIDE THE CONCRETE
C     UL2 : DEPTH OF THE WEDGE AT THE ATTACK END
C     FC : CONCRETE STRENGTH
C     P : LOADING
C     ADISP : DISPLACEMENT
C     DISP1-DISP8 : SLIP LIMIT
C     AADISP1-AADISP8 : MODIFIED SLIP LIMIT TO CONTROL PROGRAM
```

```
C       AT : LOCAL BOND STRESS FOR EACH SEGMENT
C       AS : LOCAL BOND SLIP FOR EACH SEGMENT
C       SMAX1 : LARGEST + EXPERIENCED LOCAL SLIP
C       SMAX2 : SECOND LARGEST + EXPERIENCED LOCAL SLIP
C       SMIN1 : LARGEST - EXPERIENCED LOCAL SLIP
C       SECOND LARGEST - EXPE
C       SMIN2 : SECOND LARGEST - EXPERIENCED LOCAL SLIP
C       KK1-KK6 : STIFFNESSES FOR LOCAL BOND STRESS-SLIP CURVE
C       TO : LOCAL BOND STRESS FOR CUT-OFF
C       TC : LOCAL BOND STRESS INDUCES DIAGONAL CRACKING
C       SC : LOCAL BOND SLIP CORRESPONDING TO TC
C       TMAX : MAX LOCAL BOND STRESS
C       SMAX : LOCAL SLIP CORRESPONDING TO TMAX
C       TTMAX : MODIFIED TMAX FOR CYCLIC CURVE
C       FY : YIELD STRESS
C       E1 : STIFFNESS FOR ELASTIC RANGE
C       E2 : STIFFNESS FOR STRAIN-HARDENING
C       EPSILOY : YIELD STRAIN
C       EPSISH : STRAIN WHERE STRAIN-HARDENING OCCURS
C       ASIGMA : AVERAGE STEEL STRESS
C       EPSILO : STEEL STRAIN
C       SIGMAA : MAX EXPERIENCED STRESS
C       EPSILOA : STRAIN CORRESPONDING TO SIGMAA
C       SIGMAT : TRANSITION STRESS IN REVERSED LOADING
C       EPSILOT : RANSITION STRAIN IN REVERSED LOADING
C       SIGMAT1-SIGMAT5 : TRANSITION STRESSES IN FOLLOWING CYCLES
C       K,M,N, : NO. OF SEGMENTS FOR L1,L2,L3
C       JC1-JC5 : THE LAST HALF CYCLE NO. FOR EACH SLIP
C       JC : NO. OF HALF CYCLES TO BE PRINTED OUT
C       JT : THE LAST HALF CYCLE NO. FOR PREVIOUS SLIP USED
        READ(5,100)A1,B1,A2,B2,A3,B3,L1,L2,L3,L,UL1,UL2,KK1,KK2,KK3,K1,K2,
       1K3,TO,TC,SC,TMAX,SMAX,SPACE,PERI,A,AA,D,FY,FC,E1,E2,EPSISH,DP1,DP2
       1,DP3,PC1,PC2,PC3,PT1,PT2,PT3,DISP1,DISP2,DISP3,DISP4,DISP5,DISP6,D
       1ISP7,DISP8,DISP9,DISP10
  100 FORMAT(8F10.5)
        READ(5,101)K,M,N,JC1,JC2,JC3,JC4,JC5,JC,JT
```



```
  101 FORMAT(10I8)
        WRITE(6,500)A1,B1,A2,B2,A3,B3,L1,L2,L3,L,UL1,UL2,KK1,KK2,KK3,K1,K2
       1,K3,TO,TC,SC,TMAX,SMAX,SPACE,PERI,A,AA,D,FY,FC,E1,E2,EPSISH,DP1,DP
       12,DP3,PC1,PC2,PC3,PT1,PT2,PT3,DISP1,DISP2,DISP3,DISP4,DISP5,DISP6,
       1DISP7,DISP8,DISP9,DISP10
  500 FORMAT(1H1,10X,*MATERIAL PROPERTIES AND DATA OBTAINED IN MONOTONIC
       1 LOADING PROGRAM :*/,5(10X,10F12.5//),10X,2F12.5)
        WRITE(6,501)K,M,N,JC1,JC2,JC3,JC4,JC5,JC,JT
  501 FORMAT(10X,10I12)
        IF(JT.GT.1)GO TO 102
        EPSILOY=FY/E1
        AADISP1=DISP1-DP1
        AADISP3=DISP3-DP2
        AADISP5=DISP5-DP3
        AADISP7=DISP7-DP3
        AADISP9=DISP9-DP3
        AADISP2=DISP2+DP1
        AADISP4=DISP4+DP2
        AADISP6=DISP6+DP3
        AADISP8=DISP8+DP3
        ADISP10=DISP10+DP3
        TL=L1+L2+L3+SPACE
        MR=0
        DO 11 J=1,25
        DO 11 I=1,100
        AT(J,I)=0
        AS(J,I)=0
        SIGMA(J,I)=0
        ASIGMA(J,I)=0
        EPSILO(J,I)=0
   11 CONTINUE
        DO 15 I=1,100
        SMAX1(I)=0
        SMAX2(I)=0
        SMIN1(I)=0
        SMIN2(I)=0
```

```
      SIGMAT(I)=0
      EPSILOT(I)=0
      EPSILOA(I)=0
      DL(I)=0
      EPSA(I)=0
      BETA(I)=0
      ALPH(I)=0
      DSIG1(I)=0
      DSIG2(I)=0
      SIGMAT1(I)=0
      SIGMAT2(I)=0
      SIGMAT3(I)=0
      SIGMAT4(I)=0
      SIGMAT5(I)=0
   15 CONTINUE
      X(1)=0
      IF(L1.EQ.0.)GO TO 51
      KK=K+1
      DO 1 I=1,KK
      T(I)=A*K1/PERI*(A1*EXP(K1*X(I))-B1*EXP(-K1*X(I)))
      ST(I)=A1*EXP(K1*X(I))+B1*EXP(-K1*X(I))
    1 X(I+1)=X(I)+L1/K
      IF(L2.EQ.0.)NNN=KK
      IF(L2.EQ.0.)GO TO 21
      MM=KK+1
      X(MM)=L2/M
   51 IF(L1.EQ.0.)MM=1
      MMM=K+M+1
      DO 2 I=MM,MMM
      T(I)=A*K2/PERI*(A2*EXP(K2*X(I))-B2*EXP(-K2*X(I)))
      IF(T(MM).LE.TC)GO TO 10
      ST(I)=A2*EXP(K2*X(I))+B2*EXP(-K2*X(I))
      GO TO 2
   10 ST(I)=A2*EXP(K2*X(I))+B2*EXP(-K2*X(I))+(FY-E2*EPSISH)
    2 X(I+1)=X(I)+L2/M
```



```
      IF(L3.EQ.0.)NNN=MMM
      IF(L3.EQ.0.)GO TO 21
      NN=MMM+1
      X(NN)=L3/N
      NNN=K+M+N+1
      DO 3 I=NN,NNN
      T(I)=A*K3/PERI*(A3*EXP(K3*X(I))-B3*EXP(-K3*X(I)))
      ST(I)=A3*EXP(K3*X(I))+B3*EXP(-K3*X(I))+(FY-E2*EPSISH)
    3 X(I+1)=X(I)+L3/N
   21 NNNN=NNN+1
      DO 4 I=1,NNN
      J=NNNN-I
      T1(I)=T(J)
    4 SIGMA1(I)=ST(J)
      IF(TL.LE.L)601,602
  601 T1(NNN)=TO
      T1(NNNN)=TO
      SIGMA1(NNNN)=0
      GO TO 603
  602 TL=L
      NNN=NNN-1
      NNNN=NNN+1
  603 MP=NNN
      DO 6 I=1,MP
      AT1(I)=(T1(I+1)+T1(I))/2.
      ASIGMA1(I)=(SIGMA1(I+1)+SIGMA1(I))/2.
      IF(AT1(I).LE.TC)AS1(I)=AT1(I)/KK1
      IF(AT1(I).GT.TC)AS1(I)=(AT1(I)-TC)/KK2+SC
      IF(ASIGMA1(I).LE.FY)EPSILO1(I)=ASIGMA1(I)/E1
    6 IF(ASIGMA1(I).GT.FY)EPSILO1(I)=(ASIGMA1(I)-FY)/E2+EPSISH
      N1=N+1
      MN=M+N
      MN1=MN+1
      KMN=K+M+N
      IF(L2.EQ.0.)GO TO 22
      IF(L3.EQ.0.)GO TO 23
```

```
      DO 7 I=1,N
    7 DL(I)=L3/N
   23 DO 8 I=N1,MN
    8 DL(I)=L2/M
      IF(L1.EQ.0.)GO TO 52
   22 DO 9 I=MN1,KMN
    9 DL(I)=L1/K
      IF(KMN.NE.NNN)DL(NNN)=SPACE
   52 ATCRACK=12.5664*SQRT(FC)*(UL2+D)/PERI/1000.
      J=1
      DO 5 I=1,NNN
      AT(J,I)=AT1(I)
      AS(J,I)=AS1(I)
      SIGMA(J,I)=SIGMA1(I)
      ASIGMA(J,I)=ASIGMA1(I)
      EPSILO(J,I)=EPSILO1(I)
    5 CONTINUE
      ASIGMA(J,99)=SIGMA1(1)*A/AA
      IF(ASIGMA(J,99).LE.FY)EPSILO(J,99)=ASIGMA(J,99)/E1
      IF(ASIGMA(J,99).GT.FY)EPSILO(J,99)=(ASIGMA(J,99)-FY)/E2+EPSISH
      ASIGMA(J,100)=SIGMA1(1)
      IF(ASIGMA(J,100).LE.FY)EPSILO(J,100)=ASIGMA(J,100)/E1
      IF(ASIGMA(J,100).GT.FY)EPSILO(J,100)=(ASIGMA(J,100)-FY)/E2+EPSISH
      WRITE(6,200)(AT(J,I),I=1,NNN),(AS(J,I),I=1,NNN),(SIGMA(J,I),I=1,NN
     1NN),(ASIGMA(J,I),I=1,NNN),(EPSILO(J,I),I=1,NNN)
  200 FORMAT(1H1,10X,*BOND STRESS DISTRIBUTION BEFORE UNLOADING :*/,5(10
     1X,10F10.4/),
     110X,*LOCAL SLIP DISTRIBUTION BEFORE UNLOADING :*/,5(10X,10F10.7/),
     210X,*STEEL STRESS DISTRIBUTION BEFORE UNLOADING :*/,5(10X,10F10.4/
     3),10X,F10.4/,
     110X,*AVERAGE STEEL STRESS DISTRIBUTION BEFORE UNLOADING : */,5(10X
     1,10F10.4/),
     410X,*STEEL STRAIN DISTRIBUTION BEFORE UNLOADING :*/,5(10X,10F10.7/
     4),///)
  102 WRITE(6,300)
  300 FORMAT(1H1,*THE FOLLOWING ARE THEORECTICAL RESULTS : *///)
```



```
      IF(JT.EQ.1)77,103
  103 READ(2)((SIGMA(J,I),I=1,100),J=1,25),(DL(I),I=1,100),ATCRACK,TL,MR
     1,NNN,AADISP1,AADISP2,AADISP3,AADISP4,AADISP5,AADISP6,AADISP7,AADIS
     1P8,AADISP9,ADISP10,((AT(J,I),I=1,100),J=1,25),((AS(J,I),I=1,100),J
     1=1,25),(SMAX1(I),I=1,100),(SMAX2(I),I=1,100),(SMIN1(I),I=1,100),(S
     1MIN2(I),I=1,100),EPSILOY,((ASIGMA(J,I),I=1,100),J=1,25),((EPSILO(J
     1,I),I=1,100),J=1,25),(SIGMAA(I),I=1,100),(EPSILOA(I),I=1,100),(SIG
     1MAT(I),I=1,100),(EPSILOT(I),I=1,100),(EPSA(I),I=1,100),(BETA(I),I=
     11,100),(ALPH(I),I=1,100),(DSIG1(I),I=1,100),(DSIG2(I),I=1,100),(SI
     1GMAT1(I),I=1,100),(SIGMAT2(I),I=1,100),(SIGMAT3(I),I=1,100),(SIGMA
     1T4(I),I=1,100),(SIGMAT5(I),I=1,100)
      REWIND 2
      J=JT
      AADISP1=DISP1-DP1
      AADISP3=DISP3-DP2
      AADISP5=DISP5-DP3
      AADISP7=DISP7-DP3
      AADISP9=DISP9-DP3
      AADISP2=DISP2+DP1
      AADISP4=DISP4+DP2
      AADISP6=DISP6+DP3
      AADISP8=DISP8+DP3
      ADISP10=DISP10+DP3
      GO TO 104
   77 DO 18 I=1,NNN
      IF(AS(J,I).GT.SMAX1(I))40,18
   40 SMAX2(I)=SMAX1(I)
      SMAX1(I)=AS(J,I)
   18 CONTINUE
      DO 19 I=1,NNN
      IF(SIGMAA(I).GE.-FY.AND.ASIGMA(J,I).GT.SIGMAA(I))41,19
   41 SIGMAA(I)=ASIGMA(J,I)
      EPSILOA(I)=EPSILO(J,I)
   19 CONTINUE
      DO 199 I=99,100
      IF(SIGMAA(I).GE.-FY.AND.ASIGMA(J,I).GT.SIGMAA(I))411,199
```

```
411 SIGMAA(I)=ASIGMA(J,I)
    EPSILOA(I)=EPSILO(J,I)
199 CONTINUE
104 J=J+1
    IF(J.GE.JC)GO TO 99
    CALL CASEU1(J)
    IF(J.LT.JC1.AND.ADISP.LT.DISP2)GO TO 78
    IF(J.GE.JC1.AND.J.LT.JC2.AND.ADISP.LT.DISP4)GO TO 78
    IF(J.GE.JC2.AND.J.LT.JC3.AND.ADISP.LT.DISP6)GO TO 78
    IF(J.GE.JC3.AND.J.LT.JC4.AND.ADISP.LT.DISP8)GO TO 78
    IF(J.GE.JC4.AND.J.LT.JC5.AND.ADISP.LT.DISP10)GO TO 78
 12 CALL CASEU2(J)
    IF(J.LT.JC1.AND.ADISP.LT.DISP2)GO TO 78
    IF(J.GE.JC1.AND.J.LT.JC2.AND.ADISP.LT.DISP4)GO TO 78
    IF(J.GE.JC2.AND.J.LT.JC3.AND.ADISP.LT.DISP6)GO TO 78
    IF(J.GE.JC3.AND.J.LT.JC4.AND.ADISP.LT.DISP8)GO TO 78
    IF(J.GE.JC4.AND.J.LT.JC5.AND.ADISP.LT.DISP10)GO TO 78
    IF(AT(J,NNN).LT.-ATCRACK)GO TO 79
    CALL CASEU3(J)
    IF(J.LT.JC1.AND.ADISP.LT.DISP2)GO TO 78
    IF(J.GE.JC1.AND.J.LT.JC2.AND.ADISP.LT.DISP4)GO TO 78
    IF(J.GE.JC2.AND.J.LT.JC3.AND.ADISP.LT.DISP6)GO TO 78
    IF(J.GE.JC3.AND.J.LT.JC4.AND.ADISP.LT.DISP8)GO TO 78
    IF(J.GE.JC4.AND.J.LT.JC5.AND.ADISP.LT.DISP10)GO TO 78
    IF(TL.GE.L)GO TO 12
 79 CALL CASEU4(J)
 78 DO 17 I=1,NNN
    IF(AS(J,I).LT.SMIN1(I))30,17
 30 SMIN2(I)=SMIN1(I)
    SMIN1(I)=AS(J,I)
 17 CONTINUE
    DO 20 I=1,NNN
    IF(SIGMAA(I).LE.FY.AND.ASIGMA(J,I).LT.SIGMAA(I))31,20
 31 SIGMAA(I)=ASIGMA(J,I)
    EPSILOA(I)=EPSILO(J,I)
    IF(SIGMAA(I).LT.-FY)GO TO 98
```



```
 20 CONTINUE
    J=J+1
    CALL CASER1(J)
    IF(J.LT.JC1.AND.ADISP.GT.DISP1)GO TO 77
    IF(J.GE.JC1.AND.J.LT.JC2.AND.ADISP.GT.DISP3)GO TO 77
    IF(J.GE.JC2.AND.J.LT.JC3.AND.ADISP.GT.DISP5)GO TO 77
    IF(J.GE.JC3.AND.J.LT.JC4.AND.ADISP.GT.DISP7)GO TO 77
    IF(J.GE.JC4.AND.J.LE.JC5.AND.ADISP.GT.DISP9)GO TO 77
 14 CALL CASER2(J)
    IF(J.LT.JC1.AND.ADISP.GT.DISP1)GO TO 77
    IF(J.GE.JC1.AND.J.LT.JC2.AND.ADISP.GT.DISP3)GO TO 77
    IF(J.GE.JC2.AND.J.LT.JC3.AND.ADISP.GT.DISP5)GO TO 77
    IF(J.GE.JC3.AND.J.LT.JC4.AND.ADISP.GT.DISP7)GO TO 77
    IF(J.GE.JC4.AND.J.LE.JC5.AND.ADISP.GT.DISP9)GO TO 77
    CALL CASER3(J)
    IF(J.LT.JC1.AND.ADISP.GT.DISP1)GO TO 77
    IF(J.GE.JC1.AND.J.LT.JC2.AND.ADISP.GT.DISP3)GO TO 77
    IF(J.GE.JC2.AND.J.LT.JC3.AND.ADISP.GT.DISP5)GO TO 77
    IF(J.GE.JC3.AND.J.LT.JC4.AND.ADISP.GT.DISP7)GO TO 77
    IF(J.GE.JC4.AND.J.LE.JC5.AND.ADISP.GT.DISP9)GO TO 77
    IF(TL.GE.L)GO TO 14
 98 WRITE(6,400)(SIGMAA(I),I=1,NNN)
400 FORMAT(10X,*SOME SEGMENTS YIELD IN COMPRESSION FIRST, USE ANOTHER
   1SET OF STRESS_STRAIN CURVES, OR MODIFY SEGMENT LENGTH :*/,5(10X,10
   1F10.4/))
 99 WRITE(2)((SIGMA(J,I),I=1,100),J=1,25),(DL(I),I=1,100),ATCRACK,TL,M
   1R,NNN,AADISP1,AADISP2,AADISP3,AADISP4,AADISP5,AADISP6,AADISP7,AADI
   1SP8,AADISP9,ADISP10,((AT(J,I),I=1,100),J=1,25),((AS(J,I),I=1,100),
   1J=1,25),(SMAX1(I),I=1,100),(SMAX2(I),I=1,100),(SMIN1(I),I=1,100),(
   1SMIN2(I),I=1,100),EPSILOY,((ASIGMA(J,I),I=1,100),J=1,25),((EPSILO(
   1J,I),I=1,100),J=1,25),(SIGMAA(I),I=1,100),(EPSILOA(I),I=1,100),(SI
   1GMAT(I),I=1,100),(EPSILOT(I),I=1,100),(EPSA(I),I=1,100),(BETA(I),I
   1=1,100),(ALPH(I),I=1,100),(DSIG1(I),I=1,100),(DSIG2(I),I=1,100),(S
   1IGMAT1(I),I=1,100),(SIGMAT2(I),I=1,100),(SIGMAT3(I),I=1,100),(SIGM
   1AT4(I),I=1,100),(SIGMAT5(I),I=1,100)
    END FILE 2
```

```
      STOP
      END
```



```
      SUBROUTINE CASEU1(J)
      REAL KK1,KK2,KK3,KK4,KK5,KK6,K1,K2,K3,L1,L2,L3,L
      COMMON/BOND/SIGMA(25,100),DL(100),ATCRACK,TL,MR,MP,NNN,L1,L2,L3,L,
     $SPACE,PERI,A,AA,UL1,UL2,FC,P,ADISP,DISP1,DISP2,DISP3,DISP4,DISP5,D
     $ISP6,DISP7,DISP8,AADISP1,AADISP2,AADISP3,AADISP4,AADISP5,AADISP6,A
     $ADISP7,AADISP8,D,DISP9,DISP10,AADISP9,ADISP10,JC,JC1,JC2,JC3,JC4,J
     $C5,PC1,PC2,PC3,PT1,PT2,PT3
      COMMON/LB/AT(25,100),AS(25,100),SMAX1(100),SMAX2(100),SMIN1(100),S
     $MIN2(100),KK1,KK2,KK3,KK4,KK5,KK6,AALPH,BBETA,TO,TC,SC,TMAX,SMAX,T
     $TMAX
      COMMON/STRAIN/FY,E1,E2,EPSILOY,EPSISH,ASIGMA(25,100),EPSILO(25,100
     $),SIGMAA(100),EPSILOA(100),SIGMAT(100),EPSILOT(100),EPSA(100),BETA
     $(100),ALPH(100),DSIG1(100),DSIG2(100),SIGMAT1(100),SIGMAT2(100),SI
     $GMAT3(100),SIGMAT4(100),SIGMAT5(100)
      DO 1 I=1,NNN
      AT(J,I)=AT(J-1,I)
      AS(J,I)=AS(J-1,I)
      EPSILO(J,I)=EPSILO(J-1,I)
    1 SIGMA(J,I)=SIGMA(J-1,I)
      I1=0
    4 I1=I1+5
      I=I1
      IF(I.GE.NNN)GO TO 99
      AT(J,I)=AT(J,I)-0.05*AT(J,I)
      AS(J,I)=AS(J-1,I)-(AT(J-1,I)-AT(J,I))/KK4
    2 CALL LOCAL(J,I)
      SIGMA(J,I)=AT(J,I)*DL(I)*PERI/A+SIGMA(J,I+1)
      ASIGMA(J,I)=(SIGMA(J,I)+SIGMA(J,I+1))/2.
      CALL STEEL(J,I)
      IF(I.EQ.1)GO TO 3
      AS(J,I-1)=AS(J,I)+EPSILO(J,I)*DL(I)
      I=I-1
      GO TO 2
    3 ADISP2=AS(J,I)+EPSILO(J,I)*DL(I)
      I3=100
      ASIGMA(J,I3)=SIGMA(J,I)
```

```
      CALL STEEL(J,I3)
      ADISP1=ADISP2+EPSILO(J,I3)*UL2
      I2=99
      ASIGMA(J,I2)=SIGMA(J,I)*A/AA
      CALL STEEL(J,I2)
      P=SIGMA(J,I)*A
      ADISP=ADISP1+UL1*EPSILO(J,I2)
      NNNN=NNN+1
      WRITE(6,200)P,ADISP
  200 FORMAT(6X,4H****,*FORCE = *,F10.6/
     110X,*DISPLACEMENT = *,F9.5/)
      WRITE(6,201)
  201 FORMAT(10X,*BOND STRESS DISTRIBUTION :*)
      WRITE(6,202)(AT(J,I),I=1,NNN)
  202 FORMAT(10X,10F10.4)
      WRITE(6,203)
  203 FORMAT(10X,*STEEL STRESS DISTRIBUTION :*)
      WRITE(6,204)(SIGMA(J,I),I=1,NNNN)
  204 FORMAT(10X,10F10.4)
      IF(J.LT.JC1.AND.ADISP.LT.DISP2)GO TO 99
      IF(J.GE.JC1.AND.J.LT.JC2.AND.ADISP.LT.DISP4)GO TO 99
      IF(J.GE.JC2.AND.J.LT.JC3.AND.ADISP.LT.DISP6)GO TO 99
      IF(J.GE.JC3.AND.J.LT.JC4.AND.ADISP.LT.DISP8)GO TO 99
      IF(J.GE.JC4.AND.J.LT.JC5.AND.ADISP.LT.DISP10)GO TO 99
      GO TO 4
   99 RETURN
      END
```



```
      SUBROUTINE CASEU2(J)
      REAL KK1,KK2,KK3,KK4,KK5,KK6,K1,K2,K3,L1,L2,L3,L
      COMMON/BOND/SIGMA(25,100),DL(100),ATCRACK,TL,MR,MP,NNN,L1,L2,L3,L,
     $SPACE,PERI,A,AA,UL1,UL2,FC,P,ADISP,DISP1,DISP2,DISP3,DISP4,DISP5,D
     $ISP6,DISP7,DISP8,AADISP1,AADISP2,AADISP3,AADISP4,AADISP5,AADISP6,A
     $ADISP7,AADISP8,D,DISP9,DISP10,AADISP9,ADISP10,JC,JC1,JC2,JC3,JC4,J
     $C5,PC1,PC2,PC3,PT1,PT2,PT3
      COMMON/LB/AT(25,100),AS(25,100),SMAX1(100),SMAX2(100),SMIN1(100),S
     $MIN2(100),KK1,KK2,KK3,KK4,KK5,KK6,AALPH,BBETA,TO,TC,SC,TMAX,SMAX,T
     $TMAX
      COMMON/STRAIN/FY,E1,E2,EPSILOY,EPSISH,ASIGMA(25,100),EPSILO(25,100
     $),SIGMAA(100),EPSILOA(100),SIGMAT(100),EPSILOT(100),EPSA(100),BETA
     $(100),ALPH(100),DSIG1(100),DSIG2(100),SIGMAT1(100),SIGMAT2(100),SI
     $GMAT3(100),SIGMAT4(100),SIGMAT5(100)
    4 I=NNN
      IF(J.LT.JC1)GO TO 41
      IF(J.GE.JC1.AND.J.LT.JC2)GO TO 42
      IF(J.GE.JC2.AND.J.LT.JC3)GO TO 43
      IF(J.GE.JC3.AND.J.LT.JC4)GO TO 44
      IF(J.GE.JC4.AND.J.LT.JC5)GO TO 45
   41 IF(ADISP.LT.AADISP2.OR.P.LT.PC1)51,52
   51 AS(J,I)=AS(J,I)-0.0000125
      GO TO 7
   52 AS(J,I)=AS(J,I)-0.0002
      GO TO 7
   42 IF(ADISP.LT.AADISP4.OR.P.LT.PC2)51,52
   43 IF(ADISP.LT.AADISP6.OR.P.LT.PC3)51,52
   44 IF(ADISP.LT.AADISP8.OR.P.LT.PC3)51,52
   45 IF(ADISP.LT.ADISP10.OR.P.LT.PC3)51,52
    7 IF(TL.LT.L)9,10
    9 AT(J,I)=AS(J,I)*KK1
      IF(AT(J,I).LT.-TO)GO TO 99
      GO TO 1
   10 CALL LOCAL(J,I)
    1 SIGMA(J,I)=AT(J,I)*DL(I)*PERI/A+SIGMA(J,I+1)
      ASIGMA(J,I)=(SIGMA(J,I)+SIGMA(J,I+1))/2.
```

```
      CALL STEEL(J,I)
      IF(I.EQ.1)GO TO 3
      AS(J,I-1)=AS(J,I)+EPSILO(J,I)*DL(I)
      I=I-1
      GO TO 10
    3 ADISP2=AS(J,I)+EPSILO(J,I)*DL(I)
      I3=100
      ASIGMA(J,I3)=SIGMA(J,I)
      CALL STEEL(J,I3)
      ADISP1=ADISP2+EPSILO(J,I3)*UL2
      I2=99
      ASIGMA(J,I2)=SIGMA(J,I)*A/AA
      CALL STEEL(J,I2)
      P=SIGMA(J,I)*A
      ADISP=ADISP1+UL1*EPSILO(J,I2)
      NNNN=NNN+1
      WRITE(6,200)P,ADISP
  200 FORMAT(6X,4H****,*FORCE = *,F10.6/
     110X,*DISPLACEMENT = *,F9.5/)
      WRITE(6,201)
  201 FORMAT(10X,*BOND STRESS DISTRIBUTION :*)
      WRITE(6,202)(AT(J,I),I=1,NNN)
  202 FORMAT(10X,10F10.4)
      WRITE(6,203)
  203 FORMAT(10X,*STEEL STRESS DISTRIBUTION :*)
      WRITE(6,204)(SIGMA(J,I),I=1,NNNN)
  204 FORMAT(10X,10F10.4)
      IF(J.LT.JC1.AND.ADISP.LT.DISP2)GO TO 99
      IF(J.GE.JC1.AND.J.LT.JC2.AND.ADISP.LT.DISP4)GO TO 99
      IF(J.GE.JC2.AND.J.LT.JC3.AND.ADISP.LT.DISP6)GO TO 99
      IF(J.GE.JC3.AND.J.LT.JC4.AND.ADISP.LT.DISP8)GO TO 99
      IF(J.GE.JC4.AND.J.LT.JC5.AND.ADISP.LT.DISP10)GO TO 99
      IF(MR.EQ.0)11,4
   11 IF(AT(J,NNN).LE.-ATCRACK)12,4
   12 I=NNN
      AL=L-UL2
```



```
      AAL=L
   15 AAL=AAL-DL(I)
      IF(AAL.LE.AL)13,14
   14 I=I-1
      GO TO 15
   13 NNN=I-1
      SIGMA(J,NNN+1)=0
      WRITE(6,300)
  300 FORMAT(1H1,*WEDGE AT DEAD END HAS DROPPED *,//)
   99 RETURN
      END
```

```
      SUBROUTINE CASEU3(J)
      REAL KK1,KK2,KK3,KK4,KK5,KK6,K1,K2,K3,L1,L2,L3,L
      COMMON/BOND/SIGMA(25,100),DL(100),ATCRACK,TL,MR,MP,NNN,L1,L2,L3,L,
     $SPACE,PERI,A,AA,UL1,UL2,FC,P,ADISP,DISP1,DISP2,DISP3,DISP4,DISP5,D
     $ISP6,DISP7,DISP8,AADISP1,AADISP2,AADISP3,AADISP4,AADISP5,AADISP6,A
     $ADISP7,AADISP8,D,DISP9,DISP10,AADISP9,ADISP10,JC,JC1,JC2,JC3,JC4,J
     $C5,PC1,PC2,PC3,PT1,PT2,PT3
      COMMON/LB/AT(25,100),AS(25,100),SMAX1(100),SMAX2(100),SMIN1(100),S
     $MIN2(100),KK1,KK2,KK3,KK4,KK5,KK6,AALPH,BBETA,TO,TC,SC,TMAX,SMAX,T
     $TMAX
      COMMON/STRAIN/FY,E1,E2,EPSILOY,EPSISH,ASIGMA(25,100),EPSILO(25,100
     $),SIGMAA(100),EPSILOA(100),SIGMAT(100),EPSILOT(100),EPSA(100),BETA
     $(100),ALPH(100),DSIG1(100),DSIG2(100),SIGMAT1(100),SIGMAT2(100),SI
     $GMAT3(100),SIGMAT4(100),SIGMAT5(100)
      DDL=0.1
      I=NNN
      AT(J,I)=-TO
      AS(J,I)=AT(J,I)/KK1
      GO TO 1
    4 NNN=NNN+1
      I=NNN
      AT(J,I)=-TO
      AS(J,I)=AT(J,I)/KK1
      DL(I)=DDL
      TL=TL+DL(I)
      IF(TL.GE.L)GO TO 8
      GO TO 1
   10 CALL LOCAL(J,I)
    1 SIGMA(J,I)=AT(J,I)*DL(I)*PERI/A+SIGMA(J,I+1)
      ASIGMA(J,I)=(SIGMA(J,I)+SIGMA(J,I+1))/2.
      CALL STEEL(J,I)
      IF(I.EQ.1)GO TO 3
      AS(J,I-1)=AS(J,I)+EPSILO(J,I)*DL(I)
      I=I-1
      GO TO 10
    3 ADISP2=AS(J,I)+EPSILO(J,I)*DL(I)
```



```
      I3=100
      ASIGMA(J,I3)=SIGMA(J,I)
      CALL STEEL(J,I3)
      ADISP1=ADISP2+EPSILO(J,I3)*UL2
      I2=99
      ASIGMA(J,I2)=SIGMA(J,I)*A/AA
      CALL STEEL(J,I2)
      P=SIGMA(J,I)*A
      ADISP=ADISP1+UL1*EPSILO(J,I2)
      NNNN=NNN+1
      WRITE(6,200)P,ADISP
  200 FORMAT(6X,4H****,*FORCE = *,F10.6/
     110X,*DISPLACEMENT = *,F9.5/)
      WRITE(6,201)
  201 FORMAT(10X,*BOND STRESS DISTRIBUTION :*)
      WRITE(6,202)(AT(J,I),I=1,NNN)
  202 FORMAT(10X,10F10.4)
      WRITE(6,203)
  203 FORMAT(10X,*STEEL STRESS DISTRIBUTION :*)
      WRITE(6,204)(SIGMA(J,I),I=1,NNNN)
  204 FORMAT(10X,10F10.4)
      IF(J.LT.JC1.AND.ADISP.LT.DISP2)GO TO 99
      IF(J.GE.JC1.AND.J.LT.JC2.AND.ADISP.LT.DISP4)GO TO 99
      IF(J.GE.JC2.AND.J.LT.JC3.AND.ADISP.LT.DISP6)GO TO 99
      IF(J.GE.JC3.AND.J.LT.JC4.AND.ADISP.LT.DISP8)GO TO 99
      IF(J.GE.JC4.AND.J.LT.JC5.AND.ADISP.LT.DISP10)GO TO 99
      GO TO 4
    8 DL(I)=DDL+L-TL
   99 RETURN
      END
```

```
      SUBROUTINE CASE04(J)
      REAL KK1,KK2,KK3,KK4,KK5,KK6,K1,K2,K3,L1,L2,L3,L
      COMMON/BOND/SIGMA(25,100),DL(100),ATCRACK,TL,MR,MP,NNN,L1,L2,L3,L,
     $SPACE,PERI,A,AA,UL1,UL2,FC,P,ADISP,DISP1,DISP2,DISP3,DISP4,DISP5,D
     $ISP6,DISP7,DISP8,AADISP1,AADISP2,AADISP3,AADISP4,AADISP5,AADISP6,A
     $ADISP7,AADISP8,D,DISP9,DISP10,AADISP9,ADISP10,JC,JC1,JC2,JC3,JC4,J
     $C5,PC1,PC2,PC3,PT1,PT2,PT3
      COMMON/LB/AT(25,100),AS(25,100),SMAX1(100),SMAX2(100),SMIN1(100),S
     $MIN2(100),KK1,KK2,KK3,KK4,KK5,KK6,AALPH,BBETA,TO,TC,SC,TMAX,SMAX,T
     $TMAX
      COMMON/STRAIN/FY,E1,E2,EPSILOY,EPSISH,ASIGMA(25,100),EPSILO(25,100
     $),SIGMAA(100),EPSILOA(100),SIGMAT(100),EPSILOT(100),EPSA(100),BETA
     $(100),ALPH(100),DSIG1(100),DSIG2(100),SIGMAT1(100),SIGMAT2(100),SI
     $GMAT3(100),SIGMAT4(100),SIGMAT5(100)
    4 I=NNN
      IF(MR.EQ.0)17,18
   17 AS(J,I)=AS(J,I)-0.0078
      GO TO 7
   18 IF(J.LT.JC1)GO TO 41
      IF(J.GE.JC1.AND.J.LT.JC2)GO TO 42
      IF(J.GE.JC2.AND.J.LT.JC3)GO TO 43
      IF(J.GE.JC3.AND.J.LT.JC4)GO TO 44
      IF(J.GE.JC4.AND.J.LT.JC5)GO TO 45
   41 IF(ADISP.LT.AADISP2.OR.P.LT.PC1)51,52
   51 AS(J,I)=AS(J,I)-0.0000125
      GO TO 7
   52 AS(J,I)=AS(J,I)-0.0002
      GO TO 7
   42 IF(ADISP.LT.AADISP4.OR.P.LT.PC2)51,52
   43 IF(ADISP.LT.AADISP6.OR.P.LT.PC3)51,52
   44 IF(ADISP.LT.AADISP8.OR.P.LT.PC3)51,52
   45 IF(ADISP.LT.ADISP10.OR.P.LT.PC3)51,52
    7 CALL LOCAL(J,I)
      SIGMA(J,I)=AT(J,I)*DL(I)*PERI/A+SIGMA(J,I+1)
      ASIGMA(J,I)=(SIGMA(J,I)+SIGMA(J,I+1))/2.
      CALL STEEL(J,I)
```



```
      IF(I.EQ.1)GO TO 3
      AS(J,I-1)=AS(J,I)+EPSILO(J,I)*DL(I)
      I=I-1
      GO TO 7
    3 ADISP2=AS(J,I)+EPSILO(J,I)*DL(I)
      I3=100
      ASIGMA(J,I3)=SIGMA(J,I)
      CALL STEEL(J,I3)
      ADISP1=ADISP2+EPSILO(J,I3)*UL2
      I2=99
      ASIGMA(J,I2)=SIGMA(J,I)*A/AA
      CALL STEEL(J,I2)
      P=SIGMA(J,I)*A
      ADISP=ADISP1+UL1*EPSILO(J,I2)
      NNNN=NNN+1
      WRITE(6,200)P,ADISP
  200 FORMAT(6X,4H****,*FORCE = *,F10.6/
     110X,*DISPLACEMENT = *,F9.5/)
      WRITE(6,201)
  201 FORMAT(10X,*BOND STRESS DISTRIBUTION :*)
      WRITE(6,202)(AT(J,I),I=1,NNN)
  202 FORMAT(10X,10F10.4)
      WRITE(6,203)
  203 FORMAT(10X,*STEEL STRESS DISTRIBUTION :*)
      WRITE(6,204)(SIGMA(J,I),I=1,NNNN)
  204 FORMAT(10X,10F10.4)
      IF(J.LT.JC1.AND.ADISP.LT.DISP2)GO TO 99
      IF(J.GE.JC1.AND.J.LT.JC2.AND.ADISP.LT.DISP4)GO TO 99
      IF(J.GE.JC2.AND.J.LT.JC3.AND.ADISP.LT.DISP6)GO TO 99
      IF(J.GE.JC3.AND.J.LT.JC4.AND.ADISP.LT.DISP8)GO TO 99
      IF(J.GE.JC4.AND.J.LT.JC5.AND.ADISP.LT.DISP10)GO TO 99
      MR=1
      GO TO 4
   99 MR=1
      RETURN
      END
```

```
      SUBROUTINE CASER1(J)
      REAL KK1,KK2,KK3,KK4,KK5,KK6,K1,K2,K3,L1,L2,L3,L
      COMMON/BOND/SIGMA(25,100),DL(100),ATCRACK,TL,MR,MP,NNN,L1,L2,L3,L,
     $SPACE,PERI,A,AA,UL1,UL2,FC,P,ADISP,DISP1,DISP2,DISP3,DISP4,DISP5,D
     $ISP6,DISP7,DISP8,AADISP1,AADISP2,AADISP3,AADISP4,AADISP5,AADISP6,A
     $ADISP7,AADISP8,D,DISP9,DISP10,AADISP9,ADISP10,JC,JC1,JC2,JC3,JC4,J
     $C5,PC1,PC2,PC3,PT1,PT2,PT3
      COMMON/LB/AT(25,100),AS(25,100),SMAX1(100),SMAX2(100),SMIN1(100),S
     $MIN2(100),KK1,KK2,KK3,KK4,KK5,KK6,AALPH,BBETA,TO,TC,SC,TMAX,SMAX,T
     $TMAX
      COMMON/STRAIN/FY,E1,E2,EPSILOY,EPSISH,ASIGMA(25,100),EPSILO(25,100
     $),SIGMAA(100),EPSILOA(100),SIGMAT(100),EPSILOT(100),EPSA(100),BETA
     $(100),ALPH(100),DSIG1(100),DSIG2(100),SIGMAT1(100),SIGMAT2(100),SI
     $GMAT3(100),SIGMAT4(100),SIGMAT5(100)
      DO 1 I=1,NNN
      AT(J,I)=AT(J-1,I)
      AS(J,I)=AS(J-1,I)
      EPSILO(J,I)=EPSILO(J-1,I)
    1 SIGMA(J,I)=SIGMA(J-1,I)
      I1=0
    4 I1=I1+5
      I=I1
      IF(I.GE.NNN)GO TO 99
      AT(J,I)=AT(J,I)-0.05*AT(J,I)
      AS(J,I)=AS(J-1,I)-(AT(J-1,I)-AT(J,I))/KK4
    2 CALL LOCAL(J,I)
      SIGMA(J,I)=AT(J,I)*DL(I)*PERI/A+SIGMA(J,I+1)
      ASIGMA(J,I)=(SIGMA(J,I)+SIGMA(J,I+1))/2.
      CALL STEEL(J,I)
      IF(I.EQ.1)GO TO 3
      AS(J,I-1)=AS(J,I)+EPSILO(J,I)*DL(I)
      I=I-1
      GO TO 2
    3 ADISP2=AS(J,I)+EPSILO(J,I)*DL(I)
      I3=100
      ASIGMA(J,I3)=SIGMA(J,I)
```

283

```
      CALL STEEL(J,I3)
      ADISP1=ADISP2+EPSILO(J,I3)*UL2
      I2=99
      ASIGMA(J,I2)=SIGMA(J,I)*A/AA
      CALL STEEL(J,I2)
      P=SIGMA(J,I)*A
      ADISP=ADISP1+UL1*EPSILO(J,I2)
      NNNN=NNN+1
      WRITE(6,200)P,ADISP
  200 FORMAT(6X,4H****,*FORCE = *,F10.6/
     110X,*DISPLACEMENT = *,F9.5/)
      WRITE(6,201)
  201 FORMAT(10X,*BOND STRESS DISTRIBUTION :*)
      WRITE(6,202)(AT(J,I),I=1,NNN)
  202 FORMAT(10X,10F10.4)
      WRITE(6,203)
  203 FORMAT(10X,*STEEL STRESS DISTRIBUTION :*)
      WRITE(6,204)(SIGMA(J,I),I=1,NNNN)
  204 FORMAT(10X,10F10.4)
      IF(J.LT.JC1.AND.ADISP.GT.DISP1)GO TO 99
      IF(J.GE.JC1.AND.J.LT.JC2.AND.ADISP.GT.DISP3)GO TO 99
      IF(J.GE.JC2.AND.J.LT.JC3.AND.ADISP.GT.DISP5)GO TO 99
      IF(J.GE.JC3.AND.J.LT.JC4.AND.ADISP.GT.DISP7)GO TO 99
      IF(J.GE.JC4.AND.J.LE.JC5.AND.ADISP.GT.DISP9)GO TO 99
      GO TO 4
   99 RETURN
      END
```



```
      SUBROUTINE CASER2(J)
      REAL KK1,KK2,KK3,KK4,KK5,KK6,K1,K2,K3,L1,L2,L3,L
      COMMON/BOND/SIGMA(25,100),DL(100),ATCRACK,TL,MR,MP,NNN,L1,L2,L3,L,
     $SPACE,PERI,A,AA,UL1,UL2,FC,P,ADISP,DISP1,DISP2,DISP3,DISP4,DISP5,D
     $ISP6,DISP7,DISP8,AADISP1,AADISP2,AADISP3,AADISP4,AADISP5,AADISP6,A
     $ADISP7,AADISP8,D,DISP9,DISP10,AADISP9,ADISP10,JC,JC1,JC2,JC3,JC4,J
     $C5,PC1,PC2,PC3,PT1,PT2,PT3
      COMMON/LB/AT(25,100),AS(25,100),SMAX1(100),SMAX2(100),SMIN1(100),S
     $MIN2(100),KK1,KK2,KK3,KK4,KK5,KK6,AALPH,BBETA,TO,TC,SC,TMAX,SMAX,T
     $TMAX
      COMMON/STRAIN/FY,E1,E2,EPSILOY,EPSISH,ASIGMA(25,100),EPSILO(25,100
     $),SIGMAA(100),EPSILOA(100),SIGMAT(100),EPSILOT(100),EPSA(100),BETA
     $(100),ALPH(100),DSIG1(100),DSIG2(100),SIGMAT1(100),SIGMAT2(100),SI
     $GMAT3(100),SIGMAT4(100),SIGMAT5(100)
    4 I=NNN
      IF(J.LT.JC1)GO TO 41
      IF(J.GE.JC1.AND.J.LT.JC2)GO TO 42
      IF(J.GE.JC2.AND.J.LT.JC3)GO TO 43
      IF(J.GE.JC3.AND.J.LT.JC4)GO TO 44
      IF(J.GE.JC4.AND.J.LE.JC5)GO TO 45
   41 IF(ADISP.GT.AADISP1.OR.P.GT.PT1)51,52
   51 AS(J,I)=AS(J,I)+0.0000125
      GO TO 7
   52 AS(J,I)=AS(J,I)+0.0002
      GO TO 7
   42 IF(ADISP.GT.AADISP3.OR.P.GT.PT2)51,52
   43 IF(ADISP.GT.AADISP5.OR.P.GT.PT3)51,52
   44 IF(ADISP.GT.AADISP7.OR.P.GT.PT3)51,52
   45 IF(ADISP.GT.AADISP9.OR.P.GT.PT3)51,52
    7 IF(TL.LT.L)9,10
    9 AT(J,I)=AS(J,I)*KK1
      IF(AT(J,I).GT.TO)GO TO 99
      GO TO 1
   10 CALL LOCAL(J,I)
    1 SIGMA(J,I)=AT(J,I)*DL(I)*PERI/A+SIGMA(J,I+1)
      ASIGMA(J,I)=(SIGMA(J,I)+SIGMA(J,I+1))/2.
```

```
      IF(I.EQ.1)GO TO 3
      AS(J,I-1)=AS(J,I)+EPSILO(J,I)*DL(I)
      I=I-1
      GO TO 10
    3 ADISP2=AS(J,I)+EPSILO(J,I)*DL(I)
      I3=100
      ASIGMA(J,I3)=SIGMA(J,I)
      CALL STEEL(J,I3)
      ADISP1=ADISP2+EPSILO(J,I3)*UL2
      I2=99
      ASIGMA(J,I2)=SIGMA(J,I)*A/AA
      CALL STEEL(J,I2)
      P=SIGMA(J,I)*A
      ADISP=ADISP1+UL1*EPSILO(J,I2)
      NNNN=NNN+1
      WRITE(6,200)P,ADISP
  200 FORMAT(6X,4H****,*FORCE = *,F10.6/
     110X,*DISPLACEMENT = *,F9.5/)
      WRITE(6,201)
  201 FORMAT(10X,*BOND STRESS DISTRIBUTION :*)
      WRITE(6,202)(AT(J,I),I=1,NNN)
  202 FORMAT(10X,10F10.4)
      WRITE(6,203)
  203 FORMAT(10X,*STEEL STRESS DISTRIBUTION :*)
      WRITE(6,204)(SIGMA(J,I),I=1,NNNN)
  204 FORMAT(10X,10F10.4)
      IF(J.LT.JC1.AND.ADISP.GT.DISP1)GO TO 99
      IF(J.GE.JC1.AND.J.LT.JC2.AND.ADISP.GT.DISP3)GO TO 99
      IF(J.GE.JC2.AND.J.LT.JC3.AND.ADISP.GT.DISP5)GO TO 99
      IF(J.GE.JC3.AND.J.LT.JC4.AND.ADISP.GT.DISP7)GO TO 99
      IF(J.GE.JC4.AND.J.LE.JC5.AND.ADISP.GT.DISP9)GO TO 99
      GO TO 4
   99 RETURN
      END
```



```
      SUBROUTINE CASER3(J)
      REAL KK1,KK2,KK3,KK4,KK5,KK6,K1,K2,K3,L1,L2,L3,L
      COMMON/BOND/SIGMA(25,100),DL(100),ATCRACK,TL,MR,MP,NNN,L1,L2,L3,L,
     $SPACE,PERI,A,AA,UL1,UL2,FC,P,ADISP,DISP1,DISP2,DISP3,DISP4,DISP5,D
     $ISP6,DISP7,DISP8,AADISP1,AADISP2,AADISP3,AADISP4,AADISP5,AADISP6,A
     $ADISP7,AADISP8,D,DISP9,DISP10,AADISP9,ADISP10,JC,JC1,JC2,JC3,JC4,J
     $C5,PC1,PC2,PC3,PT1,PT2,PT3
      COMMON/LB/AT(25,100),AS(25,100),SMAX1(100),SMAX2(100),SMIN1(100),S
     $MIN2(100),KK1,KK2,KK3,KK4,KK5,KK6,AALPH,BBETA,TO,TC,SC,TMAX,SMAX,T
     $TMAX
      COMMON/STRAIN/FY,E1,E2,EPSILOY,EPSISH,ASIGMA(25,100),EPSILO(25,100
     $),SIGMAA(100),EPSILOA(100),SIGMAT(100),EPSILOT(100),EPSA(100),BETA
     $(100),ALPH(100),DSIG1(100),DSIG2(100),SIGMAT1(100),SIGMAT2(100),SI
     $GMAT3(100),SIGMAT4(100),SIGMAT5(100)
      DDL1=0.25
      DDL2=0.1
      DDL3=0.03
      I=NNN
      AT(J,I)=TO
      AS(J,I)=AT(J,I)/KK1
      GO TO 1
    4 NNN=NNN+1
      I=NNN
      AT(J,I)=TO
      AS(J,I)=AT(J,I)/KK1
      DL(I)=DDL1
      IF(J.LT.JC1.AND.ADISP.GT.AADISP1)DL(I)=DDL2
      IF(J.GE.JC1.AND.J.LT.JC2.AND.ADISP.GT.AADISP3)DL(I)=DDL2
      IF(J.GE.JC2.AND.J.LT.JC3.AND.ADISP.GT.AADISP5)DL(I)=DDL2
      IF(J.GE.JC3.AND.J.LT.JC4.AND.ADISP.GT.AADISP7)DL(I)=DDL2
      IF(J.GE.JC4.AND.J.LE.JC5.AND.ADISP.GT.AADISP9)DL(I)=DDL2
      IF(DL(I).EQ.DDL2.AND.D.LE.0.75)DL(I)=DDL3
      TL=TL+DL(I)
      IF(TL.GE.L)GO TO 8
      GO TO 1
   10 CALL LOCAL(J,I)
```

```
  1 SIGMA(J,I)=AT(J,I)*DL(I)*PERI/A+SIGMA(J,I+1)
    ASIGMA(J,I)=(SIGMA(J,I)+SIGMA(J,I+1))/2.
    CALL STEEL(J,I)
    IF(I.EQ.1)GO TO 3
    AS(J,I-1)=AS(J,I)+EPSILO(J,I)*DL(I)
    I=I-1
    GO TO 10
  3 ADISP2=AS(J,I)+EPSILO(J,I)*DL(I)
    I3=100
    ASIGMA(J,I3)=SIGMA(J,I)
    CALL STEEL(J,I3)
    ADISP1=ADISP2+EPSILO(J,I3)*UL2
    I2=99
    ASIGMA(J,I2)=SIGMA(J,I)*A/AA
    CALL STEEL(J,I2)
    P=SIGMA(J,I)*A
    ADISP=ADISP1+UL1*EPSILO(J,I2)
    NNNN=NNN+1
    WRITE(6,200)P,ADISP
200 FORMAT(6X,4H****,*FORCE = *,F10.6/
   110X,*DISPLACEMENT = *,F9.5/)
    WRITE(6,201)
201 FORMAT(10X,*BOND STRESS DISTRIBUTION :*)
    WRITE(6,202)(AT(J,I),I=1,NNN)
202 FORMAT(10X,10F10.4)
    WRITE(6,203)
203 FORMAT(10X,*STEEL STRESS DISTRIBUTION :*)
    WRITE(6,204)(SIGMA(J,I),I=1,NNNN)
204 FORMAT(10X,10F10.4)
    IF(J.LT.JC1.AND.ADISP.GT.DISP1)GO TO 99
    IF(J.GE.JC1.AND.J.LT.JC2.AND.ADISP.GT.DISP3)GO TO 99
    IF(J.GE.JC2.AND.J.LT.JC3.AND.ADISP.GT.DISP5)GO TO 99
    IF(J.GE.JC3.AND.J.LT.JC4.AND.ADISP.GT.DISP7)GO TO 99
    IF(J.GE.JC4.AND.J.LE.JC5.AND.ADISP.GT.DISP9)GO TO 99
    GO TO 4
  8 DL(I)=DL(I)+L-TL

     99 RETURN
        END
```

288

289

```
      SUBROUTINE LOCAL(J,I)
      REAL KK1,KK2,KK3,KK4,KK5,KK6,K1,K2,K3,L1,L2,L3,L
      COMMON/LB/AT(25,100),AS(25,100),SMAX1(100),SMAX2(100),SMIN1(100),S
     $MIN2(100),KK1,KK2,KK3,KK4,KK5,KK6,AALPH,BBETA,TO,TC,SC,TMAX,SMAX,T
     $TMAX
      AALPH=-0.15
      KK4=3000.
      TTMAX=0.9*TMAX
      KK5=(TTMAX-TC)/(SMAX-SC)
      KK6=0.9*KK3
      J1=J-1
      DO 1 I1=1,J1
      IF(AT(I1,I).GT.TO.OR.AT(I1,I).LT.-TO)GO TO 2
    1 CONTINUE
      CALL LCASE1(J,I)
      GO TO 99
    2 IF(J.LE.2)GO TO 98
      J2=J1-1
      DO 3 I2=1,J2
      IF(AT(I2,I).GT.TO.OR.AT(I2,I).LT.-TO)GO TO 4
    3 CONTINUE
   98 IF(AT(J1,I).GT.TO)CALL LCASE2(J,I)
      IF(AT(J1,I).LT.-TO)CALL LCASE21(J,I)
      GO TO 99
    4 IF(AT(J1,I).LT.0)5,6
    5 DO 7 I3=1,J2
      IF(AT(I3,I).GT.TC)GO TO 8
    7 CONTINUE
      CALL LCASE4(J,I)
      GO TO 99
    8 CALL LCASE3(J,I)
      GO TO 99
    6 DO 9 I4=1,J2
      IF(AT(I4,I).LT.-TC)GO TO 10
    9 CONTINUE
      CALL LCASE41(J,I)
```

```
      GO TO 99
   10 CALL LCASE31(J,I)
   99 RETURN
      END
```

```
 SUBROUTINE LCASE2(J,I)
 REAL KK1,KK2,KK3,KK4,KK5,KK6,K1,K2,K3,L1,L2,L3,L
 COMMON/LB/AT(25,100),AS(25,100),SMAX1(100),SMAX2(100),SMIN1(100),S
$MIN2(100),KK1,KK2,KK3,KK4,KK5,KK6,AALPH,BBETA,TO,TC,SC,TMAX,SMAX,T
$TMAX
 ASA=AS(J-1,I)-(1-AALPH)*AT(J-1,I)/KK4
 ASB=AALPH*AT(J-1,I)/KK1
 IF(AS(J,I).GT.ASA.AND.AS(J,I).LE.AS(J-1,I))AT(J,I)=AT(J-1,I)-(AS(J
1-1,I)-AS(J,I))*KK4
 IF(AS(J,I).GT.ASB.AND.AS(J,I).LE.ASA)AT(J,I)=AALPH*AT(J-1,I)
 IF(AS(J,I).GT.-SC.AND.AS(J,I).LE.ASB)AT(J,I)=AS(J,I)*KK1
 IF(AS(J,I).GT.-SMAX.AND.AS(J,I).LE.-SC)AT(J,I)=(AS(J,I)+SC)*KK2-TC
 RETURN
 END
```

293

```
 SUBROUTINE LCASE1(J,I)
 REAL KK1,KK2,KK3,KK4,KK5,KK6,K1,K2,K3,L1,L2,L3,L
 COMMON/LB/AT(25,100),AS(25,100),SMAX1(100),SMAX2(100),SMIN1(100),S
$MIN2(100),KK1,KK2,KK3,KK4,KK5,KK6,AALPH,BBETA,TO,TC,SC,TMAX,SMAX,T
$TMAX
 IF(AS(J,I).GE.-SC.AND.AS(J,I).LE.SC)AT(J,I)=AS(J,I)*KK1
 IF(AS(J,I).GT.SC.AND.AS(J,I).LE.SMAX)AT(J,I)=(AS(J,I)-SC)*KK2+TC
 IF(AS(J,I).LT.-SC.AND.AS(J,I).GE.-SMAX)AT(J,I)=(AS(J,I)+SC)*KK2-TC
 IF(AS(J,I).GT.SMAX)AT(J,I)=TMAX-(AS(J,I)-SMAX)*KK3
 IF(AS(J,I).LT.-SMAX)AT(J,I)=-TMAX-(AS(J,I)+SMAX)*KK3
 RETURN
 END
```

292

```
      SUBROUTINE LCASE21(J,I)
      REAL KK1,KK2,KK3,KK4,KK5,KK6,K1,K2,K3,L1,L2,L3,L
      COMMON/LB/AT(25,100),AS(25,100),SMAX1(100),SMAX2(100),SMIN1(100),S
     $MIN2(100),KK1,KK2,KK3,KK4,KK5,KK6,AALPH,BBETA,TO,TC,SC,TMAX,SMAX,T
     $TMAX
      ASA=AS(J-1,I)-(1-AALPH)*AT(J-1,I)/KK4
      ASB=AALPH*AT(J-1,I)/KK1
      IF(AS(J,I).GE.AS(J-1,I).AND.AS(J,I).LT.ASA)AT(J,I)=AT(J-1,I)-KK4*(
     1AS(J-1,I)-AS(J,I))
      IF(AS(J,I).GE.ASA.AND.AS(J,I).LT.ASB)AT(J,I)=AALPH*AT(J-1,I)
      IF(AS(J,I).GE.ASB.AND.AS(J,I).LT.SC)AT(J,I)=AS(J,I)*KK1
      IF(AS(J,I).GE.SC.AND.AS(J,I).LT.SMAX)AT(J,I)=(AS(J,I)-SC)*KK2+TC
      IF(AS(J,I).GE.SMAX)AT(J,I)=TMAX-(AS(J,I)-SMAX)*KK3
      RETURN
      END
```



```
      SUBROUTINE LCASE3(J,I)
      REAL KK1,KK2,KK3,KK4,KK5,KK6,K1,K2,K3,L1,L2,L3,L
      COMMON/LB/AT(25,100),AS(25,100),SMAX1(100),SMAX2(100),SMIN1(100),S
     $MIN2(100),KK1,KK2,KK3,KK4,KK5,KK6,AALPH,BBETA,TO,TC,SC,TMAX,SMAX,T
     $TMAX
      IF(AS(J-2,I).GE.SMAX1(I))1,2
    1 DSMAX=SMAX1(I)-SMAX2(I)
      IF(DSMAX.GE.0.01)3,4
    3 BBETA=0.75
      GO TO 5
    4 BBETA=0.9-(SMAX1(I)-SMAX2(I))*15.
      GO TO 5
    2 BBETA=0.9
    5 ASA=AS(J-1,I)-(1-AALPH)*AT(J-1,I)/KK4
      ATB=AALPH*AT(J-1,I)
      ASB=AS(J-1,I)-AT(J-1,I)/KK4+0.65*(AS(J-2,I)-AS(J-1,I))
      ATC=BBETA*AT(J-2,I)
      ASC=AS(J-2,I)-(AT(J-2,I)-ATC)/KK4
      AK=(ATC-ATB)/(ASC-ASB)
      IF(AS(J,I).GE.AS(J-1,I).AND.AS(J,I).LT.ASA)AT(J,I)=AT(J-1,I)-KK4*(
     1AS(J-1,I)-AS(J,I))
      IF(AS(J,I).GE.ASA.AND.AS(J,I).LT.ASB)AT(J,I)=AALPH*AT(J-1,I)
      IF(AS(J,I).GE.ASB)AT(J,I)=AK*(AS(J,I)-ASB)+ATB
      IF(AS(J,I).GT.SC)6,99
    6 TM2=TC+(AS(J,I)-SC)*KK5
      TM3=TTMAX-(AS(J,I)-SMAX)*KK6
      IF(AS(J,I).LE.SMAX.AND.AT(J,I).GT.TM2)AT(J,I)=TM2
      IF(AS(J,I).GT.SMAX.AND.AT(J,I).GT.TM3)AT(J,I)=TM3
   99 RETURN
      END
```

```
      SUBROUTINE LCASE31(J,I)
      REAL KK1,KK2,KK3,KK4,KK5,KK6,K1,K2,K3,L1,L2,L3,L
      COMMON/LB/AT(25,100),AS(25,100),SMAX1(100),SMAX2(100),SMIN1(100),S
     $MIN2(100),KK1,KK2,KK3,KK4,KK5,KK6,AALPH,BBETA,TO,TC,SC,TMAX,SMAX,T
     $TMAX
      IF(AS(J-2,I).LE.SMIN1(I))1,2
    1 DSMIN=SMIN1(I)-SMIN2(I)
      IF(DSMIN.LE.-0.01)3,4
    3 BBETA=0.75
      GO TO 5
    4 BBETA=0.9+(SMIN1(I)-SMIN2(I))*15.
      GO TO 5
    2 BBETA=0.9
    5 ASA=AS(J-1,I)-(1-AALPH)*AT(J-1,I)/KK4
      ATB=AALPH*AT(J-1,I)
      ASB=AS(J-1,I)-AT(J-1,I)/KK4+0.65*(AS(J-2,I)-AS(J-1,I))
      ATC=BBETA*AT(J-2,I)
      ASC=AS(J-2,I)-(AT(J-2,I)-ATC)/KK4
      AK=(ATC-ATB)/(ASC-ASB)
      IF(AS(J,I).LE.AS(J-1,I).AND.AS(J,I).GT.ASA)AT(J,I)=AT(J-1,I)-KK4*(
     1AS(J-1,I)-AS(J,I))
      IF(AS(J,I).LE.ASA.AND.AS(J,I).GT.ASB)AT(J,I)=AALPH*AT(J-1,I)
      IF(AS(J,I).LE.ASB)AT(J,I)=AK*(AS(J,I)-ASB)+ATB
      IF(AS(J,I).LT.-SC)6,99
    6 TM2=-TC+(AS(J,I)+SC)*KK5
      TM3=-TTMAX-(AS(J,I)+SMAX)*KK6
      IF(AS(J,I).GE.-SMAX.AND.AT(J,I).LT.TM2)AT(J,I)=TM2
      IF(AS(J,I).LT.-SMAX.AND.AT(J,I).LT.TM3)AT(J,I)=TM3
   99 RETURN
      END
```



```
      SUBROUTINE LCASE4(J,I)
      REAL KK1,KK2,KK3,KK4,KK5,KK6,K1,K2,K3,L1,L2,L3,L
      COMMON/LB/AT(25,100),AS(25,100),SMAX1(100),SMAX2(100),SMIN1(100),S
     $MIN2(100),KK1,KK2,KK3,KK4,KK5,KK6,AALPH,BBETA,TO,TC,SC,TMAX,SMAX,T
     $TMAX
      BBETA=0.9
      ATA=AALPH*AT(J-1,I)
      ASA=AS(J-1,I)-(1-AALPH)*AT(J-1,I)/KK4
      ATB=ATA
      ASB=AS(J-1,I)-AT(J-1,I)/KK4+0.65*(AS(J-2,I)-AS(J-1,I))
      ATC=BBETA*AT(J-2,I)
      ASC=AS(J-2,I)-(AT(J-2,I)-ATC)/KK4
      AK=(ATC-ATB)/(ASC-ASB)
      ATOP=ATA
      ASOP=ATOP/KK1
      IF(ASOP.GE.ASB)1,2
    1 IF(AS(J,I).GE.AS(J-1,I).AND.AS(J,I).LT.ASA)AT(J,I)=AT(J-1,I)-KK4*(
     1AS(J-1,I)-AS(J,I))
      IF(AS(J,I).GE.ASA.AND.AS(J,I).LT.ASB)AT(J,I)=AALPH*AT(J-1,I)
      IF(AS(J,I).GE.ASB)AT(J,I)=AK*(AS(J,I)-ASB)+ATB
      IF(AS(J,I).GT.SC)3,99
    3 TM2=TC+(AS(J,I)-SC)*KK2
      TM3=TMAX-(AS(J,I)-SMAX)*KK3
      IF(AS(J,I).LE.SMAX.AND.AT(J,I).GT.TM2)AT(J,I)=TM2
      IF(AS(J,I).GT.SMAX.AND.AT(J,I).GT.TM3)AT(J,I)=TM3
      GO TO 99
    2 IF(AS(J,I).GE.AS(J-1,I).AND.AS(J,I).LT.ASA)AT(J,I)=AT(J-1,I)-KK4*(
     1AS(J-1,I)-AS(J,I))
      IF(AS(J,I).GE.ASA.AND.AS(J,I).LT.ASB)AT(J,I)=AALPH*AT(J-1,I)
      IF(AS(J,I).GE.ASB)AT(J,I)=AK*(AS(J,I)-ASB)+ATB
      IF(AT(J,I).GT.AT(J-2,I))6,99
    6 TM1=KK1*AS(J,I)
      TM2=TC+(AS(J,I)-SC)*KK2
      TM3=TMAX-(AS(J,I)-SMAX)*KK3
      IF(AS(J,I).LE.SC.AND.AT(J,I).GT.TM1)AT(J,I)=TM1
      IF(AS(J,I).GT.SC.AND.AS(J,I).LE.SMAX.AND.AT(J,I).GT.TM2)AT(J,I)=TM
```

```
      IF(AS(J,I).GT.SMAX.AND.AT(J,I).GT.TM3)AT(J,I)=TM3
   99 RETURN
      END
```



```
      SUBROUTINE LCASE41(J,I)
      REAL KK1,KK2,KK3,KK4,KK5,KK6,K1,K2,K3,L1,L2,L3,L
      COMMON/LB/AT(25,100),AS(25,100),SMAX1(100),SMAX2(100),SMIN1(100),S
     $MIN2(100),KK1,KK2,KK3,KK4,KK5,KK6,AALPH,BBETA,TC,TC,SC,TMAX,SMAX,T
     $TMAX
      BBETA=0.9
      ATA=AALPH*AT(J-1,I)
      ASA=AS(J-1,I)-(1-AALPH)*AT(J-1,I)/KK4
      ATB=ATA
      ASB=AS(J-1,I)-AT(J-1,I)/KK4+0.65*(AS(J-2,I)-AS(J-1,I))
      ATC=BBETA*AT(J-2,I)
      ASC=AS(J-2,I)-(AT(J-2,I)-ATC)/KK4
      AK=(ATC-ATB)/(ASC-ASB)
      ATOP=ATA
      ASOP=ATOP/KK1
      IF(ASOP.LT.ASB)1,2
    1 IF(AS(J,I).LE.AS(J-1,I).AND.AS(J,I).GT.ASA)AT(J,I)=AT(J-1,I)-KK4*(
     1AS(J-1,I)-AS(J,I))
      IF(AS(J,I).LE.ASA.AND.AS(J,I).GT.ASB)AT(J,I)=AALPH*AT(J-1,I)
      IF(AS(J,I).LE.ASB)AT(J,I)=AK*(AS(J,I)-ASB)+ATB
      IF(AS(J,I).LT.-SC)3,99
    3 TM2=-TC+(AS(J,I)+SC)*KK2
      TM3=-TMAX-(AS(J,I)+SMAX)*KK3
      IF(AS(J,I).GE.-SMAX.AND.AT(J,I).LT.TM2)AT(J,I)=TM2
      IF(AS(J,I).LT.-SMAX.AND.AT(J,I).LT.TM3)AT(J,I)=TM3
      GO TO 99
    2 IF(AS(J,I).LE.AS(J-1,I).AND.AS(J,I).GT.ASA)AT(J,I)=AT(J-1,I)-KK4*(
     1AS(J-1,I)-AS(J,I))
      IF(AS(J,I).LE.ASA.AND.AS(J,I).GT.ASB)AT(J,I)=AALPH*AT(J-1,I)
      IF(AS(J,I).LE.ASB)AT(J,I)=AK*(AS(J,I)-ASB)+ATB
      IF(AT(J,I).LT.AT(J-2,I))6,99
    6 TM1=KK1*AS(J,I)
      TM2=-TC+(AS(J,I)+SC)*KK2
      TM3=-TMAX-(AS(J,I)+SMAX)*KK3
      IF(AS(J,I).GE.-SC.AND.AT(J,I).LT.TM1)AT(J,I)=TM1
      IF(AS(J,I).LT.-SC.AND.AS(J,I).GE.-SMAX.AND.AT(J,I).LT.TM2)AT(J,I)=
```

```
      IF(AS(J,I).LT.-SMAX.AND.AT(J,I).LT.TM3)AT(J,I)=TM3
   99 RETURN
      END
```

300

```
      SUBROUTINE STEEL(J,I)
      COMMON/STRAIN/FY,E1,E2,EPSILOY,EPSISH,ASIGMA(25,100),EPSILO(25,100
     $),SIGMAA(100),EPSILOA(100),SIGMAT(100),EPSILOT(100),EPSA(100),BETA
     $(100),ALPH(100),DSIG1(100),DSIG2(100),SIGMAT1(100),SIGMAT2(100),SI
     $GMAT3(100),SIGMAT4(100),SIGMAT5(100)
      J1=J-1
      DO 1 I1=1,J1
      IF(ASIGMA(I1,I).GT.FY.OR.ASIGMA(I1,I).LT.-FY)GO TO 2
    1 CONTINUE
      CALL SCASE1(J,I)
      GO TO 99
    2 DO 10 I2=1,J1
      IF(ASIGMA(I2,I).EQ.SIGMAA(I))GO TO 3
   10 CONTINUE
    3 JJ1=I2
      JJ=J-JJ1
      IF(JJ.EQ.1)CALL SCASE2(J,I)
      IF(JJ.EQ.2)CALL SCASE3(J,I)
      IF(JJ.EQ.3)CALL SCASE4(J,I)
      IF(JJ.EQ.4)CALL SCASE5(J,I)
      IF(JJ.EQ.5)CALL SCASE6(J,I)
      IF(JJ.EQ.6)CALL SCASE7(J,I)
   99 RETURN
      END
```

301

```
 COMMON/STRAIN/FY,E1,E2,EPSILOY,EPSISH,ASIGMA(25,100),EPSILO(25,100
$),SIGMAA(100),EPSILOA(100),SIGMAT(100),EPSILOT(100),EPSA(100),BETA
$(100),ALPH(100),DSIG1(100),DSIG2(100),SIGMAT1(100),SIGMAT2(100),SI
$GMAT3(100),SIGMAT4(100),SIGMAT5(100)
 SSS=(AASIGMA-FY+SIGMAA(I)-ASIGMA(J2-1,I))/(2.*FY)
 SS=ABS(SSS)
 ES=BETA(I)*(SSS-ALPH(I)*(SS**6.))
 EPRO2=EPSILO(J2-1,I)+EPSA(I)-EPSILOA(I)+2.*EPSILOY*ES
 RETURN
 END
```

302

```
 FUNCTION EPRO3(J3,I,AASIGMA)
 COMMON/STRAIN/FY,E1,E2,EPSILOY,EPSISH,ASIGMA(25,100),EPSILO(25,100
$),SIGMAA(100),EPSILOA(100),SIGMAT(100),EPSILOT(100),EPSA(100),BETA
$(100),ALPH(100),DSIG1(100),DSIG2(100),SIGMAT1(100),SIGMAT2(100),SI
$GMAT3(100),SIGMAT4(100),SIGMAT5(100)
 SSSM=(SIGMAA(I)+ASIGMA(J3-1,I)-AASIGMA-FY)/(2.*FY)
 SSM=ABS(SSSM)
 ESM=BETA(I)*(SSSM-ALPH(I)*(SSM**6.))
 EPRO3=EPSILOA(I)+EPSILO(J3-1,I)-EPSA(I)-ESM*EPSILOY*2.
 RETURN
 END
```

303

```
 COMMON/STRAIN/FY,E1,E2,EPSILOY,EPSISH,ASIGMA(25,100),EPSILO(25,100
$),SIGMAA(100),EPSILOA(100),SIGMAT(100),EPSILOT(100),EPSA(100),BETA
$(100),ALPH(100),DSIG1(100),DSIG2(100),SIGMAT1(100),SIGMAT2(100),SI
$GMAT3(100),SIGMAT4(100),SIGMAT5(100)
 SIGMAS=-FY
3 SSS=(SIGMAS-FY)/(2.*FY)
 SS=ABS(SSS)
 ES1=BETA(I)*(SSS-ALPH(I)*(SS**6.))
 ES=ES1*EPSILOY*2.+EPSA(I)
 EES1=(E16-ES)
 EEES1=ABS(EES1)
 IF(EEES1.LE.0.0001)1,2
2 SIGMAS=SIGMAS+0.01
 GO TO 3
1 TSIGMA=SIGMAS
 RETURN
 END
```



```
 SUBROUTINE SCASE1(J,I)
 COMMON/STRAIN/FY,E1,E2,EPSILOY,EPSISH,ASIGMA(25,100),EPSILO(25,100
$),SIGMAA(100),EPSILOA(100),SIGMAT(100),EPSILOT(100),EPSA(100),BETA
$(100),ALPH(100),DSIG1(100),DSIG2(100),SIGMAT1(100),SIGMAT2(100),SI
$GMAT3(100),SIGMAT4(100),SIGMAT5(100)
 IF(ASIGMA(J,I).GE.-FY.AND.ASIGMA(J,I).LE.FY)EPSILO(J,I)=ASIGMA(J,I
1)/E1
 IF(ASIGMA(J,I).GT.FY)EPSILO(J,I)=(ASIGMA(J,I)-FY)/E2+EPSISH
 IF(ASIGMA(J,I).LT.-FY)EPSILO(J,I)=(ASIGMA(J,I)+FY)/E2-EPSISH
 RETURN
 END
```

```
      COMMON/STRAIN/FY,E1,E2,EPSILOY,EPSISH,ASIGMA(25,100),EPSILO(25,100
     $),SIGMAA(100),EPSILOA(100),SIGMAT(100),EPSILOT(100),EPSA(100),BETA
     $(100),ALPH(100),DSIG1(100),DSIG2(100),SIGMAT1(100),SIGMAT2(100),SI
     $GMAT3(100),SIGMAT4(100),SIGMAT5(100)
      EPSA(I)=EPSILOA(I)-(SIGMAA(I)-FY)/E1
      EPPMAX=EPSA(I)-FY/E1
      EPMAX=ABS(EPPMAX)
      EP=EPMAX/0.07
      ALPH(I)=3.1*EPMAX/0.016
      IF(ALPH(I).GE.3.1)ALPH(I)=3.1
      BETA(I)=1.+0.8*EP-0.3*(EP**3.)
      IF(BETA(I).GE.1.5)BETA(I)=1.5
      EO=EPRO2(J,I,0.)
      E16=EO-0.016
      EFFY=EPRO2(J,I,-FY)
      IF(EFFY.GE.E16)1,2
    1 SIGMAT(I)=-FY
      EPSILOT(I)=EFFY
      GO TO 3
    2 SIGMAT(I)=TSIGMA(I,E16)
      EPSILOT(I)=E16
    3 IF(ASIGMA(J,I).GE.FY)EPSILO(J,I)=EPSILOA(I)-(SIGMAA(I)-ASIGMA(J,I)
     1)/E1
      IF(ASIGMA(J,I).GE.SIGMAT(I).AND.ASIGMA(J,I).LT.FY)EPSILO(J,I)=EPRO
     12(J,I,ASIGMA(J,I))
      IF(ASIGMA(J,I).LT.SIGMAT(I))EPSILO(J,I)=(ASIGMA(J,I)-SIGMAT(I))/E2
     1+EPSILOT(I)
      RETURN
      END
```



```
      SUBROUTINE SCASE3(J,I)
      COMMON/STRAIN/FY,E1,E2,EPSILOY,EPSISH,ASIGMA(25,100),EPSILO(25,100
     $),SIGMAA(100),EPSILOA(100),SIGMAT(100),EPSILOT(100),EPSA(100),BETA
     $(100),ALPH(100),DSIG1(100),DSIG2(100),SIGMAT1(100),SIGMAT2(100),SI
     $GMAT3(100),SIGMAT4(100),SIGMAT5(100)
      DSIG1(I)=SIGMAA(I)-FY
      DSIG2(I)=FY-SIGMAT(I)
      SIGMATT=ASIGMA(J-1,I)+DSIG1(I)
      SIGMAT1(I)=ASIGMA(J-1,I)+DSIG1(I)+DSIG2(I)
      IF(ASIGMA(J-1,I).GE.SIGMAT(I))5,6
    5 IF(ASIGMA(J,I).GE.ASIGMA(J-1,I).AND.ASIGMA(J,I).LT.SIGMATT)EPSILO(
     1J,I)=EPSILO(J-1,I)-(ASIGMA(J-1,I)-ASIGMA(J,I))/E1
      IF(ASIGMA(J,I).GE.SIGMATT.AND.ASIGMA(J,I).LT.SIGMAA(I))EPSILO(J,I)
     1=EPRO3(J,I,ASIGMA(J,I))
      IF(ASIGMA(J,I).GE.SIGMAA(I))EPSILO(J,I)=EPSILOA(I)-(SIGMAA(I)-ASIG
     1MA(J,I))/E2
      GO TO 99
    6 IF(ASIGMA(J,I).GE.ASIGMA(J-1,I).AND.ASIGMA(J,I).LT.SIGMATT)EPSILO(
     1J,I)=EPSILO(J-1,I)-(ASIGMA(J-1,I)-ASIGMA(J,I))/E1
      IF(ASIGMA(J,I).GE.SIGMATT.AND.ASIGMA(J,I).LT.SIGMAT1(I))EPSILO(J,I
     1)=EPRO3(J,I,ASIGMA(J,I))
      IF(ASIGMA(J,I).GE.SIGMAT1(I))EPSILO(J,I)=EPSILOA(I)-(SIGMAA(I)-ASI
     1GMA(J,I))/E2
   99 RETURN
      END
```

```
      SUBROUTINE SCASE4(J,I)
      COMMON/STRAIN/FY,E1,E2,EPSILOY,EPSISH,ASIGMA(25,100),EPSILO(25,100
     $),SIGMAA(100),EPSILOA(100),SIGMAT(100),EPSILOT(100),EPSA(100),BETA
     $(100),ALPH(100),DSIG1(100),DSIG2(100),SIGMAT1(100),SIGMAT2(100),SI
     $GMAT3(100),SIGMAT4(100),SIGMAT5(100)
      SIGMATT=ASIGMA(J-1,I)-DSIG1(I)
      SIGMAT2(I)=ASIGMA(J-1,I)-DSIG1(I)-DSIG2(I)
      IF(ASIGMA(J-2,I).GE.SIGMAT(I))1,2
    1 IF(ASIGMA(J,I).LE.ASIGMA(J-1,I).AND.ASIGMA(J,I).GT.SIGMATT)EPSILO(
     1J,I)=EPSILO(J-1,I)-(ASIGMA(J-1,I)-ASIGMA(J,I))/E1
      IF(ASIGMA(J,I).LE.SIGMATT.AND.ASIGMA(J,I).GT.ASIGMA(J-2,I))EPSILO(
     1J,I)=EPRO2(J,I,ASIGMA(J,I))
      IF(ASIGMA(J,I).LE.ASIGMA(J-2,I).AND.ASIGMA(J,I).GT.SIGMAT(I))EPSIL
     1O(J,I)=EPRO2(J-2,I,ASIGMA(J,I))
      IF(ASIGMA(J,I).LE.SIGMAT(I))EPSILO(J,I)=EPSILOT(I)+(ASIGMA(J,I)-SI
     1GMAT(I))/E2
      GO TO 99
    2 IF(ASIGMA(J-1,I).GE.SIGMAT1(I))3,4
    3 IF(ASIGMA(J,I).LE.ASIGMA(J-1,I).AND.ASIGMA(J,I).GT.SIGMATT)EPSILO(
     1J,I)=EPSILO(J-1,I)-(ASIGMA(J-1,I)-ASIGMA(J,I))/E1
      IF(ASIGMA(J,I).LE.SIGMATT.AND.ASIGMA(J,I).GT.SIGMAT2(I))EPSILO(J,I
     1)=EPRO2(J,I,ASIGMA(J,I))
      IF(ASIGMA(J,I).LE.SIGMAT2(I))EPSILO(J,I)=EPSILOT(I)+(ASIGMA(J,I)-S
     1IGMAT(I))/E2
      GO TO 99
    4 IF(ASIGMA(J,I).LE.ASIGMA(J-1,I).AND.ASIGMA(J,I).GT.SIGMATT)EPSILO(
     1J,I)=EPSILO(J-1,I)-(ASIGMA(J-1,I)-ASIGMA(J,I))/E1
      IF(ASIGMA(J,I).LE.SIGMATT.AND.ASIGMA(J,I).GT.ASIGMA(J-2,I))EPSILO(
     1J,I)=EPRO2(J,I,ASIGMA(J,I))
      IF(ASIGMA(J,I).LE.ASIGMA(J-2,I))EPSILO(J,I)=EPSILOT(I)+(ASIGMA(J,I
     1)-SIGMAT(I))/E2
   99 RETURN
      END
```



```
      SUBROUTINE SCASE5(J,I)
      COMMON/STRAIN/FY,E1,E2,EPSILOY,EPSISH,ASIGMA(25,100),EPSILO(25,100
     $),SIGMAA(100),EPSILOA(100),SIGMAT(100),EPSILOT(100),EPSA(100),BETA
     $(100),ALPH(100),DSIG1(100),DSIG2(100),SIGMAT1(100),SIGMAT2(100),SI
     $GMAT3(100),SIGMAT4(100),SIGMAT5(100)
      SIGMATT=ASIGMA(J-1,I)+DSIG1(I)
      SIGMAT3(I)=ASIGMA(J-1,I)+DSIG1(I)+DSIG2(I)
      IF(ASIGMA(J-3,I).GE.SIGMAT(I))1,2
    1 IF(ASIGMA(J-1,I).GE.ASIGMA(J-2,I))GO TO 3
      IF(ASIGMA(J-1,I).LT.ASIGMA(J-3,I).AND.ASIGMA(J-1,I).GE.SIGMAT(I))G
     1O TO 4
      IF(ASIGMA(J-1,I).LT.SIGMAT(I))GO TO 5
    3 IF(ASIGMA(J,I).GE.ASIGMA(J-1,I).AND.ASIGMA(J,I).LT.SIGMATT)EPSILO(
     1J,I)=EPSILO(J-1,I)-(ASIGMA(J-1,I)-ASIGMA(J,I))/E1
      IF(ASIGMA(J,I).GE.SIGMATT.AND.ASIGMA(J,I).LT.ASIGMA(J-2,I))EPSILO(
     1J,I)=EPRO3(J,I,ASIGMA(J,I))
      IF(ASIGMA(J,I).GE.ASIGMA(J-2,I).AND.ASIGMA(J,I).LT.SIGMAA(I))EPSIL
     1O(J,I)=EPRO3(J-2,I,ASIGMA(J,I))
      IF(ASIGMA(J,I).GE.SIGMAA(I))EPSILO(J,I)=EPSILOA(I)+(ASIGMA(J,I)-SI
     1GMAA(I))/E2
      GO TO 99
    4 IF(ASIGMA(J,I).GE.ASIGMA(J-1,I).AND.ASIGMA(J,I).LT.SIGMATT)EPSILO(
     1J,I)=EPSILO(J-1,I)-(ASIGMA(J-1,I)-ASIGMA(J,I))/E1
      IF(ASIGMA(J,I).GE.SIGMATT.AND.ASIGMA(J,I).LT.SIGMAA(I))EPSILO(J,I)
     1=EPRO3(J,I,ASIGMA(J,I))
      IF(ASIGMA(J,I).GE.SIGMAA(I))EPSILO(J,I)=EPSILOA(I)+(ASIGMA(J,I)-SI
     1GMAA(I))/E2
      GO TO 99
    5 IF(ASIGMA(J,I).GE.ASIGMA(J-1,I).AND.ASIGMA(J,I).LT.SIGMATT)EPSILO(
     1J,I)=EPSILO(J-1,I)-(ASIGMA(J-1,I)-ASIGMA(J,I))/E1
      IF(ASIGMA(J,I).GE.SIGMATT.AND.ASIGMA(J,I).LT.SIGMAT3(I))EPSILO(J,I
     1)=EPRO3(J,I,ASIGMA(J,I))
      IF(ASIGMA(J,I).GE.SIGMAT3(I))EPSILO(J,I)=EPSILOA(I)+(ASIGMA(J,I)-S
     1IGMAA(I))/E2
      GO TO 99
    2 IF(ASIGMA(J-2,I).GE.SIGMAT1(I))6,7
```

```
      IF(ASIGMA(J-1,I).LT.SIGMAT2(I))GO TO 9
    8 IF(ASIGMA(J,I).GE.ASIGMA(J-1,I).AND.ASIGMA(J,I).LT.SIGMATT)EPSILO(
     1J,I)=EPSILO(J-1,I)-(ASIGMA(J-1,I)-ASIGMA(J,I))/E1
      IF(ASIGMA(J,I).GE.SIGMATT.AND.ASIGMA(J,I).LT.ASIGMA(J-2,I))EPSILO(
     1J,I)=EPRO3(J,I,ASIGMA(J,I))
      IF(ASIGMA(J,I).GE.ASIGMA(J-2,I))EPSILO(J,I)=EPSILOA(I)+(ASIGMA(J,I
     1)-SIGMAA(I))/E2
      GO TO 99
    9 IF(ASIGMA(J,I).GE.ASIGMA(J-1,I).AND.ASIGMA(J,I).LT.SIGMATT)EPSILO(
     1J,I)=EPSILO(J-1,I)-(ASIGMA(J-1,I)-ASIGMA(J,I))/E1
      IF(ASIGMA(J,I).GE.SIGMATT.AND.ASIGMA(J,I).LT.SIGMAT3(I))EPSILO(J,I
     1)=EPRO3(J,I,ASIGMA(J,I))
      IF(ASIGMA(J,I).GE.SIGMAT3(I))EPSILO(J,I)=EPSILOA(I)+(ASIGMA(J,I)-S
     1IGMAA(I))/E2
      GO TO 99
    7 IF(ASIGMA(J-1,I).GE.ASIGMA(J-3,I))GO TO 10
      IF(ASIGMA(J-1,I).LT.ASIGMA(J-3,I))GO TO 9
   10 IF(ASIGMA(J,I).GE.ASIGMA(J-1,I).AND.ASIGMA(J,I).LT.SIGMATT)EPSILO(
     1J,I)=EPSILO(J-1,I)-(ASIGMA(J-1,I)-ASIGMA(J,I))/E1
      IF(ASIGMA(J,I).GE.SIGMATT.AND.ASIGMA(J,I).LT.ASIGMA(J-2,I))EPSILO(
     1J,I)=EPRO3(J,I,ASIGMA(J,I))
      IF(ASIGMA(J,I).GE.ASIGMA(J-2,I).AND.ASIGMA(J,I).LT.SIGMAT1(I))EPSI
     1LO(J,I)=EPRO3(J-2,I,ASIGMA(J,I))
      IF(ASIGMA(J,I).GE.SIGMAT1(I))EPSILO(J,I)=EPSILOA(I)+(ASIGMA(J,I)-S
     1IGMAA(I))/E2
   99 RETURN
      END
```



```
      SUBROUTINE SCASE6(J,I)
      COMMON/STRAIN/FY,E1,E2,EPSILOY,EPSISH,ASIGMA(25,100),EPSILO(25,100
     $),SIGMAA(100),EPSILOA(100),SIGMAT(100),EPSILOT(100),EPSA(100),BETA
     $(100),ALPH(100),DSIG1(100),DSIG2(100),SIGMAT1(100),SIGMAT2(100),SI
     $GMAT3(100),SIGMAT4(100),SIGMAT5(100)
      SIGMATT=ASIGMA(J-1,I)-DSIG1(I)
      SIGMAT4(I)=ASIGMA(J-1,I)-DSIG1(I)-DSIG2(I)
      IF(ASIGMA(J-4,I).GE.SIGMAT(I))1,2
    1 IF(ASIGMA(J-2,I).GE.ASIGMA(J-4,I))GO TO 3
      IF(ASIGMA(J-2,I).LT.ASIGMA(J-4,I).AND.ASIGMA(J-2,I).GE.SIGMAT(I))G
     1O TO 4
      IF(ASIGMA(J-2,I).LT.SIGMAT(I))GO TO 5
    3 IF(ASIGMA(J-1,I).GE.ASIGMA(J-3,I))6,7
    6 IF(ASIGMA(J,I).LE.ASIGMA(J-1,I).AND.ASIGMA(J,I).GT.SIGMATT)EPSILO(
     1J,I)=EPSILO(J-1,I)-(ASIGMA(J-1,I)-ASIGMA(J,I))/E1
      IF(ASIGMA(J,I).LE.SIGMATT.AND.ASIGMA(J,I).GT.ASIGMA(J-4,I))EPSILO(
     1J,I)=EPRO2(J,I,ASIGMA(J,I))
      IF(ASIGMA(J,I).LE.ASIGMA(J-4,I).AND.ASIGMA(J,I).GT.SIGMAT(I))EPSIL
     1O(J,I)=EPRO2(J-4,I,ASIGMA(J,I))
      IF(ASIGMA(J,I).LE.SIGMAT(I))EPSILO(J,I)=EPSILOT(I)+(ASIGMA(J,I)-SI
     1GMAT(I))/E2
      GO TO 99
    7 IF(ASIGMA(J,I).LE.ASIGMA(J-1,I).AND.ASIGMA(J,I).GT.SIGMATT)EPSILO(
     1J,I)=EPSILO(J-1,I)-(ASIGMA(J-1,I)-ASIGMA(J,I))/E1
      IF(ASIGMA(J,I).LE.SIGMATT.AND.ASIGMA(J,I).GT.ASIGMA(J-2,I))EPSILO(
     1J,I)=EPRO2(J,I,ASIGMA(J,I))
      IF(ASIGMA(J,I).LE.ASIGMA(J-2,I).AND.ASIGMA(J,I).GT.ASIGMA(J-4,I))E
     1PSILO(J,I)=EPRO2(J-2,I,ASIGMA(J,I))
      IF(ASIGMA(J,I).LE.ASIGMA(J-4,I).AND.ASIGMA(J,I).GT.SIGMAT(I))EPSIL
     1O(J,I)=EPRO2(J-4,I,ASIGMA(J,I))
      IF(ASIGMA(J,I).LE.SIGMAT(I))EPSILO(J,I)=EPSILOT(I)+(ASIGMA(J,I)-SI
     1GMAT(I))/E2
      GO TO 99
    4 IF(ASIGMA(J,I).LE.ASIGMA(J-1,I).AND.ASIGMA(J,I).GT.SIGMATT)EPSILO(
     1J,I)=EPSILO(J-1,I)-(ASIGMA(J-1,I)-ASIGMA(J,I))/E1
      IF(ASIGMA(J,I).LE.SIGMATT.AND.ASIGMA(J,I).GT.ASIGMA(J-2,I))EPSILO(
```

```
      IF(ASIGMA(J,I).LE.ASIGMA(J-2,I).AND.ASIGMA(J,I).GT.SIGMAT(I))EPSIL
     1O(J,I)=EPRO2(J-4,I,ASIGMA(J,I))
      IF(ASIGMA(J,I).LE.SIGMAT(I))EPSILO(J,I)=EPSILOT(I)+(ASIGMA(J,I)-SI
     1GMAT(I))/E2
      GO TO 99
    5 IF(ASIGMA(J-1,I).GE.SIGMAT3(I))8,9
    8 IF(ASIGMA(J,I).LE.ASIGMA(J-1,I).AND.ASIGMA(J,I).GT.SIGMATT)EPSILO(
     1J,I)=EPSILO(J-1,I)-(ASIGMA(J-1,I)-ASIGMA(J,I))/E1
      IF(ASIGMA(J,I).LE.SIGMATT.AND.ASIGMA(J,I).GT.SIGMAT4(I))EPSILO(J,I
     1)=EPRO2(J,I,ASIGMA(J,I))
      IF(ASIGMA(J,I).LE.SIGMAT4(I))EPSILO(J,I)=EPSILOT(I)+(ASIGMA(J,I)-S
     1IGMAT(I))/E2
      GO TO 99
    9 IF(ASIGMA(J,I).LE.ASIGMA(J-1,I).AND.ASIGMA(J,I).GT.SIGMATT)EPSILO(
     1J,I)=EPSILO(J-1,I)-(ASIGMA(J-1,I)-ASIGMA(J,I))/E1
      IF(ASIGMA(J,I).LE.SIGMATT.AND.ASIGMA(J,I).GT.ASIGMA(J-2,I))EPSILO(
     1J,I)=EPRO2(J,I,ASIGMA(J,I))
      IF(ASIGMA(J,I).LE.ASIGMA(J-2,I))EPSILO(J,I)=EPSILOT(I)+(ASIGMA(J,I
     1)-SIGMAT(I))/E2
      GO TO 99
    2 IF(ASIGMA(J-3,I).GE.SIGMAT1(I))10,11
   10 IF(ASIGMA(J-2,I).GE.SIGMAT2(I))12,13
   12 IF(ASIGMA(J-1,I).GE.ASIGMA(J-3,I))14,15
   14 IF(ASIGMA(J,I).LE.ASIGMA(J-1,I).AND.ASIGMA(J,I).GT.SIGMATT)EPSILO(
     1J,I)=EPSILO(J-1,I)-(ASIGMA(J-1,I)-ASIGMA(J,I))/E1
      IF(ASIGMA(J,I).LE.SIGMATT.AND.ASIGMA(J,I).GT.SIGMAT4(I))EPSILO(J,I
     1)=EPRO2(J,I,ASIGMA(J,I))
      IF(ASIGMA(J,I).LE.SIGMAT4(I))EPSILO(J,I)=EPSILOT(I)+(ASIGMA(J,I)-S
     1IGMAT(I))/E2
      GO TO 99
   15 IF(ASIGMA(J,I).LE.ASIGMA(J-1,I).AND.ASIGMA(J,I).GT.SIGMATT)EPSILO(
     1J,I)=EPSILO(J-1,I)-(ASIGMA(J-1,I)-ASIGMA(J,I))/E1
      IF(ASIGMA(J,I).LE.SIGMATT.AND.ASIGMA(J,I).GT.ASIGMA(J-2,I))EPSILO(
     1J,I)=EPRO2(J,I,ASIGMA(J,I))
      IF(ASIGMA(J,I).LE.ASIGMA(J-2,I).AND.ASIGMA(J,I).GT.SIGMAT2(I))EPSI
```



```
     1LO(J,I)=EPRO2(J-2,I,ASIGMA(J,I))
      IF(ASIGMA(J,I).LE.SIGMAT2(I))EPSILO(J,I)=EPSILOT(I)+(ASIGMA(J,I)-S
     1IGMAT(I))/E2
      GO TO 99
   13 IF(ASIGMA(J-1,I).GE.SIGMAT3(I))20,21
   20 IF(ASIGMA(J,I).LE.ASIGMA(J-1,I).AND.ASIGMA(J,I).GT.SIGMATT)EPSILO(
     1J,I)=EPSILO(J-1,I)-(ASIGMA(J-1,I)-ASIGMA(J,I))/E1
      IF(ASIGMA(J,I).LE.SIGMATT.AND.ASIGMA(J,I).GT.SIGMAT4(I))EPSILO(J,I
     1)=EPRO2(J,I,ASIGMA(J,I))
      IF(ASIGMA(J,I).LE.SIGMAT4(I))EPSILO(J,I)=EPSILOT(I)+(ASIGMA(J,I)-S
     1IGMAT(I))/E2
      GO TO 99
   21 IF(ASIGMA(J,I).LE.ASIGMA(J-1,I).AND.ASIGMA(J,I).GT.SIGMATT)EPSILO(
     1J,I)=EPSILO(J-1,I)-(ASIGMA(J-1,I)-ASIGMA(J,I))/E1
      IF(ASIGMA(J,I).LE.SIGMATT.AND.ASIGMA(J,I).GT.ASIGMA(J-2,I))EPSILO(
     1J,I)=EPRO2(J,I,ASIGMA(J,I))
      IF(ASIGMA(J,I).LE.ASIGMA(J-2,I))EPSILO(J,I)=EPSILOT(I)+(ASIGMA(J,I
     1)-SIGMAT(I))/E2
      GO TO 99
   11 IF(ASIGMA(J-2,I).GE.ASIGMA(J-4,I))16,17
   16 IF(ASIGMA(J-1,I).LE.ASIGMA(J-3,I))GO TO 22
      IF(ASIGMA(J-1,I).GT.ASIGMA(J-3,I).AND.ASIGMA(J-1,I).LE.SIGMAT1(I))
     1GO TO 23
      IF(ASIGMA(J-1,I).GT.SIGMAT1(I))GO TO 24
   22 IF(ASIGMA(J,I).LE.ASIGMA(J-1,I).AND.ASIGMA(J,I).GT.SIGMATT)EPSILO(
     1J,I)=EPSILO(J-1,I)-(ASIGMA(J-1,I)-ASIGMA(J,I))/E1
      IF(ASIGMA(J,I).LE.SIGMATT.AND.ASIGMA(J,I).GT.ASIGMA(J-2,I))EPSILO(
     1J,I)=EPRO2(J,I,ASIGMA(J,I))
      IF(ASIGMA(J,I).LE.ASIGMA(J-2,I).AND.ASIGMA(J,I).GT.ASIGMA(J-4,I))E
     1PSILO(J,I)=EPRO2(J-2,I,ASIGMA(J,I))
      IF(ASIGMA(J,I).LE.ASIGMA(J-4,I))EPSILO(J,I)=EPSILOT(I)+(ASIGMA(J,I
     1)-SIGMAT(I))/E2
      GO TO 99
   23 IF(ASIGMA(J,I).LE.ASIGMA(J-1,I).AND.ASIGMA(J,I).GT.SIGMATT)EPSILO(
     1J,I)=EPSILO(J-1,I)-(ASIGMA(J-1,I)-ASIGMA(J,I))/E1
      IF(ASIGMA(J,I).LE.SIGMATT.AND.ASIGMA(J,I).GT.ASIGMA(J-4,I))EPSILO(
```

```
     1J,I)=EPRO2(J,I,ASIGMA(J,I))
      IF(ASIGMA(J,I).LE.ASIGMA(J-4,I))EPSILO(J,I)=EPSILOT(I)+(ASIGMA(J,I
     1)-SIGMAT(I))/E2
      GO TO 99
   24 IF(ASIGMA(J,I).LE.ASIGMA(J-1,I).AND.ASIGMA(J,I).GT.SIGMATT)EPSILO(
     1J,I)=EPSILO(J-1,I)-(ASIGMA(J-1,I)-ASIGMA(J,I))/E1
      IF(ASIGMA(J,I).LE.SIGMATT.AND.ASIGMA(J,I).GT.SIGMAT4(I))EPSILO(J,I
     1)=EPRO2(J,I,ASIGMA(J,I))
      IF(ASIGMA(J,I).LE.SIGMAT4(I))EPSILO(J,I)=EPSILOT(I)+(ASIGMA(J,I)-S
     1IGMAT(I))/E2
      GO TO 99
   17 IF(ASIGMA(J-1,I).GE.SIGMAT3(I))18,19
   18 IF(ASIGMA(J,I).LE.ASIGMA(J-1,I).AND.ASIGMA(J,I).GT.SIGMATT)EPSILO(
     1J,I)=EPSILO(J-1,I)-(ASIGMA(J-1,I)-ASIGMA(J,I))/E1
      IF(ASIGMA(J,I).LE.SIGMATT.AND.ASIGMA(J,I).GT.SIGMAT4(I))EPSILO(J,I
     1)=EPRO2(J,I,ASIGMA(J,I))
      IF(ASIGMA(J,I).LE.SIGMAT4(I))EPSILO(J,I)=EPSILOT(I)+(ASIGMA(J,I)-S
     1IGMAT(I))/E2
      GO TO 99
   19 IF(ASIGMA(J,I).LE.ASIGMA(J-1,I).AND.ASIGMA(J,I).GT.SIGMATT)EPSILO(
     1J,I)=EPSILO(J-1,I)-(ASIGMA(J-1,I)-ASIGMA(J,I))/E1
      IF(ASIGMA(J,I).LE.SIGMATT.AND.ASIGMA(J,I).GT.ASIGMA(J-2,I))EPSILO(
     1J,I)=EPRO2(J,I,ASIGMA(J,I))
      IF(ASIGMA(J,I).LE.ASIGMA(J-2,I))EPSILO(J,I)=EPSILOT(I)+(ASIGMA(J,I
     1)-SIGMAT(I))/E2
   99 RETURN
      END
```



```
      SUBROUTINE SCASE7(J,I)
      COMMON/STRAIN/FY,E1,E2,EPSILOY,EPSISH,ASIGMA(25,100),EPSILO(25,100
     $),SIGMAA(100),EPSILOA(100),SIGMAT(100),EPSILOT(100),EPSA(100),BETA
     $(100),ALPH(100),DSIG1(100),DSIG2(100),SIGMAT1(100),SIGMAT2(100),SI
     $GMAT3(100),SIGMAT4(100),SIGMAT5(100)
      SIGMATT=ASIGMA(J-1,I)+DSIG1(I)
      SIGMAT5(I)=ASIGMA(J-1,I)+DSIG1(I)+DSIG2(I)
      IF(ASIGMA(J-5,I).GE.SIGMAT(I))1,2
    1 IF(ASIGMA(J-3,I).GE.ASIGMA(J-5,I))GO TO 3
      IF(ASIGMA(J-3,I).LT.ASIGMA(J-5,I).AND.ASIGMA(J-3,I).GE.SIGMAT(I))G
     1O TO 4
      IF(ASIGMA(J-3,I).LT.SIGMAT(I))GO TO 5
    3 IF(ASIGMA(J-2,I).GE.ASIGMA(J-4,I))6,7
    6 IF(ASIGMA(J-1,I).GE.ASIGMA(J-5,I))GO TO 8
      IF(ASIGMA(J-1,I).LT.ASIGMA(J-5,I).AND.ASIGMA(J-1,I).GE.SIGMAT(I))G
     1O TO 9
      IF(ASIGMA(J-1,I).LT.SIGMAT(I))GO TO 10
    8 IF(ASIGMA(J,I).GE.ASIGMA(J-1,I).AND.ASIGMA(J,I).LT.SIGMATT)EPSILO(
     1J,I)=EPSILO(J-1,I)-(ASIGMA(J-1,I)-ASIGMA(J,I))/E1
      IF(ASIGMA(J,I).GE.SIGMATT.AND.ASIGMA(J,I).LT.ASIGMA(J-2,I))EPSILO(
     1J,I)=EPRO3(J,I,ASIGMA(J,I))
      IF(ASIGMA(J,I).GE.ASIGMA(J-2,I).AND.ASIGMA(J,I).LT.SIGMAA(I))EPSIL
     1O(J,I)=EPRO3(J-4,I,ASIGMA(J,I))
      IF(ASIGMA(J,I).GE.SIGMAA(I))EPSILO(J,I)=EPSILOA(I)+(ASIGMA(J,I)-SI
     1GMAA(I))/E2
      GO TO 99
    9 IF(ASIGMA(J,I).GE.ASIGMA(J-1,I).AND.ASIGMA(J,I).LT.SIGMATT)EPSILO(
     1J,I)=EPSILO(J-1,I)-(ASIGMA(J-1,I)-ASIGMA(J,I))/E1
      IF(ASIGMA(J,I).GE.SIGMATT.AND.ASIGMA(J,I).LT.SIGMAA(I))EPSILO(J,I)
     1=EPRO3(J-4,I,ASIGMA(J,I))
      IF(ASIGMA(J,I).GE.SIGMAA(I))EPSILO(J,I)=EPSILOA(I)+(ASIGMA(J,I)-SI
     1GMAA(I))/E2
      GO TO 99
   10 IF(ASIGMA(J,I).GE.ASIGMA(J-1,I).AND.ASIGMA(J,I).LT.SIGMATT)EPSILO(
     1J,I)=EPSILO(J-1,I)-(ASIGMA(J-1,I)-ASIGMA(J,I))/E1
      IF(ASIGMA(J,I).GE.SIGMATT.AND.ASIGMA(J,I).LT.SIGMAT5(I))EPSILO(J,I
```

```
     1)=EPRO3(J,I,ASIGMA(J,I))
      IF(ASIGMA(J,I).GE.SIGMAT5(I))EPSILO(J,I)=EPSILOA(I)+(ASIGMA(J,I)-S
     1IGMAA(I))/E2
      GO TO 99
    7 IF(ASIGMA(J-1,I).GE.ASIGMA(J-3,I))GO TO 11
      IF(ASIGMA(J-1,I).LT.ASIGMA(J-3,I).AND.ASIGMA(J-1,I).GE.ASIGMA(J-5,
     1I))GO TO 12
      IF(ASIGMA(J-1,I).LT.ASIGMA(J-5,I).AND.ASIGMA(J-1,I).GE.SIGMAT(I))G
     1O TO 13
      IF(ASIGMA(J-1,I).LT.SIGMAT(I))GO TO 14
   11 IF(ASIGMA(J,I).GE.ASIGMA(J-1,I).AND.ASIGMA(J,I).LT.SIGMATT)EPSILO(
     1J,I)=EPSILO(J-1,I)-(ASIGMA(J-1,I)-ASIGMA(J,I))/E1
      IF(ASIGMA(J,I).GE.SIGMATT.AND.ASIGMA(J,I).LT.ASIGMA(J-2,I))EPSILO(
     1J,I)=EPRO3(J,I,ASIGMA(J,I))
      IF(ASIGMA(J,I).GE.ASIGMA(J-2,I).AND.ASIGMA(J,I).LT.ASIGMA(J-4,I))E
     1PSILO(J,I)=EPRO3(J-2,I,ASIGMA(J,I))
      IF(ASIGMA(J,I).GE.ASIGMA(J-4,I).AND.ASIGMA(J,I).LT.SIGMAA(I))EPSIL
     1O(J,I)=EPRO3(J-4,I,ASIGMA(J,I))
      IF(ASIGMA(J,I).GE.SIGMAA(I))EPSILO(J,I)=EPSILOA(I)+(ASIGMA(J,I)-SI
     1GMAA(I))/E2
      GO TO 99
   12 IF(ASIGMA(J,I).GE.ASIGMA(J-1,I).AND.ASIGMA(J,I).LT.SIGMATT)EPSILO(
     1J,I)=EPSILO(J-1,I)-(ASIGMA(J-1,I)-ASIGMA(J,I))/E1
      IF(ASIGMA(J,I).GE.SIGMATT.AND.ASIGMA(J,I).LT.ASIGMA(J-4,I))EPSILO(
     1J,I)=EPRO3(J,I,ASIGMA(J,I))
      IF(ASIGMA(J,I).GE.ASIGMA(J-4,I).AND.ASIGMA(J,I).LT.SIGMAA(I))EPSIL
     1O(J,I)=EPRO3(J-4,I,ASIGMA(J,I))
      IF(ASIGMA(J,I).GE.SIGMAA(I))EPSILO(J,I)=EPSILOA(I)+(ASIGMA(J,I)-SI
     1GMAA(I))/E2
      GO TO 99
   13 IF(ASIGMA(J,I).GE.ASIGMA(J-1,I).AND.ASIGMA(J,I).LT.SIGMATT)EPSILO(
     1J,I)=EPSILO(J-1,I)-(ASIGMA(J-1,I)-ASIGMA(J,I))/E1
      IF(ASIGMA(J,I).GE.SIGMATT.AND.ASIGMA(J,I).LT.SIGMAA(I))EPSILO(J,I)
     1=EPRO3(J,I,ASIGMA(J,I))
      IF(ASIGMA(J,I).GE.SIGMAA(I))EPSILO(J,I)=EPSILOA(I)+(ASIGMA(J,I)-SI
     1GMAA(I))/E2
```



```
   14 IF(ASIGMA(J,I).GE.ASIGMA(J-1,I).AND.ASIGMA(J,I).LT.SIGMATT)EPSILO(
     1J,I)=EPSILO(J-1,I)-(ASIGMA(J-1,I)-ASIGMA(J,I))/E1
      IF(ASIGMA(J,I).GE.SIGMATT.AND.ASIGMA(J,I).LT.SIGMAT5(I))EPSILO(J,I
     1)=EPRO3(J,I,ASIGMA(J,I))
      IF(ASIGMA(J,I).GE.SIGMAT5(I))EPSILO(J,I)=EPSILOA(I)+(ASIGMA(J,I)-S
     1IGMAA(I))/E2
      GO TO 99
    4 IF(ASIGMA(J-1,I).GE.ASIGMA(J-3,I))GO TO 15
      IF(ASIGMA(J-1,I).LT.ASIGMA(J-3,I).AND.ASIGMA(J-1,I).GE.SIGMAT(I))G
     1O TO 16
      IF(ASIGMA(J-1,I).LT.SIGMAT(I))GO TO 17
   15 IF(ASIGMA(J,I).GE.ASIGMA(J-1,I).AND.ASIGMA(J,I).LT.SIGMATT)EPSILO(
     1J,I)=EPSILO(J-1,I)-(ASIGMA(J-1,I)-ASIGMA(J,I))/E1
      IF(ASIGMA(J,I).GE.SIGMATT.AND.ASIGMA(J,I).LT.ASIGMA(J-2,I))EPSILO(
     1J,I)=EPRO3(J,I,ASIGMA(J,I))
      IF(ASIGMA(J,I).GE.ASIGMA(J-2,I).AND.ASIGMA(J,I).LT.SIGMAA(I))EPSIL
     1O(J,I)=EPRO3(J-2,I,ASIGMA(J,I))
      IF(ASIGMA(J,I).GE.SIGMAA(I))EPSILO(J,I)=EPSILOA(I)+(ASIGMA(J,I)-SI
     1GMAA(I))/E2
      GO TO 99
   16 IF(ASIGMA(J,I).GE.ASIGMA(J-1,I).AND.ASIGMA(J,I).LT.SIGMATT)EPSILO(
     1J,I)=EPSILO(J-1,I)-(ASIGMA(J-1,I)-ASIGMA(J,I))/E1
      IF(ASIGMA(J,I).GE.SIGMATT.AND.ASIGMA(J,I).LT.SIGMAA(I))EPSILO(J,I)
     1=EPRO3(J,I,ASIGMA(J,I))
      IF(ASIGMA(J,I).GE.SIGMAA(I))EPSILO(J,I)=EPSILOA(I)+(ASIGMA(J,I)-SI
     1GMAA(I))/E2
      GO TO 99
   17 IF(ASIGMA(J,I).GE.ASIGMA(J-1,I).AND.ASIGMA(J,I).LT.SIGMATT)EPSILO(
     1J,I)=EPSILO(J-1,I)-(ASIGMA(J-1,I)-ASIGMA(J,I))/E1
      IF(ASIGMA(J,I).GE.SIGMATT.AND.ASIGMA(J,I).LT.SIGMAT5(I))EPSILO(J,I
     1)=EPRO3(J,I,ASIGMA(J,I))
      IF(ASIGMA(J,I).GE.SIGMAT5(I))EPSILO(J,I)=EPSILOA(I)+(ASIGMA(J,I)-S
     1IGMAA(I))/E2
      GO TO 99
    5 IF(ASIGMA(J-2,I).GE.SIGMAT3(I))18,19
   18 IF(ASIGMA(J-1,I).GE.SIGMAT4(I))20,21
```

```
 1J,I)=EPSILO(J-1,I)-(ASIGMA(J-1,I)-ASIGMA(J,I))/E1
  IF(ASIGMA(J,I).GE.SIGMATT.AND.ASIGMA(J,I).LT.ASIGMA(J-2,I))EPSILO(
 1J,I)=EPRO3(J,I,ASIGMA(J,I))
  IF(ASIGMA(J,I).GE.ASIGMA(J-2,I))EPSILO(J,I)=EPSILOA(I)+(ASIGMA(J,I
 1)-SIGMAA(I))/E2
  GO TO 99
21 IF(ASIGMA(J,I).GE.ASIGMA(J-1,I).AND.ASIGMA(J,I).LT.SIGMATT)EPSILO(
 1J,I)=EPSILO(J-1,I)-(ASIGMA(J-1,I)-ASIGMA(J,I))/E1
  IF(ASIGMA(J,I).GE.SIGMATT.AND.ASIGMA(J,I).LT.SIGMAT5(I))EPSILO(J,I
 1)=EPRO3(J,I,ASIGMA(J,I))
  IF(ASIGMA(J,I).GE.SIGMAT5(I))EPSILO(J,I)=EPSILOA(I)+(ASIGMA(J,I)-S
 1IGMAA(I))/E2
  GO TO 99
19 IF(ASIGMA(J-1,I).GE.ASIGMA(J-3,I))22,23
22 IF(ASIGMA(J,I).GE.ASIGMA(J-1,I).AND.ASIGMA(J,I).LT.SIGMATT)EPSILO(
 1J,I)=EPSILO(J-1,I)-(ASIGMA(J-1,I)-ASIGMA(J,I))/E1
  IF(ASIGMA(J,I).GE.SIGMATT.AND.ASIGMA(J,I).LT.ASIGMA(J-2,I))EPSILO(
 1J,I)=EPRO3(J,I,ASIGMA(J,I))
  IF(ASIGMA(J,I).GE.ASIGMA(J-2,I).AND.ASIGMA(J,I).LT.SIGMAT3(I))EPSI
 1LO(J,I)=EPRO3(J-2,I,ASIGMA(J,I))
  IF(ASIGMA(J,I).GE.SIGMAT3(I))EPSILO(J,I)=EPSILOA(I)+(ASIGMA(J,I)-S
 1IGMAA(I))/E2
  GO TO 99
23 IF(ASIGMA(J,I).GE.ASIGMA(J-1,I).AND.ASIGMA(J,I).LT.SIGMATT)EPSILO(
 1J,I)=EPSILO(J-1,I)-(ASIGMA(J-1,I)-ASIGMA(J,I))/E1
  IF(ASIGMA(J,I).GE.SIGMATT.AND.ASIGMA(J,I).LT.SIGMAT5(I))EPSILO(J,I
 1)=EPRO3(J,I,ASIGMA(J,I))
  IF(ASIGMA(J,I).GE.SIGMAT5(I))EPSILO(J,I)=EPSILOA(I)+(ASIGMA(J,I)-S
 1IGMAA(I))/E2
  GO TO 99
 2 IF(ASIGMA(J-4,I).GE.SIGMAT1(I))24,25
24 IF(ASIGMA(J-3,I).GE.SIGMAT2(I))26,27
26 IF(ASIGMA(J-2,I).GE.ASIGMA(J-4,I))28,29
28 IF(ASIGMA(J-1,I).GE.SIGMAT4(I))30,31
30 IF(ASIGMA(J,I).GE.ASIGMA(J-1,I).AND.ASIGMA(J,I).LT.SIGMATT)EPSILO(
```



```
 1J,I)=EPSILO(J-1,I)-(ASIGMA(J-1,I)-ASIGMA(J,I))/E1
  IF(ASIGMA(J,I).GE.SIGMATT.AND.ASIGMA(J,I).LT.ASIGMA(J-2,I))EPSILO(
 1J,I)=EPRO3(J,I,ASIGMA(J,I))
  IF(ASIGMA(J,I).GE.ASIGMA(J-2,I))EPSILO(J,I)=EPSILOA(I)+(ASIGMA(J,I
 1)-SIGMAA(I))/E2
  GO TO 99
31 IF(ASIGMA(J,I).GE.ASIGMA(J-1,I).AND.ASIGMA(J,I).LT.SIGMATT)EPSILO(
 1J,I)=EPSILO(J-1,I)-(ASIGMA(J-1,I)-ASIGMA(J,I))/E1
  IF(ASIGMA(J,I).GE.SIGMATT.AND.ASIGMA(J,I).LT.SIGMAT5(I))EPSILO(J,I
 1)=EPRO3(J,I,ASIGMA(J,I))
  IF(ASIGMA(J,I).GE.SIGMAT5(I))EPSILO(J,I)=EPSILOA(I)+(ASIGMA(J,I)-S
 1IGMAA(I))/E2
  GO TO 99
29 IF(ASIGMA(J-1,I).GE.ASIGMA(J-3,I))GO TO 32
  IF(ASIGMA(J-1,I).LT.ASIGMA(J-3,I).AND.ASIGMA(J-1,I).GE.SIGMAT2(I))
 1GO TO 33
  IF(ASIGMA(J-1,I).LT.SIGMAT2(I))GO TO 34
32 IF(ASIGMA(J,I).GE.ASIGMA(J-1,I).AND.ASIGMA(J,I).LT.SIGMATT)EPSILO(
 1J,I)=EPSILO(J-1,I)-(ASIGMA(J-1,I)-ASIGMA(J,I))/E1
  IF(ASIGMA(J,I).GE.SIGMATT.AND.ASIGMA(J,I).LT.ASIGMA(J-2,I))EPSILO(
 1J,I)=EPRO3(J,I,ASIGMA(J,I))
  IF(ASIGMA(J,I).GE.ASIGMA(J-2,I).AND.ASIGMA(J,I).LT.ASIGMA(J-4,I))E
 1PSILO(J,I)=EPRO3(J-2,I,ASIGMA(J,I))
  IF(ASIGMA(J,I).GE.ASIGMA(J-4,I))EPSILO(J,I)=EPSILOA(I)+(ASIGMA(J,I
 1)-SIGMAA(I))/E2
  GO TO 99
33 IF(ASIGMA(J,I).GE.ASIGMA(J-1,I).AND.ASIGMA(J,I).LT.SIGMATT)EPSILO(
 1J,I)=EPSILO(J-1,I)-(ASIGMA(J-1,I)-ASIGMA(J,I))/E1
  IF(ASIGMA(J,I).GE.SIGMATT.AND.ASIGMA(J,I).LT.ASIGMA(J-4,I))EPSILO(
 1J,I)=EPRO3(J,I,ASIGMA(J,I))
  IF(ASIGMA(J,I).GE.ASIGMA(J-4,I))EPSILO(J,I)=EPSILOA(I)+(ASIGMA(J,I
 1)-SIGMAA(I))/E2
  GO TO 99
34 IF(ASIGMA(J,I).GE.ASIGMA(J-1,I).AND.ASIGMA(J,I).LT.SIGMATT)EPSILO(
 1J,I)=EPSILO(J-1,I)-(ASIGMA(J-1,I)-ASIGMA(J,I))/E1
  IF(ASIGMA(J,I).GE.SIGMATT.AND.ASIGMA(J,I).LT.SIGMAT5(I))EPSILO(J,I
```

```
      IF(ASIGMA(J,I).GE.SIGMAT5(I))EPSILO(J,I)=EPSILOA(I)+(ASIGMA(J,I)-S
     1IGMAA(I))/E2
      GO TO 99
   27 IF(ASIGMA(J-2,I).GE.SIGMAT3(I))35,36
   35 IF(ASIGMA(J-1,I).GE.SIGMAT4(I))37,34
   37 IF(ASIGMA(J,I).GE.ASIGMA(J-1,I).AND.ASIGMA(J,I).LT.SIGMATT)EPSILO(
     1J,I)=EPSILO(J-1,I)-(ASIGMA(J-1,I)-ASIGMA(J,I))/E1
      IF(ASIGMA(J,I).GE.SIGMATT.AND.ASIGMA(J,I).LT.ASIGMA(J-2,I))EPSILO(
     1J,I)=EPRO3(J,I,ASIGMA(J,I))
      IF(ASIGMA(J,I).GE.ASIGMA(J-2,I))EPSILO(J,I)=EPSILOA(I)+(ASIGMA(J,I
     1)-SIGMAA(I))/E2
      GO TO 99
   36 IF(ASIGMA(J-1,I).GE.ASIGMA(J-3,I))39,34
   39 IF(ASIGMA(J,I).GE.ASIGMA(J-1,I).AND.ASIGMA(J,I).LT.SIGMATT)EPSILO(
     1J,I)=EPSILO(J-1,I)-(ASIGMA(J-1,I)-ASIGMA(J,I))/E1
      IF(ASIGMA(J,I).GE.SIGMATT.AND.ASIGMA(J,I).LT.ASIGMA(J-2,I))EPSILO(
     1J,I)=EPRO3(J,I,ASIGMA(J,I))
      IF(ASIGMA(J,I).GE.ASIGMA(J-2,I).AND.ASIGMA(J,I).LT.SIGMAT3(I))EPSI
     1LO(J,I)=EPRO3(J-2,I,ASIGMA(J,I))
      IF(ASIGMA(J,I).GE.SIGMAT3(I))EPSILO(J,I)=EPSILOA(I)+(ASIGMA(J,I)-S
     1IGMAA(I))/E2
      GO TO 99
   25 IF(ASIGMA(J-3,I).GE.ASIGMA(J-5,I))41,42
   41 IF(ASIGMA(J-2,I).LE.ASIGMA(J-4,I))GO TO 43
      IF(ASIGMA(J-2,I).GT.ASIGMA(J-4,I).AND.ASIGMA(J-2,I).LE.SIGMAT1(I))
     1GO TO 44
      IF(ASIGMA(J-2,I).GT.SIGMAT1(I))GO TO 45
   43 IF(ASIGMA(J-1,I).GE.ASIGMA(J-3,I))GO TO 46
      IF(ASIGMA(J-1,I).LT.ASIGMA(J-3,I).AND.ASIGMA(J-1,I).GE.ASIGMA(J-5,
     1I))GO TO 47
      IF(ASIGMA(J-1,I).LT.ASIGMA(J-5,I))GO TO 34
   46 IF(ASIGMA(J,I).GE.ASIGMA(J-1,I).AND.ASIGMA(J,I).LT.SIGMATT)EPSILO(
     1J,I)=EPSILO(J-1,I)-(ASIGMA(J-1,I)-ASIGMA(J,I))/E1
      IF(ASIGMA(J,I).GE.SIGMATT.AND.ASIGMA(J,I).LT.ASIGMA(J-2,I))EPSILO(
     1J,I)=EPRO3(J,I,ASIGMA(J,I))
```

320

```
      IF(ASIGMA(J,I).GE.ASIGMA(J-2,I).AND.ASIGMA(J,I).LT.ASIGMA(J-4,I))E
     1PSILO(J,I)=EPRO3(J-2,I,ASIGMA(J,I))
      IF(ASIGMA(J,I).GE.ASIGMA(J-4,I).AND.ASIGMA(J,I).LT.SIGMAT1(I))EPSI
     1LO(J,I)=EPRO3(J-4,I,ASIGMA(J,I))
      IF(ASIGMA(J,I).GE.SIGMAT1(I))EPSILO(J,I)=EPSILOA(I)+(ASIGMA(J,I)-S
     1IGMAA(I))/E2
      GO TO 99
   47 IF(ASIGMA(J,I).GE.ASIGMA(J-1,I).AND.ASIGMA(J,I).LT.SIGMATT)EPSILO(
     1J,I)=EPSILO(J-1,I)-(ASIGMA(J-1,I)-ASIGMA(J,I))/E1
      IF(ASIGMA(J,I).GE.SIGMATT.AND.ASIGMA(J,I).LT.ASIGMA(J-4,I))EPSILO(
     1J,I)=EPRO3(J,I,ASIGMA(J,I))
      IF(ASIGMA(J,I).GE.ASIGMA(J-4,I).AND.ASIGMA(J,I).LT.SIGMAT1(I))EPSI
     1LO(J,I)=EPRO3(J-4,I,ASIGMA(J,I))
      IF(ASIGMA(J,I).GE.SIGMAT1(I))EPSILO(J,I)=EPSILOA(I)+(ASIGMA(J,I)-S
     1IGMAA(I))/E2
      GO TO 99
   44 IF(ASIGMA(J-1,I).GE.ASIGMA(J-5,I))49,34
   49 IF(ASIGMA(J,I).GE.ASIGMA(J-1,I).AND.ASIGMA(J,I).LT.SIGMATT)EPSILO(
     1J,I)=EPSILO(J-1,I)-(ASIGMA(J-1,I)-ASIGMA(J,I))/E1
      IF(ASIGMA(J,I).GE.SIGMATT.AND.ASIGMA(J,I).LT.ASIGMA(J-2,I))EPSILO(
     1J,I)=EPRO3(J,I,ASIGMA(J,I))
      IF(ASIGMA(J,I).GE.ASIGMA(J-2,I).AND.ASIGMA(J,I).LT.SIGMAT1(I))EPSI
     1LO(J,I)=EPRO3(J-4,I,ASIGMA(J,I))
      IF(ASIGMA(J,I).GE.SIGMAT1(I))EPSILO(J,I)=EPSILOA(I)+(ASIGMA(J,I)-S
     1IGMAA(I))/E2
      GO TO 99
   45 IF(ASIGMA(J-1,I).GE.SIGMAT4(I))30,34
   42 IF(ASIGMA(J-2,I).GE.SIGMAT3(I))53,54
   53 IF(ASIGMA(J-1,I).GE.SIGMAT4(I))30,34
   54 IF(ASIGMA(J-1,I).GE.ASIGMA(J-3,I))39,34
   99 RETURN
      END
```

321

| | | | | | | | |
|---|---|---|---|---|---|---|---|
| 2.3152 | -1.7208 | 95.5121 | -53.8638 | 14.2285 | -9.9385 | 16.1 | 2.4 |
| 0.72 | 21.47 | 0.6875 | 2.53 | 320.1562 | 25.11698 | 4. | 0.17962 |
| 0.05031 | 0.32371 | 0.243 | 2.51941 | 0.00787 | 3.30193 | 0.03902 | 0.82 |
| 3.49 | 1.17 | 1.27 | 1.27 | 60. | 4100. | 29600. | 715. |
| 0.006 | 0.03 | 0.03 | 0.03 | -60. | -50. | -50. | 50. |
| 50. | 50. | 0.05 | -0.025 | 0.098 | -0.043 | 0.098 | |

40 5 4 7 13 19 25 31 13 1



# APPENDIX C

## MEASURED AND PREDICTED CYCLIC LOADING STRESS-STRAIN RELATIONSHIPS FOR REINFORCING BARS

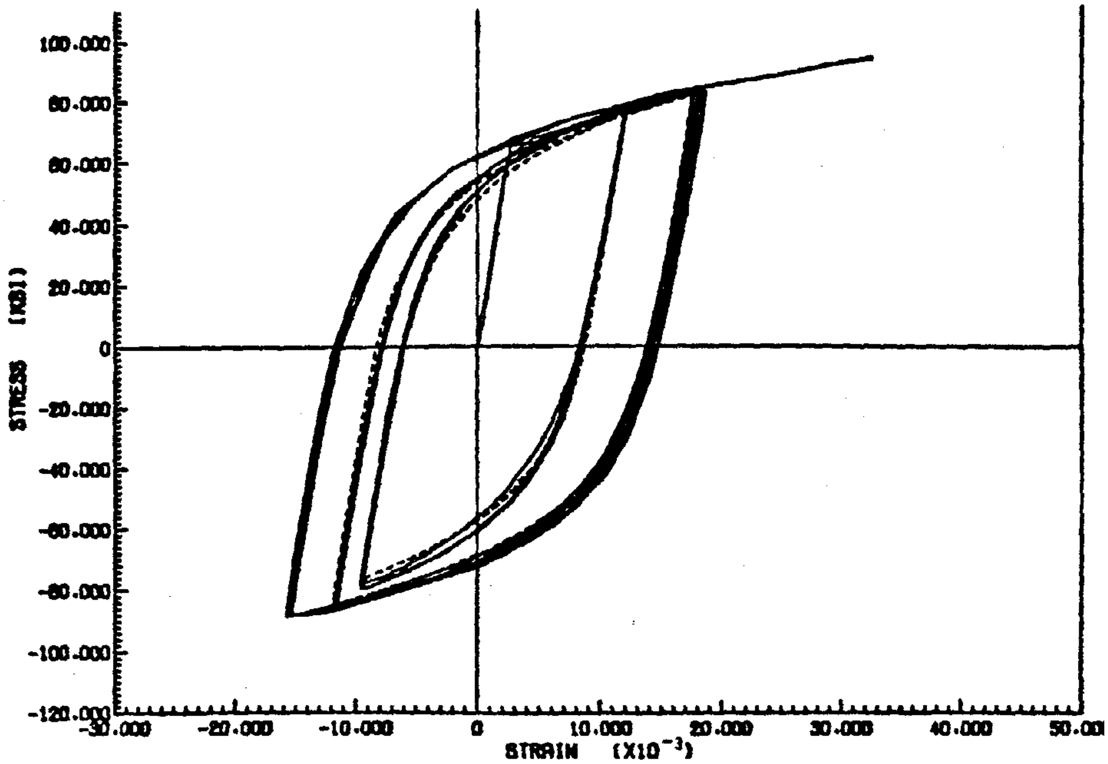


FIG. C-2 COMPARISON OF RAMBERG-OSGOOD EQUATION AND EXPERIMENTAL RESULT FOR SPECIMEN R-04 (29)

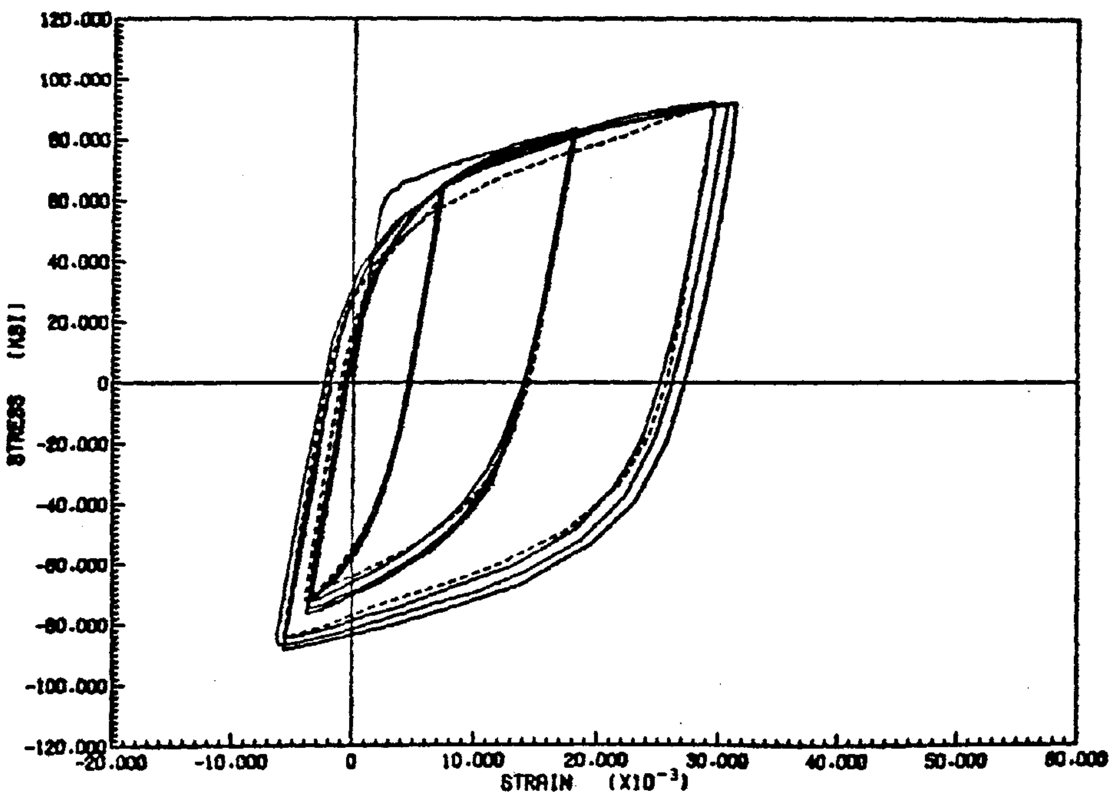


FIG. C-1 COMPARISON OF RAMBERG-OSGOOD EQUATION AND EXPERIMENTAL RESULT FOR SPECIMEN R-03 (29)

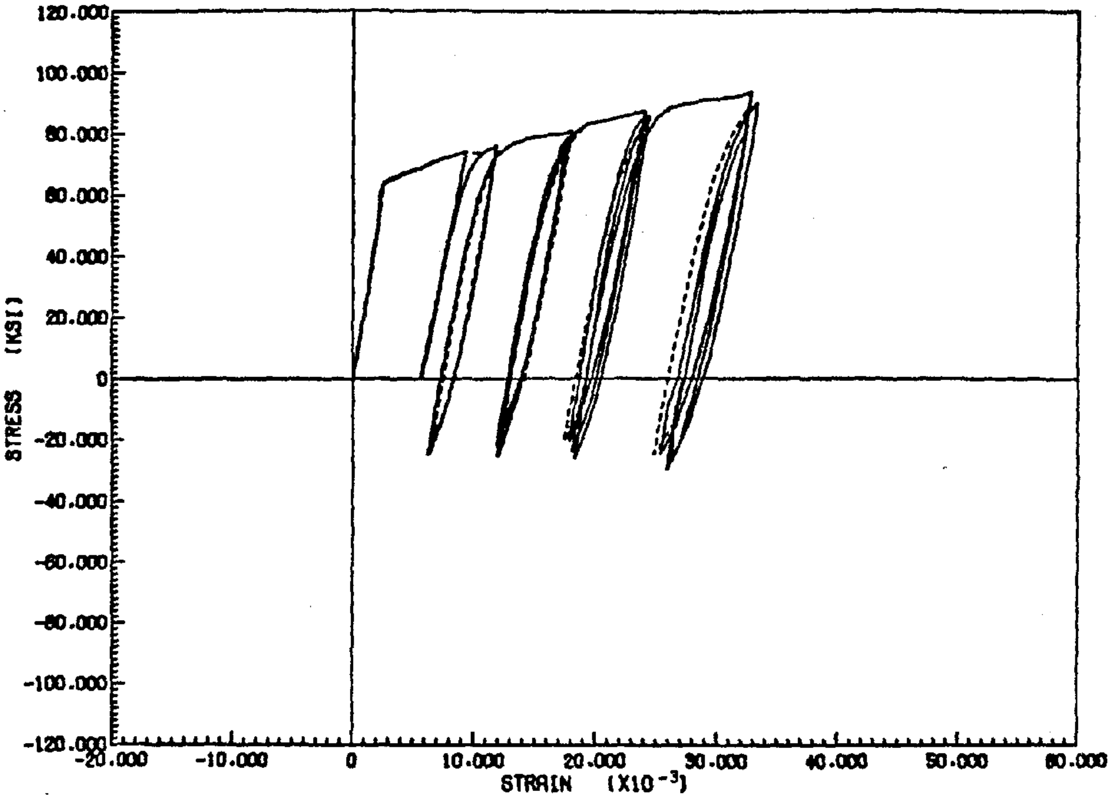


FIG. C-3 COMPARISON OF RAMBERG-OSGOOD EQUATION AND EXPERIMENTAL RESULT FOR SPECIMEN R-06 (29)